

University of Strathclyde
Department of Mechanical & Aerospace
Engineering

Controllability of Building Systems

By

Yousaf Ali Khalid

A thesis presented in fulfilment of the
requirements of the degree of Doctor of
Philosophy, 2011

Copyright statement:

This thesis is the result of the author's original research. It has been composed by the author and has not been previously submitted for examination which has led to the award of a degree.

The copyright of this thesis belongs to the author under the terms of the United Kingdom Copyright Acts as qualified by University of Strathclyde Regulation 3.50. Due acknowledgement must always be made of the use of any material contained in, or derived from, this thesis.'

Signed:

Date:

Acknowledgements

I enjoyed a wonderful working relationship with my supervisors, Professor John M Counsell, Dr Nick Kelly, and Dr John Holden. I thank you all for always willing to spend time with me when I had a question or new results for discussion. I am grateful to them for the background ideas that I have contributed to this thesis and advice in formal and informal discussion sessions throughout the research period.

Particularly, I should like to thank my colleges Matt Stewart, Alastair Scot, Gavin Murphy, Obadah Zaher, Ala Hisham, James Johnston and Joseph Brindley. They helped me a lot in clarifying, communicating and analysing ideas. I learned a great deal from Joseph Brindley about the control and analysis of systems. I am very thankful for them for always being willing to spend time with me when I had a burning experimental work or a hot new experimental results to share.

The author would like to thank Professor Allan Bradshaw of the Lancaster University, for this comments and discussion relation to RIDE Control. I also want to thank all the staff in Energy Systems Research Unit (ESRU) for inputs and discussions throughout my project.

The author acknowledges the financial support derived from the BRE, BRE trust and contribution in kind from Archial group for providing case study for my project.

Publications

The following articles by the thesis author, arising from the work in this thesis, have been published.

Journal Papers

J. Counsell, Y. Khalid, J. Brindley “Controllability of Buildings A multi-input multi-output stability assessment method for buildings with **slow** acting heating systems”
Journal of Simulation Modelling Practice and Theory, Elsevier, Volume 19, issue 4
April 2011, pages 1185-1200

Conference Papers

J. Counsell, Y. Khalid “Controllability of Buildings: A multi-input multi-output stability assessment method for buildings with **fast** acting heating systems” CIBSE Technical Symposium, 6th Sept 2011, De Montfort University, Leicester, UK

J. Counsell and Y. Khalid “A Holistic Analysis method to assess the controllability of commercial buildings and their systems” SEEP 09 14 Aug conference Dublin (Sustainable Energy and Environmental Protection)

J. Counsel and Y. Khalid “Controllability of modern commercial buildings”
WRECX conference 21-25 July 08

Nomenclature

PID = Proportional Integral Differential

CAB = Climate Adaptive Building

SISO = single input single output

RIDE = Robust Inverse Dynamics Estimation

MIMO = multiple inputs and multiple outputs

MV = Mechanical Ventilation,

NV = Natural ventilation

PSV = Passive stack ventilation

A - Area (m^2) NOTE: A with subscript is defined as area. In some places in the thesis, Capital A without subscript is defined as a matrix. This is the A matrix for the linearised model of the building which is represented in the state space form.

b – Number of occupancy

c_p – Specific heat capacity (J/kgK)

C_D – Discharge coefficient of vent opening

C_v – Effectiveness of openings (C_v is assumed to be 0.5 to 0.6 for perpendicular winds and 0.25 to 0.35 for diagonal winds)

d – Differential operator

G – Heat generation rate per person (kg/s)

G – Gravitational acceleration (m/s^2)

ΔH – height difference between upper and lower vents (m)

h – Convective heat transfer coefficient (W/m^2K)

I – Solar radiation (W/m^2)

j – Represents the j^{th} element i.e. number of wall in range 1-4

k – Constant of proportionality

k_e - Proportion of light power converted to heat

L – Lux

n – Air change rate (s^{-1})

P – Electrical power into lights (W)

\dot{Q} – Heat transfer rate (W)
q – Volume flow rate (m^3/s)
 s_x – switching surface for sliding mode
s – laplace variable
T – Temperature (K)
t – Time (s)
U – Heat transfer coefficient ($\text{W}/\text{m}^2\text{K}$)
V – Volume (m^3)
 v – Wind speed (m/s)
W – Humidity (vapour) transfer rate

Symbols:

ρ - Density of (kg/m^3)
 α – Fraction of total transmitted solar gain through the window that goes into the element such as wall, mass etc.
 σ – Transmissivity (determines the total transmitted solar gain through the windows)
 ε – Emissivity of the plant
 λ – Daylight factor
 τ – time constant

Subscripts:

1,2,3,4 - Wall numbers
a – air
ap – appliances
b – Boltzmann's constant
cm – comfort
cp – convection heat transfer from plant to air
d – Internal humidity gain
dr – direct
df – diffuse

f – Floor
i – Internal
L – Lights
m – Internal mass
mv – mechanical ventilation
t – Buoyancy (thermal)
v – Wind pressure
ni – infiltration
o – External
oc – occupancy
p – Plant
pr – radiation component of the plant
pc – convection component of the plant
pp – per person
r – Roof
rp – Radiant component of plant
s – Solar
sa – Sol-air
sf – Solar radiation falling on the floor
v – Wind
w – Wall
win – Window

1 : Controllability of buildings and the building's industry	7
1.1 Comfort in Buildings	8
1.2 Comfort in the case of Climate Adaptive Building	11
1.3 Control of Comfort	13
1.4 Problem Statement	15
1.4.1 Building Design Process, Regulations and Designers	15
1.4.2 New Technologies, Building Automation systems and Building Services Engineers	19
1.4.3 Modelling & Simulation Community and Control Engineers	21
1.4.4 Conclusions	23
1.5 Research Objectives	25
1.6 Thesis Overview and main contributions	26
2 : Guide to modelling buildings for Controllability	27
2.1 Literature Review	29
2.1.1 Modelling Method(s)	31
2.2 Building Model.....	35
2.2.1 History and evolution.....	36
2.2.2 Thermodynamics.....	41
2.2.3 Natural Ventilation and air change rate	54
2.2.4 Daylight.....	56
2.2.5 Internal and external long wave radiation exchange (sky temperature & solar radiation)	59
2.2.6 CO ₂ concentration	63
2.2.7 Humidity	65
2.2.8 Modelling of plant and sensor dynamics	66
2.3 Model Appropriateness	68

2.4	Model for Industry.....	75
2.4.1	Assessment of the model's valid bandwidth.....	76
2.4.2	Test case model.....	80
2.4.3	Simulation Method.....	82
2.4.4	Simulation Results.....	83
2.4.5	Model order reduction.....	87
2.4.6	Singular perturbation analysis.....	90
2.4.7	Frequency response and empirical verification.....	95
2.5	Conclusions to modelling for controllability.....	103
3	: Theory of Controllability Assessment.....	105
3.1	Philosophy of Ideal System Response (ISR).....	106
3.2	Theory of Ideal System Response (ISR).....	108
3.2.1	High Gain Control.....	108
3.2.2	Variable Structure Control (VSC) & Sliding Mode Control (SMC) .	110
3.2.3	Equivalent Control.....	113
3.2.4	Feasibility of ISR.....	116
3.2.5	Factors that prevent inverting the dynamics and ISR tracking.....	118
3.2.6	Degree of ease in achieving ISR.....	122
3.2.7	Fast and Slow modes.....	124
3.2.8	Inverse dynamics input (U_{eq}) and slow modes.....	128
3.2.9	Control of first order systems for achieving ISR.....	134
3.2.10	Robust Inverse Dynamics Estimation (RIDE).....	137
3.2.11	Criterion for safe operation.....	145
4	: START-OF-ABC*.....	150
4.1	ISR Philosophy in simple words.....	152
4.2	STaR Theory of buildings.....	153

4.2.1	Stability	155
4.2.2	Trackability	158
4.2.3	Reachability.....	163
4.2.4	STaR Theory and the present state of building's industry.....	167
5	: Case studies.....	169
5.1	Stability of Heating Systems with Slow Actuation	170
5.1.1	Mathematical Modelling	171
5.1.2	Stability of air temperature control	175
5.1.3	Stability of temperature plus its rate of change control	181
5.1.4	Stability of comfort temperature control.....	188
5.1.5	Conclusions	190
5.2	Controllability of Heating Systems with Fast Actuation.....	193
5.2.1	Mathematical Modelling	194
5.2.2	Stability of air temperature and humidity control	197
5.2.3	Trackability of air temperature and humidity control	202
5.2.4	Reachability of air temperature control.....	203
5.2.5	Reachability of humidity control	212
5.2.6	Conclusions	213
5.3	Simplified Controllability of Air Temperature for Systems with Fast Actuation (Convactor Heater)	216
5.3.1	Mathematical Modelling	217
5.3.2	Stability	220
5.3.3	Reachability.....	225
5.3.4	Conclusions	238
5.4	Simplified Controllability of Comfort temperature for Systems with Fast Actuation (Convactor heater).....	240

5.4.1	Stability	240
5.4.2	Reachability.....	243
5.4.3	Conclusions	249
5.5	Simplified Controllability of Comfort temperature control with a conventional Radiator	251
5.5.1	Stability	251
5.5.2	Reachability.....	253
5.5.3	Conclusions	255
6	Conclusions, industrial impact and further work	257
6.1	Conclusions	258
6.2	Industrial Impact for Heating System Control	262
6.3	Further work	268
7	References	276
8	Appendix 1 - Thermodynamics.....	291
9	Appendix 2 – external thermal mass equation derivation.....	294
10	Appendix 3 – Test house data	295
11	Appendix 4 – chapter two symbolic models and data	303
12	Appendix 5 – U_{trim} equation derivation for proof	314
13	Appendix 6 – Case-study 1	315
14	Appendix 7 – Case study 2	321
15	Appendix 8 – Case study 3	325
16	Appendix 9 – Proof of controller bandwidth to be 3 times slower	327
17	Appendix 10 – standard SAP values.....	329
18	Appendix 11 – ESL code for dynamic simulation.....	330
19	Table of figures	361

Abstract

What is Controllability of Building Systems?

Controllability is a property of the total building system and hence depends on how the building has been designed, what systems are used and what conditions in the building are to be controlled. Controllability establishes how easy or difficult it is to control the response of a building to changes in temperature, lighting level and air quality. The controllability is assessed in three fundamental parts:

- *Stability*: Can the control system guarantee that the desired temperature, lighting and air quality can be held at a constant level?
- *Trackability*: Can it track a specified set point level?
- *Reachability*: Can it reach that set point?

This thesis is concerned with improving the controllability of modern buildings and their systems using simplified modelling and simulation techniques. The present work attempts to overcome certain inadequacies of contemporary simulation applications with respect to environmental control systems, by developing novel building control system's modelling and controllability assessment methods. These methods are then integrated within a robust dynamic simulation environment so that the controllability science can be employed in practice to improve current control strategies in the buildings industry.

The first part of this thesis reviews the current building design process and problems faced by building services in commissioning advanced building energy management systems for delivering energy efficient performance and high quality of comfort for occupants. The advantages and disadvantages of the existing techniques and various approaches to control systems modelling, simulation and appraisal within the research community are reviewed. Based on this review, the resulting problem statement is defined to conclude that research is required to develop a science comprising of a holistic modelling method of building systems, for controllability assessment and simulation of modern buildings and their control systems.

The second part of the thesis focuses on development and verification of a holistic model of a building for controllability assessment. Then the thesis expands the

methodology to assess the controllability of a building and its servicing systems, such as heating, lighting and ventilation. The knowledge for these methods has been transferred from design processes and methods used in the design of aircraft flight control systems to establish a modelling and design process for assessing the controllability of buildings. The thesis describes a holistic approach to the modelling of the nonlinear and linear dynamics of the integrated building and its systems. This model is used to analyse the controllability of the building systems using Nonlinear Dynamic Inverse (NDI) controller design methods [(Counsell J. M., 1992)] used in the aerospace and robotics industry. The Controllability is assessed in terms of four fundamental multi-input multi-output controller design properties for continuous-time tracking systems: Asymptotes, Transmission Zeros, safe control and bandwidth. The results demonstrate how the same method can assist the control systems designer in developing complex control systems for buildings.

The results of controllability analyses are verified through simulation of the building and its systems using simple controllers (e.g. PID). The controllability science is used to improve the performance of current PID controllers using inverse dynamics to aid in their application to multi-input multi-output building systems. The results show that in cases where advanced controls are desirable for high performance energy control and comfort, simple PID controls can be sufficient for satisfying the comfort criteria. The results show that this method can also aid in easier commissioning and rescheduling of PID controllers already employed in the building.

Finally, the future work required to increase the applicability and accuracy of controllability science is discussed in terms of improvements to the mathematical model of the building and systems. Practical application of the science is elaborated in terms of the required integration with other software programs to develop a tool which can aid designers (e.g. architect & building services engineers) in designing controllable buildings and for building services engineers to understand why the building is difficult to control.

1 : Controllability of buildings and the building's industry



“As you climb the ladder of success, be sure it's leaning against the right building”

H. Jackson Brown, Jr.

1.1 Comfort in Buildings

People spend most of their time indoors. The main factors affecting people's comfort, health and performance include thermal conditions, indoor air quality, acoustic conditions and lighting conditions. In particular, for thermal comfort there is no absolute standard. This is not surprising, as humans can and do live in range of climates from the tropics to high latitudes. An internationally accepted definition of thermal comfort, as given by ASHRAE is 'that condition of mind which expresses satisfaction with the thermal environment'. [(Fanger, 1973), (Darby & White, 2005)]

When we try to comprehend general thermal comfort, it is common to analyse Fanger's PMV (Predicted Mean Vote) model; this model is based on thermoregulation and heat balance of the human body. In 1967, Fanger investigated the human body's physiological processes, when it is close to neutral to define the actual comfort equation. [(Garcia)]

According to Fanger [(Fanger, 1973)], what is required in practice is that the comfort conditions are expressed in controllable factors, which Fanger has given in terms of six fundamental parameters: air temperature, radiant temperature, relative humidity, air velocity, activity and clothing.

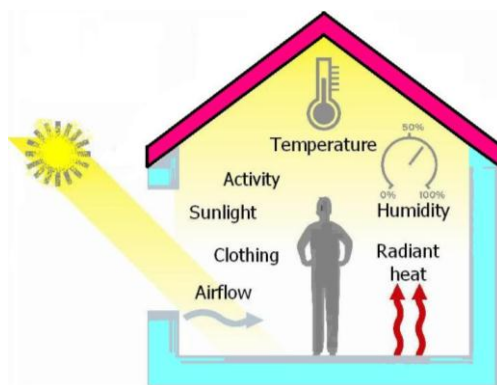


Figure 1: Schematic of the Fanger's comfort criteria

Thermal Comfort = function { air temperature, radiant temperature, relative humidity, air velocity, activity and clothing }

This comfort equation obtained by Fanger (1970) is too complicated to be solved through manual procedures [(Orosa, 2011)]. As it is difficult, certainly taking into consideration the accuracy levels of measuring instrumentation, to verify thermal conditions point by point which is why there are concerns regarding predictions of comfort temperatures by Fanger's equation [(Truong, 2010)].

The important question is how do you quantify and control thermal comfort in a building in practice?

In countries of the world where active cooling is not required most of the year and passively cooling is sufficient such as in the UK, in most buildings only heating systems are installed. From the above equation it can be concluded that strictly with a heating system, only the air temperature and radiant temperature can be directly controlled to influence the thermal comfort. Air velocity, activity levels, clothing and relative humidity are disturbances to the heating control system. These disturbance factors can be estimated so that set-points of air temperature and radiant temperature can be calculated accurately in a building for the heating system to achieve thermal comfort.

Hence for practice, controllability of air and radiant temperature are important to assess and not the Fanger or academic interpretation of thermal comfort. The building designer has to decide whether to control air temperature only or radiant temperature only or a function of the two (as given in equation 1.1 below) based on the responsiveness of the heating system and design of the building. Thus in reality when designing a building a designer is fundamentally asking the following three questions:

- 1) Control air temperature only or air temperature plus radiant temperature?**
- 2) Use a fast or a slow heating system?**
- 3) Response of the building to change in thermal conditions i.e. use high or low thermal mass?**

In practice the equivalent operative temperature is used as a defining parameter for thermal comfort [(ASHRAE, 2009), (Sourbron & Helsen, 2011), (BCO, 2009)]. The British Council for Offices (BCO, 2009) have stated this to be the combined effect of the air temperature, radiant temperature and air movement. The operative temperature as defined by ASHRAE and CIBSE is: the average of the mean radiant and ambient air temperatures. [(ASHRAE, 2009), (CIBSE, Environmental Design, Guide A, 2006) p167].

In the UK, in practice the CIBSE guidelines on comfort, given in CIBSE Guide A, are often taken as a good practice indication of thermal comfort and used for design purposes. In CIBSE Guide A, the operative temperature is defined as the environmental temperature. The environmental temperature determines rate of heat flow into a room surface by convection from the room and radiation from surrounding surfaces and other radiant sources. It is the temperature at the environmental node and traditionally taken as:

$$T_{environmental} = \frac{1}{3}T_{air} + \frac{2}{3}T_{mean\,radiant} \quad (1.1)$$

In CIBSE this operative temperature has also been referred to as the comfort temperature. Hence in this thesis where the term comfort temperature is used, it means the operative temperature (i.e. air temperature + means radiant temperature) rather than absolute comfort temperature of the occupant.

Therefore it must be noted here that there are more than one interpretation of the term comfort temperature. In the research institutions generally the term thermal comfort or comfort temperature refer to the absolute value of thermal comfort based on the research and concept of Fanger et al. As mentioned earlier this comfort temperature is difficult to predict accurately and control in practice due to errors in the measurements of the various variables such as skin temperature etc. This is the reason why in industry comfort temperature is generally referred to as given in equation 1.1.

Over the past few decades, people's expectations for indoor comfort have risen. Regardless of the outside environmental conditions people expect and demand a comfortable indoor environment [(ASHRAE, 2009)]. The quality of life in buildings (comfort conditions) is determined by mainly three factors: Thermal comfort, visual comfort, and indoor air quality. In recent times special emphasis has been given to the architecture of complex Climate Adaptive Building (CAB) that is geared towards better control of comfort and energy savings [(Wang, 2010)]. Climate Adaptive Buildings can have intelligent building management systems; active solar shading, under-floor heating and cooling, passive stack ventilation, which are just a few of the new technologies that are now being employed to keep occupants comfortable with minimum energy costs.

1.2 Comfort in the case of Climate Adaptive Building

'Climate Adaptive' means that the building's facade and systems can respond to different climatic conditions, to weather-related changes and to shifting day/night conditions. Thus by definition it can be understood that a Climate Adaptive Building can be active or passive. Even with the energy crisis, buildings in the extremely hot climates such the Middle East, employ active techniques for controlling comfort in the design of CAB type buildings. However it is agreed upon that one of the fundamental principals is to design buildings 'low tech', where passive strategies are employed before active ones. In this thesis controllability of both types is analysed as this research is for application in all cases.

Hence it is also important to understand what does the control of comfort temperature mean in a Climate Adaptive Building which is either passive or active. Recent Standards [(EN15251)] and guidance [(CIBSE, Environmental Design, Guide A, 2006), (ASHRAE-Standard-55-2004)] advice that comfort temperatures vary through the year as people adapt to changes in outside temperatures. As comfort temperatures vary, so heating and cooling set-points should be adjusted in harmony to main optimum comfort. Maintaining accurate control of set-point is easier in air conditioned or actively cooled "close control" buildings and thus smaller bands of

minimum and maximum comfort temperature are considered appropriate. However a greater margin of error is acceptable in free running or passively cooled buildings. Thus it is very important how controllability is assessed as the type of control in passive and actively cooled CAB type buildings is different. Hence, the thermal comfort standards use the Fanger's model to recommend acceptable thermal comfort conditions or comfort bands. For example, the recommendations made by ASHRAE 2004, ISO 7730:2005 and ISO 7726:2002 are seen in Table 1. These thermal conditions should ensure that at least 90% of occupants feel thermally satisfied [(Garcia)].

	Operative	Acceptable
Winter	22 °C	20-23 °C
Summer	24.5 °C	23-26 °C

Table 1 ASHRAE standard recommendations

For bands within which comfortable conditions lie, CIBSE has stated the upper and lower margins for operation of the comfort temperature in both free running and controlled environments [(CIBSE, Environmental Design, Guide A, 2006)].

	Acceptable
Winter	21-23 °C
Summer	22-24 °C

Table 2: Comfort Criteria for CIBSE Guide A

In the British Council for offices (BCO) Guide to specification of offices [(BCO, 2009)], recommended standards for offices are: air temperature of 24°C for summer design and 20 °C minimum for winter design. The range of temperatures achieved in the space will depends on the selected control band which can vary for different system types. BCO suggests a typical control band and operational tolerance of ± 2 °C. This specification is for air temperature control for providing good comfort [(BCO, 2009)]. For mixed mode and naturally ventilated offices (i.e. free running buildings), BCO (2009) has stated that the internal temperature should not exceed 25 °C for more than 5% of the occupied hours and 28 °C for no more than 1%.

Hence in buildings where there is active cooling then a single set-point can be used for temperature control where as in passively cooled buildings an upper and a lower band of acceptable temperature is defined. This insures that building is allowed to cool down within acceptable limits. **In this thesis controllability at a specific set-point as well as in terms of upper and lower bands has been assessed for a Climate Adaptive Building for both active and passive strategies. Therefore the science is applicable to systems with: 1) heating and cooling, 2) heating only and 3) cooling only.**

1.3 Control of Comfort

Much of the energy use of buildings, such as all of the energy used for heating, ventilating, and air conditioning, is for effectively controlling the indoor environmental conditions. These very buildings are also one of the largest consumers of energy and the built environment accounts for an estimated 40% of total UK energy consumption while arguably more than 50% of all UK carbon emissions can be attributed to energy use in buildings [(Clarke & Johnstone, 2008)]. The amount of wasted energy in buildings due to poor control, resulting in unnecessary heating, fabric and ventilation losses and unneeded lighting can be enormous. The construction sector covers one eighth of the total economic activity in the European Union (EU), employing more than eight million people. The intense activity in building construction, in conjunction with the need for energy savings and environmental protection policy, dictate for more reasonable design practices for buildings and their control systems. For this reason, one of the main goals of control systems [(Dounis & Caraiscos, 2009)], as applied to buildings, is to minimize energy consumption and provide a comfortable working environment.

Today buildings combine the latest technology, and have the ability to actively adapt to the environmental conditions in order to obtain the optimum solution. They can change their properties, their parameters, based on external conditions to best provide acceptable thermal comfort levels [(Wigginton & Harris, 2002)]. This might mean reducing the level of sunlight entering the building, perhaps by external shading or

by using glass with variable transparency properties, or increasing the ventilation rate by adjusting the envelope or introducing mechanical ventilation. One of the key factors when considering MIMO building systems is that these systems are systemic and dynamic in nature [(Clarke J. A., 2001)] and changing one parameter often has unforeseen consequences.

Unfortunately, whilst the flexibility and adaptability of these buildings and their plant systems to respond to changes in occupancy and outside climate conditions is theoretically superior to more conventional buildings of the 1990's; they are in many cases failing to deliver improved comfort and significant energy savings [(Brown, 2009)]. Consider, as an example, attempting to reduce the incident solar radiation into a zone, perhaps with the objective of reducing solar heat gains. The subsequent decrease in natural light may require artificial light to compensate, or attempting to reduce internal CO₂ concentration levels by ventilation would in turn decrease or increase internal heat gains and affecting the heating system. The extensive cross coupling between parameters and the differing time constants involved leads to difficulties in controlling the system [(Clarke J. A., 2001)]. As insulation and air tightness levels have improved in modern constructions, the room heat balance has become delicate and dynamic [(CIBSE, 1998), (BRE-SAP, 2005) Table S7, (EST, 2004)].

This delicate and sensitive nature of these buildings is such that poor control of the environment may lead to buildings becoming 'sick' [(Singh & Yu, 2010)]. Sick Building Syndrome (SBS) is an umbrella term which is used to loosely describe buildings which are unpleasant for, or in the extreme can pose a health hazard to occupants [(McMullan, 2007), (Hanie & Aryan, 2010)]. In part, this refers to unsuitable heating levels, cold draughts, excessive glare or poor ventilation, which can often be attributed to poor design and control [(Hanie & Aryan, 2010), (Health & safety Executive, 1995)]. This is perhaps an indication that the current knowledge and tools used by those in the building design and construction industry are not able to provide a clear explanation for the reasons behind uncontrollable occupant comfort even with latest technologies installed in latest buildings.

1.4 Problem Statement

1.4.1 Building Design Process, Regulations and Designers

Buildings are inevitably subject to a very wide range of influences and must be designed to give a satisfactory performance over the whole range of variation of the many phenomena concerned and at the same time, to establish a balance between the often-conflicting demands of these phenomena. As mentioned in [(Ralegaonkar & Gupta, 2010)], the very difficult problem of architectural design which this situation poses is made yet more complex. The other functional and economic requirements which the building must meet will very often lead to design solutions that are different to those which would best meet the energy needs and a trade off has to be made in the final solution. Therefore, interest in low energy building design continues to increase demand for architectural design tools, which can assist building designers in evaluating building designs [(Crawley & Hand, 2008)]. For example in the UK industry, the full dynamic simulation tools include IES, Energy Plus, Trnsys, ESP-r & Modelica and compliance tools such as SBEM & SAP are also commonly used.

In the industry, current tools which are available to the architects and design engineers range from simple hand calculations through to advanced integrated simulation packages. These are briefly outlined below. The simplest of these are design guidelines or rules of thumb, which are usually based on past experience and often applied without understanding of the underlying issues. They offer a quick check, which can prove useful at the early design stage [(Guthrie, 2003)].

Following these are simple hand calculations, such as calculations of heat loss and gain. These are almost exclusively based on the assumption of steady state conditions and are often one-dimensional and the compliance (Energy Performance Certificate) EPC production tool used in the UK is SAP & SBEM. SAP is the government's standard assessment procedure for energy rating of dwellings [(BRE-SAP, 2005)] and SBEM [(BRE-NCM)] is for buildings. These tools can provide an acceptable

approximation of performance and are still widely used across the buildings industry [(CIBSE, Environmental Design, Guide A, 2006)]. Computational time is minimum, whether the calculations are performed by hand or using a computer as an aid and are also transparent i.e. calculations are visible. However these methods have limited accuracy when the effect of variation in parameters i.e. dynamics need to be known during detailed design stages or when designing buildings [(CIBSE, Building Energy and Environmental Modelling, 1998)]. Furthermore, simplified modelling methods have also been developed for building-plant simulations e.g. Modelica, ISO 13790, however these programs [(Sodja & Zupancic, 2009)] and methods [(Corrado & Mechri, 2007)] are for evaluating energy consumption rather than assessing the controllability of building and its systems [(Robinson, 1996)].

In the industry, computer programs for building design and simulation have developed to become very sophisticated and precise, but in the process the user of the tools have a very steep learning curve and require large amounts of data and time to produce useful results [(Crawley & Hand, 2008)]. Dynamic building simulation packages such as Energy Plus [(Energy, 2010)] and ESP-r [(ESRU, 2010)], require a detailed description of the building and its system that is often unavailable at early design stage [(Xia & Zhu, 2008)]. While all these methods remain valuable tools for the designer at different stages of a building's life cycle, they all simply provide results, and do not quantify the internal workings of a system. An extensive simulation experience must be used in a lengthy iterative manner to gain a modicum of understanding of the relationships between parameters. Also, these programs and methods are for proof of design and evaluating energy consumption rather than assessing the scientific controllability of the building and its systems [(Robinson, 1996)].

It is important that in designing buildings the environmental control systems design must be considered in relation to their suitability to the building envelope design and external conditions. In any particular design the parameters which significantly contribute to control systems becoming unstable inside the building are to be assessed in terms of their compatibility with the building design. These

considerations at the moment are not taken into account by the current tools or the building design process.

The conceptual phase of any design project is potentially the most vibrant, dynamic and creative stage of the overall design process. In reality the design process is very complicated [(Tunstall, 2006)]. However a simplified viewpoint with fundamental processes where this project adds to the design process is illustrated as follows:

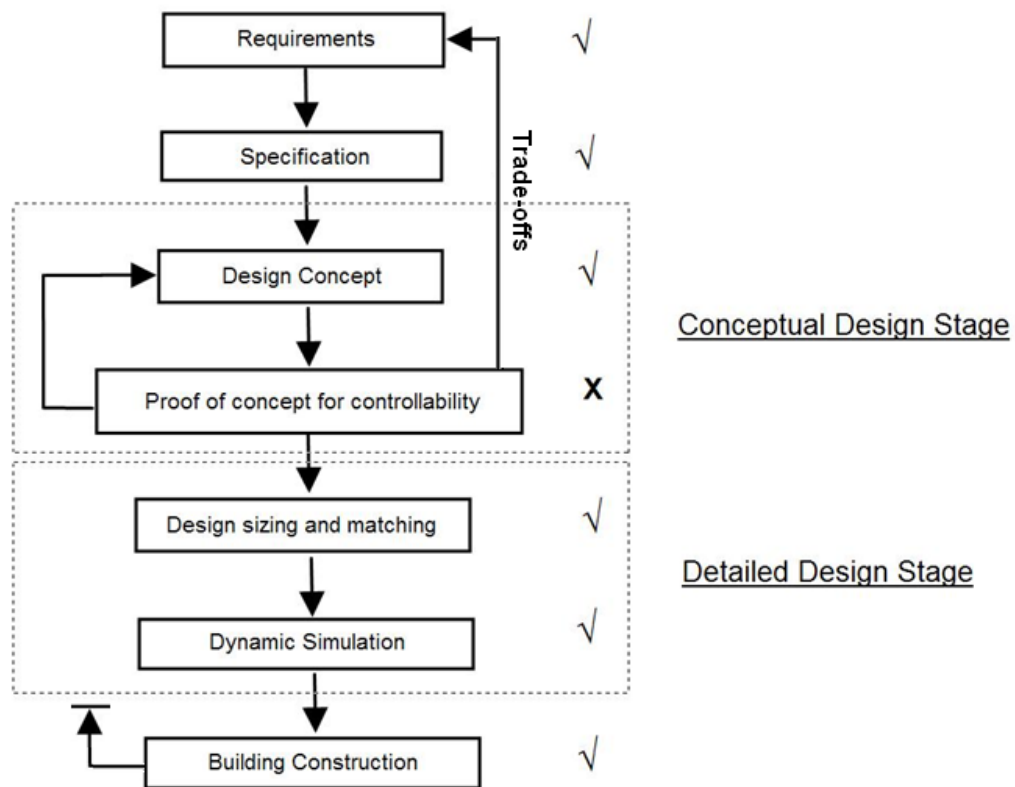


Figure 2 Current building design process (√= included x = not included) [see (French, 1985) for conceptual and detailed design stages]

Controllability assessment of the building and its systems at conceptual stage is important because it will solve the current problems of control which arise later in the detailed design phase or at post construction stage where the building services engineer is brought to control the building components. However, currently the

industry doesn't have the science or the tools to carry out such assessments. Current compliance tools in the industry are SAP for dwellings and SBEM for buildings. These tools do not take account of the dynamics of the plant and instead assume Ideal control i.e. the exact plant setting needed based on heat transfers and basic plant information [(BRE-SAP, 2005), (BRE-NCM)]. Generally the building and systems are approved based on compliance with the building regulations which take no account of their dynamics and control. This leaves a difficult design task for building services engineer to control an uncontrollable building.

There are many additional driving forces which affect the architectural community and the building industry. As the scientific evidence surrounding climate change has mounted, political will has manifested itself in an outpouring of 'green' and 'sustainable' policies. Perhaps the most important when considering the built environment are the Building Regulations. The Building Regulations are produced with the aim of ensuring the health and safety of people in and around all types of buildings and to provide for energy conservation [(Minister, 2005)]. At the time of writing, all new build and refurbishments must comply with the Part L regulations (Part J for Scotland), which require a building to conform to a minimum environmental standard [(BRE, 2006)]. Compliance is measured based on the energy transfer through the fabric, ventilation and responsivity of the heating systems. Lower overall energy use gives a better energy rating. The building regulations include a number of ways to prove compliance with the energy performance requirements such as, the elemental method, the whole building method or the carbon assessment method. However, low energy rated building in compliance with the requirements doesn't guarantee controllability of the building environment with its systems once it is commissioned. Thus, understanding the relationship between the properties of building envelope such (i.e. thermal capacities, heat transfer coefficients and densities) and control systems (i.e. controllers and actuators etc) is very important for designers to design high performance buildings for which they can be confident will comply with building regulations and be robust in performance when faced with design uncertainties.

1.4.2 New Technologies, Building Automation systems and Building Services Engineers

The level of automated control in modern buildings has risen steadily over the years [(Wang, 2010)]. This is not only due to the increasing demand for more control of comfort and convenience, but also the benefits building automation brings with regard to saving and managing energy [(Merz, Hansemann, & Hubner, 2009)]. Building automation systems are used to operate a diverse array of energy-using and producing equipment in buildings. These systems are increasing in prevalence and becoming more technologically sophisticated. Some of these technologies are in their infancy, others are centuries old. This list might include;

- Photovoltaic (PV) cells or solar hot water collectors
- Passive stack ventilation
- Chilled beams and Under-floor heating
- Sun-shading /louvers
- More recently, advanced property changing glass
- Wind turbines
- Natural light shelves and automatic lighting
- Phase change material walls

These technologies, coupled with strategies such as minimizing demand, improving efficiency, recovering heat and cold, and matching demand and supply can be used to achieve a marked reduction in energy consumption in the built environment [(Smith, 2007)]. It has been shown that better use of daylight, natural ventilation or passive heating and cooling strategies can, if well designed, provide indoor environmental conditions that occupants find more pleasant than in some air conditioned buildings [(CIBSE, Building Energy and Environmental Modelling, 1998)]. However, without proper implementation and control of these solutions will achieve very little, and given their relatively high capital costs will continue to be overlooked [(Smith, 2007)]. Although the energy efficiency of individual pieces of equipment may be improving, the overall efficiency of buildings often falls short of the potential. Poor coordination i.e. unsafe control of equipment operation and the development of faults are common causes of sub-optimal performance and poor comfort [(Salsbury, 2005)].

It is easy to perceive that the building services control industry is a low-tech field with mostly relay type controllers for room temperature regulation e.g. thermostats. The conventional image of a thermostat on a wall turning a heater on if it gets too cold and off again if it gets too hot is therefore still mostly pervasive. Although these kinds of controllers remain common, they represent only one part of an ever-broadening spectrum of technology that is being applied to buildings. The application of technology is also highly stratified with the residential sector usually having the simplest and least costly controls and the higher-end laboratory or clean-room type environments having the most advanced systems [(UK Government, 2006)].

As mentioned in [(Robins, 2007)]; commissioning of these controllers is probably the most important physical aspect of a building project. Unfortunately, it is rarely given the priority and attention that it deserves and without its proper implementation the host building will never perform to anyone's satisfaction. Ironically, since commissioning is also the last activity in any programme of works, it is also the least likely to have its full implementation time. As contracts proceed and delays occur, the actual time for commissioning becomes condensed to fit the time available within the overall contract programme. Inevitably the commissioning remains incomplete at handover and causes poor post-occupancy satisfaction and high energy usage. The commissioning phase can sometimes be perceived as a hindrance to achieving the main aims of a building project completion on time and on budget.

Furthermore, as explained by [(Salsbury, 2005)], in such circumstances, the mixture of control logic and systems that are found in today's buildings, the single input-single-output (SISO) feedback loop represents a basic element that is consistent in its form across applications. These loops, which frequently use PID (Proportional, Integral and Derivative) control, often act as the final interface between the control logic and the energy-using equipment. A problem with using PID control in buildings is that most systems are time-variant and are inherently non-linear. Control performance then varies as conditions change and loops may become sluggish or oscillatory at certain times. Gain scheduling is sometimes used to overcome non-

linearity, but this is rare because of the time required to determine an appropriate schedule. This has been solved through auto-tuning techniques [(Lui & Cai, 2009)], however these are limited to HVAC systems that are single input single output rather than multivariable.

A constant problem for building services engineers is that when different engineers work on the same project there is a tendency to alter the software because one engineer thinks their way is better. Incorrect selection of control strategies and a lack of commissioning are often found to be the major reason for poor building energy performance. This can become a very difficult situation to manage, and the costs that follow are often overlooked when the systems are being selected in the initial design [(Robins, 2007)]. Poor design and selection of control strategies is often due to lack of knowledge of the building physics, the dynamics of the whole system including the plant systems and control systems. Thus, understanding the dynamic interactions between building and new plant systems along with assessing the feasibility of basic (e.g. PID) or high performance controls in the light of underlying building physics and control theory has become even more relevant for building services engineers.

1.4.3 Modelling & Simulation Community and Control Engineers

The ultimate goal of control systems is to provide flexibility and a high degree of autonomy; effective systems control requires that the underlying system be understood and modelled (Richard C. Dorf, 2008). On one hand the academic community has utilised modelling and simulation to emulate reality to some degree and to extract conclusions which can be used to improve design [(CIBSE, Building Energy and Environmental Modelling, 1998)]. For maximum accuracy, there are integrated simulation packages [(Clarke J. A., 2001)], such as ESP-r [(ESRU, 2010), IES [(Crawley & Hand, 2008)] and Energy plus [(Energy, 2010)]. These methods attempt to emulate reality, by discretising a system and solving the describing equations numerically. The vast number of nodes required to obtain an accurate picture means that using computer processing is the only practicable way of achieving this. Where possible these tools do not rely on simplifying assumptions [

(Clarke J. A., 2001)]. This implies that accurate results will be obtained if the data input is of good quality. As a consequence of this a great deal of information (geometry, materials, climate boundary conditions etc) must be input before meaningful results can be extracted. The input and processing required in obtaining accurate results means that this method of modelling can be time consuming. The modelling and simulation is normally done at the detailed design stage where control strategies are also tested. However, because there is no assessment of controllability in the earlier design stages, there is no guarantee that at the detailed design stage the building and its systems will work in harmony under a particular control strategy offered by the control engineers or selected by the modeller. One further drawback is that although high fidelity results are achieved, the detailed simulation of building, systems and controllers makes it difficult to identify the factors affecting controllability. This is due to the large amount of parameters and underlying connections that are not visibly quantified.

Today's buildings are delicate and dynamic therefore require that the control of these buildings be suitable. Traditionally, indoor environmental control worked on a closed loop, with the occupant(s) acting as both sensor and actuator (i.e. feeling cold and increasing the heating). As technology improved this was automated to a simple closed loop control strategy and developed into to what we now know as modern Building Energy Management Systems (BEMS) [(Grimm & Mahlkecht, 2011), (Levermore, 2000)]. As discussed above, many of these systems currently in use do not provide acceptable comfort at all times [(McMullan, 2007)]. This may be attributed to current control systems not taking account of the real nature of these buildings; that they are systemic, dynamic, and often non-linear.

The control engineers have also been active in proposing replacements for PID in buildings. New controllers have been proposed based on fuzzy logic [(Tan & Dexter, 2000), (Jian & Wenjian, 2000)], neural networks [(Ahmed, Mitchell, & Klein, 1996)], and plant models [(S.Virk & Loveday, 1994)]. However, the research has concentrated on controller design rather than assessing controllability of the whole system in the light of nonlinear building physics, plant dynamics and control

theory. At the same time, as mentioned by [(Salsbury, 2005)] the industry has been slow to adopt replacements for PID for a number of reasons. Firstly, robustness can be difficult to guarantee, especially for the non-linear methods, when subjected to the kind of anomalous phenomena that can occur in building systems [(A.L.Dexter, Geng, & Haves, 1990)]. Also, any increases in set-up time due to the methods requiring specification of additional parameters will normally make them impractical. Furthermore, some methods turn out to be too computationally demanding for the type of low-cost hardware used in buildings. Lastly, the building industry is generally reluctant to adopt something that may have to be treated like a black box after only recently developing an understanding of PID control.

The control engineers developed control theory for designing feedback controllers that remove uncertainty to poor prediction where as modelling and simulation was developed to improve prediction; however both are important to designing buildings. Thus having knowledge and understanding of controllability of the building and its systems at very early stages of building design will help both disciplines to contribute and work together more effectively in designing controllable high performance buildings.

1.4.4 Conclusions

The evolution of design, operation and maintenance of buildings has changed significantly in the last few decades as energy savings, comfort and controllability become more important to both building designers and building occupants. As a result new innovations in the field are constantly under investigation. Many of the changes that can be made to existing buildings, building designs and operational practices to improve controllability will modify aspects of indoor environmental quality with potential impacts, on comfort, health, and performance. Consequently, controllability of building plant & control systems and indoor environmental quality must be addressed in a holistic and coordinated manner. Any tools and knowledge which can facilitate these improvements will be very important to industry.

The building regulations are at present the only standard that requires compliance used for quantifying the environmental performance of buildings in the U.K. As clients, architects and building engineers become more concerned about improved control of comfort of the internal environment, methods such as presented in this thesis will help designers and building regulations to be flexible enough to allow for innovative design and systems solutions for the industry. As the complexity of modern built environment has increased, the efficient control, economic and safe operation of mechanical services has become a more complex issue. Assisting building services engineers to understand the underlying physics and interaction between building and its plant systems in a holistic manner at the conceptual design stage will help to prevent problems of control and improve the performance of Building Automated Systems in modern buildings.

In consideration of what overall has been said in the problem statement it is obvious that there is a need to adopt a holistic approach to assessing controllability of building, plant and controls. There is a need to integrate the architects, building services engineers, control engineers, modelling and simulation community for designing high performance controllable buildings. However in the author's opinion buildings industry is still not mature enough to adopt the ideas of control engineering where a multivariable controller is still thought to be several PID's put together. An engineering science which can give insight into controllability of building and systems that the building industry can understand and use effectively will lead to better design of buildings by addressing problems at their root and not just treating their symptoms.

1.5 Research Objectives

It was against the background outlined in the previous sections that the present research project commenced in 2007. The following visions of the future of building industry were observed:

- The complexity of the built environment (i.e. buildings and dwellings) will continue to increase and therefore will require safe and efficient simultaneous control of their various systems.
- The building industry has still many years before it shifts to high performance controls from the traditional PID.

Consequently, this research work has encompassed the following specific objectives:

- To develop engineering science for assessment of controllability of complex Buildings and their systems at the conceptual design stage of the building design process.
- To assist in improving the performance of current controls in building industry.

1.6 Thesis Overview and main contributions

Chapter 2 of this thesis describes the development of a symbolic nonlinear mathematical building model for controllability assessment, describing heat, light, CO₂ and humidity transfer in a single zone. Chapter 3 describes the Ideal system Response Theory behind the controllability science. Chapter 4 presents this controllability science. Chapter 5 and 6 present case studies in theory and practice. And Chapter 7 contains the conclusions drawn from the present project, the industrial impact of this work and indicates the possible directions for further work.

The contributions of this research work are:

- Controllability assessment science for modern buildings and their systems.
- Cause and affect mathematical model of a single zone in a building for controllability assessment.
- Extension of RIDE control theory to a new class of MIMO systems where there is at least one direct transmission zero from an input variable to an output variable.
- Methodology to assist in improving current controls in industry i.e. PID.
- Best practice controllability guide for designers on heavy and light weight buildings.
- Best practice guide for designers on controllability of fast and slow actuator systems.
- An Ideal System Response (ISR) control guide for academic community researching in building controls.

The energy crisis of the 1970s acted as a stimulant to research in the area of building energy efficiency with activity significantly boosted during this time. Realization of the fact that buildings can account for up to a third of the total energy used in [(Toepfer, 2007), (Friedman, 2009), (Brugmann, 2009)] developed countries heralded increases in government funding for buildings research in an attempt to reduce national energy demands. Market forces also triggered greater industrial research and development into energy efficiency products and services. The main focus of these initial research efforts was on improving the efficiency of building envelopes and the energy-using equipment within them, such as chillers, boilers, heat exchangers, pumps, etc [(Salsbury, 2006)]. For this reason until now the UK government's compliance tools such as SAP and SBEM were created to focus on energy consumption and plant performance parameters rather than the actual dynamics of the whole system.

Control problems in the buildings industry are not trivial. However, the consequences of failure of plant through bad control are rarely catastrophic. The industry has been able to treat many problems through regular maintenance and commissioning schedules. This has sometimes led to surprisingly good results, but frequently fails to satisfy all the essential occupants and owner's comfort, energy use, operating cost and capital cost requirements. The research community has been active in proposing new controller algorithms for buildings [(Dounis & Caraiscos, 2009), (Salsbury, 2005)]. However, the building industry has been generally reluctant to adopt them due to difficulty in practical implementations and uncertainty in guaranteeing performance.

One aspect that has not attracted as much attention is the interaction between the building envelope, individual pieces of equipment and weather as a holistic control system. Implementing operational strategies that take account of these interactions may, in many cases, impact the overall controllability and thus energy use more than the efficiency of individual devices. Past research in building design has concentrated on controller design rather than controllability. Controllability is a property of the total system and hence depends on how the building has been

designed, what systems are used and what conditions in the building are to be controlled using feedback sensors, e.g. temperature, light intensity and CO₂ levels.

Mathematical models describing the building-plant system dynamics are becoming useful tools in the process of building design and designing appropriate control strategies [(Nakanishi et al, 1973), (Macqueen, 1997) (Gouda, Underwood, & Danaher, 2003), (Daskalov & Arvenitis, 2006)]. In order to design better control systems, a comprehensive yet simple cause and affect dynamic model of a building space representing heat, light and CO₂ transfer is presented. The nonlinear symbolic model enjoys flexibility, transparency and computational efficiency essential for the specialist case of investigating controllability of a MIMO building and its systems. The nonlinear model is simulated in ESL (European Simulation Language) and to verify the dynamics of the model, comparisons were made between simulations results of ESL and actual measured data for a case-study (see model validation section). Simulations for various cases relating to thermal transient response, internal thermal mass (furniture), and contaminants (CO₂) transfer have been performed. The results show that the model can accurately represent the important dynamics of the system and can be used for basic simulation and symbolic controllability analysis by designers for design and validation of advanced control systems in the conceptual design phase of the building design process.

2.1 Literature Review

The drive towards advanced buildings has seen an increase in utilising many different systems simultaneously, such as solar blinds, perimeter wall heating, electric storage systems, warm air systems, mechanical ventilation, chilled beams, under floor heating and renewable offerings. This has presented control systems designers the challenge to design advanced building management systems to successfully control them all simultaneously [(Dounis & Caraiscos, 2009), (Salsbury, 2005)]. In reality, building services engineers face huge problems in commissioning these complex building management systems to work reliably all year round [(Salsbury, 2005), (Salsbury, 2006)]. Often control systems of lighting,

heating and ventilation become unstable as one system fights against another resulting in poor comfort and high energy consumption [(Salsbury, 2006), (Erbe, 2006)]. Controllability assessment at the conceptual design stage [(Counsell & Porter, 1999)] will help to prevent current problems of poor control which arise later in the detailed design phase or at post construction stage. The cost of removing poor control performance in the later stages of design is normally excessive and must be avoided if possible [(Xia & Zhu, 2008) (French, 1985) (Bownass, 2001)].

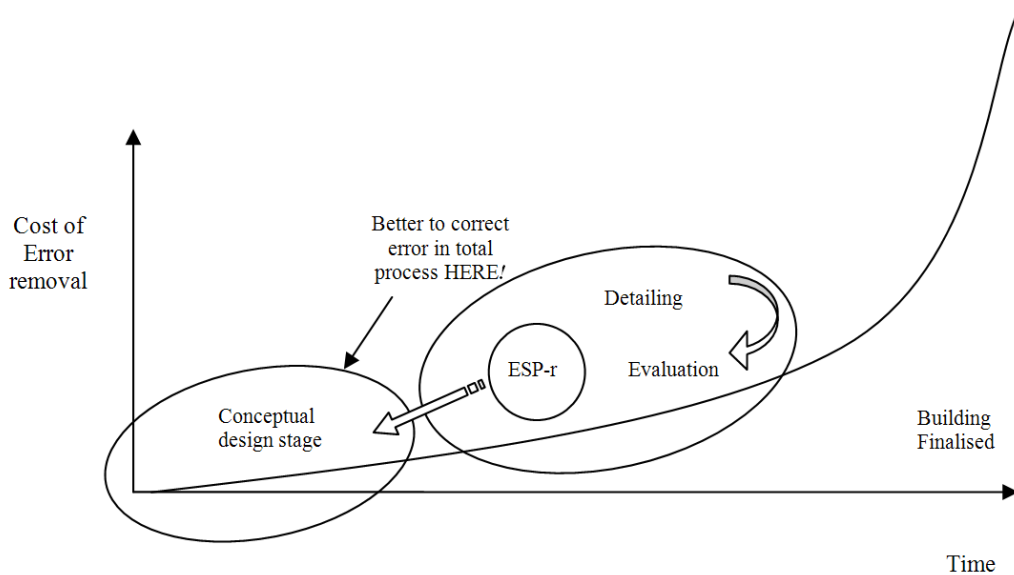


Figure 3 Graph of cost of error removal over time in design process

As shown in this thesis, this can be achieved through the use of simple nonlinear and linear dynamics models for addressing the fundamental scientific issues of controllability of the building and its systems at the conceptual design stage.

It is acknowledged that complex heating, ventilating and air conditioning systems in today's buildings present one of the most challenging situations to deal with from the point of view of control. Swings in day-to-day, week-to-week and season-to-season energy demand together with the infinitely complex combination of user needs at the human interface contribute to a highly non-stationary 'environment' within which control takes place.

The literature on modelling and control theory for systems analysis and design can only be described as vast, having attracted the attention of many researchers from various disciplines. Since the evolution of modern control theory techniques i.e. differential equations and state-space controller design techniques [(Davidson & Goldenberg, 1975), (Richard C. Dorf, 2008)] they have been applied extensively in the field of aerospace [(Counsell J. M., 1992)]. The aims of these techniques are to provide a control system design analysis and solution which guarantees closed-loop stability and tight non-interacting control simultaneously for MIMO systems. The foundation of these specific controllability techniques [(Counsell J. M., 1992)] that allow for assessment of controllability of a system to be assessed requires a mathematical model of the system which represents the major causes and effects of the system.

2.1.1 Modelling Method(s)

Mathematical modelling has been used for decades to help building scientists design, construct and operate buildings [(Xiaoshu, Derek, & Martti, 2009)]. Dynamic modelling of the actual processes involved is required for a thorough understanding of dynamics of building spaces and control systems. Holmes has defined the dynamic thermal model as ‘a method to predict the magnitude, duration and time of occurrence of an event’ [(Holmes, 1980)]. There are mainly three families of approaches to building, managing and solving models for buildings. As mentioned by [(Kampf & Robinson, 2007)], these modelling methods for buildings can be broadly classified as follows:

1. Explicit solution of the heat diffusion equation, by finite difference (e.g. [(Clarke J. A., 2001)]) or response function (e.g. [(Gough, 1982)]) methods.
2. Model reduction techniques, such as the grey box method [(Deque, Ollivier, & Poblador, 2000)].
3. Model simplification techniques, such as the resistance capacitance (RC) network (e.g. [(Lefebvre, Bransier, & Neveu, 1987)]) and admittance [(Milbank & Lynn, 1974)] methods.

The traditional approach to modelling involves computer simulation programs that have been developed for analysis of building processes such as DOE-2 [(Berkerley, 1993)], ESP-r [(ESRU, 2010)], TRNSYS [(SEL, 2000)] and IES [(Crawley & Hand, 2008)]. Presently, the most complex models are mainly used in research institutions since they require substantial time and expertise to use. ESP-r is an example of such a tool. Essentially, this approach extends the concept of the heat balance methodology to all relevant building and plant components. This modelling method attempts to emulate reality by finite-volume (or finite-difference) discretisation approach to the conservation of energy to represent the opaque and transparent fabric, internal air spaces and plant components and then solving the describing equations numerically. The vast number of nodes required to obtain an accurate picture means that using computer processing is the only practicable way of achieving this. The industry currently uses dynamic modelling and simulation in the design process to test the detail design of the building where the cost of error removed can be significantly high. At this stage traditional control algorithms (i.e. PID) are also applied. If the building proves not to be controllable, then it is very difficult to identify the factors affecting the controllability as there are too many effects and parameters to be identified.

While such complex models have found widespread acceptance as tools for energy analysis or thermal design of large commercial buildings, there are other methods that are more widely used for analysis and design of dynamics and control of building systems, such as Modelica [(Wetter, 2009), SPARK (Berkeley, 2003)]. These are equation based methods where all the relationships that govern a thermal building simulation problem are written down as equations (partial differential equations are first discretised in space,) one arrives at a so called hybrid model i.e. a mixture of ordinary differential and algebraic equations. The resulting system of equations will contain many different time-scales and have several nonlinear equations. These mathematical models do not always replicate reality, mainly because they are based on various assumptions and approximations. They are regarded as valid over some specific set of conditions [(Irving, 1988)].

After conducting consultation and research in industry [Building Research Establishment (BRE), Archial Group, BRE Centre] it is found that there is a need for mathematical models that designers can use in the early phases of the design process for testing their designs for controllability. This type of model should require minimum data input, give reliable indication of trends and sensitivities, and be user friendly. With little effort the designer can then evaluate the controllability of a number of different solutions or schemes [(Counsell & Porter, 1999)], make comparisons of these different systems and generate positive inputs to his/her design process. There is also a need for symbolic models which can be used for evaluation of the factors affecting controller design for designing and commissioning of control systems in building services. For this case, a simple dynamic model is needed to study the controllability of the overall building-plant system, i.e. analytical sensitivity analysis.

In the category of simple dynamic models are simplified lumped capacitance models of building envelopes with HVAC plant and control that have been developed by as a test bed for analyzing control strategies [(Macqueen, 1997), (Tashtoush & Molhim, 2005), (Gouda, Underwood, & Danaher, 2003), (Underwood, 2000) & (Arguello & Reyes, 1999)]. Others have also developed these models for thermal performance assessments using model reduction methods [(Gouda & Danaher, 2002), (Barrio & Lefebvre, 2000)]. Early developments have been due to [(Lorenz & Masy, 1982)] and [(Tindale, 1993)]. However, these low order model developments have been found to break down in certain instances, in particular when modeling heat transfer through high thermal capacity elements. For this, Gouda et al. proposed a new procedure for the element modeling of room spaces based on lumped capacities through the use of constrained optimization using second order description that resulted in a better estimate of the internal surface temperatures of the external walls. However as explained later this is only useful in estimating the correct energy consumption and not essential for controllability analysis. Whilst these models have good computational efficiency and provide accurate description of the transient dynamics, these models have not been used to assess controllability of buildings as in the case of aerospace industry [(Bradshaw & Counsell, 1992)]. In aerospace these

modeling methods have been used successfully for symbolic controllability analysis as well as nonlinear simulation of the system dynamics. Today's advanced buildings are multi-input and multi-output systems and holistic simplified models representing many different processes of the building together, such as natural ventilation, heat, moisture, CO₂, internal thermal mass, lux transfers and their plant systems are required for assessment of their controllability.

As mentioned by [(Macqueen, 1997)], the contention against this method is that the accuracy of building control system modelling in the transient domain can only be increased and optimised if all relevant aspects, features and characteristics of real systems are taken into account during the modelling process. This premise requires tools that adopt a fully integrated approach, which considers all energy flow paths and the interaction of control systems with fabric, flow, plant and power systems. However, control methods based on simple dynamic models are commonly used in the design of large, complex systems [(Magni & Bennani, 1997)]. For many years this method has been a widely used design tool in the robotics [(Roskilly, 1990)], aerospace [(Bradshaw & Counsell, 1992), (AlSwaiem, 2004)] and process control [(Skogestad, 1996), (Laknera & Hangos, 2005), (Lee & Kim, 1999)] industries for assessing controllability and designing advanced control systems. In these methods, a mathematical model of the system is constructed, utilizing, for example, first principles analysis and experimental data, which is then used for subsequent control system design and analysis.

In order to apply this concept of controllability in building design, a simplified lumped capacitance mathematical model is required with enough detail to know which factors are affecting the controllability. After conducting the survey of literature and industry the conclusion is that the building industry also requires a method for assessing the controllability of buildings which may require advanced controllers using nonlinear control and MIMO control systems (Note: The requirement for advanced controllers is in the case where simple PID controllers are unable to control the building). The controllability stage in the building design as

given in the figure earlier can be described as a three step process, modeling, controller design and simulation. The 3 Step process can be described as follows:

- 1) Simple Building Model: A simplified [(Counsell & Porter, 1999), (Magni & Bennani, 1997)] dynamic model that provides answers to fundamental questions of controllability and also accurately predicts the dynamic and cross-coupling behaviour of the total energy system.
- 2) Symbolic analysis for controller design: A scientific method originally developed in the aerospace industry is utilised consisting of linear state-space models to investigate the potential for the system to be stabilised when using near Ideal MIMO controller designs [(Bradshaw & Counsell, 1992), (Counsell J. M., 1992), (Muir & Bradshaw, 1996)]. It also utilises nonlinear models to investigate the ability of the system to track at all times a desired set point for all the buildings properties to be controlled.
- 3) Simulation: The results of the symbolic analysis are validated using the model from step 1 at the conceptual design stages. These results can be later verified at the detailed design stage of the design process with a full dynamic simulation model e.g. ESP-r.

2.2 Building Model

As mentioned above the purpose of this model is for symbolic analysis and simulation verification of controllability at the conceptual design stage where as detailed simulation models (e.g. ESP-r) are used at detailed design stage for detail simulation of all building and systems. The model is specifically developed to test the controllability of a nonlinear multivariable system. The assumptions inherent in constructing this model are numerous. However, the purpose of the model is not to emulate future reality and base design decisions around it, as advanced integrated software packages, such as ESP-r [(ESRU, 2010)] already exist. The dynamic model describes the energy and mass balance of air in the building zone having heating, ventilation and lighting.

2.2.1 History and evolution

The requirement for this model was that it should be used for both symbolic analysis and numerical simulation. Thus, here it is useful to mention a short history of the evolution of this model. The modelling part of the research involved five aspects, 1) number of zones, 2) multilayer or single layer representations of thermal mass, 3) Modes of heat transfer and other building physics, 4) disturbances and 5) plant models.

Controllability analysis requires the system to be modelled by differential equations which are then represented in the generic state space form to be used in the symbolic control theory analysis. Initially in this project a multi-zone case study school building was chosen. It had five zones and a schematic is represented as follows:

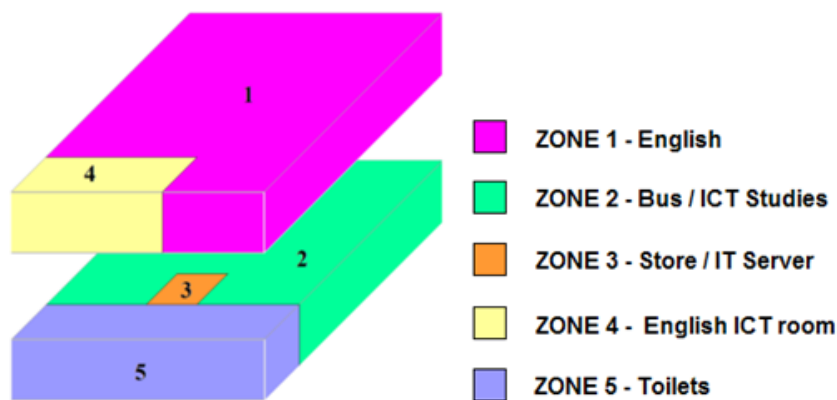


Figure 4 2D representation of a model zone building case study

This case study building was a multi-story school building. Initially all class rooms were modelled for a chosen floor. However this produced very large models and later the building was divided into zones according to the chosen HVAC strategy in different rooms.

For example in zone 1 there were 7 classrooms with all having the same ventilation and heating strategy. The five zones were modelled with each zone's model of heat transfer, lux and CO₂ levels. This still resulted in a very high order state space model

for controllability analysis. This posed difficulty for symbolic analysis as solving large determinants was very complex and difficult even with software such as Mathematica. Therefore this was not suitable for conceptual design stage where quick analysis and fundamental results are required. Also the aim was that this would be used by designers who do not have time or deeper understanding of mathematics and control theory. Also each zone had many classrooms with internal masses. Also, modelling so many classrooms as one zone was considered inappropriate for representing dynamics for controller design as it would be difficult to model so many causes and effects accurately. It was considered that each class would have its own zone control and analysing a single class room or zone would be enough where all the class rooms were having the same HVAC control strategies. Thus in this thesis a generic single zone model is represented for explanation of the controllability science and its results in theory and practice.

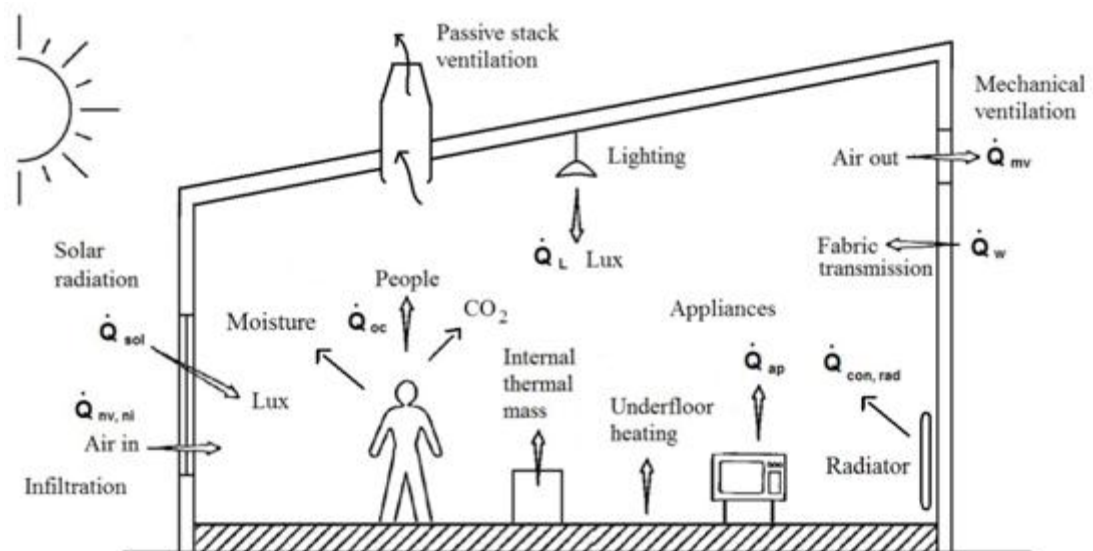


Figure 5 Schematic of the building's energy flows, CO₂ and lux balance showing the factors affecting the internal environment of the zone.

Another important aspect of the modelling was how to represent the multi layer elements of the zone such as walls etc. Although previous studies have shown that second order model predicts accurate dynamics of the wall [(Gouda & Danaher, 2002), (Kampf & Robinson, 2007)], however it is also shown [(Hudson & Underwood, 1999)] that the results are not very different from the first order model if

the resistances are calculated accurately on both sides of the thermal capacitance layer. Obviously modelling all the layers of a wall would increase the number of equations and the order of the model. Initially a second order model i.e. two layers for each element, was constructed. This resulted in a large number of equations and the symbolic analysis had to be carried out with software. However the performance of the transient response was very accurate in intermodal comparison with ESP-r simulation package.

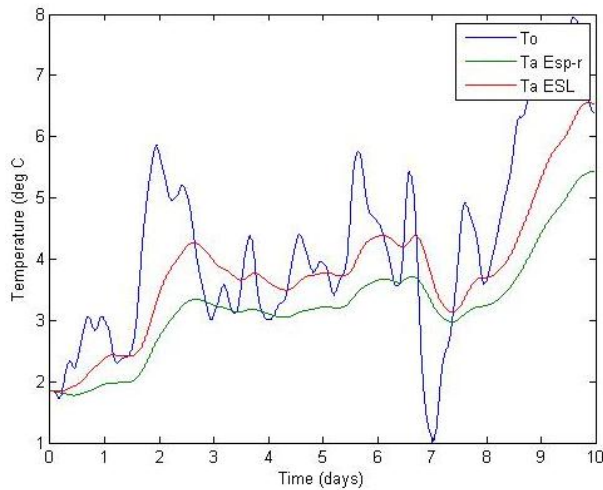


Figure 6 Internal model multilayer comparison of simplified model and ESP-r model for temperature response

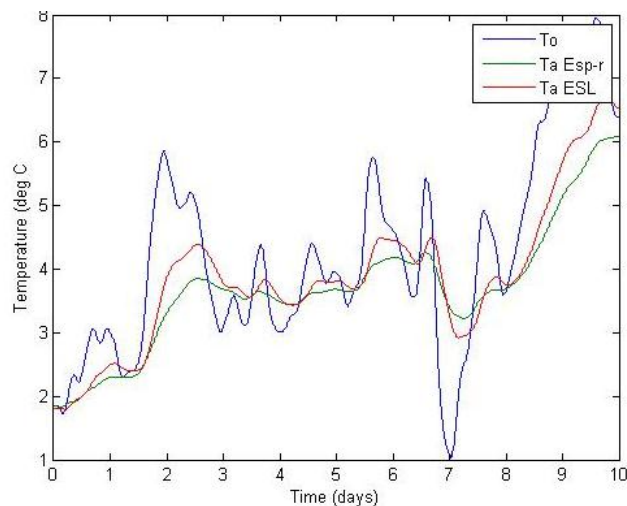


Figure 7 Internal model single layer comparison of simplified model and ESP-r model for temperature response

Then single layer lumped mass element zone was simulated as shown in figure 6 (above) and there was also difference in the results. The energy consumption results had a difference of few degrees in air temperature. Also the transient response was showing large rates of change compare to the ESP-r results. This was due to weighted average values taken for the thermal properties of the materials such as specific heat capacity, density etc. This made the zone envelope more sensitive to the internal and external disturbances. A compromise was reached by only modelling the high thermal mass layers (e.g. brick or concrete etc) and assuming the thin layers such as insulation and plastering to be in steady state. These thin layers are treated as resistances and their effect was taken into account through the overall heat transfer coefficient. This does result in differences between predicted and actual measured in terms of the energy consumption as thin layers are assumed to have little thermal mass. However, although not perfect, this method allow for dynamics to be more accurately represented than steady state methods such as SBEM and SAP.

Initially the modes of heat transfer were treated separately such as conduction, convection and radiation. This was applicable for a model where two or more layers were assumed in the zone elements such walls etc. It is important to note here that in lumped parameter method the mass is lumped into a single node and so high thermal mass and low thermal mass elements are merged. Modelling two layers is better as one can be assumed inner layer and one to be the outer [(Liao & Dexter, 2004)]. This is an advantage as ideally surface temperatures on both sides of the wall are different and this would approximate a better representation of the causes and effects. The outer layer would have temperature closer to external temperature and inner layer would have a temperature near the internal zone temperature. In this case the convection and radiation effects would have more accurate values. However with a single node (i.e. one temperature), these heat transfer effects were less accurate. With effects such as solar gain, the impact on the wall temperature was significant in the single node case and this affected the internal temperature as well. For this reason the heat transfer was modelled using U values. Here there is an obvious error that for example the wall is assumed to be only the brick layer and the U value being used is calculated based on the actual thickness of the wall with the added insulation, plaster

layers etc. This method however produced more accurate results for transient performance and energy consumption with the advantage of a simpler model. This allowed for simplification of the model for controllability analysis while retaining the essential dynamic characteristics.

The single zone considered in this thesis is modelled as a general floating zone which has boundary conditions that can be user defined for a particular case. Thus the model is applicable for controllability analysis of any zone whether in a dwelling or a commercial building office and at any level e.g. by defining the boundary conditions the floor can be considered on ground or a roof / floor in a multi-story case. Another point to note is that where needed the nonlinear elements of the model have been linearised e.g. buoyancy equation. The reason is that controllability analysis is symbolic and requires the model to be linearised about an operating point at which the controllability properties of the system are assessed. The nonlinear model is used for simulation to validate the results of the analysis.

Modelling the disturbances correctly was a challenge as it was necessary to understand their dynamics in the context of energy consumption and controllability. In this model unnecessary complex physics aspects (i.e. disturbances such as natural ventilation, solar aspects etc) have been simplified by means of empirical studies and theoretical simplifications based on physical interpretation and past research. This approach has been followed by a number of developers (Underwood et al) which resulted in various lumped or reduced order models. In this project the aim was not to develop a model equivalent to a highly detailed simulation program such as ESP-r. Thus it was decided to ignore those effects which are either very small such that their affect on energy consumption is very small or their dynamics are such that they do not affect the controllability of the building. The development of plant models is a very lengthy subject and in this project the focus was on trying to generalise the plants in terms of their speed of response. For example in industry for dwellings SAP uses responsivity factors. Thus, the plants were categorised as either fast or slow based on their inertia this determined how they would be modelled. The following sections contain more information and discussion about this and point to note is that

the modelling method presented is not new but rather the use of the model is different. The mathematical equations that govern heat, CO₂, humidity, Lux transfer and other dynamics in a single zone are represented by differential equations. The model equations are as described in the next sections.

2.2.2 Thermodynamics

There are a large variety of control system components that occur in practice, a generalized approach is useful for obtaining their mathematical models. Therefore an alternative view point to the principal of conservation is the concept of an analogous circuit. The basis for applying the principle of analogy is that two different physical systems can be described by the same mathematical model. In this work the thermodynamic equations of the system are translated to an electrical circuit model [(Wellstead, 1979)]. The procedure described in the following considers a single zone model consisting of air mass, external wall elements, floor, ceiling and internal thermal mass. Any construction element can be represented as ‘lumped’ thermal resistances and capacitances and it can be intuitive to visualise the problem as an equivalent electric R-C as shown below:

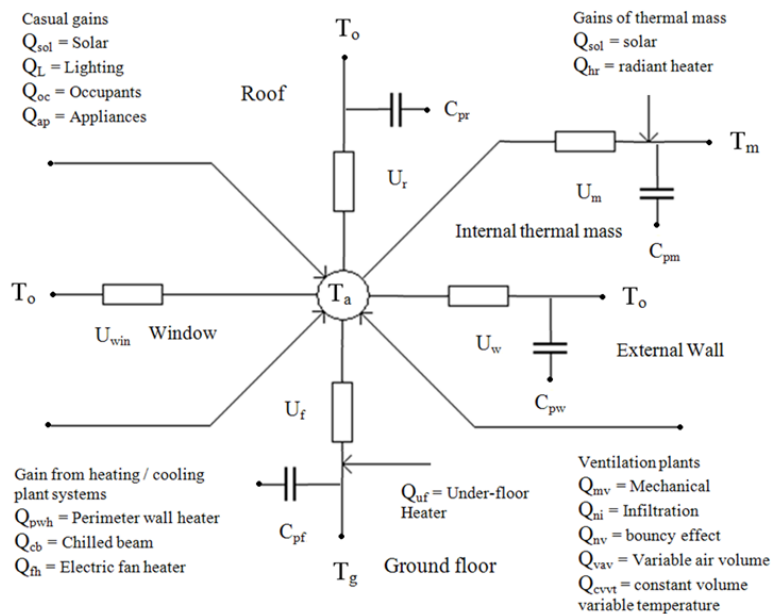


Figure 8 lumped capacitance model – building energy transfer function paths

The thermodynamic model of a building system (building, plants, walls, window etc.) can be described by the classical differential equations of heat transmission and thermodynamics. Following the principal of analogy the resulting equations are translated to an electrical circuit model making matches between the temperatures and voltages, the heat fluxes and the currents, the heat transmission resistances and the electrical resistances, the thermal capacities and the electrical capacities, etc [(Keyser & Dumortier, 1984)]. The thermal model consists of equations representing the rates of change of temperature of indoor air, walls, roof, floor and internal thermal mass. The equations which describe the system are, as it is a dynamic system, differential equations [(Richard C. Dorf, 2008)]. By making certain simplifying assumptions (mentioned above) and working from basic principles these equations can be derived (See Appendix 1).

2.2.2.1 Indoor air temperature

From a control engineers point of view we define the room air temperature as the process output that has to be controlled. This temperature is the result of the heat input through heat sources (i.e. radiators, solar etc) and the heat losses (mainly conduction through the walls, floor and windows and ventilation losses). Therefore the variation of the zone air temperature can be seen as dependent on the following physical quantities which are defined as process inputs: temperature of the outside air, casual gains, air flow through ventilation and heating / cooling plants systems.

The temperature of the zone is modelled as a single node representing an average temperature of the zone i.e. that the indoor zone air is fully mixed at constant pressure. This results in simplification stating that the air is fully stratified. This assumption is generally not valid for thermal buoyancy force-dominated flow. However this leads to far less complex dynamic equations, but are still detailed enough to analyse controllability. All the authors mentioned earlier in relation to lump parameter models have taken this assumption including Underwood et al. In reality, due to occupant behavior etc the air temperature is never uniform in all parts of the zone and this would affect controllability. However this effect is taken as a

transport lag and is discussed in chapter 3 and slow systems case study in chapter 5. The effect of transport lag is very important to controllability but in control systems design it is represented by feedback sensor lag rather than highly complex air flow equations. Such equations would make the building physics model very complex for assessing controllability contrary to the philosophy of using simple models for controllability.

$$\rho_a V_a c_{pa} \frac{dT_a}{dt} = \left[\begin{array}{l} (\dot{Q}_{sa} + \dot{Q}_L + \dot{Q}_{oc} + \dot{Q}_{ap})_{casual\ gains} \\ + (\dot{Q}_{wi1} + \dot{Q}_{wi2} + \dot{Q}_{wi3} + \dot{Q}_{wi4} + \dot{Q}_{fi} + \dot{Q}_{ri} + \dot{Q}_{win} + \dot{Q}_m)_{structure} \\ + (\dot{Q}_t + \dot{Q}_v + \dot{Q}_{ni})_{ventilation} \\ + (\dot{Q}_{mv} + \dot{Q}_{cp})_{heating/cooling} \end{array} \right] \quad (2.1)$$

The above equation shows that the rate of change of energy in the zone is equal to the difference between the energy transferred to the zone by either heat transfer through the fabric or mass flow as a temperature difference and the energy removed from the zone. Where:

Heat transfer by casual gains:

Casual heat gains are useful and can contribute towards reheats or estimating the requirement for cooling. As buildings envelopes become better insulated, casual gains can form a high proportion of the total heat needed in certain types of building. Therefore assessment of the impact of casual gains on controllability of temperature in buildings becomes very important. The amount of impact of casual gains on the internal temperature will also allow for accurate sizing of the heating and cooling plant systems. Since the heating systems are used intermittently in buildings, they are sized for early morning preheating when casual sources and solar radiation are unavailable. The availability of these sources after preheating, the heating is heavily oversized during normal operation, making controllability at light load especially crucial.

Most solar heat gain to a building space is by direct radiation through the windows [(Gouda, Danaher, & Underwood, 2000)]. The heat gain in a building by radiation from the sun depends upon site-specific factors and dynamic factors. The former consist of the surface area and angle of tilt of the glass, the composition of the glass, the geographic location of the site, the orientation of the building on the site and any local shading factors. These factors are more important for energy consumption calculation where the orientation of the building with respect to its setting will have a significant impact on the calculation results. However for controllability analysis a reasonable estimate of the amount of solar gain entering the zone is sufficient and thus a simplified model is used. Also due to direct solar radiation penetrating the window will cause the window temperature to rise. Thus a small part of the solar radiation will be included in the air due to heat transfer between the window and air. As mentioned in [(Mitalas, 1965)], that about 10% of the solar is absorbed by other surfaces apart from the floor & furniture. Majority of the other surfaces will be at room air temperature thus this 10 % can be assumed to be contributing heat directly into the air. This is due to the window being assumed to be in steady state and this gain is treated as a direct heat gain to the air temperature node. This has been assumed by other authors as well [(Liao & Dexter, 2004), (Gouda, Danaher, & Underwood, 2000)]. The solar heat gain affecting directly the air temperature through the windows is calculated as:

$$\dot{Q}_{sa} = \alpha_a \sigma_s A_{win} I_{dr} \quad (2.2)$$

Where: σ_s is known as the transmissivity of the window. The transmissivity is a function of many factors which enables the orientation of the building to be taken into account for controllability analysis. Depending on the zone being analysed (dwelling or a commercial building) the compliance method would provide a choice of appropriate factors for calculating this. For example in SAP [(BRE-SAP, 2005)] this is given as: $\sigma_s = \sigma 0.9 g_s F_f z_f$. If it is found that solar gain is important for controllability then the individual parameters can be inspected for their impact on controllability.

Not all the electrical energy is converted into light, but most of it is converted into heat due to resistance losses in the electrical system. The amount of power converted into heat is given by;

$$\dot{Q}_L = k_e P_L \quad (2.3)$$

Where, k_e is the proportion of power contributing to the gains.

The Occupancy gains are simply the number of occupants multiplied by the heat gain produced by the occupants (these can be calculated according BREDEM principles):

$$\dot{Q}_{oc} = g_{oc} n_{oc} \quad (2.4)$$

The appliances gains were considered as constant terms in the temperature equation (e.g. SAP). Dynamic appliance gains models can be used in the model, but they were not used in this thesis as they have only a small effect on controllability.

$$\dot{Q}_{ap} = \dot{Q}_{desktops} + \dot{Q}_{laptops} + \dot{Q}_{peripherals} \dots = \sum g_{ap} n_{ap} \quad (2.5)$$

Heat transfer through the structure:

The zone structural mass is a source of heat storage [(Balaras, 1996)]. The heat transfer is between the structure, external and the internal temperatures. Heat from outside is stored in the mass of the structure i.e. wall and when the temperature drops in the zone the heat is transferred into the room. In the same way when the structure temperature drops below the room temperature then heat is transferred to the structure. There are eight structural elements in this building zone, namely four walls, floor, roof, window and internal thermal mass i.e. furniture. The heat transfer rate equations for these as follows:

Note: see appendix 2 for the reason of the multiplication of factor of 2 to the wall, floor and roof equations.

$$\text{Wall 1: } \dot{Q}_{wi1} = 2U_{w1}A_{w1}(T_{w1} - T_a) \quad (2.6)$$

$$\text{Wall 2: } \dot{Q}_{wi2} = 2U_{w2}A_{w2}(T_{w2} - T_a) \quad (2.7)$$

$$\text{Wall 3: } \dot{Q}_{wi3} = 2U_{w3}A_{w3}(T_{w3} - T_a) \quad (2.8)$$

$$\text{Wall 4: } \dot{Q}_{wi4} = 2U_{w4}A_{w4}(T_{w4} - T_a) \quad (2.9)$$

$$\text{Floor: } \dot{Q}_{fi} = 2U_f A_f (T_f - T_a) \quad (2.10)$$

$$\text{Roof: } \dot{Q}_{ri} = 2U_r A_r (T_r - T_a) \quad (2.11)$$

$$\text{Window: } \dot{Q}_{win} = U_{win} A_{win} (T_o - T_a) \quad (2.12)$$

Note: Due to low thermal mass of windows they are considered to be in steady state.

$$\text{Thermal mass: } \dot{Q}_m = h_m A_m (T_m - T_a) \quad (2.13)$$

Heat transfer by ventilation:

The air leakage in the building construction; e.g. opening and closing of windows, etc. the air in the building shifts. The value is hard to predict and depends on several variables - wind speed, difference between outside and inside temperatures, the quality of the building construction (i.e. air tightness) etc. However, the heat loss caused by buoyancy effect and infiltration can be calculated as:

$$\text{Buoyancy effect (thermal force): } \dot{Q}_t = V_a n_t \rho_a c_{pa} (T_o - T_a) \quad (2.14)$$

$$\text{Buoyancy effect (wind pressure): } \dot{Q}_v = V_a n_v \rho_a c_{pa} (T_o - T_a) \quad (2.15)$$

$$\text{Air tightness (infiltration): } \dot{Q}_{in} = V_a n_{in} \rho_a c_{pa} (T_o - T_a) \quad (2.16)$$

Note: The mass flow in the zone is taken account of in terms of the heat transfer due to mass flow. Thus the pressure losses across the zone are neglected. The air is considered incompressible. Therefore the conservation of mass flow is taken account of in the conservation of energy. Since this model is predominantly aimed at thermal analysis and not driving flows thus here this assumption is applicable. This is discussed in more detail in section 2.3.

Heat transfer by heating/cooling plants:

In recent times built environments like offices, hotels, public and commercial buildings have become ever more complex. They now utilise multiple different plant systems for controlling the internal environment. Some provide fresh air while others deliver heat and cool to the building. Modelling their effects on the zone air temperature is very important for controllability assessment. For example mechanical ventilation systems provide a zone with an airflow rate. The air volume is usually based on the design cooling load for the given zone. There are a number of different ventilation systems depending on the application. The equation for mechanical ventilation based on air flow rate is:

$$\dot{Q}_{mv} = q_{mv} \rho_a c_{pa} (T_o - T_a) \quad (2.17)$$

Other systems include fan heaters, radiators etc.

A generic term for representing the heat transfers from these systems is given as follows:

$$\text{Heating or cooling plant (convection): } \dot{Q}_{cp} = h_c A_p (T_p - T_a) \quad (2.18)$$

$$\text{where: } h_c = 1.78 \left| \bar{T}_p - \bar{T}_a \right|^{0.32} \quad (\text{ASHRAE H. , 2008}) \quad (2.19)$$

The equation for the cooling or heating plant is modelling the proportion of heat transfer through convection contributing to the air. It is assumed that some of this heat transfer is between the air and some with internal & external thermal mass through radiation. The plant dynamics models are presented in section (2.2.8).

2.2.2.2 Wall Temperatures

In modern times walls are frequently consisting of several layers of different materials, is essentially a distributed parameter system its mathematical modelling would involve the solution of partial differential equations [(Keyser & Dumortier, 1984)]. In the thesis the wall is represented by a first order model by describing the wall as a capacitance and resistance.

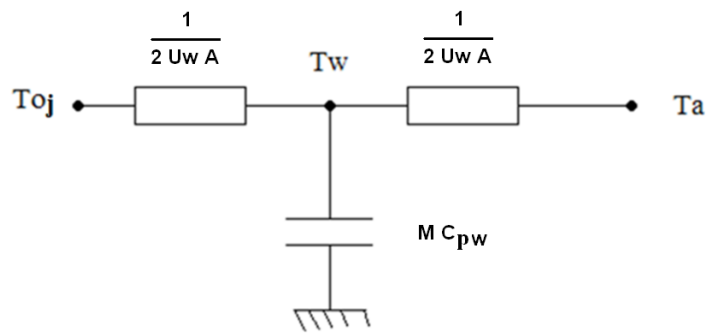


Figure 9 Resistance capacitance thermal circuit for the wall

Temperature gradients along the layers of the structure i.e. walls, floor, roof and window panes are small in comparison to those perpendicular to the surface and can be neglected [(Sodja & Zupancic, 2008)]. All elements of the envelope are thus simplified to one-dimensional heat transfer. This assumption is used by most building simulation programs and leads to far less number of equations without compromising on accuracy of results.

Often the assumption is made that the fabric solar heat gains through walls and roofs may be considered negligible for most UK applications. Little solar heat reaches the interior of the building because the high thermal capacity of ‘heavy’ constructions tends to delay transmission of the heat until its direction of flow is reversed with the arrival of evening. Low thermal capacity construction, on the other hand, tends to be well insulated, ensuring that solar heat transmission is minimised [(Gouda, Danaher, & Underwood, 2000)]. In this model for flexibility the thermal radiation of the building’s surroundings is neglected and compensation with a slightly higher outside temperature, i.e. the sol air temperature is being used to take account of the effect of solar gain on the external thermal mass [(Sodja & Zupancic, 2009)].

The number of walls to be modelled depends on the location of the zone. For example in the case of a zone connected to other zones in the building and the external environment would need the walls connected to the different zone to be modelled separately for accurately representation of the physics. To make the model more applicable in this thesis for the purpose of presenting the engineering science a simple zone is considered with four walls, floor and roof that are connected to the six

external environments and depending on the case study this can be simplified by combining the layers of the wall etc. The zone is considered a simple cube and thus the number of walls surrounding the zone is four. The basic principal of deriving the wall equations is same as presented in (Appendix 1) [for the rates of change of temperatures of walls the letter ‘j’ denotes the number of the wall (1-4), floor (5), roof (6) and their corresponding outside zones from 1 to 6]. The rate of change of wall temperature is given as follows:

$$\rho_{wj} V_{wj} c_{pwj} \frac{dT_{wj}}{dt} = [\dot{Q}_{woj} - \dot{Q}_{wij}] \quad (2.20)$$

Where heat exchange with:

$$\text{Outside: } \dot{Q}_{woj} = 2U_{wj} A_{wj} (T_{oj} - T_{wj}) \quad (2.21)$$

$$\text{Inside: } \dot{Q}_{wij} = 2U_{wj} A_{wj} (T_{wj} - T_a) \quad (2.22)$$

N.B: For heat transfer between external surroundings and the wall & roof, the external temperature is taken to be the sol-air temperature. This allows for simpler treatment of the effect of the solar radiation and sky heat exchange with the wall & roof.

2.2.2.3 Floor temperature

Composite floors are widely used in buildings nowadays. A composite floor is the general term used to denote the composite action of steel beams and concrete or composite slabs that forms a structural floor. In this thesis the floor is also modelled as a first order system. In most buildings nowadays the floors are composed of three layers mainly screed, insulation and concrete. In ground floors higher order models are more appropriate because the ground temperature will remain quite low and first order models will result in significantly higher heat transfer than in actual cases. Also for representing systems such as under-floor heating, higher order models will be more appropriate for accurate representation of the transient response. In the first case-study (section 5.1) this is shown where slow acting heating system is modelled.

However for the general case, a first order representation of the floor is presented in this chapter i.e. a capacitance and resistance.

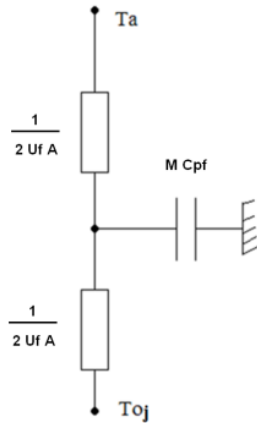


Figure 10 Resistance capacitance thermal circuit for the floor

Apart from under-floor heating, in normal floor the screed is not heated and thus it can be assumed to be in steady state as its quite thin compare to the concrete layer. Thus in the general case as discussed earlier in the evolution section using appropriate heat transfer coefficient the floor can be represented with a first order system. Again the modelling procedure is the same as shown in equations (Appendix 1). The rate of change of floor temperature is given by:

$$\rho_f V_f c_{pf} \frac{dT_f}{dt} = [\dot{Q}_{fo} - \dot{Q}_{fi}] \quad (2.23)$$

Where heat exchange with:

$$\text{Outside: } \dot{Q}_{fo} = 2U_f A_f (T_{oj} - T_f) \quad (2.24)$$

$$\text{Inside: } \dot{Q}_{fi} = 2U_f A_f (T_f - T_a) \quad (2.25)$$

Note: The floor can be connected to the ground or another zone depending on the location of the zone. For the general case it is assumed that the zone is on the ground floor. The ground temperature was assumed constant [(Cengel Y. A., 1998)].

2.2.2.4 Roof Temperature

Knowledge and understanding of heat transfer through the roof of an air-conditioned building has become increasingly important as air-conditioning penetrates more widely to attain thermal comfort. The knowledge could be utilised to rationalise and economise on the use of energy, building materials and control strategies. In a large urban environment more roof styles can be observed other than the hip roof. For the general case the roof model presented is a first order model representing a thermal mass layer surrounded by insulation i.e. a capacitance and two resistances. Generally the roofs are mainly composed of one layer (i.e. insulation) and any other layer such as steel or aluminium outer casings are thin enough to be treated as steady state. The model allows for modelling where a zone is situated below another zone and thus the roof model can be easily modelled as a floor. Again the modelling procedure is the same as shown in equations (Appendix 1). The rate of change of roof temperature is given by:

$$\rho_r V_r c_{pr} \frac{dT_r}{dt} = [\dot{Q}_{ro} - \dot{Q}_{ri}] \quad (2.26)$$

Where heat exchange with:

$$\text{Outside: } \dot{Q}_{ro} = 2U_r A_r (T_{oj} - T_r) \quad (2.27)$$

$$\text{Inside: } \dot{Q}_{ri} = 2U_r A_r (T_r - T_a) \quad (2.28)$$

2.2.2.5 Internal thermal mass temperature

Thermal mass or its thermal storage effect can be used to reduce energy consumption of mechanical and heating systems in buildings (Balaras, 1996). The working principle is very simple that thermal mass stores heat in both the building envelope materials and the interior mass such as furniture, partitions, ceiling and floor during a warm period on a summer day and releases it at a later time in the day. The peak cooling loads can be reduced thereby; similarly the stored heat during high solar

gains can be released into the building in the late afternoon, which can satisfy partly the heating needs during cold period. Two engineering questions arise: how much thermal mass should be used in a particular building design to ensure stability of the entire system and what are the quantitative impacts of thermal mass on cooling/heating and indoor air temperature. Many models have been developed for the purpose of studying the effect of thermal mass [(Yam & Li, 2002), (Zhou & Zhang, 2008)]. The model presented here is for the purpose of symbolic controllability analysis and nonlinear simulation of causes and effects of internal thermal mass (i.e. furniture, internal structure etc).

The thermal mass is assumed to be a lumped mass situated in the zone which exchanges heat with the internal air mass and the heating system. It is assumed that the thermal mass is not in equilibrium with the indoor air. Here all the internal masses are represented by one mass. However, in reality the mass will be spread throughout the zone floor. The temperature distribution in the thermal mass materials is also assumed to be uniform. This means that the thermal diffusion process is much faster than the convective heat transfer at the thermal mass surface [(Zhou & Zhang, 2008), (Yam & Li, Nonlinear coupling between thermal mass and natural ventilation in buildings, 2003)]. In this manner different types of thermal masses can be modelled for their effect on controllability. The internal mass is modelled as a rectangular block hanging in air with a heat capacity and a surface area corresponding to all the furniture pieces in the room and there is no heat transfer with the floor. At the moment even the state of the art simulation packages such as ESP-r are using this approach unless CFD models are created for analysing the effect of furniture arrangement on energy consumption. In terms of controllability the position of the furniture matters in practice, because it can determine the flow path of the heat from the heating system to the zone elements. However this effect is again caused in the transport delay (later). The rate of change of thermal mass temperature is given by the following differential equation:

$$\rho_m V_m c_{pm} \frac{dT_m}{dt} = [\dot{Q}_{sm} + \dot{Q}_{rpm} - \dot{Q}_m] \quad (2.29)$$

Where the heat exchange with:

$$\text{Air: } \dot{Q}_m = h_m A_m (T_m - T_a) \quad (2.30)$$

$$\text{Plant: } \dot{Q}_{rpm} = h_r A_p (T_p - T_m) \quad (2.31)$$

$$\text{Where: } h_r = \varepsilon \sigma_b (\bar{T}_p^2 + \bar{T}_m^2) (\bar{T}_p + \bar{T}_m) \quad (\text{Holman, 2009}) \quad (2.32)$$

$$\text{Solar gain through the window: } \dot{Q}_{sm} = \alpha_m \sigma_s A_{win} I_{dr} \quad (2.33)$$

2.2.2.6 Plant thermal dynamics

The states (e.g. temperatures etc) that are being controlled in a building will have different time constants. Different plant systems will have varying thermal responses (SAP). For example an under floor heating system is a slow plant system because the release of heat is slow due to the thermal mass of the floor. If this system was working alongside a fast acting ventilation system then due to their slow and fast thermal dynamics they will have a strong coupling between them and operating them simultaneously for tracking different requirements would be a complex process. Therefore modelling the thermal dynamics of the plants is very important in assessing the controllability of the overall system. In this thesis controllability of slow and fast acting actuator systems is also analysed (sections 5.1 & 5.2). A model of a general heating/cooling plant was created based on the model developed by [(Liao & Dexter, 2004)]. The thermal dynamics of the plant is modelled by a differential equation where the rate of change of temperature of the heating or cooling element of the plant that drives the heat transfer between the zone and the plant is given by:

$$\rho_p V_p c_{pp} \frac{dT_p}{dt} = [\dot{Q}_p - \dot{Q}_{rpm} - \dot{Q}_{cp}] \quad (2.34)$$

and where the heat exchange is with:

$$\text{The power input to the plant } \dot{Q}_p \quad (2.35)$$

$$\text{and plant to thermal mas } \dot{Q}_{rpm} = h_r A_p (T_p - T_m) \quad (2.36)$$

$$\text{and heat transfer from plant to air } \dot{Q}_{cp} = h_c A_p (T_p - T_a) \quad (2.37)$$

This is useful in modelling plants where the element with which the zone exchanges heat/cool takes time to heat/cool up/down i.e. it has thermal capacitance, for example a wet system such as radiator where the water takes time to heat up before heat transfer can take place. Of course the plant power is also variable from zero to maximum with which the temperature of the heat element of the plant is influenced. Thus, the plant power also has first order dynamics with a time constant set as required (see section 2.2.8).

2.2.3 Natural Ventilation and air change rate

The study of air flow through inlet and outlet openings has been the subject of papers by a number of authors. Natural ventilation is induced by thermal buoyancy and wind. Theoretical and experimental research of natural ventilation of buildings is broadly published in literature [(Zhang & Jacobson, 1989), (Li & Delsante, 2000), (Yang & Zhang, 2005), (Luo & Zhao, 2007), (Andersen, 2003), (Gebremedhin & Wu, 2003)]. At least two methods have appeared in literature to combine the effects of wind with thermal buoyancy [(Kavolelis & Bleizgys, 2008)]. One method superimposes wind and thermally induced pressure differences across openings, and use Bernoulli's equation to develop expressions for the speed as a function of vertical height in the opening. An alternative method is to calculate natural ventilation due to wind separately and then combine them using the equation: square of total air flow rate is equal to the sums of squares of air flow rates induced by thermal buoyancy and wind forces. It is proposed that the intensity of natural ventilation in premises is determined by many factors such as wind speed, direction and its turbulence, the size of ventilation openings and their location, heat sources, thermal conduction of outer walls, solar irradiance, etc. However, the most important thing is to evaluate ventilation induced by thermal buoyancy and wind speed [(Li & Delsante, 2001)]. Thermal buoyancy pressure is usually smaller than wind pressure, therefore, wind induced ventilation is also greater. It is difficult to forecast as wind speed and direction change invariably. For a more thorough symbolic analysis, the wind

pressure and buoyancy effects have been modelled separately [(ASHRAE, 2009)]. Their effect on the indoor air temperature is presented in equations of air change rate. Air change rate is the result of buoyancy effect and tightness of the building that is influenced by air velocity pressure difference or temperature difference between internal and external environments. With passively driven ventilation, it is known that indoor airflow is thermally stratified in some circumstances. By using the fully mixed assumption, it leads to relatively simple equations, which nonetheless display interesting cause and effect behaviour. This is a reasonable assumption because as shown in chapter 3, in practice the sensors are operated slow enough to allow for this assumption to be valid.

The air change rate induced by buoyancy due to temperature difference is given by:

$$n_i = \frac{C_D A_o}{V_a} \sqrt{2g\Delta H \left(\frac{T_i - T_o}{T_i} \right)} \quad (2.38)$$

This equation applies when internal air temperature is greater than external air temperature i.e. ($T_i > T_o$) [(ASHRAE, 2009)]. As can be seen that the above equation is nonlinear and subsequent case studies will utilise linear control theory for controllability analysis, therefore this equation is later linearised.

If in the term $(T_i - T_o)/T_i$, the temperatures are assumed to be at some operating point under analysis i.e. that the numerator term can be taken as the operating point temperature difference term ΔT and the denominator is taken as the desired operating temperature of the zone based on the internal and external temperatures. Then for small perturbation analysis this equation can be assumed constant. This is reasonable assumption because here the ΔT is only used to calculate the air change rate and the sign of ΔT is not important as that will be determined by the heat equation Q_t where small perturbations can be applied to the temperature difference. With the above assumption the equation can be written as a constant to be used in the equation as follows:

$$\bar{n}_t = \left(\frac{C_D A_o}{V_a} \sqrt{2g\Delta H} \right) \sqrt{\frac{\bar{T}_i - \bar{T}_o}{\bar{T}_i}} \quad (2.39)$$

Note as mentioned in [(ASHRAE, 2009)], denominator will change according to the magnitude of the temperature. If T_i is greater than T_o then denominator will be T_i and vice versa. This method of linearisation is similar to the linearization of radiation equation where the 4th order terms are linearised by this method [(Holman, 2009)]. Also in this way the linear and nonlinear properties of the model are preserved. Through dynamic simulation this can be inspected to see if it can be treated as a constant.

The air change rate induced by wind pressure forces is given by [(ASHRAE, 2009)]:

$$n_v = \frac{C_v A_i}{V_a} v_o \quad (2.40)$$

This equation is linear however when calculating its effect on the air temperature the heat transfer equation becomes nonlinear. Thus the heat transfer equation is linearised as shown in section 5.1. These models combine the main factors that are needed to be taken into account for symbolic controllability assessment of buildings with natural ventilation strategies. The models are created for subsequent simulation of the causes and effects of natural ventilation in a zone and its implications on the control strategies. These equations are not for predicting highly accurate air change rates through the building zone for purposes of heating/cooling load calculations and energy consumption and used for simulating causes and effects that are reasonably accurate.

2.2.4 Daylight

The level of light within a building has important implications for occupant comfort and productivity. Daylight is an important psychological factor and it has been found that occupants prefer to work by natural light [(McMullan, 2007)]. It is important for the correct level of lighting to be available for the task, without excessive glare and so usually combined lighting strategy must be used [(McMullan, 2007), (CIBSE,

2006)]. The first step in evaluating the visual performance and energy efficiency provided by daylight requires an accurate estimation of the amount of daylight entering a building. The actual daylight illuminance of a room is mainly influenced by the luminance levels and patterns of the sky in the direction of view of the window at that time.

For the purposes of modelling, the level of light can be treated as three components, the artificial light, and the direct light from the sun and the background, or reflected light from the surrounding environment. The objective of this work is not to model accurate position of the sun in the sky for formulating luminance levels. A reasonable daylight factor will allow for simulating the causes and effects in the zone by the external solar data.

Specific solar, HVAC, or day lighting applications require specific solar radiation components for simulation or monitoring purposes. For instance, the simulation of daylight distribution in complex interior spaces, which is now possible thanks to detailed simulation software [(ESRU, 2010)] requires an accurate knowledge of the distribution of light in the sky i.e. solar angles etc. Since these specific components are many and are often too expensive to measure on a routine basis, another option is to rely on conversion models that use more routinely accessible data i.e. direct and diffuse radiations. Although real lux data is always preferable there are conversion factors to generate lux values from radiation levels [(Littlefair, 1988) & (Fontoynt, 2002)]. In the model this method for calculating daylight is presented for flexibility, simpler and quicker controllability analysis. The exact conversion factor changes depending on the level of cloud cover, in that clouds alter the amount of absorption of the different wavelengths/scattering in the atmosphere and therefore reduce the total reaching the ground. There are various models presented in the literature and are mainly of three types:

1. Luminous efficacy models that relate, in terms of number of lumens per watt, the three basic radiation components (direct, global and diffuse irradiance) to their

photopic equivalent (direct, global, and diffuse illuminance), [(Littlefair, 1988), (DeRosa & Ferraro, 2008)].

2. Models that predict diffuse irradiance or illuminance received by tilted surfaces [(Tung, 2008)].

3. Models that are concerned with the angular distribution of light in the sky dome rather than with the integrated diffuse which predict the luminance at the sky's zenith and estimating luminance at any point in the sky dome [(Pirez & Ineichen, 1990)].

The purpose of this research was not to model accurate models of daylight and the type 1 model based on luminous efficacy was found to give satisfactory results and was easiest to work with. Thus that was used in the work for its simplicity compared to the other two types, as the simplicity will allow a symbolic approach to controllability analysis.

Radiant emittance from a source is in watts per square meter (Wm^{-2}). Similarly, the density or irradiance at a receiving surface is given in Wm^{-2} . For luminous emittance or illuminance, the units are lumens per square meter ($lm m^{-2}$), or commonly lux (lx) [(Hanan, 1997)].

$$\text{Luminance} = lux = \frac{lm}{m^2} \rightarrow lm = lux m^2 \quad (2.41)$$

$$\text{Luminous efficacy} = \frac{lm}{W} = \frac{lux m^2}{W} \quad (2.42)$$

In [(Littlefair, 1988)] it is shown that the luminous efficacy conversion function does not vary much with percentage of year. It mentions that the variations that do occur may be due to experimental or sampling errors. It was proposed that a single figure of $119 lm/W^{-1}$ can be used for conversion [(Littlefair, 1988)]. Therefore to calculate the amount of lux, the solar radiation has to be multiplied by the factor of 119. This is shown here as follows:

$$\frac{lm}{W} = \frac{lux m^2}{W} \rightarrow \frac{lux m^2}{W} \times Wm^{-2} = lux \quad (2.43)$$

It should be noted here that the solar radiation being converted is the diffuse one not the direct. This is a crude method where it is assumed an over cast sky so direct solar radiation and i.e. position of the sun are ignored. In this model two different effects have been combined: day light factor and radiation to lux conversion factor [(Littlefair, 1988)] which have different purposes. Day light factor determines how much of the outside lux is entering the zone. The amount of lux outside is determined by the conversion factor. This method is presented for ease of controllability analysis in the case of detail solar data not being available. The purpose of the illuminance model is for simulating causes and effects which affect the zone illuminance and is not used for energy conservation calculation. Moreover, the model is used for symbolic controllability assessment of the lighting controls strategy with respect to the overall control system and therefore doesn't require a complex day lighting model which is also out of scope of this work. The equation for this is kept simple and in case where the controllability shows this to be a crucial factor to controllability then the designer can look at the detail of solar angles etc.

Thus, the illuminance level in the zone is given as follows:

$$L_{cm} = L_i + L_s = k_L P_L + \lambda \alpha_L I_{df} \quad (2.44)$$

2.2.5 Internal and external long wave radiation exchange (sky temperature & solar radiation)

Long wave radiation between sky and solar gain on the external mass of the building are two different effects. Long-wave radiation exchange between internal surfaces of the zone is ignored. The reason is that this is a slowly varying process and depends on the temperature difference between surfaces. Majority of the time the internal surfaces have light colours and small temperature differences such that the long-wave heat transfer between them will not drastically affect the dynamics their surface temperatures. Also in comparison with other radiant effects e.g. heating system, the long-wave exchanges have a negligible effect on the internal thermal dynamics [(Mitalas, 1965)]. Thus this effect has little influence on controllability.

Regarding long wave radiation with sky vault, it is mentioned in [(Fissore, 1997)], that treating mean radiant external sky temperature to be equivalent to external air temperature produced error of less than 1 % even in cases where the temperature difference between wall surface and external air temperature was 50 °C. The account of radiative exchanges with the sky lays a problem that is common to various fields of solar energy applications, as solar collectors, thermal behaviour of outer walls or greenhouse. One method is to use Sky temperature as a fictitious temperature, introduced to model the long wave radiation exchanges with the sky and often taken as equal to the dry air temperature of the external air. Several authors offered various relations and take into consideration the external dry air temperature [(Swinbank, 1963)], the dew temperature [(Berger & Buriot, 1984)], or the degree of cloud cover. Nonetheless, this procedure remains problematic, correlations being only acceptable in certain weather conditions or for a specific site [(Clarke J. A., 2001)].

Solar radiation and ambient temperature control the net energy exchange between a building and its environment and their combined effect must be considered. Solar radiation on cooling load were compared and discussed in [(Liesen & Pedersen, 1997)], and it's shown that projecting all the solar on the floor matches actual behaviours in many cases. In most cases the floor will be obscured with the internal thermal mass such as furniture and thus it is sensible to include solar gains in the thermal mass equation. Another important aspect is that solar component directly affecting the internal surfaces of the walls is neglected because in most cases only one of the walls will be receiving solar gain. The whole of that wall will not receive direct solar gain and thus in reality a small part of the wall affected by the solar gain will have negligible effect on the indoor air temperature [(Mitalas, 1965)]. These assumptions are probably very true for floor and walls in dwellings in urban environment.

In most cases however, such as high rise flats and commercial building where solar gain will be more significant as it is noted that normally internal thermal mass is spread out and not lumped together. Thus, a fraction of the internal thermal mass will receive solar gain [(Mitalas, 1965)] and that's included in internal thermal mass

differential equation. This is limitation of the model that lumping the mass together will receive solar gain which actually will affect internal thermal dynamics more than in reality. This requires further work in the sense that alternative method of representing internal thermal mass is needed. For example modelling the thermal mass in two or more layers where majority of the heat exchange is between external layer and less from the internal layer. This is also mentioned in [(Mitalas, 1965)] where it is mentioned that the most active layer of the room envelope with respect to the heat storage is the one closest to the surface.

Note: The solar gains in this model are treated by including a percentage of the total solar gain entering the zone, in the air temperature node and the thermal mass node. Solar gains are treated as a direct heat input to the air and thermal mass temperature nodes. The flexibility of this approach is that distribution of solar gains inside the zone is easier. A fraction of the total gain can be included as a direct heat input term in the temperature equation of the object upon which solar radiation is falling in the zone. The limitation is that for example: it cannot be assumed that solar gain is affecting part of the internal mass (i.e. furniture) or part of the internal walls. It is assumed that whatever amount of solar gain hitting a structure is affecting the temperature in all parts of the structure equally. This is the limitation of the lumped parameter approach as the whole of the wall is given one temperature node, i.e. simplified model.

A more simple method is the sol-air temperature [(ASHRAE, 2009)] to account for the effect of solar radiation absorbed by the wall and for radiation from the building envelope to the cooler night sky. Sol-air temperature is the outdoor air temperature that, in the absence of all radiation changes gives the same rate of heat entry into the surface as would the combination of incident solar radiation, radiant energy exchange with the sky, other outdoor surroundings and convective heat exchange with outdoor air.

In the simplest case, it is assumed that the temperature of the radiant surroundings is at the air temperature and that the only other source for radiant energy is solar

radiation. An energy balance on the surface notes that the total rate of heat transfer at the surface is the sum of the convection and radiation exchange with the air temperature and the absorbed solar radiation [(ASHRAE, 2009)].

$$\frac{q}{A} = \alpha E_t + h_o (T_o - T_s) - \varepsilon \Delta R \quad (2.45)$$

Assuming the rate of heat transfer can be expressed in terms of the sol-air temperature T_{sa} :

$$\frac{q}{A} = h_o (T_{sa} - T_s) \quad (2.46)$$

And from the two equations above the sol-air temperature is given by (ASHRAE, 2009):

$$T_{sa} = T_o + \frac{\alpha E_t}{h_o} + \frac{\varepsilon \Delta R}{h_o} \quad (2.47)$$

This procedure was used to calculate the sol-air temperature in this work. A difference will prevail between actual solar absorption and that predicted. However the purpose here is not to emulate reality by performing complex tedious solar angle and intensity calculations, but instead using simple calculation with good representation of the causes and effects will suffice for assessment of controllability and can reduce the effort involved.

This is a valid assumption because sol-air temperature is an established method for taking account of the solar gains on the external thermal mass. If in the controllability analysis solar air temperature is found to be an important factor then the sensitivity of the variables in the equation (2.47) can be assessed. Then if any of the variables is found to be important and is a function of parameters such as solar angles etc then modelling of such complex effects will be useful.

2.2.6 CO₂ concentration

Complex relationships exist between carbon dioxide concentration and Indoor Air Quality (IAQ) in terms of occupant comfort. This includes the impact of elevated CO₂ on comfort, the association between CO₂ level and other air contaminants, and the relation between CO₂ and ventilation. Ventilation in buildings with frequent or occasional high occupancy levels, presents a problem (e.g. schools). The generation of CO₂ especially from high occupancy, is one of the major contributing factor linked to poor IAQ. Thus it is important to account for CO₂ levels in buildings with high occupancy. The model presented here predicts the concentration of CO₂ in building space/zone at any time during high occupancy and when the occupancy levels return to lower levels. A schematic representation of a building occupied space with a forced fresh air filtration and natural ventilation system is shown in Figure 3. The model presented in [(Aglan, 2003)] was used as the basis for the CO₂ concentration model in this thesis.

As mentioned in [(Never, 1995)], in air pollution literature ppm (part per million) applied to a gas, always means parts per million by volume or by mole. These are identical for an ideal gas, and practically identical for most gases of air pollution interest at 1 atm. Another way of expressing this value is ppm (V). One part per million (by volume) is equal to a volume of a given gas mixed in a million volumes of air:

$$1 \text{ ppm} = \frac{1 \text{ gas volume}}{10^6 \text{ air volumes}} \quad (2.48)$$

A micro litre volume of gas in one litre of air would therefore be equal to 1 ppm:

$$1 \text{ ppm} = \frac{1 \mu\text{L gas}}{1 \text{L air}}, \quad 1 \mu\text{L} = 1 \times 10^{-6} \text{ L}, \quad 1 \text{L} = 1 \times 10^{-3} \text{ m}^3 \quad (2.49)$$

$$1 \text{ ppm} = \frac{1 \times 10^{-6} \text{ L gas}}{1 \text{ L air}} = \frac{1 \times 10^{-6} \times 1 \times 10^{-3} \text{ m}^3 \text{ gas}}{1 \times 10^{-3} \text{ m}^3 \text{ air}} = \frac{1 \times 10^{-6} \text{ m}^3 \text{ gas}}{1 \text{ m}^3 \text{ air}} \quad (2.50)$$

$$1 \text{ ppm} = \frac{1 \times 10^{-6} \text{ m}^3 \text{ gas}}{1 \text{ m}^3 \text{ air}} \quad (2.51)$$

This is Parts per million CO₂ by volume. Multiplying parts per million CO₂ by volume by the density of CO₂ in kg/m³ gives you kg/m³. In modelling the CO₂ production or ex-filtration is measured in mass per unit time from occupancy and other source [(Aglan, 2003)]. Thus; to find the mass per unit time (kg/s), the value of concentration in m³ is multiplied by density of CO₂ and volumetric flow rate (n times the volume).

$$\dot{C}_n = \frac{1 \times 10^{-6} \text{ m}^3 \text{ gas}}{1 \text{ m}^3 \text{ air}} \rho n V = \frac{\text{m}^3}{\text{m}^3} \frac{\text{kg}}{\text{m}^3} \frac{1}{\text{m}^3} \text{m}^3 = \frac{\text{kg}}{\text{s}} \quad (2.52)$$

The differential equation which governs the generation and decay of CO₂, based on mass consideration, can be expressed as:

$$\rho_{co_2} V_a \frac{dC_a}{dt} = S - \dot{C}_{mv} - \dot{C}_t - \dot{C}_v - \dot{C}_i \quad (2.53)$$

Where:

S is internal CO₂ gain (kg/s)

$$\text{CO}_2 \text{ transferred via mechanical ventilation: } \dot{C}_{mv} = q_{mv} \rho_{co_2} (C_a - C_o) \quad (2.54)$$

$$\text{CO}_2 \text{ transferred via Buoyancy effect (wind pressure): } \dot{C}_t = \rho_{co_2} n_t V_a (C_a - C_o) \quad (2.55)$$

$$\text{CO}_2 \text{ transferred via Air tightness (infiltration): } \dot{C}_v = \rho_{co_2} n_v V_a (C_a - C_o) \quad (2.56)$$

$$\text{CO}_2 \text{ transferred via infiltration is: } \dot{C}_i = \rho_{co_2} n_i V_a (C_a - C_o) \quad (2.57)$$

2.2.7 Humidity

A high or low humidity environment is related closely to not only many health problems, but also has great influence on the construction durability and energy consumption [(Zhang & Yoshino, 2010)]. For these reasons, keeping indoor humidity environment steady at the correct level is very important for ensuring the sustainability and health of buildings. It is known that the control of moisture is of prime importance to moderate the indoor humidity level. However, the indoor humidity environment is complicated and is influenced by many factors such as moisture sources (human presence and activity, equipment, plants), ventilation and infiltration of building envelope, air flow and temperature distributions in rooms, moisture adsorption and desorption from surrounding surfaces (interior walls, floor, carpet, furniture, futon and books, etc.), as well as the absolute humidity of the outdoor air. In order to provide an acceptable indoor air quality the use of mechanical ventilation systems became more accepted. These systems are capable of providing a controlled rate of air change and respond to the varying needs of occupants and pollutant loads, regardless from outdoor conditions. Therefore, in order to make moisture mitigating strategies and to reduce moisture related damage, controllability assessment of combined humidity and temperature control systems is necessary. For this purpose a humidity model is presented to be used in the controllability assessment method. The models presented by [(Daskalov & Arvenitis, 2006), (Beghi & Cesshinato, 2008), (Enai & Kawaguchi, 1999) & (Nakanishi et al, 1973)] were used as the basis for the humidity model in this thesis. The differential equation water balances on the interior volume of the building are as follows:

$$\rho_a V_a \frac{dw_a(t)}{dt} = W_d - W_{mv} - W_t - W_v - W_i \quad (2.58)$$

Where:

W_d is internal humidity gain (kg/s).

$$W_{mv} \text{ is humidity loss by mechanical ventilation : } W_{mv} = \rho_a q_m (w_a - w_o) \quad (2.59)$$

$$W_t \text{ is humidity loss by thermal buoyancy : } W_t = \rho_a n_t V_a (w_a - w_o) \quad (2.60)$$

$$W_v \text{ is humidity loss by wind pressure : } W_v = \rho_a n_v V_a (w_a - w_o) \quad (2.61)$$

$$W_i \text{ is humidity loss by natural air change rate : } W_i = \rho_a n_i V_a (w_a - w_o) \quad (2.62)$$

2.2.8 Modelling of plant and sensor dynamics

The point to note is that some modern buildings are multi-input multi-output systems. The actuator systems installed in the building will have different response characteristics and physical limits. As mentioned before that each building system will have different degree of responsivity. For example an under floor heating system is a slow actuating system because the release of heat is slow due to the thermal mass of the floor thus it takes time to heat up the floor. On the other hand a warm air system is a fast actuating system because it is faster to warm up the air and release it into the zone with instant effect.

For a building there are mainly four categories of systems: wet, air, storage systems, radiant and direct electric systems. Depending on the requirements and application the final decision is normally based on the required performance in terms of actuator bandwidth (speed of response) [(Franklin & Powell, 2005)]. However, all these actuation systems are highly nonlinear and the effective bandwidth of the actuation system can vary significantly with the amplitude of the input signal. The cause of this variation is normally very simple, in wet systems there is a maximum flow rate and temperature which can be achieved. Further more in dc motor drives (e.g. mechanical ventilation) there is a maximum rate which is a result of having to limit the motor current to prevent damage of the motor windings. Similarly in systems such as under-floor heating the floor temperature is a restriction to prevent discomfort for the occupants walking on the floor. These complex mix of non-linearities, control algorithms, building physics, fast & slow actuator time constants and disturbances (i.e. weather etc.) requires a science that can fundamentally show the factors affecting the controllability of buildings.

The response of these plant systems depends on their thermal and actuator dynamics. For example in an electric heater the heating element doesn't take very long to heat

up thus its thermal dynamics are fast. The actuator dynamics are related to the time constant of the power input to the plant (e.g. electrical power input to the electric heater) to reach maximum. Majority of these plant systems have first order actuator responses however their time constant vary depending on the type of system being used. The actuator is modelled as a first order system:

$$\tau_p \frac{d\dot{Q}_p}{dt} = [\dot{Q}_c - \dot{Q}_p] \quad (2.63)$$

Where: τ_p = time constant of actuator, \dot{Q}_c = Controller heat input required and \dot{Q}_p = Actuator heat output.

It is important to note that modelling such effects is important because in reality these dynamics are sometimes the reason for uncontrollable effects in a building. Part of the problem is that all plants are in reality nonlinear due to their limited output. Thus even though the building physics may be relatively simple and could be approximated with linear functions, the plant dynamics are nonlinear. However the effect of this nonlinearity can be inspected with controllability analysis. This may seem contradictory as the analysis depends on a linear state space model. The reason is that when inspecting controllability at a given operating point (i.e. linearised model) the nonlinearity (i.e. limited power) can be inspected for that operating point. Meaning whether at that operating point is the available power sufficient? Therefore depending on the thermal dynamics the plant system there could be second or third order and nonlinear in its overall response and thus modelling these dynamics is very important to controllability analysis of the building.

The function of sensors is to measure the temperature and relative humidity in the zone and to give feedback signal to the control system in order to enhance the performance of the system. The high performance CAB type buildings will require more information regarding performance and more accurate data. Sensors in buildings, especially related to HVAC control and lighting, will become more sophisticated and more of them will be deployed in buildings. These will be CO₂

sensors, photoelectric cells, thermostats, even micro-sensors embedded in the walls. The result will not only be more data but more accurate data of existing conditions, allowing for more accurate control of the system.

In high performance industries such as the aerospace, taking account of the sensor dynamics in conceptual design stage is crucial in developing the right controller design and ensuring controllability at commissioning stage. Sensor dynamics become very significant for controllability of a system when working at small time steps i.e. seconds or milliseconds such as in aircraft and missile applications. In these applications how fast and how often the sensor can take measurement is very crucial. However in building control systems, time steps are typically of minutes or hours and thus sensor dynamics are considered fast and are normally ignored. However it is important to model the transport delay in the system i.e. the effect of heater input seen on the air temperature sensor takes time due to transport delay. Thus modelling this delay is important in controllability assessment. Hence for completeness and explanation of the science and the assumptions, in this work it is assumed that the sensor is a first order system with a given time constant. Therefore, the equation can be written directly as:

$$\tau_s \frac{dT_{se}}{dt} = [T_{me} - T_{se}] \quad (2.64)$$

2.3 Model Appropriateness

In the last 20 years a lot of work was done to develop methods and techniques for model validation. The main methods are code checking, analytical tests [(Bland, 1992)], inter-model comparisons [(Judkoff & Neymark, 1994)] and empirical comparisons [(Lomas, Eppel, Martin, & Bloomfield, 1997)]. For an overview see: [(Bloomfield, Lornas, & Martin, 1992) or (Bartholomew & Robinson, 1998)]. Empirical validation is potentially very powerful (depending upon measurement uncertainties), but is restricted by a small number of cases for which high quality

datasets exist. As shown in the previous sections similar models were also developed by others and verified for simulation of causes and effects.

The type of lumped capacitance models presented have been utilised by many authors for simulation of thermal dynamics, both as a tool for testing building concept designs as well as for testing of control strategies, among them include Hudson, Underwood, Kampf, Nakanishi, Daskalov and Xu who have been referenced in the earlier sections of this chapter. Thus, the lumped parameter models are widely used in academia and industry as accepted methods for verifying proof of concepts. Such types of thermal models have been verified against ESP-r with good accuracy of their dynamics [(Kampf & Robinson, 2007)]. Although there is no such thing as a truth model, following the extensive and continued validation studies that have been carried out on ESP-r [(Clarke J. A., 2001)], this is a good candidate for a virtual building with which to compare results. Others have also verified these thermal models against real data [(Xu & Wang, 2008)] and testing standards [(ASHRAE standard 140), (Yuan & O'Neill, 2008)] and found results with good accuracy. Some have also used these for investigating dynamic behaviour of thermal mass in buildings [(Yam & Li, Nonlinear coupling between thermal mass and natural ventilation in buildings, 2003) & (Zhou & Zhang, 2008)].

A constitutive CO₂ concentration dynamics model was developed [(Aglan, 2003)] to predict the generation of CO₂ in building envelopes resulting from high occupancy. The model was experimentally verified in view of experiments conducted on an affordable, energy efficient, and healthy house. It was found that the model accurately predicts the generation of CO₂ from occupancy and the decay of CO₂ after the generation ceased. Daskalov (2006) extensively used these techniques for prediction and control of temperature and humidity simultaneously. His models were adequately represented by first order dynamic models and tests showed that the air temperature and moisture productions by the models agreed well with measured data. Likewise Delsante (2001) and Kavolelis (2008) also showed this for natural ventilation and the results were very accurate.

For indoor natural lux calculation, the literature contains two distinct methods. One is presented by Littlefair (1988) which utilises a factor for converting solar radiation into lux for different sky conditions and this derived using experimental measured data. The results show that a single factor can be used with fairly good results. The most common method is the daylight factor (DF) method which utilises the assumption of standard overcast sky distribution. There are concerns regarding the accuracy of the DF method [(Mardaljevic & Heschong, 2009)] and in this thesis a combination of these two methods is used as it allows for the variation in solar radiation to be taken into account more accurately. Solar gain transfer through the building fabric is represented using the sol-air temperature which is well established method by ASHRAE (2009).

Conservation of energy, mass and momentum

As mentioned in [(Clarke J. , 2006)] A lot of programs such as ESP-r are modular programs where the building systems are broken down into small control volumes (CV) within which properties such as mass, energy, momentum and contaminant flow are represented mathematically. As discussed earlier that validation is essential for improvement in the quality of a model since it increases confidence in the predicted result. The increasing use of thermal models requires that their accuracy be also assessed in terms of their predictions fulfilling conservation of energy, mass and momentum. As mentioned in [(Clarke J. , 2006)] the network approach as used in this thesis is not applicable for driving flows as there is no way to account for the conservation of momentum in the flow. Instead the inter-element couplings are characterised by temperature difference as the model is mainly concerned with heat transfer. However, in the case of modelling carbon dioxide and humidity levels, the internal and external zones are considered as single lumped nodes where the exchange of contaminants is driven by the internal and external concentration levels or in case of humidity the ratio of moisture in the air. The differential equation(s) represent the change in the variable due to infiltration and exhalation of that variable in the zone. Thus in this case it is assumed that the air flow is incompressible and hence the heat or contaminants entering by delta terms automatically satisfy conservation of mass.

In the development of his law for electrical circuits, Georg Ohm performed experiments that modelled Fourier's law of heat conduction. Consequently, an analogy between heat and electrical conduction can be observed. As found in the referenced literature, the analogy is useful in the analysis of several steady heat transfer problems from property measurement to modelling. In modelling, a complicated heat transfer analysis can be made much simpler by creating an "electric circuit" like model of the problem. This can be seen in the illustrative example above [Figure 4]. As shown in this figure, in thermal systems, this electrical analogy gives rise to the so-called thermal network model. The relationship between thermal and electrical systems can be summarized as follows:

Quantity	Thermal system	Electrical system (resistor)
Potential	Temperature difference = ΔT	V (voltage drop)
Flow	Heat flux = q	I (current)
Resistance	Potential / flow = $R = \Delta T / q$	$R = v/i$
Capacitance	Storage / Potential = $C = \int q dt / \Delta T$ [or $C(dT / dt) = q$]	$C = \int i dt / v$ [or $C(dv / dt) = i$]

Table 3 Analogy between thermal and electrical systems

The electrical to heat conduction analogy allows one to apply laws from circuit theory to solve more complicated conduction problems, such as the heat flow through conducting layers attached in parallel or series. The conservation of mass energy and momentum can be proven through the laws of circuit analysis i.e. Kirchoff's law. Kirchoff's Current Law or KCL, states that the "total current or charge entering a junction or node is exactly equal to the charge leaving the node as it has no other place to go except to leave, as no charge is lost within the node".

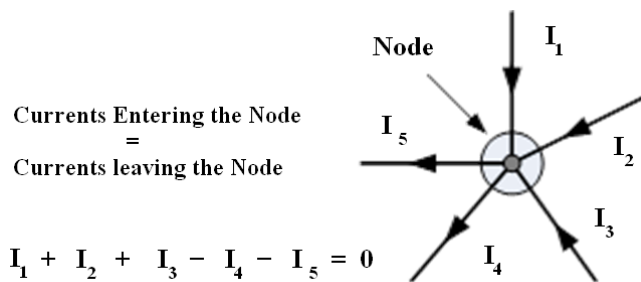


Figure 11 An electrical node through which current are entering and exiting

In other words the algebraic sum of ALL the currents entering and leaving a node must be equal to zero, $I(\text{exiting}) + I(\text{entering}) = 0$. This idea by Kirchoff is known as the Conservation of Charge. Here, the 3 currents entering the node, I_1, I_2, I_3 are all positive in value and the 2 currents leaving the node, I_4 and I_5 are negative in value. Then this means we can also rewrite the equation as: $I_1 + I_2 + I_3 - I_4 - I_5 = 0$.

The term node in an electrical circuit generally refers to a connection or junction of two or more current carrying paths or elements such as cables and components. Also for current to flow either in or out of a node a closed circuit path must exist. We can use Kirchhoff's current law when analysing heat (\dot{Q}) entering, leaving and stored in systems.

Hence an energy balance for any finite control volume can be written as follows:

$$\left[\begin{array}{l} \text{rate of change} \\ \text{of energy in V} \end{array} \right] = \left[\begin{array}{l} \text{net flow rate of} \\ \text{energy into V} \end{array} \right] + \left[\begin{array}{l} \text{internal energy} \\ \text{generation rate in V} \end{array} \right]$$

And for the i^{th} fixed volume, the rate of change of temperature given by:

$$(\rho c V)_i \frac{d}{dt} T_i = \sum_j q_{ij} + \dot{Q}_i \quad (2.65)$$

Where:

$$q_{ij} = \frac{(T_j - T_i)}{R_{ij}} = \text{net energy flow rate from node } j \text{ to node } i \quad (2.66)$$

R_{ij} = resistance between node i and j

$$(\rho c V)_i \frac{d}{dt} T_i = \sum_j \frac{(T_j - T_i)}{R_{ij}} + \dot{Q}_i \quad (2.67)$$

The above equation is referred to as the thermal network representation of the system. In thermal systems the above equation can be written as:

$$\dot{Q}_{in} - \dot{Q}_{out} - \dot{Q}_{stored} = 0 \quad (2.68)$$

Symbolically this equation can be written for the test case house as follows:

$$\dot{Q}_{in} = \left[\begin{array}{l} \dot{Q}_{sa} + \dot{Q}_{wi1} + \dot{Q}_{wi2} + \dot{Q}_{wi3} + \dot{Q}_{wi4} + \dot{Q}_{fi} + \dot{Q}_{ri} + \dot{Q}_{win} + \dot{Q}_m + \dot{Q}_{cp} \\ + \dot{Q}_{wo1} + \dot{Q}_{wo2} + \dot{Q}_{wo3} + \dot{Q}_{wo4} + \dot{Q}_{fo} + \dot{Q}_{ro} + \dot{Q}_{sm} + \dot{Q}_{rpm} + \dot{Q}_p \end{array} \right] \quad (2.69)$$

$$\dot{Q}_{out} = \left[-\dot{Q}_{wi1} - \dot{Q}_{wi2} - \dot{Q}_{wi3} - \dot{Q}_{wi4} - \dot{Q}_{fi} - \dot{Q}_{ri} - \dot{Q}_m - \dot{Q}_{rpm} - \dot{Q}_{cp} \right] \quad (2.70)$$

$$\dot{Q}_{stored} = \left[\begin{array}{l} (\dot{Q}_{sa} + \dot{Q}_{wi1} + \dot{Q}_{wi2} + \dot{Q}_{wi3} + \dot{Q}_{wi4} + \dot{Q}_{fi} + \dot{Q}_{ri} + \dot{Q}_{win} + \dot{Q}_m + \dot{Q}_{cp}) \\ + (\dot{Q}_{wo1} - \dot{Q}_{wi1}) + (\dot{Q}_{wo2} - \dot{Q}_{wi2}) + (\dot{Q}_{wo3} - \dot{Q}_{wi3}) + (\dot{Q}_{wo4} - \dot{Q}_{wi4}) \\ + (\dot{Q}_{fo} - \dot{Q}_{fi}) + (\dot{Q}_{ro} - \dot{Q}_{ri}) + (\dot{Q}_{sm} + \dot{Q}_{rpm} - \dot{Q}_m) + (\dot{Q}_p - \dot{Q}_{rpm} - \dot{Q}_{cp}) \end{array} \right] \quad (2.71)$$

Symbolically the above equations can also be verified using dynamic simulation. This result can show that the energy in the model is conserved and thus the symbolic model and simulation have correct boundary conditions and equations are taking account of all the energy transferred. This is one of the advantages of this modelling technique that if the model predictions are not accurate then symbolically the model can also be assessed for identifying the causes for inaccuracies in mathematics and physics by inspecting whether sum of all heat transfer is equal to zero or not. On the other hand, as mentioned in [(Gouda, Danaher, & Underwood, 2000)], that one of the reasons for inaccuracies in results of building models is that they are often used for conditions for which they are not valid, or their results are misinterpreted owing to poor understanding of the mathematical models on which they are based. For this reason in this thesis even though the model is not validated it has been simulated for further analysis to see if simplifications could be made to the model based on best practice principals. This has resulted in a model for industry to use which is less complicated mathematically and also preserves the dynamics of the fundamental causes and effects for analysis of the controllability of the building design and systems.

The point to note is that these models are used for symbolic analysis and simulation for investigating causes and effects and not for full blown detailed dynamic simulation and in the literature they have been extensively verified for their dynamics. As mentioned before the purpose of this model is not to emulate future reality, but to be able to use it in conceptual design phase to confirm the findings and results of the symbolic analysis method. Comprehending the model's assumptions

and limitations is more important than employing exact theories. A pragmatic approach is thus required when developing models and their validation for buildings.

So far the model presented in this thesis is for the general case of controllability analysis. However for majority of the cases in industry the thermal dynamics are the most important and further in this chapter the above model is simplified for the industry. These simplifications have been discussed in the light of controllability analysis case studies results presented later in the thesis.

2.4 Model for Industry

The mathematical model presented in the previous sections, is a full order model where all the fundamental dynamics have been modelled using differential equations (Note: the equations are explicitly given together at the start of appendix 4 for the full model). However, upon further analysis it can be concluded that a reduced order model is sufficient which can perform the same as the full order model. This requirement springs from the fact that the buildings industry in practice is low skilled in the use of dynamic simulation and modelling even though architects and building services engineers have the basic knowledge. It would be risky to assume that designers have a full understanding of mathematical models and control theory.

In high technology industries such as aerospace [(Magni & Bennani, 1997)] the mathematical models used for simulation of control systems are greatly simplified based on the controllability analysis underpinned by mathematics and control theory. A model is needed which is as simple as possible while preserves the fundamental dynamics based on best practice principals. This would allow for simple, understandable and manageable symbolic analysis and simulation for designers in industry at conceptual design stage of the building design process. Both higher and reduced order models can be used in research institutions where as the reduced order is for industrial application. The higher and lower order models can have the same dynamic performance when responding to frequency inputs below a threshold known as the bandwidth.

2.4.1 Assessment of the model's valid bandwidth

The concept of bandwidth of the model springs from a branch of control systems analysis known as the frequency response. A simple way to understand this is as mentioned in [(Distefano, 1995)]. When controlling a real system it is essential to know how it behaves when different signals are applied to it. This will give a measure of the dynamic response of the system. One way to find the response of a system is to apply a test signal to the input and look at the output to see how it responds. Many test signals are possible, but a simple and useful test signal is the sine wave. This is because ideally the output of a system with a sine wave input is also a sine wave, but with a different amplitude and phase. Although in some cases the output is not always a sine wave and this is useful because if the output is damped or constant then in frequency domain the causes can be investigated [(Clarke J. A., 2001)]. By measuring the output amplitude and phase of a system over a range of frequencies of the input sine wave, a particular version of the dynamic response is built – this is called the frequency response.

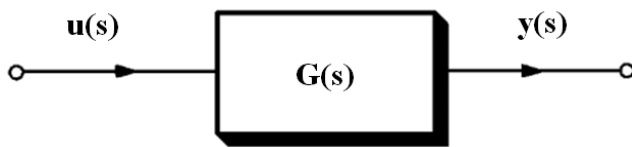


Figure 12 Linear transfer function with sine wave input

If a system has transfer function $G(s)$, then the output response at a particular frequency $\omega=2\pi f$ is given by the gain and phase of the frequency response $G(j\omega)$ at the frequency ω (i.e. $s=j\omega$). For the system shown above the input and output signals (after initial transient have gone) are in the time domain:

$$u(t) = U \sin(\omega t), \quad y(t) = Y \sin(\omega t + \phi) \quad (2.72)$$

The corresponding gain and phase are given by:

$$\text{Gain at } \omega = |G(j\omega)| = \frac{Y}{U}, \quad \text{Phase at } \omega = \angle G(j\omega) = \phi \quad (2.73)$$

By measuring the gain and phase over a range of frequencies, the full frequency response of the system can be plotted. The plot of the logarithm of the gain and phase against the frequency is called a Bode plot.

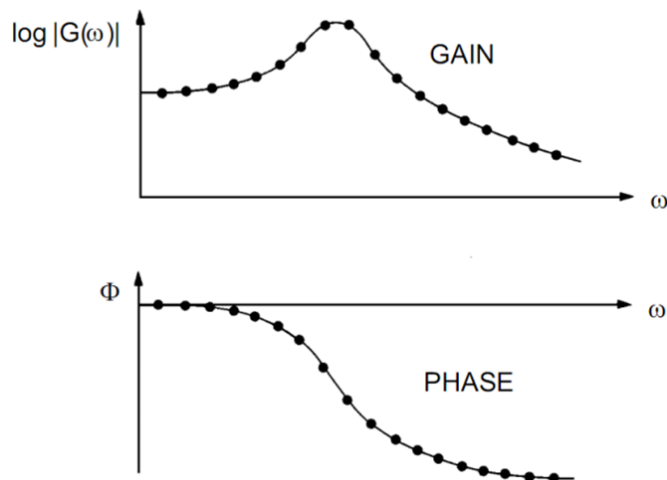


Figure 13 Presentation of frequency response data: Bode Plot

If a system has a transfer function [(Franklin & Powell, 2005)] $G(s)$, and its Bode plot is as shown in the above figure. Then it is shown that the amplitude of an output for a sine-wave input, as its frequency increases the amplitude reduces. This is basically conservation of energy, the faster your trying to move the system physically, the less it can respond, the energy is transferring less and less quickly, it gets attenuated and is being absorbed into storage elements.

The physical world does not respond at an infinite response and will eventually start to stop responding when request to respond at high speed (or frequency). The magnitude of the response of any system at some point is attenuated at that frequency. Until at a certain frequency the output is attenuated to very low levels such that in reality the measured output would have dynamics of high frequency and small magnitude also known as 'noise'. This response is so small in magnitude that the measured output can be approximated as constant.

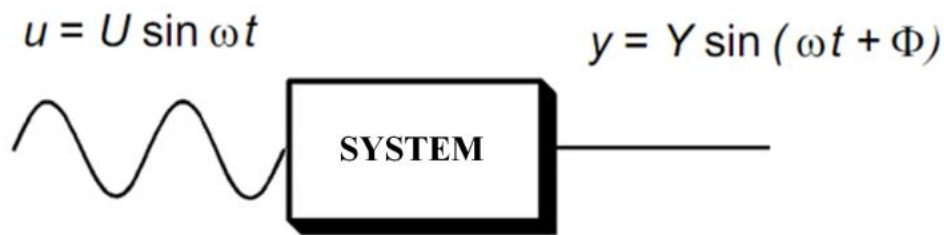


Figure 14 Response of a system to high frequency excitation (input)

Thus the signal dynamics being measured at low magnitudes and high frequency excitations is not related to the physics of the system but is all ‘noise’. Therefore modelling those inputs that result in noise only results in distorting the real output signal of the system therefore need not be modelled because in the real world the effect of those inputs will not be visible on the output signal. Hence, what is the point of modelling something in your model that you can never see in practice?

So for example modelling the dynamics of thermal capacitance of wallpaper in a building model such that if excited by a high frequency input the dynamics will reach steady state so quickly that it is not going to impact on what is being measured as the output. However as a general case it must be noted that high frequency fast dynamics attenuating is subject to stability of the system related to the resonant frequency. In general as long as the fast dynamics are attenuating beyond the resonant or unstable frequency then they can be considered ‘noise’ and ignored.

Thus, bandwidth (ω_b) is defined as the frequency at which the magnitude of the closed loop frequency response drops to 0.070 of its zero frequency value. In general, the bandwidth of a controlled system gives measure of the transient response properties, in that a large bandwidth corresponds to a faster response. Conversely, if the bandwidth is small, only signals of relatively low frequencies are passed, and time response will generally be slow and sluggish. Bandwidth also indicates the noise-filtering characteristics and the characteristics of the system in distinguishing signals from noise. Cut –off rate of the frequency response, is the slope of the closed loop frequency response at high frequencies [(Singh S. , 2009)].

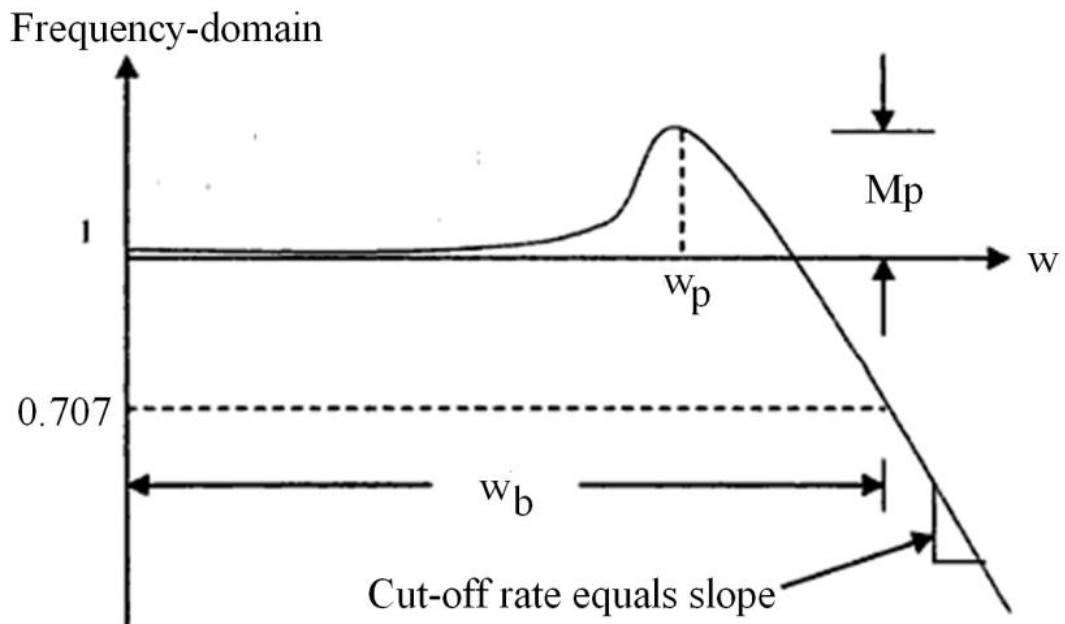


Figure 15 Frequency response specification

Hence for simplifying a higher order model to a lower order model requires the need to inspect their bandwidths. Therefore the concept of the model's bandwidth basically means that the high and low order physics models should have the same bandwidth i.e. the speed of response. By removing the high frequency or very low frequency dynamics from the higher order model, the model can be reduced to a lower order model which has the same dynamics as the higher order model. Thus the difference between the high and low order model is the removal of the high or very low frequency dynamics. Then a low order can be used instead of a complex higher order model. This is only possible upon inspecting the frequency dynamics that do not have an effect on the output signal and can be removed or assumed constant to reduce the model. To implement this for the current model singular perturbation theory is applied.

For simplification of the dynamics and bandwidth verification of the lower order model, firstly requires the simulation of the higher model. This is carried out using experimental data obtained from a test house heating experiment [Appendix 3].

2.4.2 Test case model

As shown in appendix 3, the test case is a mid terraced house in which the downstairs living room (labelled 1) was used for modelling and validation of thermal response. The measured data is from a co-heating experiment. Sensors were used to measure air temperature and the power consumed by the heater. The simulation results will be compared with these values. A basic schematic of the living room is given as follows:

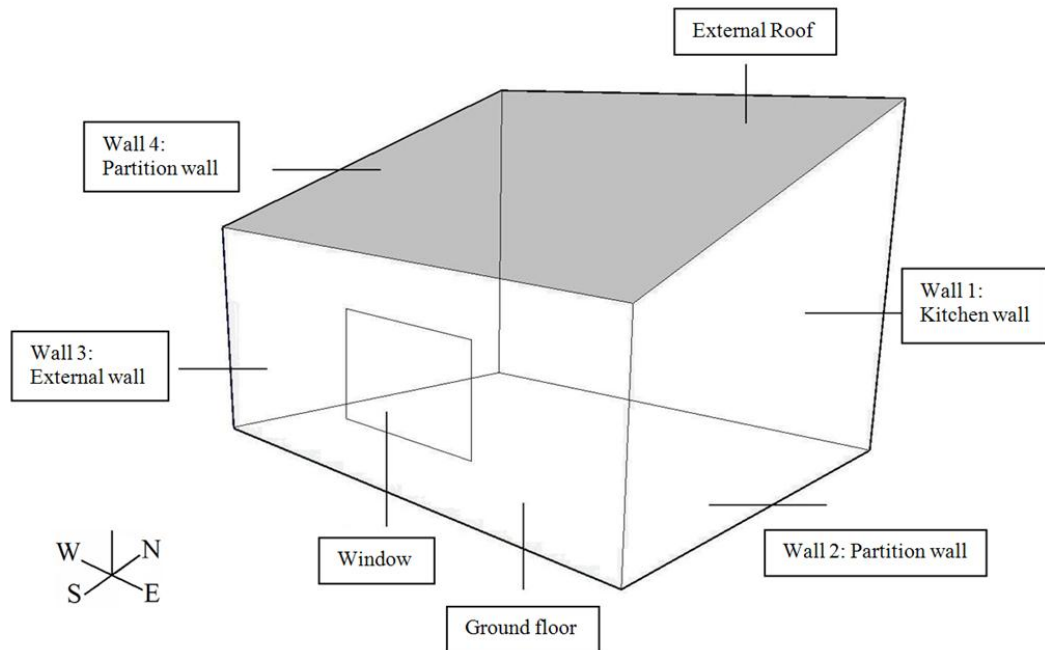


Figure 16 Three dimensional representation of the test house living room

Note: Kitchen wall is facing north, external wall south, partition wall (2) east and partition wall (4) west.

The mathematical model presented earlier takes into account the major causes and effects. However in modelling practice some of these causes and effects will have to be neglected depending on the case study. Thus for this particular test case the following points were taken into consideration:

As mentioned in appendix 3, while collecting data it was assumed that there is no heat transfer across the two partition walls. Thus walls 2 and 4 have no heat loss (i.e. no heat loss between houses) thus $\dot{Q}_{wo2} = \dot{Q}_{wo4} = 0$. The external wall (3) is connected to the outside temperature thus $T_{o3} = T_{sa}$; where T_{sa} is the sol-air temperature. The back wall of the zone is connected to the kitchen of the house. Thus, T_{o4} is the temperature of the kitchen. This house is an old 1980s mid terrace house and there is no passive stack or mechanical ventilation thus $\dot{Q}_t = \dot{Q}_v = \dot{Q}_{mv} = 0$. The natural air change rate was not taken into account as only a single room is being assessed where the air change rate is assumed to be small enough to have little effect on the heat transfer. For this experiment occupancy, appliances and lighting gains were not taken into account i.e. $\dot{Q}_{oc} = \dot{Q}_{ap} = \dot{Q}_L = 0$ as these were not active in the experiment.

The living room was furnished and it was assumed that it had a 2 piece sofa suite. For solar gain it was assumed that it was absorbed partly by the air (20 %) and majority of it by the internal thermal mass (80%). This was based on the assumption that majority of the time the temperature difference between air and thermal mass will be very small and it can be assumed that some of the solar is going directly into the air [(Gouda, Danaher, & Underwood, 2000), (Mitalas, 1965)] this was further discussed in the section 2.2.5. This ratio ($\alpha_a = 0.2$, $\alpha_m = 0.8$) was found to give satisfactory results however this is part of further work.

Oil filled Electric panel heaters were used for heating the front and back of the house on both floors [see appendix 3 for specification]. Because it's a small furnished room it was assumed that majority of the radiation from the heater goes into the internal thermal mass. The emittance was assumed to be 0.5 for a light painted radiator and the ground temperature was taken to be a constant 10 degrees Celsius. Other constants and more information are given in Appendix 3. First the full model was simulated and the results were compared. Then based on the simulation results the model was simplified from 10th order to 3rd & 4th order.

2.4.3 Simulation Method

There have been a number of developments in modular simulation programs such TRNSYS, HVACSIM etc with emphasis on HVAC plant and control. One restriction with these modular programs is that many of the plant component models are steady state or quasi-steady state making them suitable for low frequency dynamic analysis but unsuitable for high frequency disturbances, which are important in many instances for controller design.

A modelling environment that has the potential to meet these needs is ESL (European Simulation Language, ISIM Limited). ESL is a Continuous System Simulation Language (CSSL), which was originally designed for European Space Agency for satellite and spacecraft simulation. This modelling environment is a lot simpler in constructing simulations compare to SimuLink and Matlab. The main features of ESL are: (1) models can be built from sub models (2) separation of model and experiment (3) advanced discontinuity-handling (4) a parallel segment feature. Hence, this method has been used in the present work. The model was divided into sub models files representing plant, actuator and controller. The nonlinear mathematical model was entered in ESL code rather than constructing block diagrams.

ESL model is composed of three files

1. Data package file containing all the information about the building fabric
2. Building model file which includes all the mathematical equations
3. Actuator model file which contains the oil filled electric heater model
4. Controller file that contains the control algorithm for controlling the actuator
5. Main experiment file from which you can change the simulation parameters

The simulation was run for 10 days for which actual empirical data was available for comparison and validation. The simulation was run at 1 minute time step. The empirical data was at 15 minute step so for correlation a first order transfer function was fitted to allow for smooth running of the simulation.

2.4.4 Simulation Results

The empirical data was from a co-heating experiment where the heating system was used to see if the zone temperature was being maintained at different levels. Initially the temperature was maintained at 24 °C and thereafter at 28 °C. First the measured heater power setting is input to the heater model. This is part of the model and to compare the predicted and actual air temperatures. The plot of measured and estimated zone air temperature is given as follows:

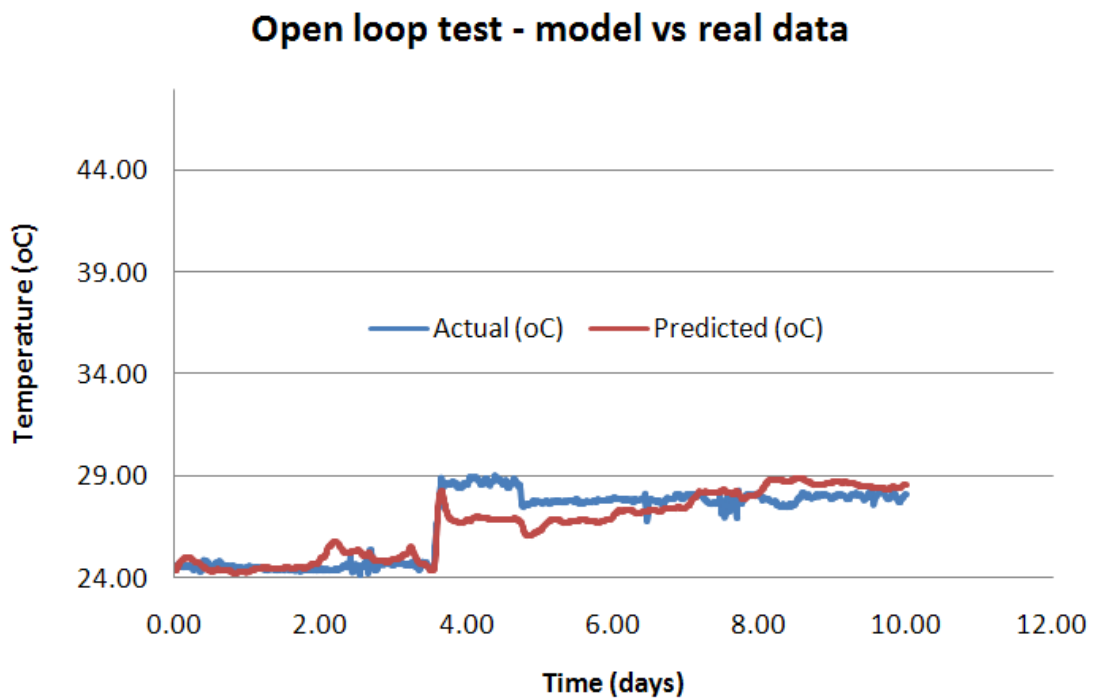


Figure 17 Comparison of the measured and estimated zone air temperature in the test house with measured heat power output (open loop test – model vs real)

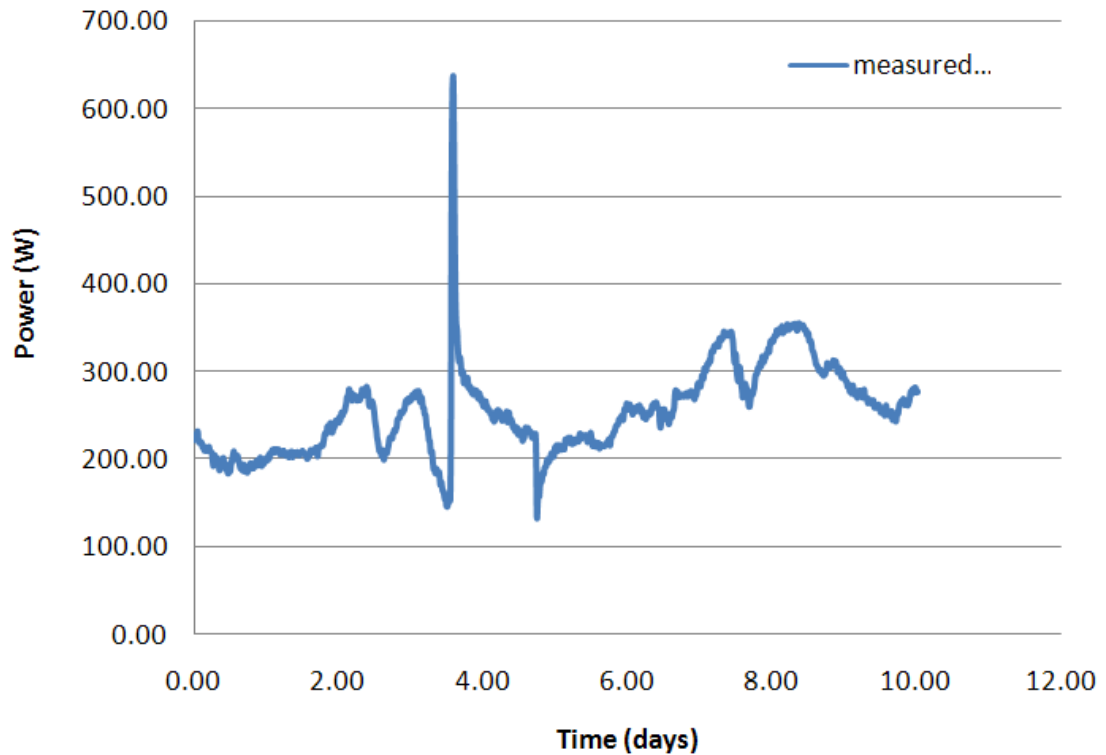


Figure 18 Measured heater power output in the test house

With injecting into the model the measured heater power the model predicts similar temperature profile to the one measured. However, it is obvious from

Figure 17 that the model is responsive. This is due to the effect of estimated parameter values especially internal thermal mass. For this case study very little information was available and a lot of values had to be approximated. The test house was built in the 1980s and upgraded to the latest regulations and the information available was very basic (such as U values etc) and detailed information such as material layers in the walls, floors etc were not available. Although the available information was not adequate never the less the estimated parameter values produced results close to the measured values. Thus, the sensitivity of the model to errors is not severe. Overall the error between field measurements and model results are within 1 to 2 degree Celsius which is reasonably good performance for a simple model.

Another simulation was carried out to test the basic plant model in comparison to the actual measured output of the heater in the test house. This test is a closed-loop test and is shown in Figure 19 which shows the modelled heater tracking the temperature. A simple PI controller was tuned to track the temperature set-points. Initially the set-point is at 24 degree Celsius and then after some time it changes to 28 degree Celsius.

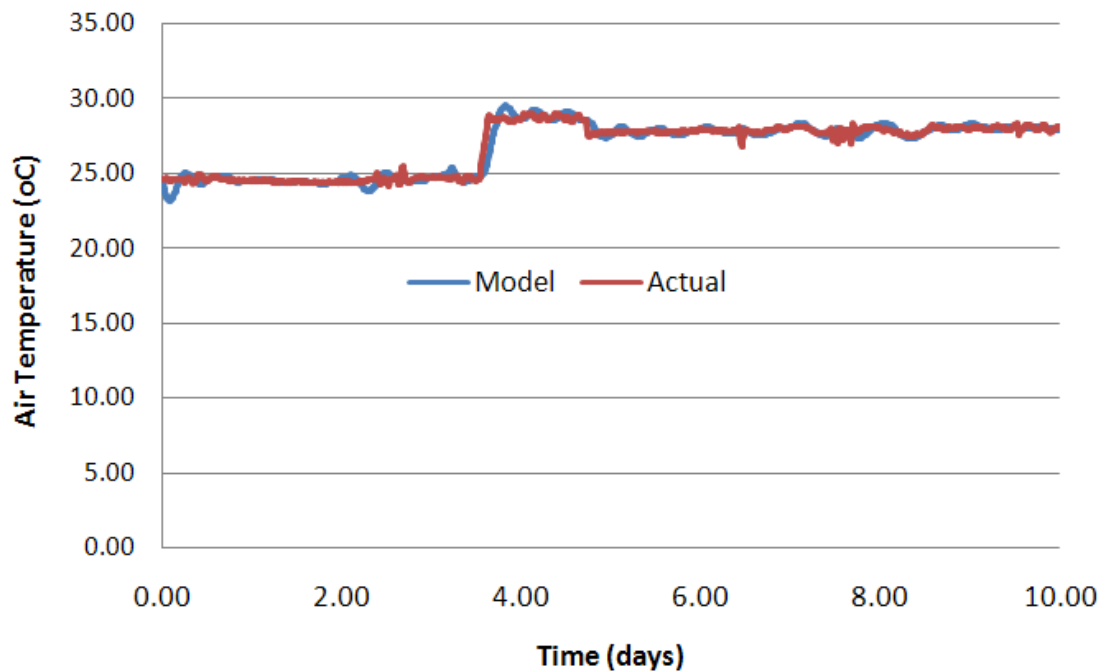


Figure 19 Comparison of the measured and estimated air temperature in the test house with model heater

Here using the modelled heater the temperature is tracked very accurately with maximum error of 0.5 degree Celsius. However the main result here is the comparison between the measured and estimated consumed power of the heater to achieve this response to desired set-point. This is shown in figure 20 below:

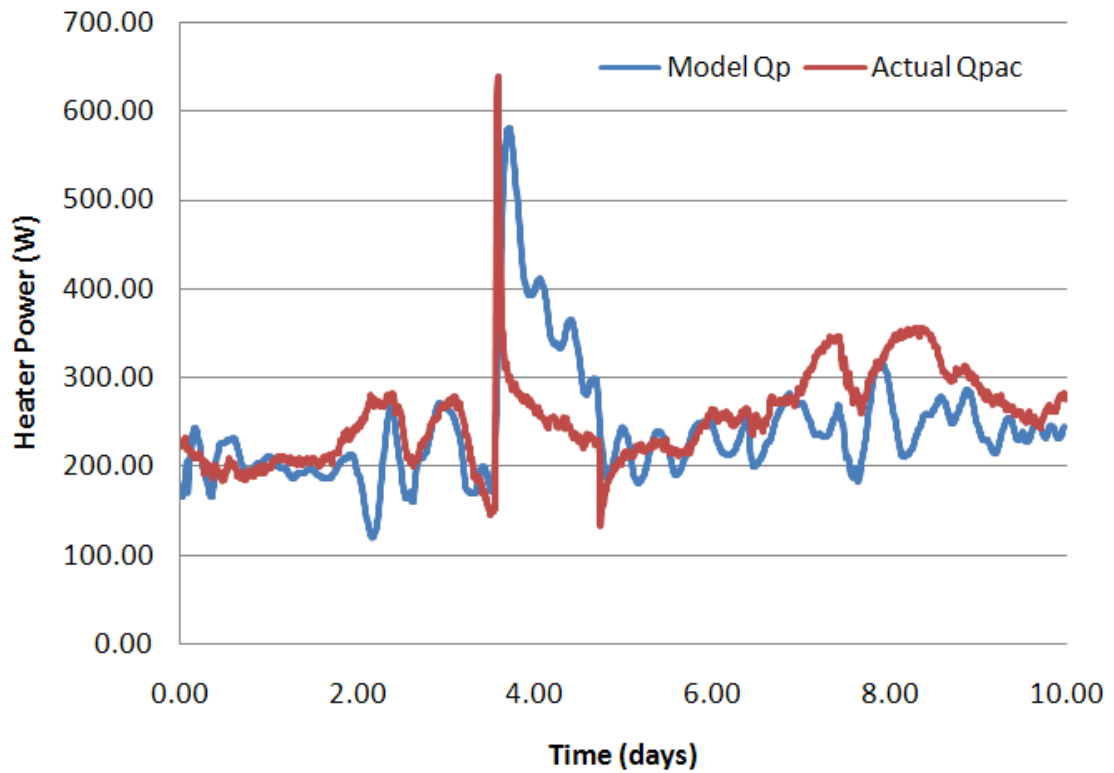


Figure 20 Comparison of the measured and estimated heat power output

Since the information about the oil filled heater parameters was limited, a rough estimate was used [see appendix 3]. In the last figure (above), the response of the heating system is shown. The error between the model predictions and field measurements is approximately 50W and at some points 100W. One of the reasons why the heater is taking more energy to maintain temperature compare to the field measurements is that it is assumed that a portion of the heat is going into the thermal mass. Obviously the position of the heater and thermal mass are not known. It was assumed that most of the energy would be transferring to the thermal mass. This would result in more energy consumption as the thermal mass such as furniture would need to be heated up to affect the internal air temperature. The detail information of the thermal properties of the internal thermal mass was not available thus the parameters for these were approximated. Thus good estimates of convection coefficients and information about where objects are placed and their thermal properties, in the room in relation to the plant have significant effect on the energy consumption. Convection coefficients may change depending on where the heater is

placed. In a lot houses the heater is hidden by the furniture arrangement and thus its effectiveness is decreased causing increase in the energy consumption. Considering that no information was available about the heater a rough estimated model performed very well. Overall the performance of the heater is showing larger energy consumption if considered over a long period; however its dynamic response and steady state gain are reasonably predicted.

2.4.5 Model order reduction

For model order reduction the temperatures of all the walls, floor, room and internal thermal mass were modelled. These modelled temperatures were simulated in closed loop heating and also open loop to inspect their dynamics over the 10 day simulation period and the results are as follows:

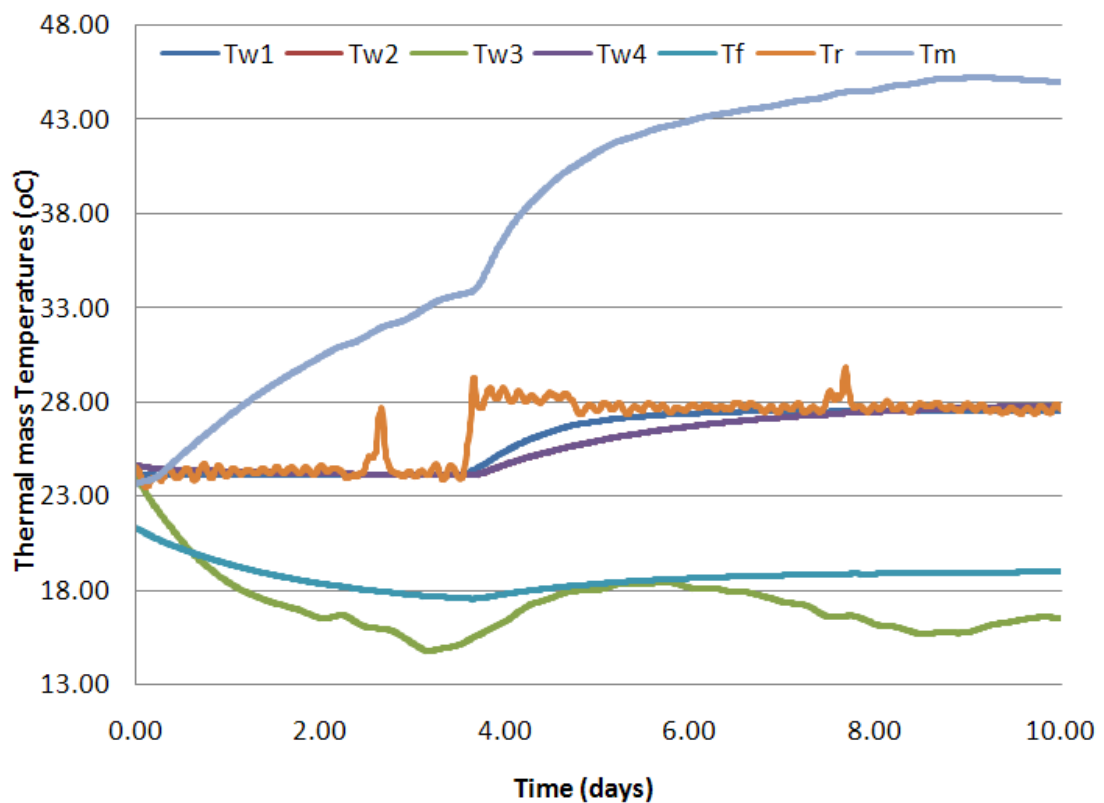


Figure 21 Thermal mass temperatures with heating (Closed loop)

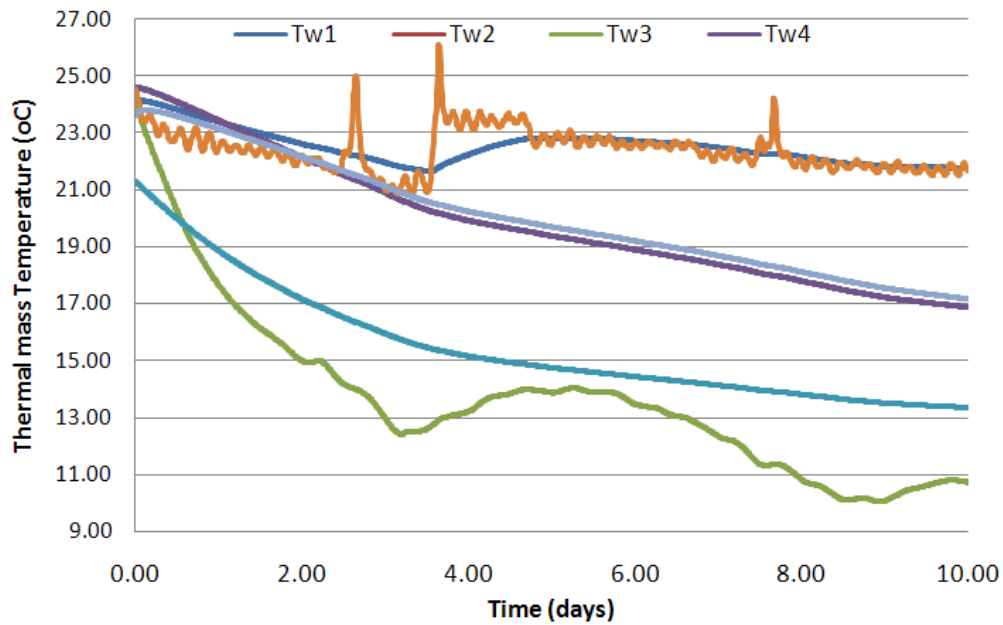


Figure 22 Thermal mass temperatures without heating (open loop)

These two figures above show clearly that apart from the wall (Tw3) that is exposed to external environment the rest of the thermal masses i.e. wall 1,2,4, floor and roof all have steady temperatures for the 10 day simulation period. The plots of Walls 2 and 4 are overlapping each other and thus only one of them is showing. Wall 3 is exposed to outside temperature and also it has thermal mass more than other elements as it has a brick layer. The other walls are also assumed to be brick layered however their temperatures are much more steady as they are exposed to temperatures from other zones of house with similar temperatures. The concrete floor having high thermal capacity has a very slow time constant and also due to the steady ground temperature. Based on this it can be concluded that for the requirement of a model for industry, only the external brick wall need to be modelled as it has thermal mass and also has dynamics that are neither too slow nor fast that they can be ignored and affect the internal temperature dynamics. However other elements such as internal walls or high capacity flooring can be assumed steady state due to dynamics that are either too slow or too fast to affect the controllability or controller design of the building systems and dynamics of the internal temperature. Internal thermal mass on the other hand needs to be modelled as furniture and other high mass elements affect the internal air temperature. Plus majority of the time the

internal thermal mass occupies the floor and receives a significant amount of the heat gain from the plant.

Obviously for long term simulations, the zone internal and external thermal mass dominates the dynamics response and energy consumption, where as for short term simulations, these dynamics could be assumed steady and in that case the dynamics of the zone air would be dominant. Apart from very slow plant systems such as under-floor, other systems such as, oil or hot water filled radiators, electric radiant or convector heaters have dynamics that are much closer to the zone air dynamics than thermal mass. Thus using simple equations for these plants still captures the key dynamics for air temperature control and therefore is sufficient for controllability assessment and controller design for industrial use [(Gouda, Danaher, & Underwood, 2000)].

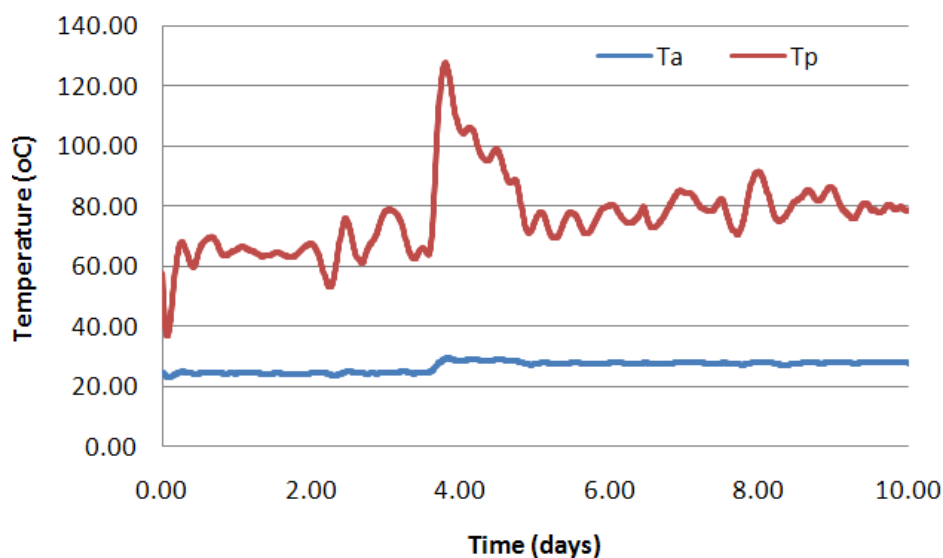


Figure 23 Comparison of dynamics of radiator temperature and air temperature for closed loop system

The above figure shows that the dynamics of the air mass are much closer to the heating system dynamics than to the internal and external thermal mass. Hence the plant temperature model can be simplified that still captures the key low frequency dynamics is in harmony with the dominant air thermal capacity effect of the space.

The zone model predicts the temperature reasonably however it all depends on the quality of information available for a building. As presented in the modelling section the actuator and sensors dynamics are modelled with first order dynamics. As shown in the next chapter these can be ignored or considered steady state as long as the controller bandwidth is at least 3 times slower than the bandwidth of the actuator and sensor dynamics [appendix 9]. Therefore the controller does not command the actuator faster than the actuator can physically respond.

This model is different in the sense that it has to balance between symbolic analysis as well as good simulation. The ways the different parts of the whole model are constructed are to allow for symbolic analysis to be carried out and the model to be modified from case to case basis which increases the flexibility of the model. The model can be modified and used for conditions for which it is more valid for. Hence in the next section it is shown how the model presented in this chapter can be further simplified which can predict the same dynamics but is much more simple and flexible for industrial use. It must be noted that this case study is not for validation but for basic analysis to understand what simplifications can be made for the reduced industrial model.

2.4.6 Singular perturbation analysis

Singular perturbation theory [(Kokotovic, Khalil, & O'Reilly, 1999)] is found to be a good approach to obtain a reduced order model. As mentioned in [(Ahmed, Schwartz, & Aitken, 2004)], the singularly perturbed system is first separated into separate approximate dynamical models for the slow and fast subsystems using quasi steady state methods. As mentioned in the earlier sections the fast subsystem usually presents the parasitic parameter that is usually neglected or unknown in normal mathematical modelling. Neglecting the parasitic element (by setting the appropriate closed loop bandwidth) is equivalent to setting the perturbed parameter 'e' to zero and the result is the reduced order system. As presented by Kokotovic 1999, the differential equations are presented in a state space format and then reduced, and for this test case house the method starts with the differential equations as follows:

$$\rho_a V_a c_{pa} \frac{dT_a}{dt} = [\dot{Q}_{sa} + \dot{Q}_{wi1} + \dot{Q}_{wi2} + \dot{Q}_{wi3} + \dot{Q}_{wi4} + \dot{Q}_{fi} + \dot{Q}_{ri} + \dot{Q}_{win} + \dot{Q}_m + \dot{Q}_{cp}] \quad (2.74)$$

$$\rho_{w1} V_{w1} c_{pw1} \frac{dT_{w1}}{dt} = [\dot{Q}_{wo1} - \dot{Q}_{wi1}] \quad (2.75)$$

$$\rho_{w2} V_{w2} c_{pw2} \frac{dT_{w2}}{dt} = [\dot{Q}_{wo2} - \dot{Q}_{wi2}] \quad (2.76)$$

$$\rho_{w3} V_{w3} c_{pw3} \frac{dT_{w3}}{dt} = [\dot{Q}_{wo3} - \dot{Q}_{wi3}] \quad (2.77)$$

$$\rho_{w4} V_{w4} c_{pw4} \frac{dT_{w4}}{dt} = [\dot{Q}_{wo4} - \dot{Q}_{wi4}] \quad (2.78)$$

$$\rho_f V_f c_{pf} \frac{dT_f}{dt} = [\dot{Q}_{fo} - \dot{Q}_{fi}] \quad (2.79)$$

$$\rho_r V_r c_{pr} \frac{dT_r}{dt} = [\dot{Q}_{ro} - \dot{Q}_{ri}] \quad (2.80)$$

$$\rho_m V_m c_{pm} \frac{dT_m}{dt} = [\dot{Q}_{sm} + \dot{Q}_{rpm} - \dot{Q}_m] \quad (2.81)$$

$$\rho_p V_p c_{pp} \frac{dT_p}{dt} = [\dot{Q}_p - \dot{Q}_{rpm} - \dot{Q}_{cp}] \quad (2.82)$$

$$\tau_p \frac{d\dot{Q}_p}{dt} = [\dot{Q}_c - \dot{Q}_p] \quad (2.83)$$

Based on the reasons given earlier about the dynamics of certain variables; equations (2.75), (2.76), (2.78)-(2.80) & (2.82),(2.83) can be reduced to steady state by setting the left side of the equations to zero. Then the corresponding equations relating to heat transfers etc are substituted and the temperature variable that was set to steady state for each equation must be made the subject. This is shown as follows:

$$T_{w1} = \frac{T_{o1} + T_a}{2} \quad (2.84)$$

$$T_{w2} = \frac{T_{o2} + T_a}{2} \quad (2.85)$$

$$T_{w4} = \frac{T_{o4} + T_a}{2} \quad (2.86)$$

$$T_f = \frac{T_{o5} + T_a}{2} \quad (2.87)$$

$$T_r = \frac{T_{o6} + T_a}{2} \quad (2.88)$$

For fast systems it was assumed that majority of the energy is directly input or taken out from the air with some energy transfer to the internal and external thermal mass. The model of a simple fast acting radiator was developed by [(Liao & Dexter, 2004)]. In the thesis, this model is used for representing an ideal fast acting heater and cooler plant. It was assumed that compared with the building zone, the radiator or cooler has a much smaller thermal inertia. The energy transfer from a radiator or cooler panel depends primarily on the temperature difference between the plant and the surrounding air. So the dynamics of the radiator can therefore be ignored and simplified as shown by [(Liao & Dexter, 2004)]. The heat transfer can be expressed as:

$$\dot{Q}_p - \dot{Q}_{rpm} - \dot{Q}_{cp} = \dot{Q}_p - h_r A_p (T_p - T_m) - h_c A_p (T_p - T_a) = 0 \quad (2.89)$$

The nonlinear terms in this equation are the radiation and convection coefficients. Because these constants depend on operating points therefore an average value was calculated for the whole range of simulation period for this case study. It was found that the variation in the values of the constants was not great and thus an average value was sufficient. These values are given in appendix 3. Hence, the steady state equation for the plant temperature T_p is given as follows:

$$T_p = \frac{\dot{Q}_p + h_r A_p T_m + h_c A_p T_a}{(h_r + h_c) A_p} \quad (2.90)$$

Lastly, based on the results in Figure 23 and the discussion, equation (2.83) can be set to steady state and substituted into the above equation:

$$\dot{Q}_c = \dot{Q}_p \quad (2.91)$$

Substituting these steady state equations into the differential equations(2.74), (2.77) & (2.81) and rearranging gives the following third order model; for air temperature:

$$\rho_a V_a c_{pa} \frac{dT_a}{dt} = \left[\begin{array}{l} \alpha_a \sigma_s A_{win} I_{dr} + U_{w1} A_{w1} (T_{o1} - T_a) + U_{w2} A_{w2} (T_{o2} - T_a) \\ + 2U_{w3} A_{w3} (T_{w3} - T_a) + U_{w4} A_{w4} (T_{o4} - T_a) + U_f A_f (T_{o5} - T_a) \\ + U_r A_r (T_{o6} - T_a) + U_{win} A_{win} (T_{o3} - T_a) + h_m A_m (T_m - T_a) \\ + h_c A_p (T_p - T_a) \end{array} \right] \quad (2.92)$$

External thermal mass:

$$\rho_{w3} V_{w3} c_{pw3} \frac{dT_{w3}}{dt} = [2U_{w3} A_{w3} (T_{o3} - T_{w3}) - 2U_{w3} A_{w3} (T_{w3} - T_a)] \quad (2.93)$$

Internal thermal mass

$$\rho_m V_m c_{pm} \frac{dT_m}{dt} = [\alpha_m \sigma_s A_{win} I_{dr} + h_r A_p (T_p - T_m) - h_m A_m (T_m - T_a)] \quad (2.94)$$

The above three equations represent the less complex reduced order model. As mentioned before the three most important components which concern the industry are the dynamics of air, internal and external thermal masses because these determine the thermal comfort of the internal environment. To be able to prove that the higher and lower models are thermodynamically the same requires them to be linearised and arranged into state space form for the frequency response analysis. The state space representations of full model (2.74)-(2.83) and the reduced model (2.92)-(2.94) are as follows (see Appendix 4 for symbolic matrix and their numerical values):

Higher order model: The vectors and matrices of constant coefficients of the state space model (i.e. A, B, C, D, E & F) are as follows:

Note: The state space model is a representation of differential equations in the form [(Richard C. Dorf, 2008)]:

$$\begin{aligned} \dot{x}(t) &= Ax(t) + Bu(t) + Fd(t) \\ y(t) &= Cx(t) + Du(t) + Ed(t) \end{aligned}$$

It must be also noted that A, B, C, D, E & F are constant coefficient matrixes of the state space representation. They are not to be confused with the symbols given in nomenclature.

$$\delta x = \left[\delta T_a \quad \delta T_{w1} \quad \delta T_{w2} \quad \delta T_{w3} \quad \delta T_{w4} \quad \delta T_f \quad \delta T_r \quad \delta T_m \quad \delta T_p \quad \delta \dot{Q}_p \right]^T$$

$$\delta u = \left[\delta \dot{Q}_p \right]^T$$

$$\delta d = \left[\delta I_{dr} \quad \delta T_{o1} \quad \delta T_{o2} \quad \delta T_{o3} \quad \delta T_{o4} \quad \delta T_{o5} \quad \delta T_{o6} \quad \delta \dot{Q}_p \right]^T$$

$$A = \begin{bmatrix} a_{11} & a_{12} & a_{13} & a_{14} & a_{15} & a_{16} & a_{17} & a_{18} & a_{19} & 0 \\ a_{21} & a_{22} & 0 & 0 & 0 & 0 & 0 & 0 & 0 & 0 \\ a_{31} & 0 & a_{33} & 0 & 0 & 0 & 0 & 0 & 0 & 0 \\ a_{41} & 0 & 0 & a_{44} & 0 & 0 & 0 & 0 & 0 & 0 \\ a_{51} & 0 & 0 & 0 & a_{55} & 0 & 0 & 0 & 0 & 0 \\ a_{61} & 0 & 0 & 0 & 0 & a_{66} & 0 & 0 & 0 & 0 \\ a_{71} & 0 & 0 & 0 & 0 & 0 & a_{77} & 0 & 0 & 0 \\ a_{81} & 0 & 0 & 0 & 0 & 0 & 0 & a_{88} & a_{89} & 0 \\ a_{91} & 0 & 0 & 0 & 0 & 0 & 0 & a_{98} & a_{99} & 0 \\ 0 & 0 & 0 & 0 & 0 & 0 & 0 & 0 & 0 & 0 \end{bmatrix}, B = \begin{bmatrix} 0 \\ 0 \\ 0 \\ 0 \\ 0 \\ 0 \\ 0 \\ 0 \\ b_{91} \\ b_{101} \end{bmatrix}$$

$$F = \begin{bmatrix} f_{11} & 0 & 0 & f_{14} & 0 & 0 & 0 & 0 \\ 0 & f_{22} & 0 & 0 & 0 & 0 & 0 & 0 \\ 0 & 0 & f_{33} & 0 & 0 & 0 & 0 & 0 \\ 0 & 0 & 0 & f_{44} & 0 & 0 & 0 & 0 \\ 0 & 0 & 0 & 0 & f_{55} & 0 & 0 & 0 \\ 0 & 0 & 0 & 0 & 0 & f_{66} & 0 & 0 \\ 0 & 0 & 0 & 0 & 0 & 0 & f_{77} & 0 \\ f_{81} & 0 & 0 & 0 & 0 & 0 & 0 & 0 \\ 0 & 0 & 0 & 0 & 0 & 0 & 0 & 0 \\ 0 & 0 & 0 & 0 & 0 & 0 & 0 & f_{108} \end{bmatrix} C = [1 \quad 0 \quad 0]$$

$$D = [0]$$

$$E = [0 \quad 0 \quad 0 \quad 0 \quad 0 \quad 0 \quad 0 \quad 0]$$

Lower order model: The vectors and matrices of constant coefficients of the state space model are as follows:

$$\delta x = [\delta T_a \quad \delta T_{w3} \quad \delta T_m]^T$$

$$\delta u = [\delta \dot{Q}_p]^T$$

$$\delta d = [\delta I_{dr} \quad \delta T_{o1} \quad \delta T_{o2} \quad \delta T_{o3} \quad \delta T_{o4} \quad \delta T_{o5} \quad \delta T_{o6}]^T$$

$$A = \begin{bmatrix} a_{11} & a_{12} & a_{13} \\ a_{21} & a_{22} & 0 \\ a_{31} & 0 & a_{33} \end{bmatrix}, B = \begin{bmatrix} b_{11} \\ 0 \\ b_{31} \end{bmatrix}, F = \begin{bmatrix} f_{11} & f_{12} & f_{13} & f_{14} & f_{15} & f_{16} & f_{17} \\ 0 & 0 & 0 & f_{24} & 0 & 0 & 0 \\ f_{31} & 0 & 0 & 0 & 0 & 0 & 0 \end{bmatrix}$$

$$C = [1 \quad 0 \quad 0], D = [0], E = [0 \quad 0 \quad 0 \quad 0 \quad 0 \quad 0 \quad 0]$$

For verification of the dynamics of the reduced model the bandwidths of the two models are compared. As discussed in earlier sections that if the bandwidths of the models i.e. speed of response, match then this means that reduced order model is sufficient for simulation in place of the higher order model for thermal analysis.

2.4.7 Frequency response and empirical verification

The dynamic performance of the reduced third order model in the frequency domain was verified by comparing Bode plots for the third order model and the equivalent higher order model response thermal circuits. The magnitude and phase gains are shown in plot below.

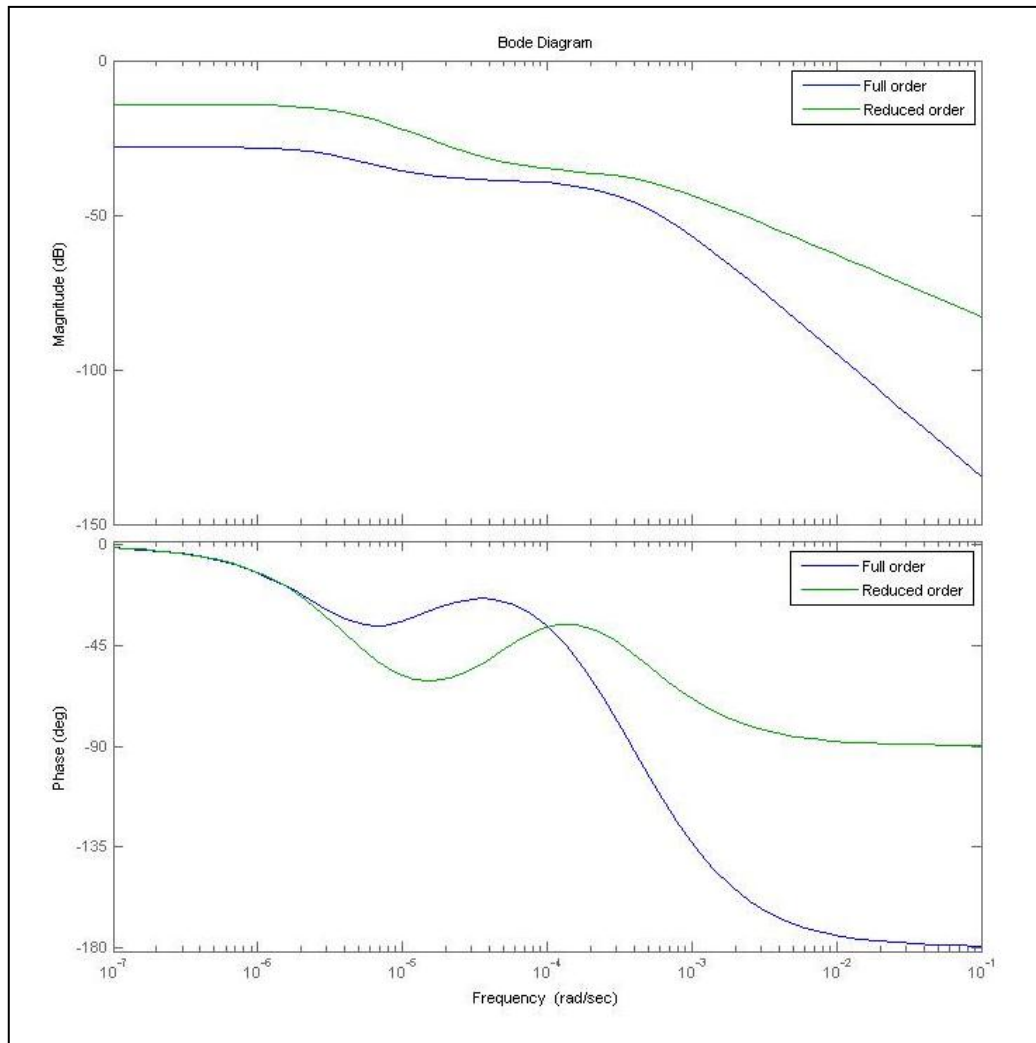


Figure 24 Bode plots of the two models for the test case house

The phase and magnitude frequency series of the two thermal circuits should ideally match – a perfect match would suggest perfect agreement in the time domain under all conditions. The plots provide a quick summary of the performance of each model network for the given room construction under sinusoidal excitation over a range of frequencies. The figure above shows the bode plot for the case study comparing the 3rd order and the full 10th order model. In both models the gain is measured at the air node so as to include the effect of the air mass and the heat considered to be injected at the air point. The error in the third order approximation to the higher order model has clearly been minimised at the 17 hours (10^{-4} rad/sec) period (Note: The error is large at 10^{-2} rad/sec because the reduced order model has difficulties dealing with

higher frequencies due to simplifications however generally this region of frequencies is ignored as it does not occur in buildings very often). The plot shows that the 3rd order model response is similar to that of the 10th order at very high frequencies (by the air mass) and at very low ones by the steady state U values of the thermal mass. There is an obvious difference in the magnitude of the gains of two models. With higher gain the reduced model is more sensitive to inputs and thus is shown by the simulation:

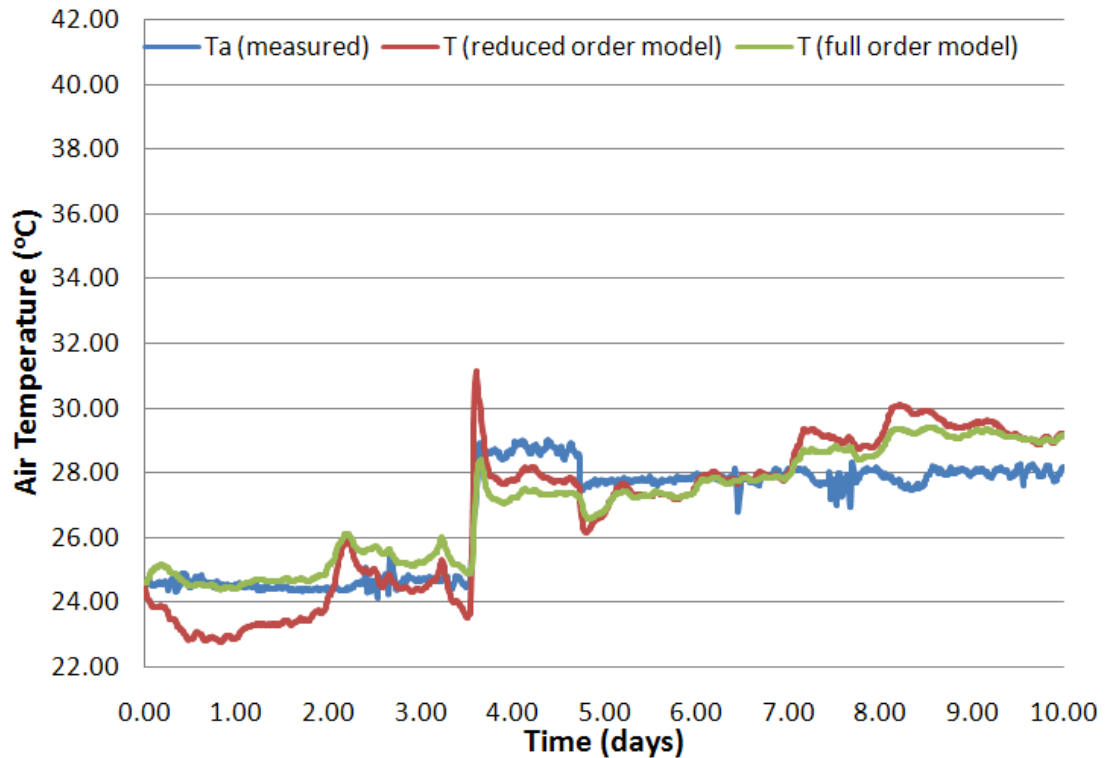


Figure 25 Comparison of the reduced and full order temperature response with measured temperature

This case study is with all the walls made of brick. It is obvious from the earlier Figure 17 & 18, that the walls temperatures of internal walls are not completely steady state. The temperatures are varying at a slow rate. Thus assuming these to be steady state will result in error as the walls are not heavy weight constructions which are enough to remain steady state. However this is not main reason for the higher gradients of the reduced order model. There are two points that are important to note

here. Firstly if the floor is assumed to be in steady state then its temperature will be much lower as the ground temperature is set very low. However in practice due to insulation or top layers such carpet or screed will restrict the flow of heat through the floor. This is the reason for the initial drop in the air temperature. Secondly the roof is composed of timber boards and insulation. This in practice would be steady state for this case study however for the general case the roof may not be in steady state due to boundary conditions and location of the zone.

Overall the dynamics of the reduced model are very close to the higher order model. As can be seen from the above simulation results above there is a slightly higher rate of change of temperature and the average maximum error is about 0.5 °C. Previous studies [(Bloomfield & Fisk, 1981)] have shown that variation of air temperature of ± 1.0 °C will have little effect on the mean radiant temperature at this frequency and the comfort temperature may vary by ± 0.5 °C. As shown in the frequency response there is a difference in the gain of the two models. The reason is that for the full model there is a convection component from the plant to the air node. When the plant temperature equation T_p is set to steady state and substituted into temperature equation it is being assumed that the plant is directly affecting the air node. Obviously due to direct injection of heat to the air node in the 3rd order causes the changes in air temperature to be faster as the dynamics of the heater are ignored. As a result of this the gain of the temperature node is slightly increased due to the substituted terms being positive causing the gain of the reduced model to be higher than the full order model. However this gain is constant for small frequencies and around the 24 hour point the gain reduces and thus response to those frequencies would be very similar to the higher order model.

Obviously from dynamics and energy consumption point of view the model is not fully acceptable as difference in gain will result in different results. It was decided to not to reduce to steady state the plant temperature equation. So that the reduced order model becomes a fourth order model. The state space model is given as follows:

Forth order model:

Note: The state space model is a representation of differential equations in the form [(Richard C. Dorf, 2008)]:

$$\dot{x}(t) = Ax(t) + Bu(t) + Fd(t)$$

$$y(t) = Cx(t) + Du(t) + Ed(t)$$

It must be also noted that A, B, C, D, E & F are constant coefficient matrixes of the state space representation. They are not to be confused with the symbols given in nomenclature.

$$\delta x = [\delta T_a \quad \delta T_{w3} \quad \delta T_m \quad \delta T_p]^T$$

$$\delta u = [0 \quad 0 \quad 0 \quad \delta \dot{Q}_p]^T$$

$$\delta d = [\delta I_{dr} \quad \delta T_{o1} \quad \delta T_{o2} \quad \delta T_{o3} \quad \delta T_{o4} \quad \delta T_{o5} \quad \delta T_{o6}]^T$$

$$A = \begin{bmatrix} a_{11} & a_{12} & a_{13} & a_{14} \\ a_{21} & a_{22} & 0 & 0 \\ a_{31} & 0 & a_{33} & a_{34} \\ a_{41} & 0 & a_{43} & a_{44} \end{bmatrix}, B = \begin{bmatrix} 0 \\ 0 \\ 0 \\ b_{41} \end{bmatrix}, F = \begin{bmatrix} f_{11} & f_{12} & f_{13} & f_{14} & f_{15} & f_{16} & f_{17} \\ 0 & 0 & 0 & f_{24} & 0 & 0 & 0 \\ f_{31} & 0 & 0 & 0 & 0 & 0 & 0 \\ 0 & 0 & 0 & 0 & 0 & 0 & 0 \end{bmatrix}$$

$$C = [1 \quad 0 \quad 0 \quad 0], D = [0], E = [0 \quad 0 \quad 0 \quad 0 \quad 0 \quad 0 \quad 0]$$

The forth row and column is for the plant temperature equation as given in the original model. The parameters are given in the Appendix 4.

It was found that the results for frequency response for the 10th order and the 4th order are almost identical. This indicates that the dynamics of the radiator are neither slow nor too fast to be completely ignored. This is very much the case in wet systems where there is a time lag in transferring of heat and part of it radiant and part convection and the liquid in the radiator takes time to change its temperature. The results are as follows:

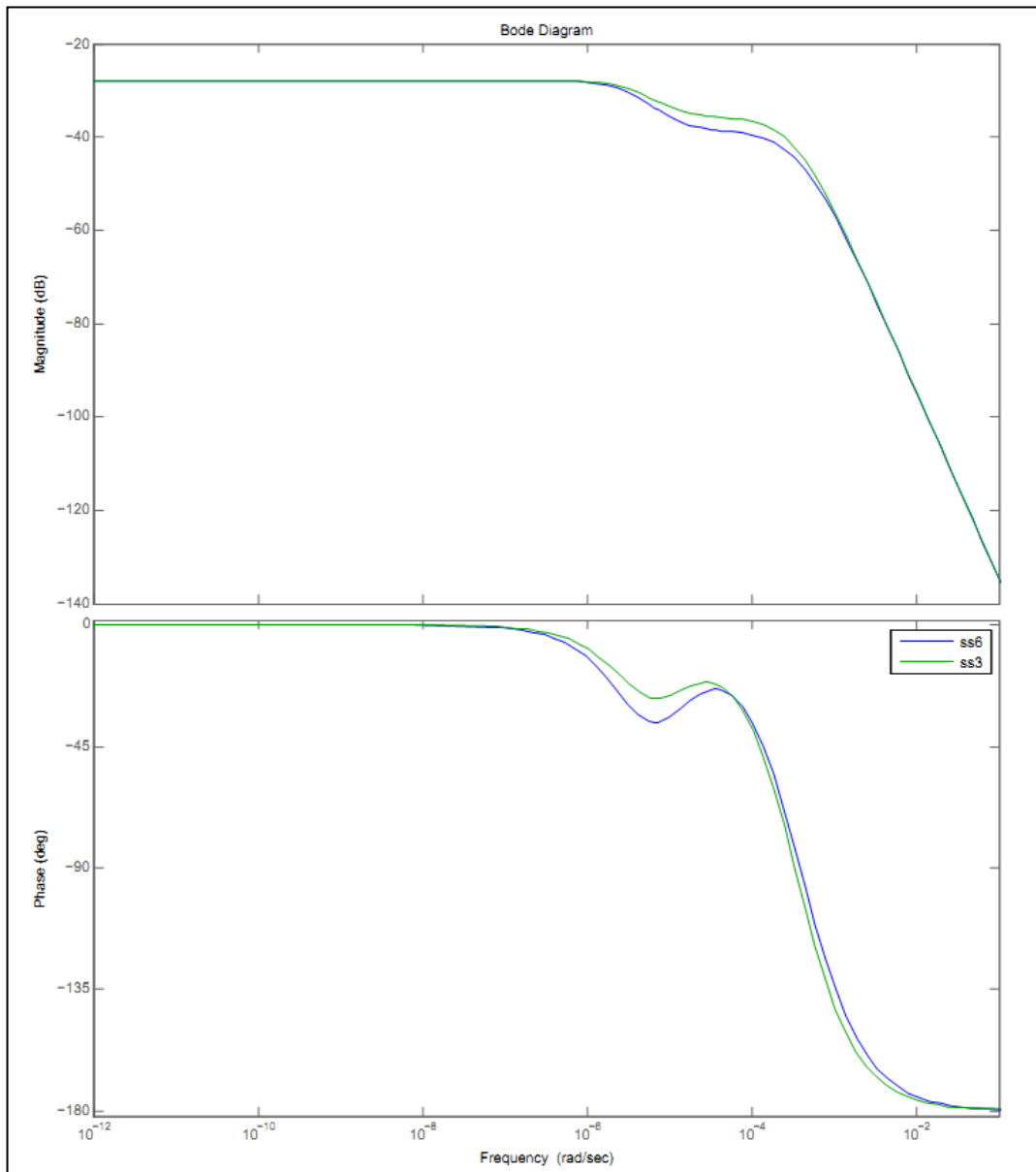


Figure 26 Bode plots of the 4th and 10th order models for the test case house

The bode plots are clearly showing that by not considering the plant to be steady state the dynamics are well matched of the two models. Here important point to note is that model order reduction for plant depends on the thermal inertia of the plant. By modelling the thermal inertia of the plant the gain of the reduced order model is reduced and thus the responses are very similar as shown below:

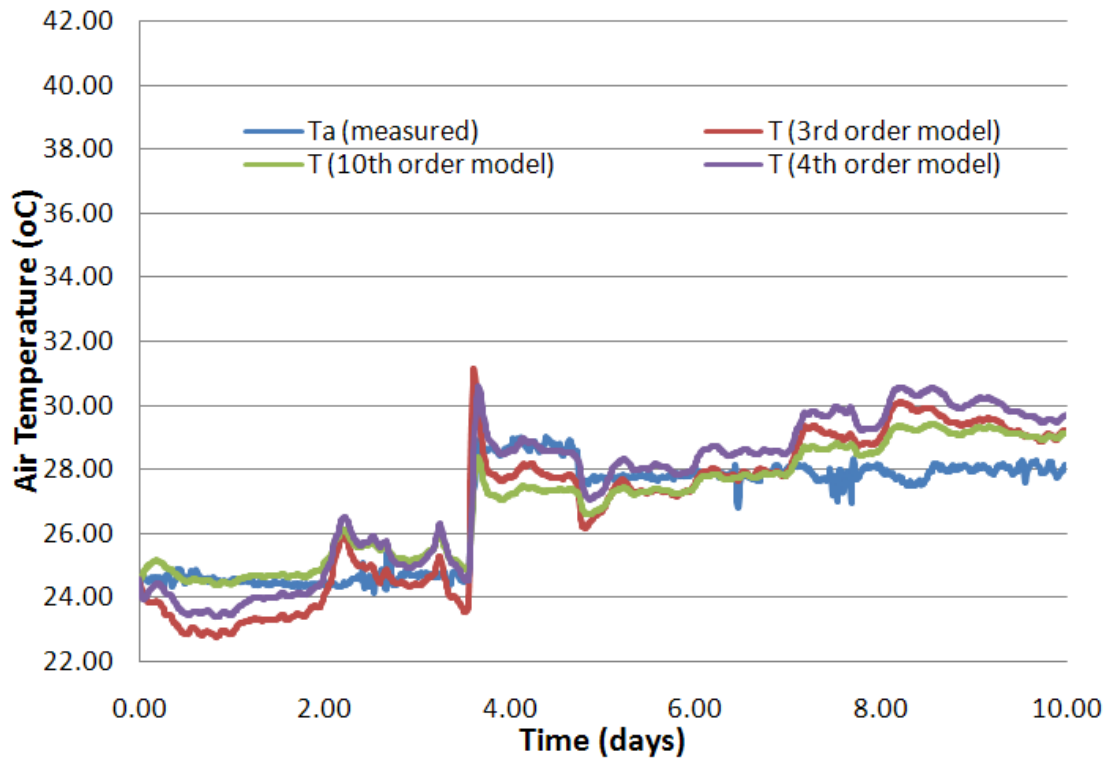


Figure 27 Comparison of the reduced and full order temperature response with measured temperature

The above figure is showing the comparison between the three models, 10th, 3rd and 4th order models. It is clear that there is very little difference between the 10th and 4th order models in terms of dynamic response. However there is a constant off set error between the three models and the 4th order model is predicting high temperature then the other two models. This can be explained from the plots of the dynamic and steady state temperatures of the heater as shown below. The plots show that the dynamic temperature is higher than the steady state and this would explain the predicted higher temperatures of the 4th order model. However, from the figure below it is obvious that by setting the heater dynamic to steady state does not have any effect on the dynamic of the heater thus the plant temperature equation can be set to steady state. From the above plots it is clear that the response of the air temperature is affected by the setting of the walls, floor and roof temperature to steady state. This is contrary to the bode plots shown earlier where the frequency response is perfectly matched. The reason is that in the simulations for this case study the boundary conditions for the partition walls were set to adiabatic and thus

there was heat transfer between the walls and the air internally. When these walls were set to steady state the internal heat transfer became zero. Therefore no heat was being absorbed by the internal partition walls causing the internal air temperature to rise.

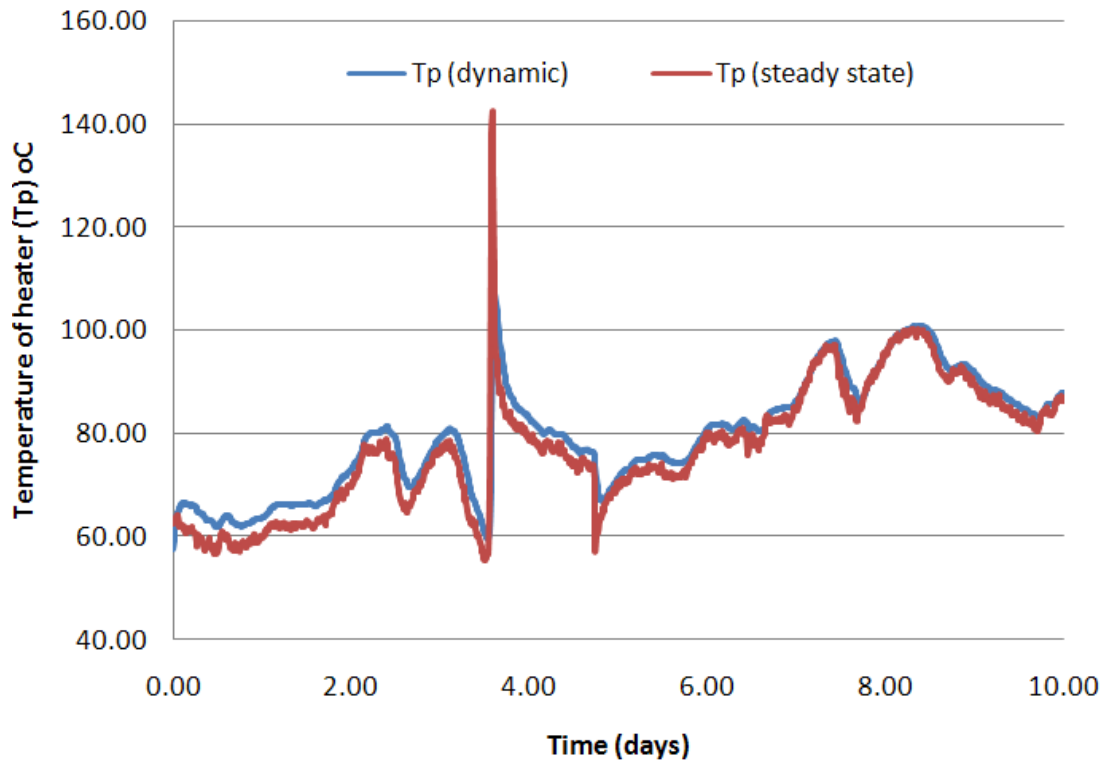


Figure 28 Comparison of the dynamic and steady state temperature predictions of the plant temperature

In the light of the above results it is suggested that the plant temperature can be set to steady state without causing large errors in results. The other errors in the results are due to the boundary conditioning rather than modelling of the zone. It is also recommended that for high thermal mass layer such as the floor it would be better modelling these as two resistances rather than one as this is a major factor in heat leakage through the zone. Thus it is a matter of dynamic accuracy which needs to be considered when looking at energy consumption and controllability. For controllability this will be less important as the third order model captures the dynamics reasonably good however for energy consumption it is more important as wrong gain values will predict for lower energy consumption than in practice which is not useful in the design process for energy efficient building design.

In conclusion the reduced order model is sufficient for assessment of both of controllability symbolic analysis as well as simulation. Based on the above results it is assuring that the model is accurate when used to model lightweight spaces such as the one presented in the case study where the walls were of normal brick. Hence the model would be sufficiently accurate for modelling heavy weight spaces. Lastly it is important to note that having good quality data would allow for more accurate analysis. However as mentioned before that control theory is used for removing errors in prediction and thus a combination of symbolic analysis with fairly accurate model predictions of dynamics are sufficient for controllability assessment as the building dynamics are less ruthless than in the case of aerospace systems.

2.5 Conclusions to modelling for controllability

There is a trade-off between accuracy and complexity in nearly all methods of analysing problems. It has been found that during the early design stage, a model which requires simple input and can be processed rapidly is often the most useful, if it can provide answers with sufficient robustness or precision for the design task. Early-stage design decisions which can have a fundamental impact on performance include, but are by no means limited to; building orientation, optimum window sizing, maximum plan width regarding natural ventilation and natural lighting [(Morbiter, 2003)].

The goal of all these tools is to inform design and contribute towards the construction of buildings more fit for purpose. It is essential that the appropriate tool is used for the task it is applied to, and the stage of the design process. It has been identified that the earlier in the design process decisions are made, the more impact those decisions have. When parameters are at their loosest and the design is to some extent flexible then design decisions can influence the end results in meaningful manner [(Lechner, 2001)].

It is therefore imperative that those charged with making these decisions at any stage in the process have access to the appropriate tools which allow for informed and

accurate decisions and so facilitate good design. Better understanding of the systemic relationships within buildings and the coupling of their parameters could improve early design and make for more meaningful impact on controllability of today's modern buildings.

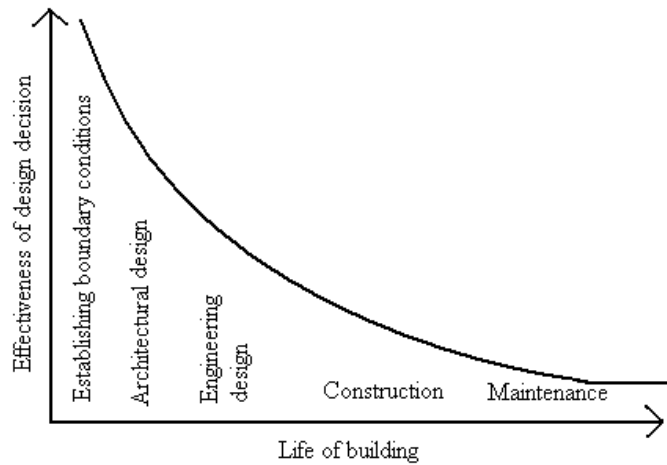


Figure 29 Decision impact vs. Building life [(Lechner, 2001)]

The mathematical single zone building models presented above fulfil the requirements for a model for controllability, simulation and controller design as will be shown later in the thesis. Overall it has been shown that both higher order and lower order models are very similar in their dynamics. It is intended that the higher order can be used by researchers who are working in fields of building design and controls for assessing the controllability of building and systems. Whereas, the low order model is aimed at providing fundamental results with quick simple analysis that can help designers currently in the building industry as will be shown in case studies (Chapter 5). The results from the case studies show consistent results between the symbolic analysis and simulations. The models have not only provided robust answers to early design stage fundamental questions, while preserving the dynamic and cross-coupled nature of the building energy system, but are able to quantify the relationships between the many variables and provide an insight into the effects of changing certain parameters. Hence the rationale of this thesis is to improve understanding of Climatic Adaptive Building systems, and hence improve the control of them.

3 : Theory of Controllability Assessment



The solar system: an example of a super nonlinear multivariable system operating perfectly.

3.1 Philosophy of Ideal System Response (ISR)

The engineering science for controllability assessment presented in this thesis is based on the ‘Ideal System Response (ISR) Philosophy’. This philosophy aims to establish for a given design, if an ideal response is feasible whilst maintaining controllability of the closed loop control system.

What is an ideal response of a system?

In theory an ideal system response is one where the system has no time delay in responding to the step change in set-point i.e. the set-point is followed exactly at all times. This is not possible because in reality the systems do not have infinite bandwidth i.e. in terms of buildings having infinite cooling and heating. **Hence an Ideal System Response achievable in practice is the first order response.** An example of a first order temperature response to step change in temperature set-point is given in the figure below:

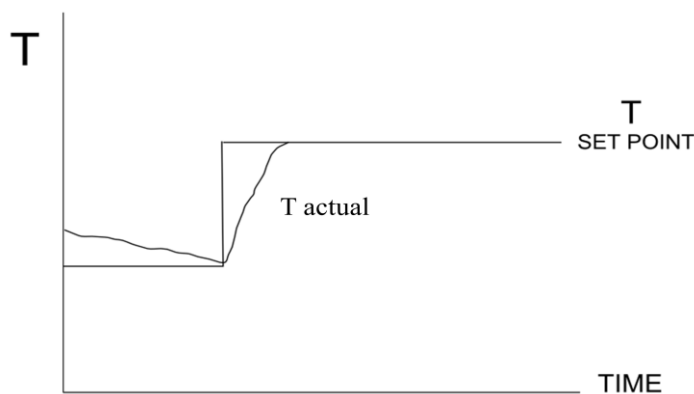


Figure 30: First order temperature response to step change in temperature

Stable First order systems behave well and are most easy to control. On the other hand, the response of real world is higher order and difficult to control i.e. there are oscillations, overshoots etc in the response. However, some higher order systems are dominantly first order. Dominantly first order system is the easiest to control in the real world. Hence the fundamental question is:

For any given system is Ideal System Response (ISR) possible?

The value of the feasibility of ISR is strictly in allowing the designer **to assess the ease in which dynamics of the system can be inverted**. The assumption is that the easier it is in theory to invert the dynamics of the system then in reality the easier it will be for the real system to achieve ISR. **This is because a nonlinear multivariable system can only achieve ISR if it is decoupled by inverting its dynamics as shown in this chapter**. The author believes that is a sound and thorough philosophy to adopt to establish the controllability of a building. In this thesis using the knowledge of inverse dynamics and control systems design developed for many years in various different disciplines, the controllability of the building model is assessed which in a modelling exercise provides the solution of ISR under feedback control. In a block diagram the ISR philosophy is composed as follows:

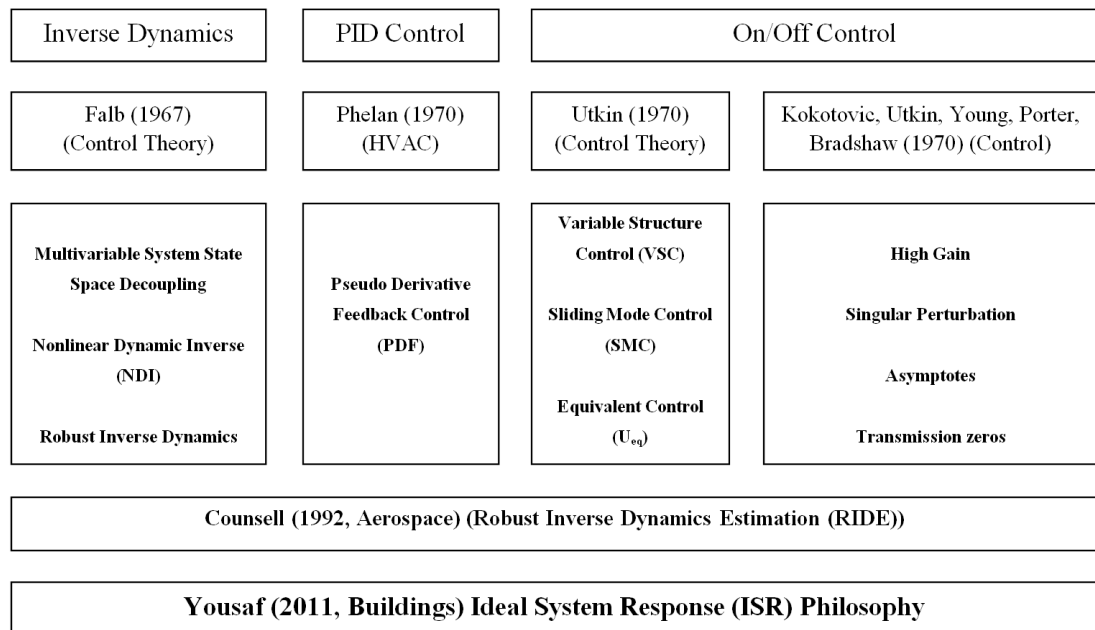


Figure 31 Block diagram of the ISR Philosophy

The following sections explain the theory of controllability assessment and the ISR philosophy:

3.2 Theory of Ideal System Response (ISR)

3.2.1 High Gain Control

Proportional feedback systems are based on the difference between the required set point and the actual value and the difference between them is called the error. For example: controlling temperature in a furnace the power is applied in direct proportion to the error. The amount of corrective action that is applied for a given error is set by the gain or sensitivity of the control system.

A proportional controller attempts to control the temperature of a furnace by applying power, P , to the heater in proportion to the difference in temperature between the furnace T_f and the set-point T_s i.e. error,

$$P = K(T_s - T_f) \quad (3.1)$$

where K is known as the *proportional gain* of the controller. As its gain is increased the system responds faster to changes in set-point. The higher the gain the fast the error will be corrected by the system.

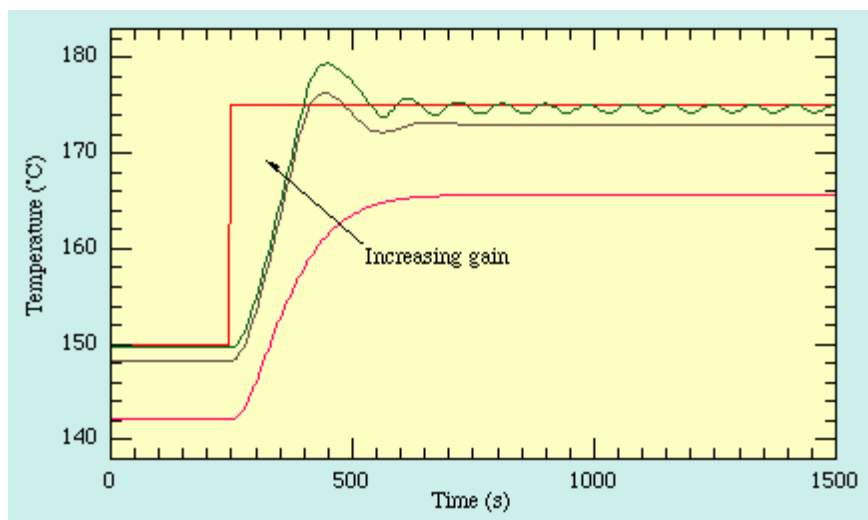


Figure 32 Temperature response as the proportional gain is increased

The concept of high gain can be understood mathematically as follows:

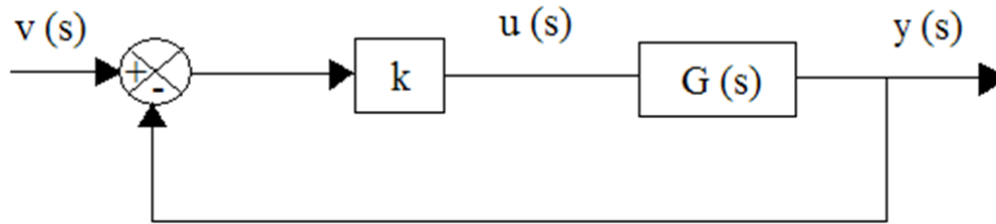


Figure 33 The simplest controller – a gain

The simplest possible controller (above) involves just multiplication of the error by a scalar gain K . The overall input ($v(s)$) and output ($y(s)$) relationship i.e. transfer function is given by:

$$\frac{y(s)}{v(s)} = \frac{K G(s)}{1 + K G(s)} \quad (3.2)$$

The principal of high gain can be applied to this system by saying that: If K (system gain) is very high (infinity) then the overall transfer function is approximately:

$$\frac{y(s)}{v(s)} = \frac{K G(s)}{1 + K G(s)} = 1 \quad (3.3)$$

i.e. provided that $K \gg 1$ ISR can be obtained. In other words, $y(s) = v(s)$, meaning that at infinite gain output is equal to the input i.e. you have reached set-point and are steady state.

Question: What happens as $k \rightarrow \infty$? Will this give better and better control?

Answer:

- (i) As K is increased, the system may become unstable and unusable.
- (ii) Assuming that the system remains within input to the system limits as $k \rightarrow \infty$, then we have arrived at a switch (relay) control system.

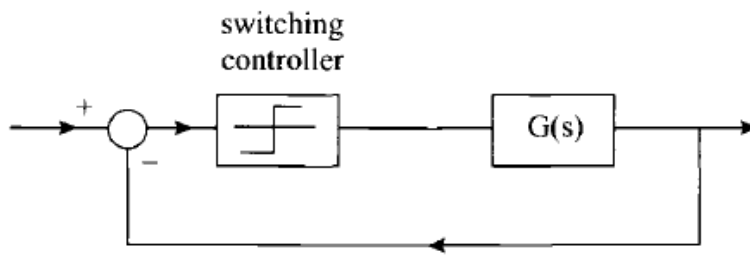


Figure 34 As $k \rightarrow \infty$, the controller becomes a relay

In reality you cannot drive the gain to infinity however it is possible to realise an infinite gain process over a small amplitude, also known as relay, on/off or bang bang control. In a bang bang control system the decisions are made based on target and threshold values, and the system decides whether to turn the controller on or off. Bang bang control has significant practical advantages that lead to it being widely applied across industry e.g. to control the temperature in the room.

Even though Bang-Bang control is very simple, it's theory is also the origin of the more advanced concepts in control engineering, such as Robust Inverse Dynamics Estimation (RIDE) (Counsell J. M., 1992) which are the basis of the controllability science presented in this thesis. As a result of the discontinuous control signal, systems that include bang-bang controllers are variable structure systems, and bang-bang controllers are thus variable structure controllers.

3.2.2 Variable Structure Control (VSC) & Sliding Mode Control (SMC)

Variable structure control, or VSC, is a form of discontinuous nonlinear control. The method alters the dynamics of a nonlinear system by application of a high-frequency switching control. The state-feedback control law is not a continuous function of time; it switches from one smooth condition to another. So the structure of the control law varies based on the position of the state trajectory; the method switches from one smooth control law to another and possibly very fast speeds. Variable structure control (VSC) and associated sliding mode behaviour was first investigated in early 1940s in the Soviet Union [(Meerov, 1947)].

To realise VSC, a switching surface or function was introduced, which was called by the Russians as “ s_x ” given by [(Utkin, Variable structure systems with sliding modes, 1977)]:

$$s_x = \begin{cases} u = L & s_x > 0 \\ u = -L & s_x \leq 0 \end{cases} \quad (3.4)$$

Which says that when s_x is greater than zero the actuator should be at maximum limit i.e. L , and when s_x is less than or equal to zero then the actuator should be at minimum limit i.e. $-L$. Sliding mode control is a particular type of variable structure system designed to drive and then constrain the system state to lie within a neighbourhood of the switching function s_x .

In other words during the sliding mode the discontinuous control chatters about the switching surface at high frequency. This sliding mode approach transforms a higher-order system into a first-order system. In this way, simple control algorithms such as PID can be applied which can be very straight forward and robust. How can this be possible? In theory it is described as follows:

Consider an on/off control system which is just one special case of VSC, when $s =$ error i.e. difference between the set-point and the output. Now the nonlinear single input dynamic system can be represented by:

$$\dot{x}(t) = f(x(t), t) + f(u(t), t) \quad (3.5)$$

Where the scalar x is the state of the system of interest (for instance, the temperature of a building), the scalar u is the control input (for instance, a heat from a heating system).

The control problem is to get the state $y(t)$ to track a specific set-point $v(t)$.

Let $e(t) = v(t) - y(t)$ be the tracking error in the variable $y(t)$, where $y(t)$ is the measured output value of the state $x(t)$. Furthermore, let a surface s_x be defined by the equation $s_x(t) = e(t)$ that varies about the surface $s(t)=0$ as the control input u switches between u^+ and u^- . Thus, the problem of tracking i.e. $y(t)=v(t)$ is equivalent to that of remaining on the surface s for all $t > 0$. When in sliding mode the surface $s_x=0$ is reached and the rate of change of $s_x(t)$ is equal to zero.

$$\dot{s}(t) = \dot{v}(t) - \dot{y}(t) = 0 \quad (3.6)$$

$$\text{when } v(t) = \text{constant} \Rightarrow \dot{v}(t)=0 \Rightarrow \dot{y}(t)=0 \quad (3.7)$$

Now consider a linear system:

$$\dot{x}(t) = Ax(t) + Bu(t) + Fd(t) \quad (3.8)$$

Where the output or measured variable $y(t)$ is related to the state $x(t)$ by:

$$y(t) = Cx(t) \quad (3.9)$$

At sliding mode i.e. steady state, the rate of change of output is equal to zero.

$$\dot{y}(t) = C\dot{x}(t) = 0 \quad (3.10)$$

Substituting the $\dot{x}(t)$ equation into $y(t)$:

$$\dot{y}(t) = CAx(t) + CBu(t) + CFd(t) = 0 \quad (3.11)$$

The input signal which drives the system dynamics $\dot{s}_x(t) = 0$ is:

$$u(t) = -(CB)^{-1} CAx(t) - (CB)^{-1} CFd(t) \quad (3.12)$$

Which, if substituted back into the original state equation:

$$\dot{x}(t) = Ax(t) + B\left(- (CB)^{-1} CAx(t) - (CB)^{-1} CFd(t)\right) + Fd(t) \quad (3.13)$$

This results in: $\dot{x}(t) = 0$

Thus in sliding mode the system of appropriate magnitude of control is immune to the external disturbances and is able to reach steady state and this is the essence of the celebrated invariant property of SMC. This virtual control input U derived above is known as the equivalent control input $U_{eq}(t)$.

3.2.3 Equivalent Control

A simple approach to robust control, and the main topic of this chapter, is the so-called sliding control methodology. Intuitively, it is based on the remark that it is much easier to control 1st order systems (i.e., systems described by 1st order differential equations), be they nonlinear or uncertain, than it is to control general n^{th} order systems (i.e., systems described by n^{th} order differential equations). It is then easy to show that, for the transformed problems, “Ideal” performance can in principal be achieved in the presence of arbitrary parameter inaccuracies. The equivalent control method [(Utkin, 1971)] in the output feedback mode yields a reduced-order system exhibiting output feedback equivalent dynamics [(Slotine & Li, 1991)]. This methodology can be viewed as a form of realisable inverse dynamics due to the use of equivalent control input which inverts the model with respect to the controlled outputs.

For a feedback control system steady state tracking [(Bradshaw & Counsell, 1992)] of a constant reference input $v(0)$ can be expressed as,

$$\lim_{t \rightarrow \infty} e(t) = v(t) - y(t) \Rightarrow 0 \quad (3.14)$$

If this condition (above) is satisfied then the tracking condition will be satisfied even in the presence of a disturbance vector $d(t)$. It is clear that the above condition depends on what is being measured? Therefore it is important that what is measured in, approaches the desired output $y(t)$ in steady state. The input $U_{eq}(t)$ uses inverse dynamics to determine the actuator inputs that are required to ensure zero rate of change of the outputs. It does this by taking into account the disturbances and system dynamics that would otherwise prevent the system from operating like an ideal integrating system.

Consider a basic control system which has a controller matrix K and an extra input $U_{eq}(t)$.

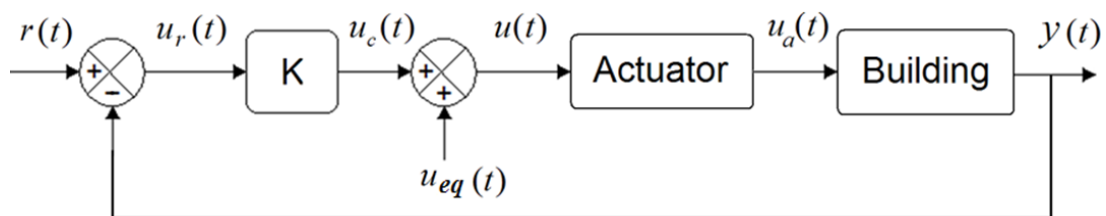


Figure 35 Block diagram of the control system with controller matrix $K(t)$ and dynamic inverse input $U_{eq}(t)$ where: $u_r(t)$ = reference input to the controller, $u_c(t)$ = controller output, $u(t)$ = control signal to the actuator, $u_a(t)$ = actuator output, $y(t)$ = actual output of the system and $r(t)$ = desired output.

Note: It is, of course, essential that all relevant actuator dynamics are represented in the state equation (3.8). However, it is also important not to include high frequency dynamical modes which would serve only to obscure the important features at the initial design stage. For this reason, the dynamical modes associated with the actuators and sensors are not included. Of course, these dynamics are important and are incorporated into the model in section on bandwidth (3.2.5) to show their effect on controllability. For demonstrating the order reducing property of $U_{eq}(t)$, here the dynamics of the actuator are assumed to be fast compare to the control system bandwidth, thus the transfer function of actuator is equal to 1. Hence $u(t)$ becomes $u_a(t)$.

From above figure, $u(t) = u_c(t) + u_{eq}(t)$. This is substituted into the state equation (3.8) to give:

$$\dot{x}(t) = Ax(t) + B(u_c(t) + u_{eq}(t)) + Fd(t) \quad (3.15)$$

The output equation (3.9) differentiated (rate of change of output) and the state equation is substituted into it. Then a Laplace transform ('s') is taken to give a transfer function from input to output and from disturbance to output:

$$sy(s) = [CAx(s) + CB(u_c(s) + u_{eq}(s)) + CFd(s)] \quad (3.16)$$

The $U_{eq}(s)$ input is chosen such that it reduces the system to a first order system. For the system under consideration the $U_{eq}(s)$ as derived earlier is given by:

$$u_{eq}(s) = [-(CB)^{-1} CAx(s) - (CB)^{-1} CFd(s)] \quad (3.17)$$

Substituting this back into equation(3.16) yields:

$$sy(s) = CBu_c(s) \quad (3.18)$$

$$\frac{y(s)}{u_c(s)} = s^{-1}ICB \quad (3.19)$$

In closed loop error actuated control with K as given above the system is represented as follows:

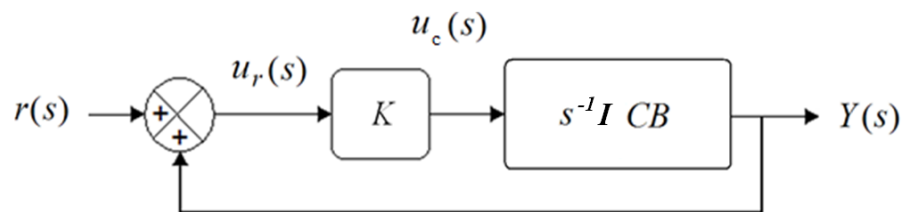


Figure 36 Block diagram of a simple feedback control system with controller matrix K

Thus it is shown that the U_{eq} can reduce a higher order system to a first order system represented by a s^{-1} ICB transfer function. This is the generic reduced order transfer function for any n^{th} order system with some controller gain K , injected with U_{eq} . Thus, U_{eq} can be assumed to be an inverse dynamics input to the system which is able to **decouple** a complex higher order system and causes it to behave like a first order system even with disturbances. Therefore in theory this is an IDEAL SYSTEM RESPONSE (ISR) PHILOSOPHY.

How to know the feasibility of ISR for a system?

3.2.4 Feasibility of ISR

The purpose of $U_{eq}(t)$ is to act as the inverse dynamics input that makes the system transfer function reduced to first order i.e. CB/sI , making the system easier to control with ideal response. Thus existence of a CB matrix for a system tells us that dynamics of the system are invert able and thus ISR is feasible.

Up to now the assumption was made that the basic equation $\dot{y}(t)=0$ is non-degenerate, and from it the equivalent control is derived uniquely. For the system considered in equations (3.8)-(3.9), this assumption means that CB matrix is full rank. It is important to know when the degenerate cases arise where this condition is violated. Theoretically this is shown as follows:

Consider the linear system described in equations (3.8)-(3.9), but with disturbance matrix $F=0$, has the general transfer function:

$$\frac{Y(s)}{U(s)} = C(sI - A)^{-1} B = \frac{\text{Adjugate}(sI - A)}{\text{determinant}(sI - A)} CB \quad (3.20)$$

A general series expansion of the transfer function gives:

$$C(sI - A)^{-1} B = \frac{CB}{s} + \frac{CAB}{s^2} + \frac{CA^2B}{s^3} + \dots \quad (3.21)$$

Where the quantities $CB, CAB, CA^2B, \dots, CA^k B, \dots$, are called the Markov parameters of the system, which are sufficient to completely determine the system transfer function. The significance of Markov parameters can be understood using the concept of relative degree. Relative degree is a concept used in the classical control theory. But it is also directly related to modern control theory as it explains the reason for CB being rank defective.

The degree of the denominator ($|sI - A| = 0$) of transfer function is always equal to the system order n , but the degree of the numerator $C \text{Adjugate}(sI - A)B$ is included between 0 and $n-1$. The relative degree of linear system also called relative order or characteristic index, is equal to the difference between the degrees of denominator and numerator of transfer function.

The relative degree of linear system is defined by [(Corriou, 2004)]:

$$CA^p B = 0 \quad \text{for all } : p < r - 1 \quad (3.22)$$

$$CA^{r-1} B \neq 0 \quad (3.23)$$

The relative degree r is the smallest integer such that: $CA^{r-1} B \neq 0$. The system will thus have a relative degree r such that:

$$\begin{aligned} r &= 1 \text{ if } CB \neq 0 \\ r &= 2 \text{ if } CB = 0 \text{ and } CAB \neq 0 \\ r &= 3 \text{ if } CB = CAB = 0 \text{ and } CA^2 B \neq 0, \dots \end{aligned} \quad (3.24)$$

The relative degree, if it exists, is necessarily such that: $1 \leq r \leq n$. The relative degree can also be considered from a different angle by taking into account the successive time derivatives of the output y :

$$\begin{aligned}
\frac{dy}{dt} &= CAx \\
&\vdots \\
\frac{d^{r-1}y}{dt^{r-1}} &= CA^{r-1}x \\
\frac{d^r y}{dt^r} &= CA^r x + CA^{r-1}Bu
\end{aligned} \tag{3.25}$$

The relative degree is thus the smallest degree of differentiation of the output y which depends explicitly on the input u [(Corriou, 2004)].

As shown in equation(3.24), the system with a relative degree of 1 has a CB matrix with rank non zero, whereas relative degree greater than 1 results in CB matrix rank equal to zero. For this reason when a complete feedback control system is modelled its CB matrix rank is inspected for ISR to be feasible i.e. CB rank should be non zero and this means the relative degree of the system is equal to 1.

3.2.5 Factors that prevent inverting the dynamics and ISR tracking

Ideally it is preferred that systems should have a first order response i.e. relative degree of 1. First order systems are simple and easiest to control. However in the real world the systems are not first order but are of higher order. Theoretically the problem above is solved by using the U_{eq} input that converts the higher order system into 1st order. The problems arise when actuator and sensor dynamics are added to the system. In reality the sensors and actuators have dynamics and they are not zeroth order. The order of actuators and sensors makes the overall closed loop system have a relative degree greater than 1. This poses a problem as relative degree greater than 1 leads to CB rank defective as shown in the last two equations.

Consider a simple block diagram of a generic control system:

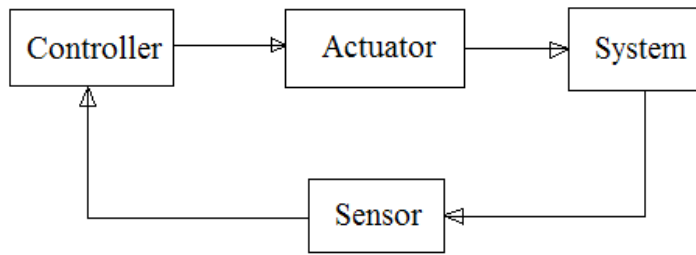


Figure 37 simple block diagram of a generic control system

Assuming that the system, actuator and sensor are all first order and the controller has a gain k , then the block diagram of this is as follows:

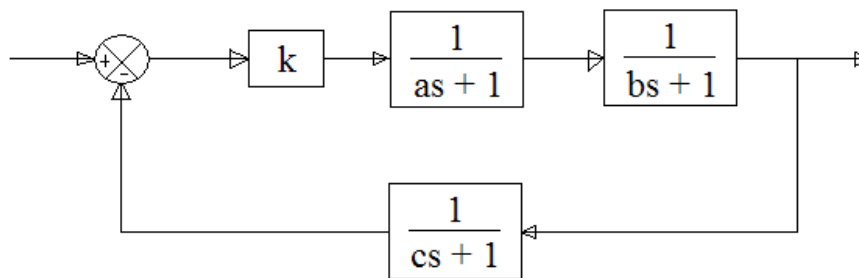


Figure 38 first order system block diagram

Where a , b and c are time constants of actuator, system and sensor respectively. For the control system in the above figure, the closed loop transfer function TF is given by:

$$TF = \frac{(cs + 1)k}{(as + 1)(bs + 1)(cs + 1) + k} \quad (3.26)$$

It is known that the difference between order of numerator and the denominator equations of the transfer function is the relative degree i.e. the difference between number of poles and zeros of the closed loop system. Here the numerator is first order and the denominator is third order. Thus here the relative degree of the overall system is $3 - 1 = 2$.

As shown the dynamics of the actuator and sensor causes the overall relative degree to be higher than 1. The dynamics of the system, plant and sensor are fixed and cannot be modified. However it is possible to operate the control system at a speed such that it can be assumed that the dynamics of the actuator and sensors are fast and thus can be neglected in controllability analysis. The speed of response is known as the bandwidth. Typically the closed loop bandwidth is kept three times slower than the bandwidth of actuator and sensors (refer appendix 9) to allow for safe operation and neglecting their dynamics as “parasitic” for ease in modelling. This is a reasonable assumption in the aerospace where the dynamics of actuation systems are very fast however in building this factor of three might be different and this requires further research for proof. Thus if these parasitics are neglected (i.e. transfer function equal to 1) then the closed loop transfer function of the system in Figure 38 would be given as:

$$TF = \frac{k}{bs + 1} \quad (3.27)$$

Thus by neglecting the parasitic the relative degree is reduced to 1.

In reality most systems that are controlled are not first order systems. Most systems are higher order however a lot of systems can be approximated by a second order transfer function. The problem of higher order modelling and relative degree greater than 1 can be solved by neglecting the actuator and sensor dynamics (if they are fast compared with the desired closed loop response) and transport lag through keeping the controller bandwidth three times slower. However it must be noted that sensor dynamics are significant in applications where reaction times are in seconds or less. In other applications such as buildings this is not very important and can be neglected however still relative degree may still remain higher than 1 due to inherent system dynamics such as transport lag in buildings cause the same problem. This means that sometimes the system being controlled (i.e. building) with the required feedbacks is still with relative degree greater than 1. In these cases the only variable that can be altered is the feedback for achieving relative degree of 1 (e.g. first case

study section 5.1) Thus assuming a unity controller gain with second order system and neglecting the “parasitic” the block diagram is be given as follows:

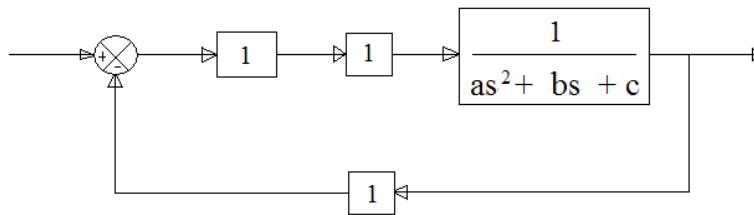


Figure 39 Second order system block diagram

For the control system above the closed loop transfer function TF is given by:

$$TF = \frac{1}{as^2 + bs + c + 1} \quad (3.28)$$

Here the numerator is zeroth order and the denominator is 2nd order. Thus here the relative degree of the system is 2-0=2. This means that the CB is rank defective and thus ISR is not feasible. Now if the order of the feedback signal is increased by differentiating the output signal; the block diagram is given as follows:

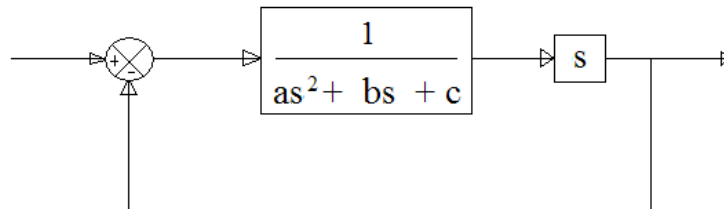


Figure 40 Second order system with derivative feedback block diagram

For the control system above the closed loop transfer function TF is given by:

$$TF = \frac{s}{as^2 + (b+1)s + c} \quad (3.29)$$

Here the relative degree is 1 i.e. 2-1=1. Thus it is shown that by analysing the system symbolically and knowing its relative degree, appropriate feedback signals can be chosen to make the system CB full rank for system to be feasible for ISR and thus in

practice this results in a simpler control problem allowing simple controller to be applied.

It is important to note that with relative degree of 1 and CB matrix being full rank does not mean that ISR will be easy to achieve as the degree of ease in achieving ISR is determined by the structure of the full rank CB matrix.

3.2.6 Degree of ease in achieving ISR

Once it is confirmed that CB is full rank then it is also important to inspect the CB for the degree of ease in which ISR that the system can achieve. The CB matrix allows for calculation of an important property of the overall system called the asymptotes. The asymptotes of the system are important in estimating the degree of ease in which ISR can be achieved.

At this point it is useful to recall the significance of CB matrix. Applying the Inverse dynamics input ($U_{eq}(t)$) to a system reduces the system to a first order, provided that CB is full rank. The reduced system in closed loop form is given in Figure 33 for which the transfer function is given as follows:

$$TF = C(sI + kCB)^{-1} kB \quad \text{where } k = \begin{bmatrix} k_{11} & 0 & 0 \\ 0 & k_{22} & 0 \\ 0 & 0 & k_{mm} \end{bmatrix} \quad (3.30)$$

The transfer function shows that for a given controller gain the poles of the system are given by the equation $|sI+kCB|=0$. This shows that CB matrix determines the closed loop stability of the system when injected with Inverse dynamics input.

As the feedback gain k of the control system is varied from zero to infinity the closed-loop poles can be traced out on a root-locus [(Franklin & Powell, 2005)] and a number of these poles equal to the number of inputs/outputs approach the

asymptotes (infinite zeros). On the root-locus, the structure of the (CB) matrix determines the direction of asymptotes which fundamentally affect the ability for the system to be stable in ISR mode.

If the matrix is found to be diagonal:

$$\begin{bmatrix} s_1 + k_{11}cb_{11} & 0 & \cdots & 0 \\ 0 & s_2 + k_{22}cb_{22} & \cdots & 0 \\ \vdots & \vdots & \ddots & \vdots \\ 0 & 0 & \cdots & s_n + k_{nn}CB_{nn} \end{bmatrix} \quad (3.31)$$

Then, it means that asymptotes are aligned with the negative real axis of the complex plane, thus greatly assisting high gain and ISR to be easily achieved. It also means that classical single input single output (SISO) controllers such as Proportional plus Integral control (PI), could be sufficient as each channel is independent and not coupled because the matrix is diagonal.

If the matrix is non diagonal meaning that there are other terms in the matrix where there are zeros shows the cross coupling between the control loops of the system.

$$\begin{matrix} u_1 & u_2 & \cdots & u_n \\ \begin{bmatrix} s_1 + k_{11}cb_{11} & 0 & \cdots & 0 \\ 0 & s_2 + k_{22}cb_{22} & \cdots & 0 \\ \vdots & \vdots & \ddots & \vdots \\ 0 & 0 & \cdots & s_n + k_{nn}CB_{nn} \end{bmatrix} & \begin{matrix} y_1 \\ y_2 \\ \vdots \\ y_n \end{matrix} \end{matrix} \quad (3.32)$$

Non diagonal matrix indicates that some of the asymptotes may be pointing towards the complex stable region or towards the unstable region. Pointing towards the unstable region means that at a certain gain the poles would cross the stable region and may enter the unstable region. A pole in the right half plane of the root locus means that the control system is unstable and thus ISR is not feasible. This would mean in practice that simple controls are not applicable and will not result in controllability. Instead a more complex controller design would be required to re-

align the asymptotes along the negative real axis. In general, in order to align these asymptotes a MIMO controller is required using a pre-filter matrix given by $(CB)^{-1}$ to re-align the asymptotes along the negative real axis and allow ISR to be achieved in this more complex situation [(Bradshaw & Counsell, 1992)].

3.2.7 Fast and Slow modes

What are poles and zeros and why are they important?

Poles and Zeros of a transfer function are the frequencies for which the value of the transfer function becomes infinity or zero respectively. The values of the poles and the zeros of a system determine whether the system is stable, and how well the system performs. Control systems, in the simplest sense, can be designed simply by assigning specific values to the poles and zeros of the system. Physically realizable control systems must have a number of poles greater than or equal to the number of zeros. Systems that satisfy this relationship are called proper [(Straete, 1995), (Franklin & Powell, 2005)]. To analyse the system's response and stability the poles and zeros are plotted on a root locus.

What is root locus? Root locus analysis is a graphical method for examining how the roots of a system change with variation of a certain system parameter, commonly the gain of a feedback system. As gain is increased the poles trace out a locus and they move towards their corresponding zeros [(Franklin & Powell, 2005)]. The root locus of an (open-loop) transfer function $G(s)$ is a plot of the locations (locus) of all possible closed loop poles with proportional gain k and unity feedback:

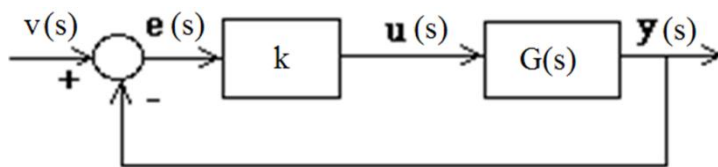


Figure 41 Generic feedback control system

The closed-loop transfer function is:

$$\frac{y(s)}{v(s)} = \frac{kG(s)}{1+kG(s)} \quad (3.33)$$

And thus the poles of the closed loop system are values of s such that $1 + k G(s) = 0$.

If we write $\mathbf{G}(s) = \mathbf{z}(s)/\mathbf{p}(s)$, then this equation have the form:

$$p(s) + kz(s) = 0 \quad (3.34)$$

$$\frac{p(s)}{k} + z(s) = 0 \quad (3.35)$$

Let $n =$ order of $p(s)$ and $m =$ order of $z(s)$ [the order of a polynomial is the highest power of s that appears in it]. If consider all positive values of k . In the limit as $k \rightarrow 0$, the poles of the closed-loop system are $p(s) = 0$ or the poles of $G(s)$. In the limit as $k \rightarrow$ infinity, the poles of the closed-loop system are $z(s) = 0$ or the zeros of $G(s)$.

No matter what we pick k to be, the closed-loop system must always have n poles, where n is the number of poles of $G(s)$. The root locus must have n branches; each branch starts at a pole of $G(s)$ and goes to a zero of $G(s)$. It also means that there are two types of poles and zeros, finite and infinite. In a modelling sense the number of state equations determines the number of poles of the system. However at this point it is important to note that not all the state(s) are being controlled. And what you feedback is what you control in a control system e.g. air temperature, lux and CO_2 . The state(s) that are being feedback and controlled are the states corresponding to the infinite poles i.e. asymptotes, branches. The infinite poles approach infinite zeros. The states that are modelled in a building physics model for completeness of the dynamics such as thermal mass temperature etc, their poles are finite poles approaches finite zeros. Also known as transmission zeros for MIMO systems [(Straete, 1995)].

In theory if $G(s)$ has more poles than zeros (as is often the case), $m < n$ and we say that $G(s)$ has zeros at infinity. In this case, the limit of $G(s)$ as $s \rightarrow$ infinity is zero. The number of zeros at infinity is $n-m$, the number of poles minus the number of

zeros, and is the number of branches of the root locus that go to infinity (asymptotes).

What are fast and slow modes?

Since the root locus is actually the locations of all possible closed loop poles, from the root locus we can select a gain such that our closed-loop system will perform the way we want. The position of poles on the root-locus determines the response and stability of the system. If any of the selected poles are on the right half plane, the closed-loop system will be unstable. Poles farthest from the imaginary axis (i.e. infinite poles or asymptotes, the state being controlled such as air temperature) have the least influence on the closed loop response and their corresponding states reach steady state quickly. That's why they are called the fast modes of the system. The poles that are closest to the imaginary axis have the greatest influence on the closed-loop response, and their corresponding states have a large time constant (i.e. wall temperature) and thus reach steady state after a long time. That's why they are called the slow modes of the system. So even though the system has three or four poles, it may still act like a second or even first order system depending on the location(s) of the dominant pole(s). However the final position(s) of the pole(s) are restricted by the position of the fixed zeros. This is why it is important to analyse the open loop zero's locations. Because open loop zeros are the closed loop poles. If open loop zeros are in the unstable region then closed loop poles will approach these open loop unstable zeros as gain increases making the system unstable.

This is SISO explanation of the concept of fast and slow modes. Modern buildings are MIMO systems. Generally MIMO systems are analysed in state space representation. As shown earlier the Inverse dynamics input (U_{eq}) reduces the system to a first order CB/s transfer function. In terms of classical control theory Inverse dynamics input (U_{eq}) places all the poles on top of zeros thus making the states controllable. That's why open loop zeros are the poles of the closed loop system. The open loop transfer function = CB/s where zeros are determined by the CB matrix. In the closed loop transfer function $|sI+kCB|=0$ determine the poles of the system. Thus,

open loop multivariable zeros are the closed loop poles of the system operating with Inverse dynamics input. Thus if open loop zeros are in RHP then ISR is not feasible.

As discussed in the earlier section, the CB matrix determines the direction of the asymptotes i.e. the poles at infinity. Therefore it is also important to determine the location of the positions of the finite poles. These are determined by the MIMO transmission zeros [(Straete, 1995), (Qui & Davison, 1993), (Calafiore & Carabelli, 1997)]. If transmission zeros are unstable then those slow states are unstable causing the whole system to be unstable. For a proper [(Straete, 1995)] system the transmission zeros can be calculated as follows:

Consider the basic system described by the equations:

$$\begin{aligned} \dot{x}(t) &= Ax(t) + Bu(t) \\ y(t) &= Cx(t) + Du(t) \end{aligned} \quad (3.36)$$

Where A,B,C and D are constant coefficient matrixes of state space model.

From the basic definition of the zero, at zero the output y is zero. Thus in Laplace domain the above equations can be written as follows:

$$\begin{aligned} 0 &= (A - sI)x(s) + Bu(s) \\ 0 &= Cx(s) + Du(s) \end{aligned} \quad (3.37)$$

In matrix form this can be written as follows:

$$\begin{bmatrix} A - sI & B \\ C & D \end{bmatrix} \begin{bmatrix} x(s) \\ u(s) \end{bmatrix} = 0 \quad (3.38)$$

Thus the transmission zeros can be calculated by solving the following determinant:

$$\det \begin{vmatrix} A - sI & B \\ C & D \end{vmatrix} = 0 \quad (3.39)$$

Thus to conclude, as the gain k tends to infinity the eigen-values tend to infinite zeros along the asymptotes defined by the directions of CB matrix which are the root locus asymptotes. These are the fast modes. For large but finite values of gain g , the eigen-values are the transmission zeros of the open loop system [(Young, Kokotovic, & Utkin, 1977)]. Therefore in practice, having the knowledge of the locations of the transmission zeros means you can understand whether a building is inherently stable or unstable as an open loop system. If its transmission zeros are unstable then to achieve ISR will be impossible and simple control will not be able to control the building. In the same way knowing the direction of the asymptotes on the root-locus determines the stability of the fast modes. If the asymptotes are pointing towards unstable region then at high gains the infinite poles might become unstable.

3.2.8 Inverse dynamics input (U_{eq}) and slow modes

It is possible in state space representation to separate the system into its fast and slow parts. This technique is useful in model order reduction through the use of singular perturbation method [(Kokotovic, Khalil, & O'Reilly, 1999)] as is shown in chapter 2. In addition to this it is very important in understanding the true nature of Inverse dynamics U_{eq} . This is shown as follows; consider the system:

$$\dot{x}(t) = Ax(t) + Bu(t) \quad (3.40)$$

This system can be decomposed into its fast and slow parts in the form [(Young, Kokotovic, & Utkin, 1977)]:

$$\dot{x}_1(t) = A_{11}x_1(t) + A_{12}x_2(t) \quad (3.41)$$

$$\dot{x}_2(t) = A_{21}x_1(t) + A_{22}x_2(t) + B_2u(t) \quad (3.42)$$

A transformation matrix J can be used for transforming one set of states into another set:

$$x(t) = \begin{bmatrix} x_1 & x_2 \end{bmatrix}^T = Jx(t) \quad (3.43)$$

Where the transformation matrix J:

$$J = \begin{bmatrix} J_1 \\ J_2 \end{bmatrix} \quad (3.44)$$

Thus:

$$JAJ^{-1} = \begin{bmatrix} A_{11} & A_{12} \\ A_{21} & A_{22} \end{bmatrix} \quad (3.45)$$

The transformation is on the condition that:

$$J_1 B = 0 \quad (3.46)$$

Thus based on the assumption that B_2 and C_2 are non singular and CB matrix is full rank:

$$JB = \begin{bmatrix} 0 \\ B_2 \end{bmatrix} \quad (3.47)$$

And

$$CJ^{-1} = [C_1 \quad C_2] \quad (3.48)$$

The state space representation would be as follows:

$$\begin{bmatrix} \dot{x}_1(t) \\ \dot{x}_2(t) \end{bmatrix} = \begin{bmatrix} A_{11} & A_{12} \\ A_{21} & A_{22} \end{bmatrix} \begin{bmatrix} x_1(t) \\ x_2(t) \end{bmatrix} + \begin{bmatrix} 0 \\ B_2 \end{bmatrix} [u(t)] \quad (3.49)$$

$$[y(t)] = [C_1 \quad C_2] \begin{bmatrix} x_1(t) \\ x_2(t) \end{bmatrix} \quad (3.50)$$

The reason for such a transformation is that the system can be divided into fast and slow parts. The fast part is the $x_2(t)$ state and the slow is the $x_1(t)$ state. The fast state ($x_2(t)$) is influenced directly by the input and the slow state ($x_1(t)$) is influenced after by the fast state. The transformation allows for B_1 to be cancelled so its response is dependent on the fast state.

When the Inverse dynamics input (U_{eq}) is applied to the system, rate of change of the switching surface s_x is zero:

$$\dot{s}_x(t) = C_1\dot{x}_1(t) + C_2\dot{x}_2(t) = 0 \quad (3.51)$$

And substituting equations (3.41)-(3.42) in (3.51) an expression for the equivalent control system is obtained in terms of slow and fast terms $x_1(t)$ and $x_2(t)$ the $U_{eq}(t)$ is given as follows:

$$U_{eq}(t) = -(C_2B_2)^{-1} \left[(C_1A_{11} + C_2A_{21})x_1(t) + (C_1A_{12} + C_2A_{22})x_2(t) \right] \quad (3.52)$$

And the switching surface is a function of the slow and fast states:

$$s_x(t) = C_1x_1(t) + C_2x_2(t) \quad (3.53)$$

The real sliding mode exhibits two types of motions: the fast motions associated with the motion across the sliding surface and the slow motions associated with the motion along the sliding surface [(Boiko, 2009)]. When Inverse dynamics $U_{eq}(t)$ is applied and the system is made to slide along the sliding surface then at that point the motion of the system is described by the equation of the slow part i.e. $U_{eq}(t)$. Thus the equivalent control system becomes:

$$\dot{x}_1(t) = A_{11}x_1(t) + A_{12}x_2(t) \quad (3.54)$$

$$\dot{s}_x(t) = 0 \quad (3.55)$$

Making $x_2(t)$ the subject from $s_x(t) = C_1x_1(t) + C_2x_2(t)$ and substituting into the slow system yields the $(n-m)^{\text{th}}$ reduced order system.

$$\dot{x}_1(t) = (A_{11} - A_{12}C_2^{-1}C_1)x_1(t) + (A_{12}C_2^{-1})s_x(t) \quad (3.56)$$

If the switching surface is zero then $s_x(t)=0$ giving the result as presented in [(Young, Kokotovic, & Utkin, 1977), (Zinober, 1990)]:

$$\dot{x}_1(t) = (A_{11} - A_{12}C_2^{-1}C_1)x_1(t) \quad (3.57)$$

The analysis above shows that when a system achieves ISR its behaviour corresponds to the ‘slow’ (reduced) subsystem. It was also shown earlier that fast eigenvalues are the asymptotes on a multivariable root locus and their direction is determined by the CB matrix. On the other hand closed loop slow eigenvalues approach the finite zeros. Thus it is clear that the eigenvalues of the equivalent control system are equal to the slow modes of the original system i.e. transmission zeros with the output $y(t)$.

This result also confirms what is shown earlier that the Inverse dynamics ($U_{\text{eq}}(t)$) reduced a higher order system into a lower first order system. This can only be done if the system can be decoupled and the fast modes are cancelled out. The $U_{\text{eq}}(t)$ decouples the system and cancels the fast dynamics thus allowing for reduction of the system to first order.

To conclude this section it can be said that in a stable system the fast modes are important only during a short initial period. Once the system reaches sliding mode the fast modes are negligible and the system is described by the slow modes. Neglecting the fast modes is equivalent to assuming that they are infinitely fast and thus have steady state [(Naidu, 1988)]. If we assume that the fast modes are over quickly and slow modes are almost constant then the system can be treated as a quasi steady state. Inspecting the Inverse dynamics input (U_{eq}) which is identical to the

slow motions can show how slow are the slow modes to be able to take them as constant i.e. steady state. This is the reason why for some systems the quasi steady state models are justified because the slow modes are very slow and fast are very fast that both can be assumed constant. This is the reason why some systems are described linear even though this may seem to be contradictory considering their nonlinear nature. This is because when the system is constrained to operate such (sliding mode) that linear assumptions are still valid.

So far in this chapter the Inverse dynamics input U_{eq} is discussed that can convert a system from higher order to a reduced first order system that can easily be controlled. Then the ease in which ISR can be achieved, of this reduced first order system is analysed. The reduced order system is analysed for its controllability by understanding the significance and structure of the CB matrix and the transmission zeros. It was shown that CB matrix and transmission zeros represent the fast and slow modes of the system. It is also found that the dynamics of the reduced order system are represented by the slow modes of the system. These slow dynamics are governed by the Inverse dynamics U_{eq} and its eigenvalues are equal to the slow modes i.e. transmission zeros.

It is important to note that this control input is not the controller of the overall system; it is only instead used to condition the higher order system (i.e. reduced its order) so that simple controllers (e.g. PI) can be used successfully to control the response of the system. Thus the Inverse dynamics input is in addition to the simple control law that would be needed to control the reduced system. This can be shown with a simple proportional controller as follows:

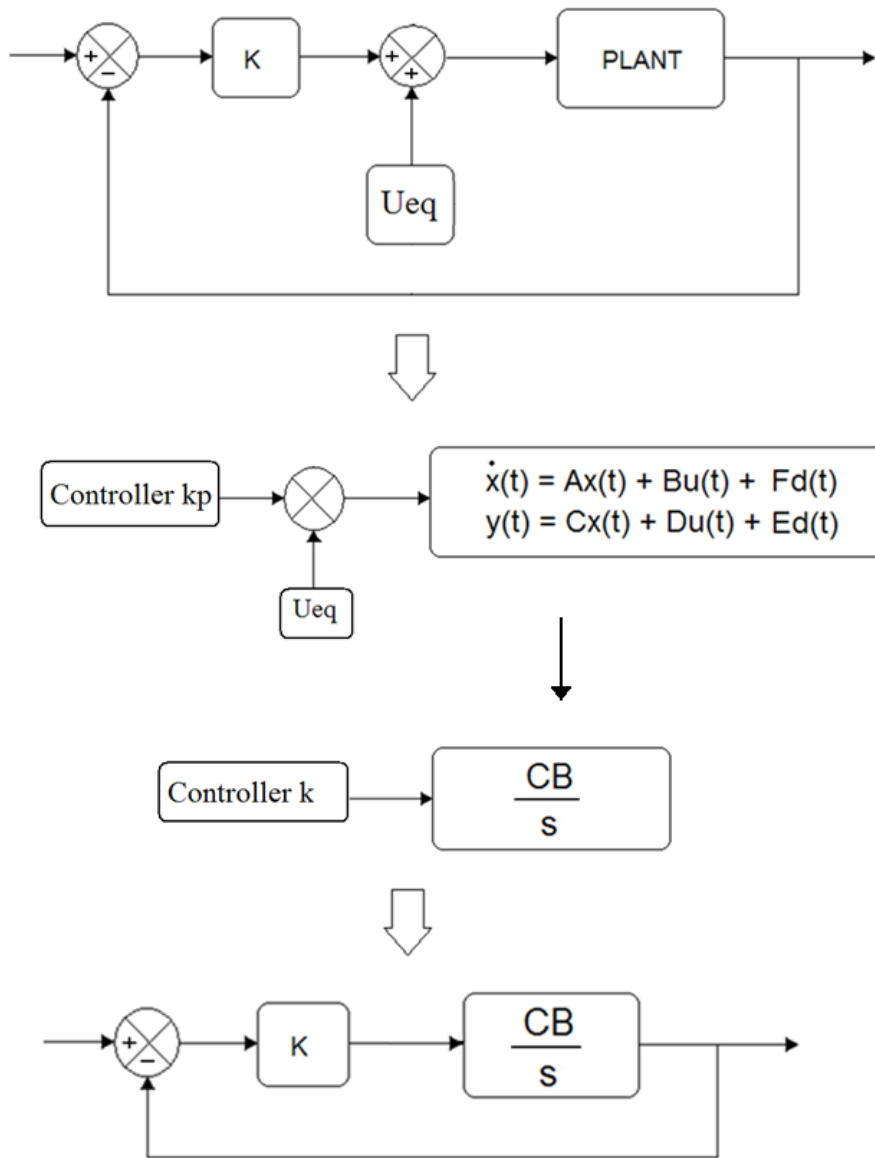


Figure 42 U_{eq} feedback makes a MIMO system behave like an ideal integrator (i.e. First Order)

In practice what is the ISR control law for controlling a first order system i.e. CB/s ?

3.2.9 Control of first order systems for achieving ISR

In modern times the decade of 1970s could be marked as an important year for control engineering as another brilliant control engineer Richard Phelan [(Phelan, 1977)] (Cornell University, NY) realized that the way most engineers and scientists go about controlling things, is not nearly as good as it could be. The first order systems are simple and easiest to control and in an elegant and mathematically simple way Richard Phelan proved mathematically and practically that his Pseudo-Derivative Feedback (PDF) controller allows the response characteristics of a first-order system to be completely controlled as explained by the equations in this section [(Phelan, 1977)]. The PDF controller in block diagram is represented as follows:

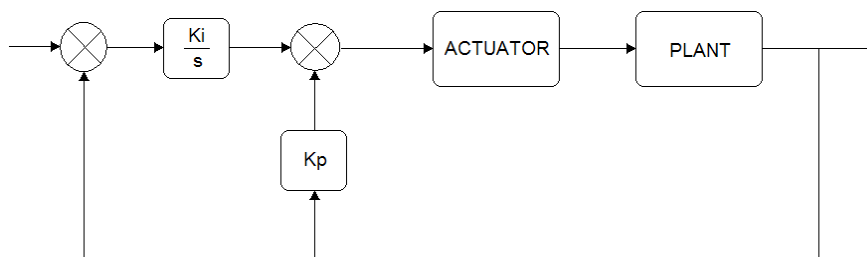


Figure 43 PDF control system block diagram

This structure provides all the control aspects of proportional integral derivative (PID) control but without system zeros that are normally introduced by a PID compensator. Phelan named this structure PDF control from the fact that the rate of the measured parameter is fed-back without having to calculate a derivative. It is important to mention about PDF in this thesis because in the later sections it is shown how this is the basis of the RIDE methodology.

Phelan showed that simple first order systems such as with transfer function '1/s', their response can be completely controlled using the structure and gains of the PDF controller. In Phelan's book (Phelan, 1977) the above PDF control system is considered and neglecting actuator dynamics and assuming the system to be an integrator (1/s) (TYPE 1), the block diagram can be simplified:

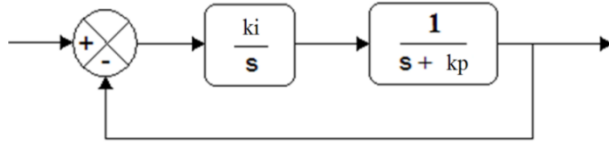


Figure 44 Simplified PDF and first order system

The closed loop transfer function is given by:

$$G_c(s) = \frac{k_i}{s^2 + k_p s + k_i} \quad (3.58)$$

This transfer function is equivalent to an ideal second order system with the transfer function:

$$G_I(s) = \frac{\omega_n^2}{s^2 + 2\zeta\omega_n s + \omega_n^2} \quad (3.59)$$

Hence for an ideal second order system, the following correlation is drawn between $G_c(s)$ and $G_I(s)$:

The system's natural frequency is given as:

$$\omega_n^2 = k_i \rightarrow \omega_n = \sqrt{k_i} \quad (3.60)$$

The system's damping is given as:

$$2\zeta\omega_n = k_p \rightarrow 2\zeta\sqrt{k_i} = k_p \rightarrow \zeta = \frac{k_p}{2\sqrt{k_i}} \quad (3.61)$$

The above equations show that by controlling a first order system with PDF control structure the resulting system is an ideal second order system. The response characteristics of such a system can be completely controlled based on the proportional and integral gains. Thus by varying the gains a first order response can

be modelled. The natural frequency w_n of the system is determined by the value of the integral gain k_i .

The natural frequency w_n of an ideal second order system is also its closed loop bandwidth w_{cb} . Therefore even with integral action (k_i) it is possible to condition the closed loop bandwidth of the system relative to the actuator dynamics. Hence the closed loop bandwidth of the system is the square root of k_i . The basic method for avoiding all operational problems with real automatic control systems is to insure that the actuator is never asked to deliver energy at a rate faster than it can. In most cases, the actuator time constant cannot be modified thus the rate of demand of the controller is conditioned so that it never demands faster than the rate at which the actuator can deliver energy. As mentioned in earlier section on CB matrix sensitivity, for sufficient gain and phase margins the controller time constant is kept equal to or less than a third of the actuator time constant. In other words the controller or closed loop bandwidth is kept three times less than the actuator and sensor bandwidths. Therefore k_i can be used to modify the tracking performance of the system.

Also as shown the damping ratio of the system can also be controlled and hence the desired over shoot can be easily achieved by varying the gains to make the damping ratio less than critical for overshoot to occur. For the case of single input single output systems this technique provides a complete control of the response of the system in an ideal way. Thus PDF controller is the optimum controller for a system that acts as an integrator or Type 1 system as Phelan called it. All the theory presented in the previous sections was to make the most complicated multivariable system look like a Phelan Type 1 system. Therefore this is ideal for being used with inverse dynamics to get the right kind of response for a system that is reduced to an integrator.

3.2.10 Robust Inverse Dynamics Estimation (RIDE)

To understand RIDE it is important to understand the theory in earlier sections in multivariable sense. In a multivariable sense the purpose of an inverse dynamics input is to decouple these control channels so that they behave like independent SISO channels in parallel that are easy to control. This is shown in earlier sections where the system transfer function reduces to first order i.e. CB/s . Thus existence of a CB matrix for a system tells us that ISR is feasible to some degree. The degree of feasibility is determined upon analysing the structure of the matrix (section 3.2.6). For a multivariable system the CB matrix shows the cross coupling between the various control channels in terms of inputs and outputs of the whole system. Therefore through the CB matrix, it can be determined whether a MIMO system can be decoupled, how strong is the coupling and is ISR feasible or not? In theory this was first shown mathematically that a multivariable system can be decoupled if the matrix CB is non-singular and this was generalised for all order of systems [(Falb & Wolovich, 1967)].

The RIDE starts with the open loop multivariable system transfer function in state space which is expanded using binomial theorem to obtain the Markov series:

$$y(s) = \frac{I}{s} \left(C + \frac{CA}{s} + \frac{CA^2}{s^2} + \frac{CA^3}{s^3} + \dots + \frac{CA^n}{s^n} \right)^{-1} Bu(s) \quad (3.62)$$

In RIDE theory it was realised from the Markov series that if CA was made to cancel out and CB was made not equal to zero then the transfer function matrix reduces to:

$$y(s) = s^{-1} I CBu(s) \quad (3.63)$$

In closed loop form the system in block diagram will be as follows:

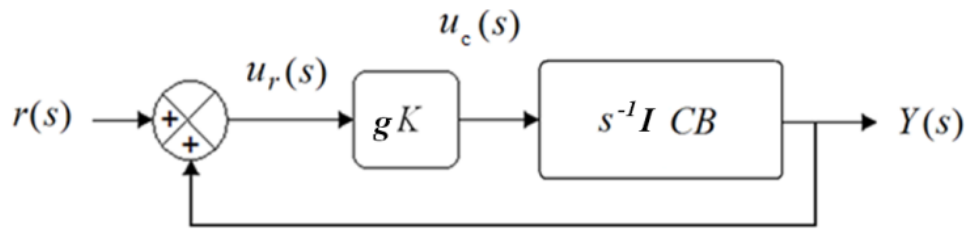


Figure 45: Block diagram of a simple feedback control system with controller matrix $K(s)$ Where: r = set-point, y = output, g = scalar gain and K = controller gain matrix

By choosing $K=(CB)^{-1}$ the system's transfer function matrix is reduced to a perfect first order system and each channel of the multivariable system behaves like a perfect integrator for each control variable, i.e. Ideal non interacting Multi - Single Input Single Output (M-SISO) system given by:

$$\begin{bmatrix} y_1(s) \\ y_2(s) \\ \vdots \\ y_n(s) \end{bmatrix} = \begin{bmatrix} g/s_1 + g & 0 & \cdots & 0 \\ 0 & g/s_2 + g & \cdots & 0 \\ \vdots & \vdots & \ddots & \vdots \\ 0 & 0 & \cdots & g/s_n + g \end{bmatrix} \begin{bmatrix} v_1(s) \\ v_2(s) \\ \vdots \\ v_n(s) \end{bmatrix} \quad (3.64)$$

Where the closed loop system time constant is $1/g$ and the bandwidth is g .

One of the ways of cancelling CA is the high gain theory that drives the closed loop transfer function to steady state and the effect is the CA is zero [(Young, Kokotovic, & Utkin, 1977)] as shown in the earlier section. But in practice it is not possible to achieve high gain (i.e. infinite gain) and thus the effect of CA is not cancelled. The A matrix is the system matrix which cannot be changed. However it is possible to change what you feedback and thus changing matrix C such that CA cancels and $CB \neq 0$. Thus Counsell [(Counsell J. M., 1992)] introduced the concept of extra measurements i.e. feeding back $w(s)$:

This change in feedback is based upon the condition $w(s)$ is chosen such that in steady state $w(s) = y(s)$, thus in steady state the controller will track $y(s)$ rather than $w(s)$. Also ideally M is chosen such that MA cancels and $MB \neq 0$ when the Inverse

dynamics input is applied. Thus the feedback equation is $w(s) = M x(s)$. Providing that MA cancels the new transfer function matrix in Laplace domain would be given by:

$$w(s) = s^{-1} I M B u(s) \quad (3.65)$$

The feedback equation is generalised for all cases for which one of the cases is where $M=C$ and $w(s) = y(s)$. Hence the new system in time domain is given as follows:

$$\dot{x}(t) = Ax(t) + Bu(t) + Fd(t) \quad (3.66)$$

$$w(t) = Mx(t) \quad (3.67)$$

Generally the problem is that by choosing the right feedback it is easy to set $MB \neq 0$ however it is difficult to cancel MA. This particular case is addressed in the RIDE methodology by adding a special input $U_{trim}(t)$ to the control law.

Consider the simple closed loop system with the special input $U_{trim}(t)$:

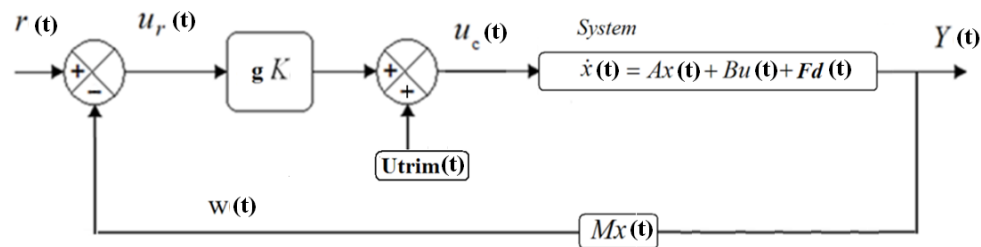


Figure 46 Block diagram of closed system with U_{trim}

If the gain matrix K is taken as $(MB)^{-1}$ then the control law can be given as follows:

$$u_c(t) = g (MB)^{-1} (r(t) - w(t)) + U_{trim}(t) \quad (3.68)$$

Differentiating $w(t)$ equation (3.67) and substituting state equation (3.66) gives:

$$\dot{w}(t) = MAx(t) + MBu(t) + MFd(t) \quad (3.69)$$

Substituting the control law Equation (3.68) results:

$$\dot{w}(t) = MAx(t) + gI(r(t) - w(t)) + MBU_{trim}(t) + MFd(t) \quad (3.70)$$

It was observed that if $U_{trim}(t)$ was given by:

$$U_{trim}(t) = -(MB)^{-1} (MAx(t) + MFd(t)) \quad (3.71)$$

And substituted into equation (3.70) then it reduces the system effectively removing the MA and MF terms. This is equivalent to being a system where $CA=0$:

$$\dot{w}(t) = gI(r(t) - w(t)) \quad (3.72)$$

Which in Laplace domain is given by:

$$w(s) = gI(sI + gI)^{-1} r(s) \quad (3.73)$$

This control law is valid for all values of the matrix MA as the U_{trim} input is able to make MA and the disturbance MF terms be cancelled out. Also substituting this into the state equation (3.66) results in $\dot{x}(t) = 0$, meaning that U_{trim} has driven the state to steady state. Thus for U_{trim} to cancel MA and MF terms only $|MB| \neq 0$ is required. The difference here is that Utkin [(Utkin, 1971)] derived this for the case of matrix A and C i.e. state output feedback where as Counsell generalised the technique for all values of matrix A and M providing $|MB| \neq 0$ based upon being consistent with the Markov series. Hence: $U_{trim} = U_{eq}$ i.e. Inverse dynamics input when the switching surface ' $s_x(t)$ ' from VSC is the error $e(t) = r(t) - w(t)$.

Therefore applying a switching surface of $r(t) - w(t)$ into a multivariable control system whereby we have a controller gain matrix $(MB)^{-1}$ followed by a identity matrix of on/off switches controlling a system and feeding back $w(t)$ such that

$|MB| \neq 0$. Then the resultant system will be a variable structure control system that is a multivariable on/off control system. Using relay switches as the actuators and providing the system from $u_c(t)$ to $w(t)$ is of relative degree of 1 the response of the multivariable system will be of ISR.

Now as shown earlier in section (3.2.9) that the ISR control law for controlling a first order system (Phelan Type 1 system) is the PDF algorithm. Using this algorithm the response of the system is completely controllable using the gains of the system as shown in equation 60-63. Therefore Counsell (1992) produced a new control law by combining PDF algorithm with U_{trim} . Therefore Counsell (1992) was able to prove that the ISR control law for a complex multivariable system (i.e. a nonlinear MIMO system) is given as:

ISR CONTROL ALGORITHM = PDF controller + Inverse dynamics Input (U_{trim})

Where the U_{trim} is able to decouple the multivariable system and reduces each control channel to a perfect integrator (Type 1) and then the PDF controller is able to completely control its response which is a function of its gains. This is shown as follows:

The ISR control algorithm is given as follows:

$$u_c(t) = k_I z(t) - k_P w(t) + U_{trim}(t) \quad (3.74)$$

Where z is the integral of error:

$$\dot{z}(t) = e(t) = r(t) - w(t) \quad [Laplace : z(s) = s^{-1}I(r(s) - w(s))] \quad (3.75)$$

Substituting the control law in the equation (3.69) gives:

$$\dot{w}(t) = MB(k_I z(t) - k_P w(t)) \quad (3.76)$$

If the controller gains k_I and k_P are given as:

$$k_I = g(MB)^{-1} \rho, \quad k_P = g(MB)^{-1} \sigma \quad (3.77)$$

Where, g = system scalar gain, ρ = diagonal Integral gain matrix and σ = diagonal proportional gain matrix. Then the equation (3.76) reduces to:

$$\dot{w}(t) = g\rho z(t) - g\sigma w(t) \quad (3.78)$$

In Laplace domain it is given as follows:

$$(sI + g\sigma)w = g\rho z \quad (3.79)$$

Substituting equation (3.75) into (3.79) results in the closed loop transfer function of the system which is the ideal second order transfer function as discussed earlier equation(3.59):

$$\frac{w}{r} = \frac{g\rho}{s^2I + g\sigma s + g\rho} \quad (3.80)$$

Thus it is shown that by applying the ISR control law results in the ideal second order system and its response characteristics are completely controllable as it's a function of the controller gains matrices.

How is RIDE a low gain theory? The origins of RIDE theory are in high gain theory however mathematically speaking it is a low gain theory that relies on a good estimate of U_{trim} to make the system more controllable.

First of all it is important to note that the building physics model is an approximation of the real causes and effects. Thus deriving U_{trim} from the model means that this U_{trim} is an approximation of the real U_{trim} . Thus in reality, in an application of the ISR control law there would be an error in the estimate of U_{trim} , thus the system would not completely behave as a decoupled first order system. It is shown the

equation (3.71) of U_{trim} derived from the model is a function of all its matrices, i.e. it is a function of all the parameters. Therefore the ISR control law in reality is:

$$u_c(t) = k_I z(t) - k_P w(t) + \hat{U}_{trim}(t) \quad (3.81)$$

Where in the equation the \hat{U}_{trim} is the measured U_{trim} in practice. Thus this necessitates the measurement of all state variables and disturbances, as well as plant parameters which are typically unknown in practice. Thus, in reality, the implementation of the equivalent control term is often ignored as it is viewed impractical. However it was showed [(Muir & Bradshaw, 1996)] that rapid estimation of U_{trim} is achievable through the above methodology. Consider the equation (3.69) and dividing through by the matrix MB gives another expression for U_{trim} that is used in practice:

$$(MB)^{-1} \dot{w}(t) = (MB)^{-1} (MAx(t) + MFd(t)) + u(t) = -U_{trim}(t) + u(t) \quad (3.82)$$

Therefore an estimate of U_{trim} can be given by:

$$U_{trim}(t) = u(t) - (MB)^{-1} \dot{w}(t) \quad (3.83)$$

Thus in practice we can estimate the U_{trim} by knowing the matrix MB, rate of the measured variable $w(t)$ i.e. sensor measurement and the actuator output $u(t)$. This means that in practice, to know whether ISR is feasible or not i.e. whether simple controllers will work or not requires only the knowledge of the M and B matrices from the system description equations. And modelling a complete system with detailed matrixes A and F i.e. the system and disturbances is not needed. Thus, it is also important to inspect the sensitivity of MB as it directly affects the feasibility of ISR control which is what was shown in section (3.2.4-3.2.6)

Then the question arises as to how to remove the sensitivity to errors in U_{trim} ?

If the control law [equation(3.81)] is substituted into this equation (3.83) then:

$$-(MB)^{-1} \dot{w}(t) = \hat{U}_{trim}(t) - U_{trim}(t) + k_I z(t) - k_P w(t) \quad (3.84)$$

Differentiating this equation twice and substituting the error equation (3.75) and then taking Laplace transform gives:

$$\left\{ (MB)^{-1} s^2 + k_P s + k_I \right\} w(s) = s \left(\hat{U}_{trim}(s) - U_{trim}(s) \right) + k_I r(s) \quad (3.85)$$

If there is good estimate of U_{trim} i.e. $\hat{U}_{trim}(s) = U_{trim}(s)$ then this results in a perfect second order closed loop response totally controllable by the controller gains as shown earlier in equation (3.80).

$$\frac{w(s)}{r(s)} = g \rho \left\{ s^2 + g \sigma s + g \rho \right\}^{-1} \quad (3.86)$$

However if the estimate of U_{trim} is poor then: In terms of high gain singular perturbation method, dividing both sides of equation (3.85) by g gives:

$$\left\{ \frac{s^2}{g} + \sigma s + \rho \right\} w(s) = \frac{sMB \left(\hat{U}_{trim}(s) - U_{trim}(s) \right)}{g} + \rho r(s) \quad (3.87)$$

As g tends to infinity s tends to zero thus $w(s) = r(s)$. However infinite gain is not possible and in slow actuator applications a lower gain g is required. Thus having a better estimate of U_{trim} will allow for ΔU_{trim} terms to be small which could then be made negligible with a lower gain. Thus good estimate of U_{trim} will make this a low gain method. If the scalar gain is not high enough to remove the effect of ΔU_{trim} then this sensitivity of ΔU_{trim} is also reduced by the PDF algorithm itself. This is shown by dividing both sides of the equation (3.85) by integral gain ρ :

$$\left\{ \frac{s^2}{\rho} + \frac{g \sigma s}{\rho} + g \right\} w(s) = \frac{sMB \left(\hat{U}_{trim}(s) - U_{trim}(s) \right)}{\rho} + g r(s) \quad (3.88)$$

As we increase the integral gain very high the system reaches steady state i.e. $w(s)=r(s)$. If however integral gain doesn't not remove the effect of ΔU_{trim} then in steady state as s tends to zero, $\Delta U_{trim} = 0$ and $w(s) = r(s)$. Thus overall it is shown that this ISR Control Law is robust against the estimated inverse dynamics i.e. U_{trim} and thus able to achieve ideal response of the system.

The ISR control law i.e. RIDE is a closed loop controller design methodology that can directly symbolically tell you what the closed loop bandwidth should be for a given building design. Having a controller design method that fixes the closed loop bandwidth is giving you certainty that your closed loop bandwidth is within the confidence level of the building model i.e. in practice the controller will be able to track the required variable such as temperature.

It is important that the ISR Control Law is able to operate the system within its limits and does not make the system perform an operation that is out of the limits of the overall control system. Therefore it is crucial to derive a criterion that governs the limits of the system's safe operation.

3.2.11 Criterion for safe operation

Previous mathematical developments are based on linearisation of the system about an operating point. Real systems are highly nonlinear in their dynamical behaviour and even though a control system can be designed based on linear assumptions; there is no guarantee that safe performance will be achieved. In many systems real problems occur when the actuator is required to deliver more energy than there is available. That is asked to do something it cannot possibly do!

To solve this problem both linear and nonlinear system behaviours will be treated together rather than two separate subjects. For stability it is still assumed that the system can be described by linear time invariant model. Even though this may seem contradictory considering the nonlinear system, however the system is constrained to operate such that linear assumptions are still valid. Thus the linear model can be used

for controllability analysis carried out earlier relating to CB matrix etc. Linear state space method will not provide safe control however it can be used for developing a more robust nonlinear controller by using the controllability analysis results because they are still valid for those specific operating conditions.

It is crucial that system can operate with actuator saturation and limit on the rate of change of demand signal safely for optimum performance. In order to guarantee optimum and safe control, it is necessary to design and analyse a safe criteria.

As shown earlier U_{trim} , a Inverse dynamics input and a system property, is a complex function of many unknown parameters and the required state vector $x(t)$ to perform the required system performance. As long as U_{trim} stays within its limits, this will ensure that the system will reach steady state. The U_{trim} corresponds with the exact control required to offset the disturbance vectors and provide the required control for cancellation of cross coupling effects from perturbation in the system states. And the system is able to perform unique limit cycle behaviour once U_{trim} reaches its limits. The safe operation of the control system under disturbances and actuator nonlinearities is governed by the safe criteria for U_{trim} [(Counsell J. M., 1992), (Bradshaw & Counsell, 1992)]. The presence of limitations on the power of the system's actuators results in limitations on maintaining stable tracking. In order to better understand this it is useful to derive a criterion which describes the tracking limits. When the actuator output, $u_a(s)$, has reached its upper (L_U) or lower (L_L) limits, the control signal to the actuator, $u(s)$, must either remain constant or decrease in order to avoid overdriving the actuator and to maintain safe control. This can be expressed as [(Counsell, Brindley, & Macdonald, 2009)];

$$u(t)\dot{u}(t) \leq 0 \rightarrow \text{Laplace } u(s)su(s) \leq 0 \quad (3.89)$$

When,

$$u(s) \geq L_U \text{ or } u(s) \leq L_L \quad (3.90)$$

Consider a generic feedback control system, which is illustrated in Figure 44, where using proportional control and Utrim the control law is given by:

$$u(s) = K(s)(r(s) - w(s)) + U_{trim}(s) \quad (3.91)$$

The above equation is then differentiated to give:

$$su(s) = sK(s)r(s) - sK(s)w(s) + sU_{trim}(s) \quad (3.92)$$

As previously shown that U_{trim} is given by equation (3.83) and in Laplace is given by:

$$u_{Trim}(s) = -(MB)^{-1} sw(s) + u(s) \quad (3.93)$$

Making $sw(s)$ the subject gives:

$$sw(s) = (MB)[u(s) - U_{trim}(s)] \quad (3.94)$$

Equation (3.94) is substituted into (3.92) to give:

$$su(s) = sK(s)r(s) - K(s)(MB)(u(s) - U_{trim}(s)) + sU_{trim}(s) \quad (3.95)$$

Then the condition for safe operation is given multiplying $u(s)$ to equation (3.95):

$$u(s)su(s) = u(s)sK(s)r(s) - u(s)K(s)(MB)(u(s) - U_{trim}(s)) + u(s)sU_{trim}(s) \leq 0 \quad (3.96)$$

Dividing throughout by $u(s)$ and $K(s)(MB)$ two criteria are formed:

When $u(s) > 0$ and $u_a(s) = L_U$

$$u_{trim}(s) \leq L_U - sK(s)^{-1} (MB)^{-1} U_{trim}(s) - s(MB)^{-1} r(s) \quad (3.97)$$

When $u(s) < 0$ and $u_a(s) = L_L$

$$u_{trim}(s) \geq L_L - sK(s)^{-1}(MB)^{-1}U_{trim}(s) - s(MB)^{-1}r(s) \quad (3.98)$$

By combining these two expressions, a single criterion can be formed as follows:

$$L_L - (MB)^{-1} \left(\frac{sU_{trim}(s)}{K(s)} + sr(s) \right) \leq U_{trim}(s) \leq L_U - (MB)^{-1} \left(\frac{sU_{trim}(s)}{K(s)} + sr(s) \right) \quad (3.99)$$

By extending the RIDE Methodology it is found that if substituting $K(s) = g(MB)^{-1}\sigma$ into equation 3.99 then the criterion in Laplace domain is given by:

$$L_L - \frac{sU_{trim}(s)}{g\sigma} - (MB)^{-1}sr(s) \leq U_{trim}(s) \leq L_U - \frac{sU_{trim}(s)}{g\sigma} - (MB)^{-1}sr(s) \quad (3.100)$$

This criterion states that providing the closed-loop response is fast i.e. $K(s)$ is relatively large compared with rates of change of $U_{trim}(s)$ (i.e. slow modes) and that rate of change of $r(s)$ is made small then the limitation on tracking is that U_{trim} must remain between the upper and lower actuator limits.

$$L_L \leq U_{trim}(s) \leq L_U \quad (3.101)$$

This criterion demonstrates that, when actuator limits are reached, safety can be ensured simply by setting the error signal to zero, providing that steady state is reachable (i.e. that the U_{trim} is within limits). This condition for reaching steady state can be readily inspected using dynamic simulation [(Counsell, Brindley, & Macdonald, 2009)]. To understand which parameters in the system could cause the U_{trim} to go out of limits, the criterion needs to be inspected symbolically and is shown in case studies later in the thesis .

In conclusion as proven the Inverse dynamics input U_{trim} with the PDF algorithm combines to give the ISR control Law that is able to control a nonlinear multivariable system perfectly. This can be shown in block diagram as follows:

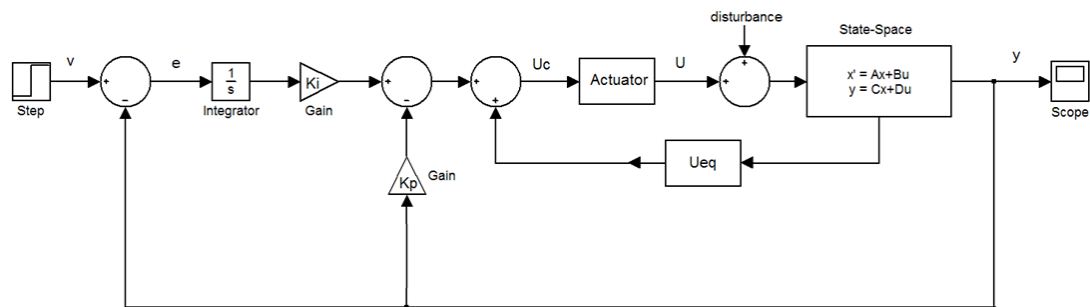


Figure 47 RIDE control system block diagram

A question that frequently arises is that this theory is all based on linear assumption where as in reality the systems are non-linear? Answer: The theory is for both linear and nonlinear systems. The symbolic analysis is carried out by constraining the system to operate such that linear assumptions are true for the operating points of significance. Secondly by applying the ISR control law a nonlinear system will decouple and reduce to integrators and thus allowing for its response to be completely controlled using simple controllers. This theory works very well in theory and practice for fast actuator systems and where there is no time delay in measurement of variables. However with slow actuator systems there is a time delay between the input to the system and the resulting change being recorded by the sensor. Then this theory takes account of this by assuming the controller bandwidth to be slower than the actuator and also extra sensor measurements. This is discussed earlier in section 3.2.5.

The Inverse dynamics input $U_{eq}(t)$ uses inverse dynamics to determine the actuator inputs that are required to ensure zero rate of change of the outputs. It does this by taking into account the disturbances (i.e. solar gains) and system dynamics that would otherwise prevent the system from operating with ISR. How to invert the physics of transport delay in buildings is very complex and this is a new area of research requiring CFD modelling (further work section).

4 : START-OF-ABC*

*Stability, Trackability And Reachability Theory OF Advanced Building Control



“Two famous types of systems exist, aerospace and buildings and they have almost everything in common for control systems design. The only difference is that F-16 goes through the air and air goes through BRE-16”

One of the aims of the work in this thesis is to upscale the building industry scientifically. It is very useful to know how systems work in practice however without a proper science for explaining the causes and effects and the relationships between systems, will result in solutions that are not robust and thus will always need to be re-commissioned. It is very clear that this up-scaling will take a long time and the buildings industry is not yet ready to take up advanced control theory for building design. Hence simple controls will still be the standard in the near future. Thus in this chapter, it is shown how this science can be used in practice to make sure that buildings designs are assessed for controllability at the conceptual design stage so that simple controls will perform better in practice. The following section presents the complex control theory from chapter 3 in terms of buildings and what it means in practice.

NOTE: The theory of controllability assessment is EQUALLY applicable for:

1. **Heating and cooling only**
2. **Heating only**
3. **Cooling only**

Majority of the theory presented in chapter 3 is utilised by the aerospace industry for assessing the controllability of aircrafts. **However the theory is such that it can be applied to any system for assessment of its controllability e.g. Climate adaptive buildings.** In today's buildings there are such types of systems that are known as multiple inputs multiple outputs (MIMO) systems just like MIMO systems in other industries. Meaning there are several control channels i.e. temperature, lighting, humidity, CO₂ etc that operate in parallel and each channel will have its own actuator (Plant) system and all are coupled together in terms of building physics. In chapter 3, with simple analysis the control theory behind ISR is presented using less complex system of equations (3.66)-(3.67).

However modern climate adaptive buildings are complex MIMO systems and thus have to be represented by the complete full version of these equations which are as follows:

$$\dot{x}(t) = Ax(t) + Bu(t) + Fd(t) \quad (4.1)$$

$$w(t) = Mx(t) + Du(t) + Ed(t) \quad (4.2)$$

The extra matrices D, E are found in cases where the plant inputs and disturbance inputs are directly affecting the feedback or sensor measurements. For example if radiant heater or solar radiation directly radiating to the sensor will result in this type of equation. In this way the sensor equation for temperature will include a direct component of radiant terms. Thus inputs and disturbances are directly affecting the sensor measurement. In the same way the lux equation is the same where the direct lux from solar and internal lights are affecting the internal lux level directly. For these reasons advanced buildings are complex MIMO systems and have to be represented with full set of equations.

For the convenience of the reader (i.e. non control theorist), the theory of ISR presented in chapter 3 can be simply explained in terms of building and systems as follows:

4.1 ISR Philosophy in simple words

Consider an actuator and a system, just like a heater/cooler and a building. The actuator can give positive input as well as negative. Just like a plant which can give both heat and cold to a building. But there is a condition. The actuator i.e. plant can only operate at its maximum or minimum limits and so at any moment in time it is either delivering maximum heat (positive) or maximum cold (negative). Now consider this switching between the two limits to be occurring very fast i.e. high frequency. Mean while in the building due to the fast switching between delivering heat and cold the temperature in the building exhibits oscillatory response around the set-point. At the same time the steady state error (i.e. set-point minus the temperature) is switching between positive and negatives around the zero error point. In control theory this is called the switching surface which is zero. The aim is to drive the error to zero so that the temperature equals set-point. At a certain switching frequency between hot and cold settings and amplitude of the plant input, the error

can be driven to zero and the temperature can be maintained constantly at the set-point. The plant input U that is able to reduce the tracking error to zero and maintain the temperature at the set-point despite the disturbances must be the Inverse dynamics input and is the low frequency average component of the input U . The average value of U as time goes on is at the equilibrium point U_{eq} also known as the equivalent control or U_{trim} or Inverse dynamics [see sections 3.3.3 & 3.4.1 for derivation]. The Inverse dynamics input can be derived for a building represented by equations (4.1)-(4.2) using steps shown in chapter 3 from equations (3.8)-(3.12). The new Inverse dynamics input U_{trim} is given by [for proof see appendix 5]:

$$U_{trim}(s) = \left[-(MB + sD)^{-1} MAX(s) - (MB + sD)^{-1} (MF + sE)d(s) \right] \quad (4.3)$$

In practice a simple building system (i.e. first order) is easier to control. Majority of the buildings are not simple (i.e. higher order). The Inverse dynamics input U_{trim} makes a complex building behave like a simple building which can then be controlled accurately by a simple controller. The controller which can control a simple (first order) system completely is called a PDF controller (see section 3.2.9). Thus combining these two can result in a **ISR CONTROL LAW** = U_{trim} + PDF (see section 3.4.1) The control theory presented in chapter 3 can be used for symbolic studies to assess the controllability of a building in terms of three fundamental controllability properties, **Stability**, **Trackability** and **Reachability** of a complete building system also known as **STaR**.

4.2 STaR Theory of buildings

The STaR theory of buildings will allow for modern buildings to be designed with a science that is utilised in the design process by aerospace, robotics, automotive and process control industries for many years [see Chapter 2 for references]. A simplified conceptual design stage is shown below with the controllability stage:

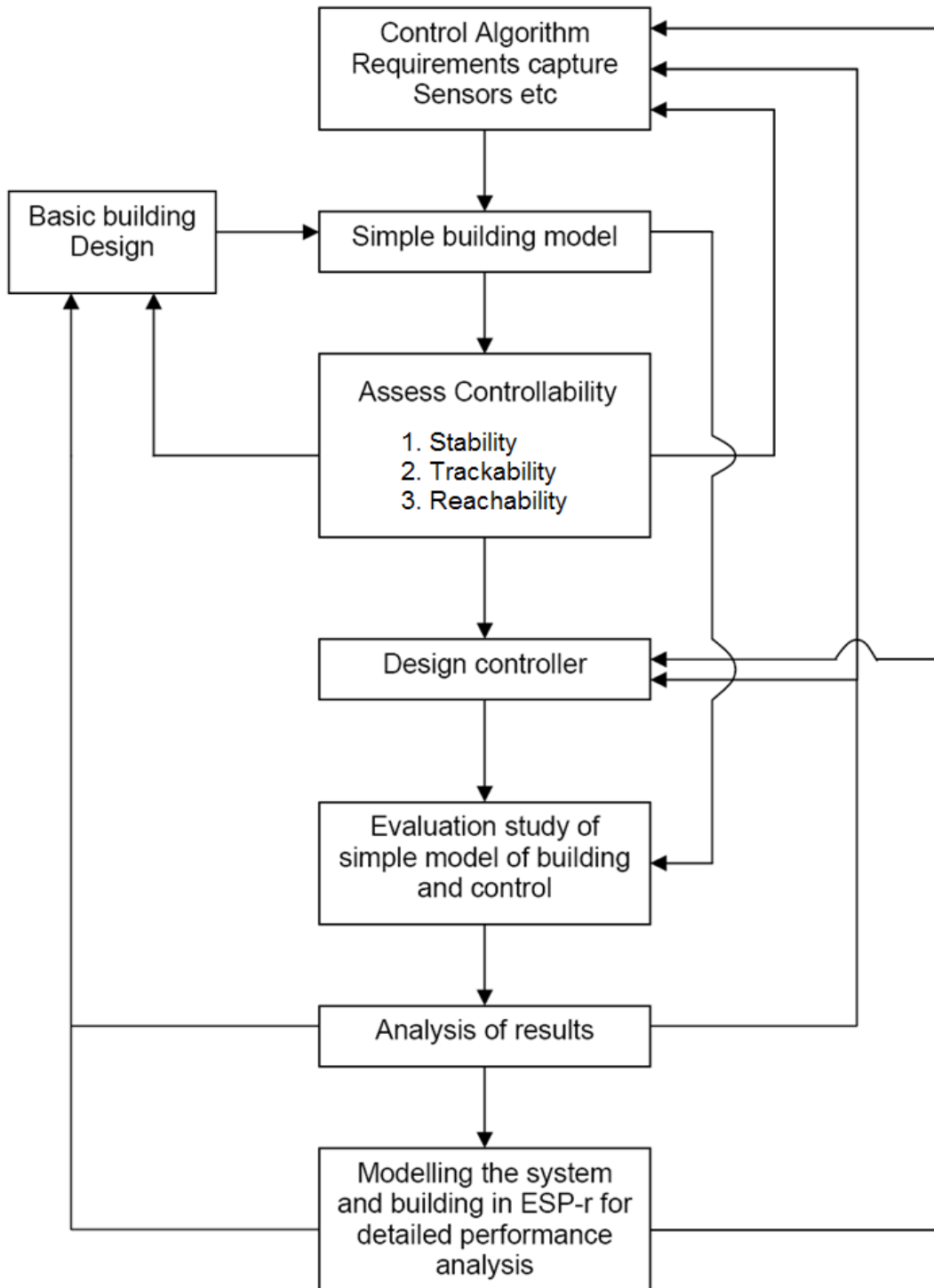


Figure 48 Proposed design process flow diagram for controllability assessment and controller design

4.2.1 Stability

The states of the building which reach steady state quickly are known as the fast modes (e.g. air temperature) and the states that are slow to reach steady state are called the slow modes (e.g. thermal mass temperature). Stability of the fast and slow components of the building responses are important to assess. If the fast mode is unstable then it will not reach steady state. If the fast mode was stable however the slow mode was unstable then over all system will still be unstable and will diverge from the set-point.

The fast modes of the building and plant dynamics can be mathematically modelled in full order however ISR philosophy shows that in slow mode the building system can be represented by an equivalent reduced order system with the dynamics same as the original full order system. The fast modes are important only during a short initial period until the state reaches the set-point. After that period the fast modes are negligible and the behaviour of the building system can be described by its slow modes at the set-point. The Inverse dynamics input decouples the fast mode from the slow mode and describes the dynamics of slow mode of the building system. Holistically assessing the fast and slow modes for feasibility of ISR is known as the **STABILITY** of the building and its systems.

4.2.1.1 Stability of fast modes (or asymptotes [section 3.2.7])

Their stability is crucial as they are the environmental parameters being controlled in the building. At conceptual design stage, if we want to find out whether a building is stable or unstable i.e. whether it will be able to maintain its comfort requirements or not, for this we have to inspect its stability matrix [sections 3.2.5-3.2.6] derived from the mathematical state space model [chapter 2]. Thus inspection of this matrix informs about the stability of fast modes and thus how easily achieve is ISR for the building.

The stability matrix for the new system of equations (4.1)-(4.2) is derived as follows. The transfer function of the new system is derived by differentiating eqn. (4.2) and substituting equation (4.1) into it. Then further substituting $u(s) = u_c(s) + U_{trim}(s)$ and U_{trim} equation (4.3) into the transfer function and then following the procedures as shown in equations (3.15) to (3.19) (Chapter 3), the building system represented by the new system equations can be reduced to a similar form as shown in equation (3.19) and the new stability matrix is given as follows:

$$\text{Stability Matrix} = (MB + sD) \quad (4.4)$$

Note: This is confirmed by the Markov series (neglecting disturbance matrices) where by making the matrix MA cancel out will result in this system [Equations (3.62)-(3.63)]. Thus it is shown that with the application of the U_{trim} input the system is reduced to a low less complex first order system.

The significance of $(MB+sD)$ matrix of a building can be explained as such that if $(MB+sD)$ is full rank i.e. its inverse exists then it means that the building can achieve stability. And that the ISR of the building also exists to some degree. The degree of ISR is determined by the structure of the matrix which shows the stability of the fast modes [chapter 3 section: 3.2.7].

The physical structure of the $(MB+sD)$ matrix shows the cross coupling between the different control channels such as humidity, lighting and temperature (section 3.2.4). If the matrix is completely diagonal then this means that the control channels are not coupled and will be easier to control with simple controllers. A non diagonal matrix is indicating cross coupling between the control channels. The stability of each control channel is found by the eigenvalues of the matrix (section 3.2.6). The eigenvalues of the matrix determine the direction of the asymptotes (fast modes) on the stability chart (root locus). If the eigenvalues are negative then it means that the asymptotes are pointing towards the stable region. This in practice implies good controllability along with easier commissioning of simple controls giving. On the other hand if eigenvalues are positive then it means that the asymptotes are pointing

towards the unstable region and thus the building is uncontrollable having no chance of simple control to work. It is possible to make these eigenvalues stable however this requires a more complex high performance controller design using pre-filter matrix $(MB+sD)^{-1}$ [(Bradshaw & Counsell, 1992), (Muir & Bradshaw, 1996)] as discussed and shown in section 3.4.1 equation (3.77).

If the stability matrix is rank defective then it becomes a trackability problem as the system is marginally stable and this is further discussed in the section on Trackability [section 4.2.2].

4.2.1.2 Stability of slow modes (transmission zeros)

The stability of slow mode(s) of a building is determined by the inherent property of the building called the transmission zero(s). As shown in chapter 3 (section 3.2.7) their values are calculated by the determinant of the matrix:

$$TZ = \det \begin{vmatrix} sI - A & B \\ C & D \end{vmatrix} = 0 \quad (4.5)$$

The transmission zeros need to be negative for the building to be inherently stable. If they are positive then the building is inherently unstable. They basically determine the stability of the building the slow parts which affect the steady state response of the system. Thus at conceptual design stage with a symbolic model the transmission zeros can be derived symbolically and sensitivity analysis can be performed to analyse their stability and also the response of the building.

The closer the transmission zeros are to the origin of the stability chart (root locus) the slower the response of the building will be and vice versa [(Straete, 1995)]. Therefore those factors that influence the response of the building can be analysed and tuned for the building requirements and systems installed. Thus for a designer changing the position of the transmission zeros can result in changing the response of

the building. This is possible because the transmission zeros are a function of all the parameters of the building, plant and sensors.

In conclusion, overall the stability of a building depends on the stability of its fast and slow parts. Their stability is governed by the rank and structure of the stability matrix and the transmissions zeros. Thus it is possible for a designer to design an inherently unstable building with positive asymptotes and transmission zeros meaning that ISR is very difficult. In practice, simple controllers will find impossible to control this building. Hence inspecting the transmission zeros and stability matrix of a building at the conceptual design stage will result in a stable building at build stage allowing easier commissioning of the control systems.

In cases where the asymptotes are pointing at an angle towards the stable region then this indicates that the response of the building states will not be a perfect first order response. In other words there may be oscillatory behaviour with overshoots and steady state error even though the building and control systems are overall stable. Thus being stable does not guarantee accurate tracking of the set point.

This section is just to analyse the structure of the stability matrix and asymptotes for determining stability. Trackability looks at the problem of stability matrix being rank defective and using extra measurements to make it full rank and then perform stability again.

4.2.2 Trackability

It is very important that while the building system is stable it is also able to effectively track the set point of the building variable being controlled. If the stability matrix ($MB+sD$) is rank defective i.e. it is not invertible and this means that the matrix has a column or row having all zeros and this leads to one or several eigenvalues being located at the origin. This results in the response of the corresponding control channel to be oscillatory as it is marginally stable. Although

not completely unstable, a marginally stable system will not be able to track the set point accurately. Therefore it's a Trackability problem.

For a rank defective stability matrix the ISR philosophy states that the ISR for the building doesn't exist or is not feasible (sections 3.2.3-3.2.4). If ISR is not possible for a building then a simple controller such as a PI controller will not be able to control this building in reality. Thus for simple controllers this building would be uncontrollable. The solution to this tracking problem is that extra sensor measurements are required and selected such that the stability matrix becomes full rank.

In control systems design you have to measure (feedback) what you are trying to control. However sometimes this results in ISR to be difficult. Thus it is sometimes useful to take extra measurements which allow for ease of ISR i.e. good Trackability. This is why the RIDE theory generalises the feedback to $w(s)$ to ensure that you select such measurements that allows for ISR control law to track accurately. This requires the modification of the feedback equation 105. Therefore at conceptual design stage the sensitivity of sensor measurements to $|MB+sD|=0$ needs to be analysed through the use of symbolic models. In this way, in practice those factors can be avoided that will cause the building system to be not trackable due to marginally stable fast modes (asymptotes).

How to know in practice whether $MB+sD$ is full rank or not without modelling?

Answer: In real systems the appearance of degenerate cases is most often due to at least one of the matrices M and B not having maximal rank. An example of degeneration of matrix M is a system in which several components of the control suffer discontinuities simultaneously. If more than one control is applied to the same inputs of the system, then the columns of matrix B corresponding to these controls will be collinear and, consequently, this matrix is degenerate. Combinations of these two cases can also lead to degeneracy [(Utkin, 1971)].

In the stable region, if the asymptotes (fast modes) are aligned to the negative real axis then this means that the tracking will be fast, accurate and with first order response. If they are at angles to the real axis i.e. complex, then the tracking will depend on the location in the complex region and its corresponding natural frequency and damping ratio will determine the tracking and response. And as mentioned above that for re-aligning the asymptotes to the real axis requires a complex controller design. However in industry only the PID controller is commonly used. A lot of times the reason for such a case where the asymptotes are pointing at angles is because of the cross coupling between the various control channels that have different bandwidths to each other e.g. temperature and CO₂ control systems are coupled by the ventilation system. If the speeds of response (i.e. bandwidth) of the heating and ventilation systems are not equal then both will not be able to reject each other's cross coupled effects as one might be slower to respond and disturbance reject. Thus here Trackability will be difficult.

Hence Trackability is dependent on the speed of the response of the control system and the choice of sensors measurements. If the response of the control system is faster than the dynamics of the plant and the sensor then the control system will never be able to track in the building. The speed of response of the control system is known as the closed loop bandwidth [chapter 3 section 3.2.5]. Thus it is very important that the closed loop bandwidth is set at three times slower than the fast dynamics of the building systems such as plant and sensors. The factor of 3 is a general rule of thumb used in the aerospace industry for setting closed loop bandwidth [appendix 9]. Thus in practice, for buildings: The time constant of controller must be set a third of the actuator and sensors time constant to ensure Trackability:

$$\tau_c = \frac{\tau_a}{3} \quad (4.6)$$

This is also useful in conceptual design stage for mathematical building models used for design and simulation of control systems. By assuming the plant and sensors to be fast compare to closed loop bandwidth these dynamics can be neglected as

parasitics in modelling of the causes and effects. This allows for simplified building models for controllability analysis where fast dynamics of plant and sensors are neglected with the assumption that their bandwidth is three times higher than the bandwidth of the closed loop system. For designers, at conceptual design stage having a building model can allow for determining the closed loop bandwidth required for trackability of the building.

At conceptual design, in theory the choice of open-loop system models for control system design and analysis depends on the desired speed of response of the feedback system [see section 2.4]. If the desired feedback system bandwidth is much lower than the actuator and sensor bandwidths then the actuator and sensor modes can be neglected as “parasitics”. However when the system bandwidth is close to the actuator-sensor bandwidth, the cautious designer includes the actuator-sensor dynamics in the open-loop model. This increases the complexity of the feedback design and may cause numerical difficulties. A more practical way is to neglect the actuator-sensor parasitics, but to develop a method which anticipates their effect on system performance in practice [see section 3.2.5].

In aerospace applications sensor dynamics are very important [(Counsell J. M., 1992)] as the control actions are taking place in milliseconds or less and here the sensor dynamics have significant effect on controllability. In most other applications such as buildings, comparatively the control actions are taking place in minutes and thus sensors are considered fast. However especially in buildings the transport delay (i.e. sensor signal delay) can causes problems in controllability. For example in buildings the transport delay is the time taken for the sensor to record the correct ambient temperature when there is a step change in the air temperature due to actuator injecting cool or heat into the zone. The transport delay is affected by the air change rate of the zone which is disrupted by disturbances in the zone such as occupancy and appliances. These are stochastic effects which are difficult to predict however occupancy patterns can be mapped for a particular zone application and according to that time taken for the temperature to settle can be roughly estimated. According to this time the bandwidth of the controller can be set so that the

controller waits for the sensor signal before commanding the actuator systems. The transport lag would be at least a first order transfer function that would cause the relative degree to be greater than 1 as shown above. Another time lag in addition to this can be due to the slow actuating systems and thus their response times also have to be taken account in the transport lag.

This is one of the reasons why for conceptual design stage the SAP [(BRE-SAP, 2005)] methodology utilises responsivity factors to account of dynamics of different plants. Because it assumes that these dynamics are fast compare to the closed loop bandwidth of the building control system. Thus their dynamics are neglected as SAP is for energy consumption analysis tool and not for assessing building/plant dynamics and control analysis.

Thus in theory when it is assumed that the actuator and sensors are fast compared to the speed of the closed loop response for making stability matrix full rank, in practice to take account of this assumption a ratio is considered between the closed loop bandwidth and the sensor and actuator bandwidths. Normally in practice a safety factor of three is used i.e. the closed loop bandwidth is a third of the actuator and sensor bandwidth. This ensures that the assumption of fast actuator and sensors is valid and the system is controllable [appendix 9].

While the actuator and sensor dynamics can be neglected by considering appropriate closed loop bandwidth, the closed loop system could still have a relative degree greater than then 1 if the system is of a higher order. In practice, systems such as climate adaptive buildings are higher order systems. Classical control theory shows that adding dynamics in the feed-forward loop e.g. actuators and controller transfer function, increasing the order of the system and thus increases the number of poles. Therefore the order of feed-back loop has to be increased and this increases the number of zeros; thus reducing the relative degree. In most cases, the order of the system (number of poles) is fixed. However, the number of zeros can be altered and thus the relative degree. This is another reason why it is important to have a physical insight into how some modifications to the system involve the number and values of

the zeros. In practice this is determined by what state of the system is being controlled, what is being measured by the sensor and what is being feedback. An appropriate feedback i.e. sensor measurement, in practice would help in making stability matrix full rank and thus allowing the system to operate with ISR.

Thus in practice **TRACKABILITY** of the building system is the speed of response of the control system and the choice of sensor measurements and the rank of the stability matrix. As shown in chapter 3 that a first order system with first order actuator and sensor dynamics would cause the closed system to have a relative degree greater than 1 meaning the MB matrix is equal to zero. This obviously means that equivalent control cannot be derived i.e. ISR is not possible. This means that for ISR to be feasible the actuator and sensors need to be fast? This is not possible in reality as most systems are not instantly fast or zeroth order. To solve this problem the concept of bandwidth is introduced for simplifying modelling and keeping the stability matrix full rank.

4.2.3 Reachability

It is useful if the control system is stable and once at the set point, it will be able to track the set point. However this is only possible if the building is able to reach the set point with its control system. Therefore it is important to assess whether a building design with all its systems will in practice be able to reach the set-point. **It is not useful that if the control system is asking the plant to deliver more than it can to be able to reach the set point. This is determined by understanding the safety criterion of U_{trim} [see section 3.2.11]. If the U_{trim} is within its safe limits then this means that the building will reach its set point. U_{trim} is a function of all the different building and plant parameters. Thus assessing symbolically which parameters will affect the building reaching its set-point is crucial to REACHABILITY of the building control system.**

The safe operation of the control system under disturbances and actuator nonlinearities is governed by the safe criteria for U_{trim} [(Counsell J. M., 1992),

(Bradshaw & Counsell, 1992)]. The presence of limitations on the power of the building's plant results in limitation on maintaining stable tracking as insufficient power directly affects the Reachability of the system. In order to better understand this it is useful to derive a criterion which describes the Reachability limits. When the plant output, $u_a(s)$, has reached its upper (L_U) or lower (L_L) limits, the control signal to the plant, $u(s)$, must either remain constant or decrease in order to avoid overdriving the plant and to maintain safe control. This is derived and discussed in section 3.2.11 following the procedures in equation (3.91)-(3.101) and for the new system of equations is given as follows:

When $u(s) > 0$ and $u_a(s) = L_U$

$$U_{trim}(s) \leq L_U - sK(s)^{-1}(MB + sD)^{-1}U_{trim}(s) - s(MB + sD)^{-1}r(s) \quad (4.7)$$

When $u(s) < 0$ and $u_a(s) = L_L$

$$U_{trim}(s) \geq L_L - sK(s)^{-1}(MB + sD)^{-1}U_{trim}(s) - s(MB + sD)^{-1}r(s) \quad (4.8)$$

By combining these two expressions, a single criterion can be formed as follows:

$$L_L - (MB + sD)^{-1} \left(\frac{sU_{trim}(s)}{K(s)} + sr(s) \right) \leq U_{trim}(s) \leq L_U - (MB + sD)^{-1} \left(\frac{sU_{trim}(s)}{K(s)} + sr(s) \right) \quad (4.9)$$

As long as the U_{trim} is within the limits derived in equations derived above the building system will reach the set points of the variables being controlled simultaneously. If providing that the rate of change of U_{trim} is small and also the rate of change of the set-point being zero compare to the bandwidth of the controller then, the limitation on tracking is that U_{trim} must remain between the upper and lower actuator limits.

$$L_L \leq U_{trim}(s) \leq L_U \quad (4.10)$$

This criterion demonstrates that, when actuator limits are reached, safety can be ensured simply by setting the error signal to zero, providing that steady state is reachable (i.e. that the U_{trim} is within limits).

In theory the original expression for U_{trim} can be symbolically expanded to see which properties of the building and its control system affect the value of U_{trim} from staying between the plant limits. Through sensitivity analysis different operating points can be inspected for Reachability and the affecting factors. This condition for Reachability can also be readily inspected using dynamic simulation.

This is very useful at the conceptual design stage where dynamic simulation can be used for assessing the Reachability before the building is built. In theory the U_{trim} governs the dynamics of the slow modes. When a building is controlled and has reached set point it's dynamics are represented by the dynamics of the U_{trim} . Thus if inspected by dynamic simulation we would expect to see that in transient mode and steady state mode the ideal required plant input (U_{trim}) and the actual plant input. This comparison will show whether actual plant input is sufficient for reaching steady state or not. And thus is very useful as a sizing tool at the conceptual design stage hence we important for assessing energy consumption.

Hence Reachability is not based on the building having cooling . Hence the equation (4.3) for U_{trim} does not depend on the system having cooling to be applicable. The U_{trim} calculates the actuator input required in response to the offset in temperature due to disturbances etc. If the U_{trim} is negative i.e. to reach set point cooling is required. then it is up to the designer whether to use active or passive cooling. terms associated with active and passive cooling are present in the U_{trim} equation as shown in (case study 3). if the designer wants to use passive means then it will try to increase thermal mass, air change or some building parameter in the U_{trim} equation to eliminate the need for active cooling.

Practically this is very useful because if the plant power is not enough then U_{trim} would be larger than the plant input showing that plant power is insufficient for reaching the set point. In practice if an accurate estimate of the U_{trim} can be constantly monitored then the buildings Reachability can be assessed.

Thus the STAR theory or buildings for controllability assessment is EQUALLY applicable for:

1. **Heating and cooling only**
2. **Heating only**
3. **Cooling only**

In conclusion what does STaR theory mean in terms of current industrial practice and are current methods in any way useful for building design?

4.2.4 STaR Theory and the present state of building's industry

As discussed in earlier chapters the science of controllability can be applied to any system whether aircrafts, buildings, robots, automotive, chemical plants etc. In all these systems there is a fundamental difference between energy controllability and energy consumption. For energy controllability the analysis of the dynamics of the system are utmost important as they determine the magnitude of rate of transmission of energy between the various parts of the system. Without accurate knowledge of dynamics of transmission of energy, it will not be possible to design efficient controls. However it is important that through conceptual design stages a method of analysis can be used to determine which dynamics are significant in affecting controllability. And they are used in the process of controller design. It may be that some effects that are significant to energy consumption are not important to energy controllability and may be ignored. This is one of the reasons for simplified models used in high performance and technology industries such as aerospace where failure is not an option. On the other hand energy consumption is not about rate of energy transmission, but about the amount of energy transferred in total. Here it can be argued that knowing all the dynamics will obviously help in estimating the amount of energy consumption. This is true however not all the dynamics have significant effect on energy consumption.

The STaR theory can be used to explain and support the justification of why in buildings SAP and SBEM utilise quasi steady state models. For example in terms of control theory, the SAP method has utilised singular perturbation technique to neglected fast dynamics of the actuators and assumed they are steady state and has incorporated them in the model using Responsivity Factors. This assumption is reasonable when the dynamics of the thermal mass are compared to the short term dynamics of the heating system in SAP. On the other hand it assumes that thermal mass dynamics are so slow that they can be assumed constant i.e. steady state. However the air temperature lies in between the fast and slow modes. This means that air temperature should have been modelled dynamically where as in SAP it is assumed steady state.

By assuming the system to be operating with Inverse dynamics input (U_{trim}), SAP has taken the temperature to be always maintained at the set-point i.e. constant. Hence, $\dot{Q}_{in} - \dot{Q}_{out} = 0$ and the energy (plant input U) required for ISR is worked out i.e. energy consumption. This input (U) is of course the same as equivalent control or U_{trim} which corresponds to the slow modes of the system. In buildings these slow modes are the thermal mass. Thus SAP's quasi steady state method could be justifiable by inspecting U_{trim} of buildings. Inspection of U_{trim} for a building will be able to show whether the slow modes are very slow and thus could be considered steady state as long as transmission zeros are stable. If U_{trim} is almost steady then slow modes are very slow and can be assumed constant i.e. steady state.

Although it is acknowledged that this justification is correct for energy consumption but obviously not for energy controllability. Although some practical ways are mentioned for ensuring controllability however STaR theory requires ultimately the building to be modelled for controllability. Presently the building industry stands on having years of experience through practice which is unlike the aerospace industry where experience and practice are justified also through an engineering science.

Assessing the stability of new systems in relation to building physics and control is important where empirical data is not available. The stability matrix describes the relationship between inputs and outputs of a complex MIMO building system. Understanding dynamics of new systems and how they affect tracking will help in delivering more efficient solutions. Operation and sizing of plant systems will also help delivering cost effective solutions that meet the demand and conserve energy.

5 : Case studies



“Good buildings come from good people, and all problems are solved by good design” Stephen Gardiner

5.1 Stability of Heating Systems with Slow Actuation

The purpose of this case study is to illustrate the important of $\det|MB| \neq 0$ for stability of the system when applied with Inverse dynamics input. The stability of the slow acting heating system is assessed when controlling the following variables for achieving thermal comfort:

- 1) Air temperature
- 2) Air temperature plus its rate of change
- 3) Comfort temperature

This section presents a case study of a school being designed in Scotland using the CAB design philosophy and is illustrated in figure below. The school will have a building management system that will utilise the latest technology to control and monitor the school's environmental conditions to aid learning and maximise energy efficiency. Some of the technologies proposed for achieving thermal comfort through a sustainable, low-energy approach incorporate under floor heating system rather than the conventional radiator system that will be of the "self-regulating" type. The temperature of the air in the zone will be controlled by means of floor embedded and air sensors connected to the BMS software to monitor and regulate the space temperature. The ventilation strategy employs natural means by manually operated windows and ventilation "stacks". The "stacks" will also incorporate axial fans which will be automatically operated via a combined temperature and CO₂ room sensor ensuring a fresh teaching environment and that the temperature is kept within the stated criteria. The school will have an intelligent lighting control system that dims down the lighting depending on the natural daylight available externally, thus reducing the energy consumption. In this case study a single class room is modelled for controllability analysis (Appendix 6).



Figure 49 Case study School Design Concept

As stated above, the mechanical ventilation (axial fans) will be used to control both temperature and CO₂ to ensure fresh teaching environment and comfort temperature are achieved. In this thesis, only the heating mode (figure below) is considered for controllability analysis where mechanical ventilation is not required for cooling and thus mechanical ventilation is only used for controlling CO₂ concentration levels.

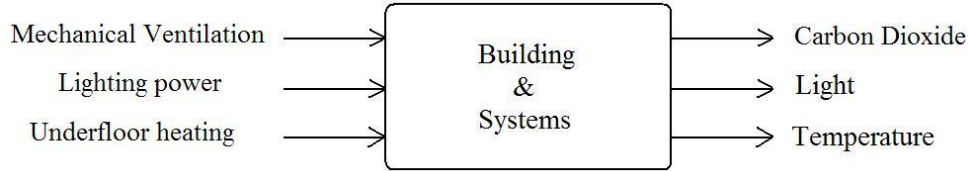


Figure 50 Heating mode, showing inputs of the whole system, where MV = Mechanical ventilation, PL = lighting power and UFH = Under-floor heating

5.1.1 Mathematical Modelling

First the mathematical equations were created that represent the physics of the above system and are as follows:

Rate of change of air temperature equation is as follows:

$$\rho_a V_a c_{pa} \frac{dT_a}{dt} = \left[\begin{array}{l} (\dot{Q}_{sa} + \dot{Q}_L + \dot{Q}_{oc})_{casual\ gains} \\ + (\dot{Q}_{wi1} + \dot{Q}_{wi2} + \dot{Q}_{wi3} + \dot{Q}_{wi4} + \dot{Q}_{ri} + \dot{Q}_{win} + \dot{Q}_m)_{structure} \\ + (\dot{Q}_t + \dot{Q}_v + \dot{Q}_{ni})_{ventilation} \\ + (\dot{Q}_{mv} + \dot{Q}_{cp})_{heating/cooling} \end{array} \right] \quad (5.1)$$

Where the heat transfers are defined as follows:

$$\dot{Q}_{sa} = \alpha_a \sigma_s A_{win} I_{dr} \quad (5.2)$$

$$\dot{Q}_L = k_e P_L \quad (5.3)$$

$$\dot{Q}_{oc} = g_{oc} n_{oc} \quad (5.4)$$

$$\dot{Q}_{wi1} = 2U_{w1}A_{w1}(T_{w1} - T_a) \quad (5.5)$$

$$\dot{Q}_{wi2} = 2U_{w2}A_{w2}(T_{w2} - T_a) \quad (5.6)$$

$$\dot{Q}_{wi3} = 2U_{w3}A_{w3}(T_{w3} - T_a) \quad (5.7)$$

$$\dot{Q}_{w4} = 2U_{w4}A_{w4}(T_{w4} - T_a) \quad (5.8)$$

$$\dot{Q}_{ri} = 2U_r A_r (T_r - T_a) \quad (5.9)$$

$$\dot{Q}_{win} = U_{win} A_{win} (T_o - T_a) \quad (5.10)$$

$$\dot{Q}_m = h_m A_m (T_m - T_a) \quad (5.11)$$

$$\dot{Q}_t = V_a n_t \rho_a c_{pa} (T_o - T_a) \quad (5.12)$$

$$\dot{Q}_v = V_a n_v \rho_a c_{pa} (T_o - T_a) \quad (5.13)$$

$$\dot{Q}_{in} = V_a n_{in} \rho_a c_{pa} (T_o - T_a) \quad (5.14)$$

$$\dot{Q}_{mv} = q_{mv} \rho_a c_{pa} (T_o - T_a) \quad (5.15)$$

$$\dot{Q}_{cp} = h_c A_s (T_s - T_a) \quad (5.16)$$

There are four walls in this zone. They are modelled in the same way as shown in chapter 2. The equations are as follows:

$$\rho_{w1} V_{w1} c_{pw1} \frac{dT_{w1}}{dt} = [\dot{Q}_{wo1} - \dot{Q}_{wi1}] \quad (5.17)$$

$$\rho_{w2} V_{w2} c_{pw2} \frac{dT_{w2}}{dt} = [\dot{Q}_{wo2} - \dot{Q}_{wi2}] \quad (5.18)$$

$$\rho_{w3} V_{w3} c_{pw3} \frac{dT_{w3}}{dt} = [\dot{Q}_{wo3} - \dot{Q}_{wi3}] \quad (5.19)$$

$$\rho_{w4} V_{w4} c_{pw4} \frac{dT_{w4}}{dt} = [\dot{Q}_{wo4} - \dot{Q}_{wi4}] \quad (5.20)$$

Where:

$$\dot{Q}_{wo1} = 2U_{w1}A_{w1}(T_{o1} - T_{w1}) \quad (5.21)$$

$$\dot{Q}_{wo2} = 2U_{w2}A_{w2}(T_{o2} - T_{w2}) \quad (5.22)$$

$$\dot{Q}_{wo3} = 2U_{w3}A_{w3}(T_{o3} - T_{w3}) \quad (5.23)$$

$$\dot{Q}_{wo4} = 2U_{w4}A_{w4}(T_{o4} - T_{w4}) \quad (5.24)$$

The heating system in this case study is the under-floor heating system and thus the modelling of the floor is crucial to understanding the controllability of the slow heating system. The floor has three sections: screed, insulation and concrete. Since the floor is heated, each section of the floor is modelled separately for heat transfer. The heat interchange is assumed to be between the floor screed and the air. Thus, the temperature of the screed T_s is given by:

$$\rho_s V_s c_{ps} \frac{dT_s}{dt} = [\dot{Q}_{in} + \dot{Q}_p - \dot{Q}_{cp} - \dot{Q}_{rpm}] \quad (5.25)$$

The floor's insulation layer which is in the middle of screed and concrete is assumed to be in a steady state condition and the heat transfer through the insulation is:

$$\dot{Q}_{in} = U_{in} A_{in} (T_c - T_s) \quad (5.26)$$

The radiation transfer from floor to internal thermal mass is given by:

$$\dot{Q}_{rpm} = h_r A_s (T_s - T_m) \quad (5.27)$$

The temperature of the floor's concrete layer T_c is given by:

$$\rho_c V_c c_{pc} \frac{dT_c}{dt} = [\dot{Q}_{ci} - \dot{Q}_{in}] \quad (5.28)$$

Where:

$$\dot{Q}_{ci} = U_c A_c (T_{o5} - T_c) \quad (5.29)$$

The roof temperature T_r is modelled simple as shown in chapter 2 as follows:

$$\rho_r V_r c_{pr} \frac{dT_r}{dt} = [\dot{Q}_{ro} - \dot{Q}_{ri}] \quad (5.30)$$

Where:

$$\dot{Q}_{ro} = 2U_r A_r (T_{o6} - T_r) \quad (5.31)$$

The differential equation which governs the generation and decay of CO₂, based on mass consideration, can be expressed as:

$$\rho_{co2} V_a \frac{dC_a}{dt} = S - \dot{C}_{mv} - \dot{C}_t - \dot{C}_v - \dot{C}_i \quad (5.32)$$

Where:

S is internal CO₂ gain (kg/s)

$$\dot{C}_{mv} = q_{mv} \rho_{co2} (C_a - C_o) \quad (5.33)$$

$$\dot{C}_t = \rho_{co2} n_t V_a (C_a - C_o) \quad (5.34)$$

$$\dot{C}_v = \rho_{co2} n_v V_a (C_a - C_o) \quad (5.35)$$

$$\dot{C}_i = \rho_{co2} n_i V_a (C_a - C_o) \quad (5.36)$$

Rate of change of lighting power:

Lighting systems are constrained to limiting the frequency at which their lux levels can power on and off [(Newsham & C.Donnely, 2006)]. Consequently, it is sensible to control the rate-of-change of power delivered to the lighting system such that,

$$\frac{dP_L}{dt} = u_L \quad (5.37)$$

The rate of change of internal thermal mass (furniture) is given by:

$$\rho_m V_m c_{pm} \frac{dT_m}{dt} = [\dot{Q}_{sm} + \dot{Q}_{rpm} - \dot{Q}_m] \quad (5.38)$$

Where:

$$\dot{Q}_m = h_m A_m (T_m - T_a) \quad (5.39)$$

$$\dot{Q}_{sm} = \alpha_m \sigma_s A_{win} I_{dr} \quad (5.40)$$

5.1.2 Stability of air temperature control

A feedback control system can only control (i.e. track) what it feeds back as measured system outputs. Thus, to analyse the controllability of these measurements, they must be defined and are as follows:

$$\text{Measured Comfort CO}_2 \text{ is given by: } C_{cm} = C_a \quad (5.41)$$

$$\text{Measured Comfort lux level is given by: } L_{cm} = L_i + L_s = k_L P_L + \lambda \alpha_L I_{df} \quad (5.42)$$

$$\text{Measured Air Temperature level is given by: } T_{cm} = T_a \quad (5.43)$$

In order to apply the aerospace controllability science, the nonlinear dynamic equations must be linearised about a steady state operating point. As mentioned before this is science for both linear and nonlinear systems, however the symbolic can only be done as a linearised system. The nonlinear effects have not been compromised by linearisation because of how the nonlinear effects have modelled. A good example is the natural ventilation air change equation in chapter 2. The linearization's are as follows:

$$\text{Nonlinear: } \dot{Q}_v = V_a n_v \rho_a c_{pa} (T_o - T_a) = V_a n_v \rho_a c_{pa} T_o - V_a n \rho_a c_{pa} T_a \quad (5.44)$$

$$\text{Linear: } \delta \dot{Q}_v = V_a \rho_a c_{pa} \bar{n}_v \delta T_o - V_a \rho_a c_{pa} \bar{n}_v \delta T_a + V_a \rho_a c_{pa} (\bar{T}_o - \bar{T}_a) \delta n_v \quad (5.45)$$

$$\text{Nonlinear: } \dot{Q}_{mv} = q_{mv} \rho_a c_{pa} (T_o - T_a) = \rho_a c_{pa} q_{mv} T_o - \rho_a c_{pa} q_{mv} T_a \quad (5.46)$$

$$\text{Linear: } \delta \dot{Q}_{mv} = \rho_a c_{pa} \bar{q}_{mv} \delta T_o - \rho_a c_{pa} \bar{q}_{mv} \delta T_a + \rho_a c_{pa} (\bar{T}_o - \bar{T}_a) \delta q_{mv} \quad (5.47)$$

$$\text{Nonlinear: } \dot{C}_{mv} = q_{mv} \rho_{co2} (C_a - C_o) = q_{mv} \rho_{co2} C_a - q_{mv} \rho_{co2} C_o \quad (5.48)$$

$$\text{Linear: } \delta \dot{C}_{mv} = \bar{q}_{mv} \rho_{co2} \delta C_a + \rho_{co2} (\bar{C}_a - \bar{C}_o) \delta q_{mv} - \bar{q}_{mv} \rho_{co2} \delta C_o \quad (5.49)$$

$$\text{Nonlinear: } \dot{C}_v = \rho_{co2} n_v V_a (C_a - C_o) = \rho_{co2} n_v V_a C_a - \rho_{co2} n_v V_a C_o \quad (5.50)$$

$$\text{Linear: } \delta \dot{C}_v = \rho_{co2} \bar{n}_v V_a \delta C_a + \rho_{co2} V_a (\bar{C}_a - \bar{C}_o) \delta n_v - \rho_{co2} \bar{n}_v V_a \delta C_o \quad (5.51)$$

The results of this linearisation enable the total system to be represented in the state-space form:

$$\dot{x}(t) = Ax(t) + Bu(t) + Fd(t) \quad (5.52)$$

$$y(t) = Mx(t) + Du(t) + Ed(t) \quad (5.53)$$

This linear model describes the dynamic behaviour of the building and its systems for a small amplitude perturbation δ about a steady state equilibrium condition. Where $y(t)$ is the measured output vector, $x(t)$ is a vector of state variables, $u(t)$ is a vector of system inputs (i.e. controller outputs) and $d(t)$ is a vector of disturbances. A, B, M, D, E and F are time invariant matrices consisting of constants. The vectors associated with these matrices are given as follows:

$$\begin{aligned} \delta x &= [\delta T_a, \delta T_{w1}, \delta T_{w2}, \delta T_{w3}, \delta T_{w4}, \delta T_s, \delta T_c, \delta T_r, \delta C_a, \delta P_L, \delta T_m]^T \\ \delta u &= [\delta q_{mv}, \delta u_L, \delta \dot{Q}_p]^T \\ \delta y &= [\delta C_{cm}, \delta L_{cm}, \delta T_{cm}]^T \\ \delta d &= [\delta I_{dr}, \delta n_{oc}, \delta T_o, \delta T_{o1}, \delta T_{o2}, \delta T_{o3}, \delta T_{o4}, \delta T_{o5}, \delta T_{o6}, \delta n_v, \delta S, \delta C_o, \delta I_{df}]^T \end{aligned} \quad (5.54)$$

State space model matrixes are given as follows and matrix elements are given in Appendix 6:

$$A = \begin{bmatrix} a_{11} & a_{12} & a_{13} & a_{14} & a_{15} & a_{16} & 0 & a_{18} & 0 & a_{110} & a_{111} \\ a_{21} & a_{22} & 0 & 0 & 0 & 0 & 0 & 0 & 0 & 0 & 0 \\ a_{31} & 0 & a_{33} & 0 & 0 & 0 & 0 & 0 & 0 & 0 & 0 \\ a_{41} & 0 & 0 & a_{44} & 0 & 0 & 0 & 0 & 0 & 0 & 0 \\ a_{51} & 0 & 0 & 0 & a_{55} & 0 & 0 & 0 & 0 & 0 & 0 \\ a_{61} & 0 & 0 & 0 & 0 & a_{66} & a_{67} & 0 & 0 & 0 & a_{611} \\ 0 & 0 & 0 & 0 & 0 & a_{76} & a_{77} & 0 & 0 & 0 & 0 \\ a_{81} & 0 & 0 & 0 & 0 & 0 & 0 & a_{88} & 0 & 0 & 0 \\ 0 & 0 & 0 & 0 & 0 & 0 & 0 & 0 & a_{99} & 0 & 0 \\ 0 & 0 & 0 & 0 & 0 & 0 & 0 & 0 & 0 & 0 & 0 \\ a_{111} & 0 & 0 & 0 & 0 & a_{116} & 0 & 0 & 0 & 0 & a_{1111} \end{bmatrix}, B = \begin{bmatrix} b_{11} & 0 & 0 \\ 0 & 0 & 0 \\ 0 & 0 & 0 \\ 0 & 0 & 0 \\ 0 & 0 & 0 \\ 0 & 0 & b_{63} \\ 0 & 0 & 0 \\ 0 & 0 & 0 \\ b_{91} & 0 & 0 \\ 0 & b_{102} & 0 \\ 0 & 0 & 0 \end{bmatrix}$$

$$F = \begin{bmatrix} f_{11} & f_{12} & f_{13} & 0 & 0 & 0 & 0 & 0 & 0 & f_{110} & 0 & 0 & 0 \\ 0 & f_{22} & 0 & 0 & 0 & 0 & 0 & 0 & 0 & 0 & 0 & 0 & 0 \\ 0 & 0 & f_{33} & 0 & 0 & 0 & 0 & 0 & 0 & 0 & 0 & 0 & 0 \\ 0 & 0 & 0 & f_{44} & 0 & 0 & 0 & 0 & 0 & 0 & 0 & 0 & 0 \\ 0 & 0 & 0 & 0 & f_{55} & 0 & 0 & 0 & 0 & 0 & 0 & 0 & 0 \\ 0 & 0 & 0 & 0 & 0 & 0 & 0 & 0 & 0 & 0 & 0 & 0 & 0 \\ 0 & 0 & 0 & 0 & 0 & 0 & 0 & f_{78} & 0 & 0 & 0 & 0 & 0 \\ 0 & 0 & 0 & 0 & 0 & 0 & 0 & f_{88} & 0 & 0 & 0 & 0 & 0 \\ 0 & 0 & 0 & 0 & 0 & 0 & 0 & 0 & 0 & f_{910} & f_{911} & f_{912} & 0 \\ 0 & 0 & 0 & 0 & 0 & 0 & 0 & 0 & 0 & 0 & 0 & 0 & 0 \\ f_{111} & 0 & 0 & 0 & 0 & 0 & 0 & 0 & 0 & 0 & 0 & 0 & 0 \end{bmatrix}$$

Initially the controllability was assessed for a feedback strategy where air temperature, lux level and internal CO₂ concentration levels were fed back and controlled. The M, D and E matrices for this strategy are as follows:

$$M = \begin{bmatrix} 0 & 0 & 0 & 0 & 0 & 0 & 0 & 0 & m_{19} & 0 & 0 \\ 0 & 0 & 0 & 0 & 0 & 0 & 0 & 0 & 0 & m_{210} & 0 \\ m_{31} & 0 & 0 & 0 & 0 & 0 & 0 & 0 & 0 & 0 & 0 \end{bmatrix}, D = \begin{bmatrix} 0 & 0 & 0 \\ 0 & 0 & 0 \\ 0 & 0 & 0 \end{bmatrix}$$

$$E = \begin{bmatrix} 0 & 0 & 0 & 0 & 0 & 0 & 0 & 0 & 0 & 0 & 0 & 0 & 0 \\ 0 & 0 & 0 & 0 & 0 & 0 & 0 & 0 & 0 & 0 & 0 & 0 & f_{213} \\ 0 & 0 & 0 & 0 & 0 & 0 & 0 & 0 & 0 & 0 & 0 & 0 & 0 \end{bmatrix}$$

The stability matrix MB+sD for this control strategy is given as follows:

$$MB + sD = \begin{bmatrix} q_{mv} & u_L & \dot{Q}_p \\ m_{19}b_{91} & 0 & 0 \\ 0 & m_{210}b_{102} & 0 \\ m_{31}b_{11} & 0 & 0 \end{bmatrix} \begin{matrix} CO_2 \\ Lux \\ Temperature \end{matrix} \quad (5.55)$$

The stability matrix is showing the cross coupling between the three control systems of CO₂, lighting and temperature. In the first column of the matrix there is an obvious coupling of CO₂ and temperature controls through ventilation. Meaning that when

running mechanical ventilation both the CO₂ concentration and air temperature are going to be affected. This will causes problems when mechanical ventilation will be turned ON for controlling CO₂ level and this will cause the temperature to be effected resulting in heating to come ON for maintaining the correct temperature. However as can be seen that this is a one way coupling as the mechanical ventilation in the heating mode is only used for controlling CO₂ level and therefore when CO₂ levels will increase then the mechanical ventilation will affect the internal temperature.

In the second column the lighting is considered independent and does not affect the other controls. Thus lighting control is completely decoupled and here simple proportional controller will be able to control lux levels easily and accurately.

From the third column it is noted that when air temperature T_a is controlled for achieving the required temperature i.e. T_{cm} = T_a, the matrix (MB+sD) is not of full rank (i.e. not invertible) as shown above. This means that the temperature control of air temperature has a problem. To understand stability of this MIMO control system, the eigenvalues of the stability matrix are calculated which show the direction of the asymptotes of each control channel from which the stability can be determined.

The RIDE theory states that the asymptotes for a multivariable design are given by Eigen-values: $|sI + g(MB + sD)\sigma| = 0$ where, g is the global gain from zero to infinity and σ is a scalar gain. Therefore the asymptotes are the solutions for s of the following determinant:

$$|sI + g(MB + sD)\sigma| = \begin{bmatrix} s_1 + gm_{19}b_{91}\sigma_1 & 0 & 0 \\ 0 & s_2 + gm_{210}b_{102}\sigma_2 & 0 \\ m_{31}b_{11} & 0 & s_3 \end{bmatrix} = 0 \quad (5.56)$$

The eigenvalues are given as follows:

$$s_1 = -gm_{19}b_{91}\sigma_1, s_2 = -gm_{210}b_{102}\sigma_2, s_3 = 0 \quad (5.57)$$

Where:

$$s_1 = g \frac{(\bar{C}_a - \bar{C}_o)}{V_a} (-\sigma_1), s_2 = -gk_L \sigma_2, s_3 = 0 \quad (5.58)$$

The eigenvalues for CO₂ and lighting are stable (i.e. negative) and their asymptotes are pointing towards left half plains. The first eigenvalue corresponding to CO₂ control channel is positive however using the negative gain this can be made negative. For air temperature control the eigenvalue is at the origin. This means that the system will be marginally stable and will result in oscillatory behaviour. Thus it means that feeding back just air temperature is not sufficient for control of air temperature with under-floor heating. This also indicates that ISR of air temperature is not feasible with slow system such as under floor heating and thus extra measurements from the sensors are needed for ISR. On a root locus this is shown as follows:

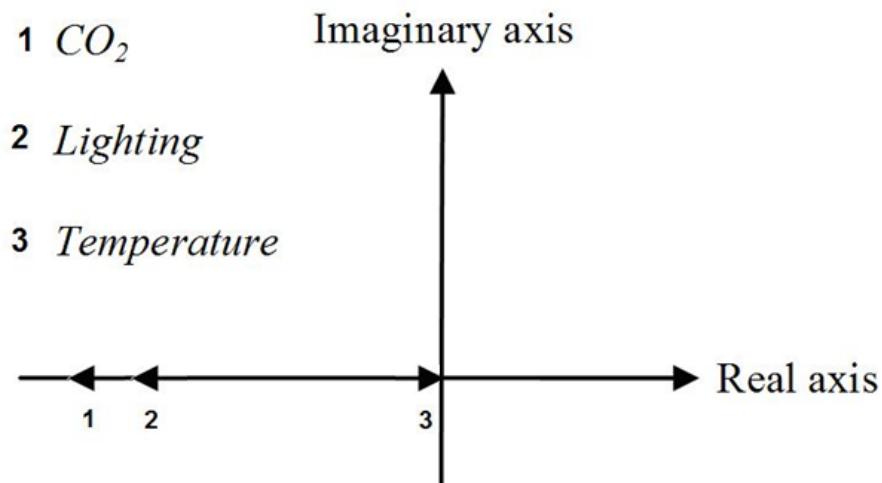


Figure 51 Asymptote directions on a root locus for the three control channels with control strategy 1

It is important at this point that the transmission zeros be also analysed to understand the total stability of the system. The transmission zeros are given by the determinant of the following matrix:

$$TZ = \det \begin{vmatrix} a_{11}-s & a_{12} & a_{13} & a_{14} & a_{15} & a_{16} & 0 & a_{18} & 0 & a_{110} & a_{111} & b_{11} & 0 & 0 \\ a_{21} & a_{22}-s & 0 & 0 & 0 & 0 & 0 & 0 & 0 & 0 & 0 & 0 & 0 & 0 \\ a_{31} & 0 & a_{33}-s & 0 & 0 & 0 & 0 & 0 & 0 & 0 & 0 & 0 & 0 & 0 \\ a_{41} & 0 & 0 & a_{44}-s & 0 & 0 & 0 & 0 & 0 & 0 & 0 & 0 & 0 & 0 \\ a_{51} & 0 & 0 & 0 & a_{55}-s & 0 & 0 & 0 & 0 & 0 & 0 & 0 & 0 & 0 \\ a_{61} & 0 & 0 & 0 & 0 & a_{66}-s & a_{67} & 0 & 0 & 0 & a_{611} & 0 & 0 & b_{63} \\ 0 & 0 & 0 & 0 & 0 & a_{76} & a_{77}-s & 0 & 0 & 0 & 0 & 0 & 0 & 0 \\ a_{81} & 0 & 0 & 0 & 0 & 0 & 0 & a_{88}-s & 0 & 0 & 0 & 0 & 0 & 0 \\ 0 & 0 & 0 & 0 & 0 & 0 & 0 & 0 & a_{99}-s & 0 & 0 & b_{91} & 0 & 0 \\ 0 & 0 & 0 & 0 & 0 & 0 & 0 & 0 & 0 & -s & 0 & 0 & b_{102} & 0 \\ a_{111} & 0 & 0 & 0 & 0 & a_{116} & 0 & 0 & 0 & 0 & a_{1111}-s & 0 & 0 & 0 \\ 0 & 0 & 0 & 0 & 0 & 0 & 0 & 0 & m_{19} & 0 & 0 & 0 & 0 & 0 \\ 0 & 0 & 0 & 0 & 0 & 0 & 0 & 0 & 0 & m_{210} & 0 & 0 & 0 & 0 \\ m_{21} & 0 & 0 & 0 & 0 & 0 & 0 & 0 & 0 & 0 & 0 & 0 & 0 & 0 \end{vmatrix} = 0$$

This matrix can be simplified to an equivalent reduced matrix.

$$TZ = \det \begin{vmatrix} a_{16} & a_{111} \\ a_{116} & a_{1111}-s \end{vmatrix} = 0 \quad (5.59)$$

Here there is one transmission zero given as follows:

$$s = \frac{a_{16}a_{1111} - a_{111}a_{116}}{a_{16}} \quad (5.60)$$

Where:

$$s = \left(-\frac{h_r A_s + h_m A_m}{\rho_m V_m c_{pm}} - \frac{h_m A_m h_r}{\rho_m V_m c_{pm} h_c} \right) \quad (5.61)$$

The transmission zero is negative and thus is located in the stable left half plane of the root locus. This is necessary to guarantee the internal stability of the whole system.

5.1.3 Stability of temperature plus its rate of change control

For the system to be fully stable the stability matrix needs to be full rank. In cases where air dominant temperature sensor is used to control the under-floor heating, this will result in unstable oscillatory behaviour. In this case study where air temperature needs to be controlled, it has been shown that the addition of rate of measured output feedback to the sensors have been successfully deployed in the aerospace industry [(Bradshaw & Counsell, 1992), (Muir & Bradshaw, 1996)] and the electric motor based systems [(Roskilly, 1990)]. This technique can be successfully used here for controlling air temperature accurately. Thus the second feedback strategy for temperature is to feedback the temperature plus rate of change of temperature. Hence in transient response the feedback will be $T_a + \dot{T}_a$, and when steady state is reached $\dot{T}_a = 0$ and thus in steady state air temperature T_a will be controlled. Thus the new feedback equation and M and D matrices are given as follows:

$$M = \begin{bmatrix} 0 & 0 & 0 & 0 & 0 & 0 & 0 & 0 & m_{19} & 0 & 0 \\ 0 & 0 & 0 & 0 & 0 & 0 & 0 & 0 & 0 & m_{210} & 0 \\ a_{11}+1 & a_{12} & a_{13} & a_{14} & a_{15} & a_{16} & 0 & a_{18} & 0 & a_{110} & a_{111} \end{bmatrix}, D = \begin{bmatrix} 0 & 0 & 0 \\ 0 & 0 & 0 \\ b_{11} & 0 & 0 \end{bmatrix}$$

$$E = \begin{bmatrix} 0 & 0 & 0 & 0 & 0 & 0 & 0 & 0 & 0 & 0 & 0 & 0 \\ 0 & 0 & 0 & 0 & 0 & 0 & 0 & 0 & 0 & 0 & 0 & f_{213} \\ f_{11} & f_{12} & f_{13} & 0 & 0 & 0 & 0 & 0 & 0 & f_{110} & 0 & 0 \end{bmatrix}$$

With the new output variable the new stability matrix is given as follows:

$$(MB + sD) = \begin{bmatrix} m_{19}b_{91} & 0 & 0 \\ 0 & m_{210}b_{102} & 0 \\ (a_{11}+1)b_{11} + b_{11}s & a_{110}b_{102} & a_{16}b_{63} \end{bmatrix} \quad (5.62)$$

The constants shown in the matrix above are function of building parameters and operating conditions as given in appendix 6:

$$m_{19} = 1, b_{91} = \frac{-(\bar{C}_a - \bar{C}_o)}{V_a}, m_{210} = k_L, b_{102} = 1,$$

$$a_{11} = \frac{1}{\rho_a V_a c_{pa}} \left(-2U_{w1} A_{w1} - 2U_{w2} A_{w2} - 2U_{w3} A_{w3} - 2U_{w4} A_{w4} - 2U_r A_r - U_{win} A_{win} \right)$$

$$b_{11} = \frac{(\bar{T}_o - \bar{T}_a)}{V_a}, a_{110} = \frac{k_e}{\rho_a V_a c_{pa}}, a_{16} = \frac{h_c A_s}{\rho_a V_a c_{pa}}, b_{63} = \frac{1}{\rho_s V_s c_{ps}}$$

The cross coupling between the inputs and outputs in the MB+sD matrix is indicated as follows:

$$(MB + sD) = \begin{bmatrix} q_{mv} & u_L & \dot{Q}_p \\ m_{19} b_{91} & 0 & 0 \\ 0 & m_{210} b_{102} & 0 \\ (a_{11} + 1) b_{11} + b_{11} s & a_{110} b_{102} & a_{16} b_{63} \end{bmatrix} \begin{bmatrix} CO_2 \\ Lux \\ Temp \end{bmatrix} \quad (5.63)$$

The matrix is not diagonal and it is also important to inspect the asymptotes and they are given by the follow determinant:

$$|sI + g(MB + sD)\sigma| = 0 \quad (5.64)$$

$$s = g m_{19} b_{91} \sigma_1, s = g m_{210} b_{102} \sigma_2, s = g a_{16} b_{63} \sigma_3 \quad (5.65)$$

$$s_1 = g \frac{(\bar{C}_a - \bar{C}_o)}{V_a} (-\sigma_1), s_2 = -g k_L \sigma_2, s_3 = -g \frac{h_c A_s}{\rho_a V_a c_{pa} \rho_s V_s c_{ps}} \sigma_3 \quad (5.66)$$

From the symbolic analysis it can be shown in figure below that the asymptotes will be displayed on the root loci as follows as g (system gain) tends to infinity:

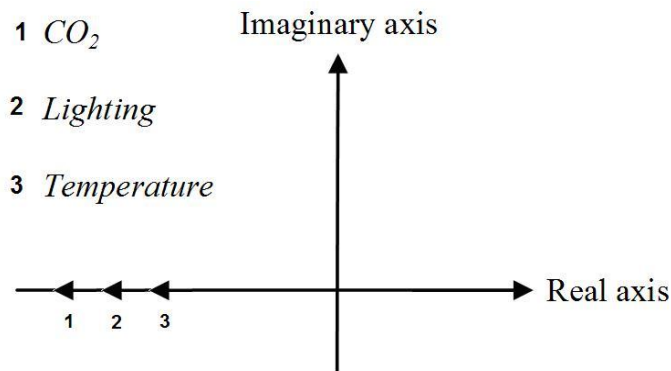


Figure 52 Asymptote directions on a root locus for the three control channels with control strategy 2

Note: It is difficult to perform asymptote direction analysis for all the possible operating points, thus the asymptotes are analysed symbolically in terms of differences between parameters rather than each individual operating point parameters i.e. $(\bar{C}_a - \bar{C}_o) = \Delta\bar{C}_{ao}$ and $|\bar{T}_s - \bar{T}_a| = |\Delta\bar{T}_{sa}|$. The difference between the operating temperatures of the floor (screed) and the air is included in the equation of the convection coefficient. However this is not as important because through simulation it was found that this remains constant and thus an average value is sufficient to make the analysis simple.

The first asymptote s_1 for CO_2 level, is pointing towards the positive real axis as the negative signs cancel to make the asymptote positive. This asymptote can be aligned to the negative real axis by making the scalar gain negative (σ) in the control law. The other two asymptotes for lighting and temperature are already negatively aligned.

The (MB+sD) matrix is not diagonal and in some cases, but not this one, this could mean that some of the asymptotes are pointing at angles to the negative real axis of the root-locus. In this case when high gain is used, which is desirable to reject disturbances such as changes in solar gains and outside temperature, the system is more likely to become oscillatory in its response.

It is clear that there is cross coupling between temperature and CO₂ controls via the Mechanical ventilation. Also there is coupling between lighting and temperature modes through the heat emitted by the lighting power. However, as can be seen, the coupling between the temperature and CO₂ controls is only one way, i.e. rate of change of temperature control has no effect on CO₂ control. The $d_{31}s$ term shows that the coupling is due to the rate of change of ventilation which has a significant effect on the temperature control. Hence controlling rate of change of temperature causes coupling with the rate of change of ventilation. This coupling can be very strong because the ventilation system has a faster time constant than the heating system. Thus, the heating system cannot respond faster to the change in ventilation. This is the reason for the non-diagonal terms in (MB+sD) matrix.

The (MB+sD) matrix gives an indication of which properties of the building such as U values, wall area etc. embedded in the constants could be changed to give as near a diagonal matrix as physically possible and thus allowing simple PI controllers to be successfully utilised. As can be seen from the (MB+sD) matrix that asymptote directions are affected by coupling of constants ($a_{11}b_{11}+b_{11}s$) and ($a_{110}b_{102}$). These constants correspond to the building parameters as well as operating points. This shows that the stability is dependent on the operating internal and external temperatures, CO₂ levels, floor temperature, wind speed and air outside to inside exchange rate. The direction of asymptotes is also a function of the temperature difference between the internal and external operating temperatures ΔT . This indicates that as ΔT changes with the seasons, the stability of the system will be affected.

In the first column the terms ($a_{11}b_{11}+b_{11}s$) are going to be negligible as long as the constant b_{11} is small. This constant is a function of the internal and external operating air temperatures. Thus in winter this coupling will be very strong as the temperature difference will be large and in summer the coupling will be weak due to small temperature difference. Also higher occupancy levels will increase CO₂ concentration levels and this will have a greater impact on the temperature control stability due to the coupling with rate of change of ventilation. However higher

occupancy levels also means higher casual gains and this would reduce the impact of mechanical ventilation on temperature control.

In winter lighting power will be at its greatest and will have a greater impact on temperature control stability than in the summer season. As shown in the second column the coupling is due to the constant a_{110} . Thus in winter lighting will be used more and thus this coupling will have more effect in winter than summer.

In the third column the heating system is only affecting the air temperature. The response of the heating system is affected by the third asymptote. The direction of the asymptote is pointing towards negative real axis however as can be seen from the constants $a_{16}b_{63}$ the asymptote is a function of the thermal mass of the screed. Therefore due to high thermal mass this asymptote will affect the responsivity of the heating system. Hence the air temperature control is a function of the thermal mass of the screed, the heat transfer coefficient and air thermal properties ONLY. It is also interesting to note that the thermal mass of the construction (i.e. walls and roof) has NO impact on the asymptote direction, and thus no impact on cross coupling that could prevent the high performance control of the system in controlling air temperature.

For this system the transmission zeros are given by the determinant as follows:

$$TZ = \det \begin{vmatrix} a_{11} - s & a_{12} & a_{13} & a_{14} & a_{15} & a_{16} & 0 & a_{18} & 0 & a_{110} & a_{111} & b_{11} & 0 & 0 \\ a_{21} & a_{22} - s & 0 & 0 & 0 & 0 & 0 & 0 & 0 & 0 & 0 & 0 & 0 & 0 \\ a_{31} & 0 & a_{33} - s & 0 & 0 & 0 & 0 & 0 & 0 & 0 & 0 & 0 & 0 & 0 \\ a_{41} & 0 & 0 & a_{44} - s & 0 & 0 & 0 & 0 & 0 & 0 & 0 & 0 & 0 & 0 \\ a_{51} & 0 & 0 & 0 & a_{55} - s & 0 & 0 & 0 & 0 & 0 & 0 & 0 & 0 & 0 \\ a_{61} & 0 & 0 & 0 & 0 & a_{66} - s & a_{67} & 0 & 0 & 0 & a_{611} & 0 & 0 & b_{63} \\ 0 & 0 & 0 & 0 & 0 & a_{76} & a_{77} - s & 0 & 0 & 0 & 0 & 0 & 0 & 0 \\ a_{81} & 0 & 0 & 0 & 0 & 0 & 0 & a_{88} - s & 0 & 0 & 0 & 0 & 0 & 0 \\ 0 & 0 & 0 & 0 & 0 & 0 & 0 & 0 & a_{99} - s & 0 & 0 & b_{91} & 0 & 0 \\ 0 & 0 & 0 & 0 & 0 & 0 & 0 & 0 & 0 & -s & 0 & 0 & b_{102} & 0 \\ a_{111} & 0 & 0 & 0 & 0 & a_{116} & 0 & 0 & 0 & 0 & a_{1111} - s & 0 & 0 & 0 \\ 0 & 0 & 0 & 0 & 0 & 0 & 0 & 0 & m_{19} & 0 & 0 & 0 & 0 & 0 \\ 0 & 0 & 0 & 0 & 0 & 0 & 0 & 0 & 0 & m_{210} & 0 & 0 & 0 & 0 \\ (a_{11} + 1) & a_{12} & a_{13} & a_{14} & a_{15} & a_{16} & 0 & a_{18} & 0 & a_{110} & a_{111} & b_{11} & 0 & 0 \end{vmatrix} = 0$$

$$TZ = (-s-1)(a_{22}-s)(a_{33}-s)(a_{44}-s)(a_{55}-s)(a_{88}-s)(a_{116}a_{111}-a_{16}(a_{1111}-s))=0 \quad (5.67)$$

$$s = -1, s = a_{22}, s = a_{33}, s = a_{44}, s = a_{55}, s = a_{88}, s = a_{1111} - \frac{a_{116}a_{111}}{a_{16}} \quad (5.68)$$

Symbolically the transmission zeros are given as follows:

$$s = -1, a_{22} = \frac{-4U_{w1}A_{w1}}{\rho_{w1}V_{w1}c_{pw1}}, a_{33} = \frac{-4U_{w2}A_{w2}}{\rho_{w2}V_{w2}c_{pw2}}, a_{44} = \frac{-4U_{w3}A_{w3}}{\rho_{w3}V_{w3}c_{pw3}}, a_{55} = \frac{-4U_{w4}A_{w4}}{\rho_{w4}V_{w4}c_{pw4}},$$

$$a_{88} = \frac{-4U_r A_r}{\rho_r V_r c_{pr}}, s = \frac{-h_r A_s - h_m A_m}{\rho_m V_m c_{pm}} - \frac{h_r h_m A_m}{\rho_m V_m c_{pm} h_c}$$

Due to the stability matrix being full rank the slow modes of the system are now observable and are located at the transmission zero locations shown above.

Here the transmission zeros correspond to the four walls, roof, and internal thermal mass. The transmission zeros are stable as they are always negative i.e. on the left half plane of the root-locus. In this case they are not a function of operating conditions such as outside temperature, but are a function of thermal properties; area, mass and thermal capacitance of the walls, roof and internal thermal and heat transfer coefficients. This shows that the transmission zeros will always remain negative and therefore stable since the building parameters will never have negative values. There is a transmission zero at -1. This is due to rate of change of temperature being a function of temperature. For this a cascade control solution is required where temperature feedback is utilised to produce a rate of change of temperature command for the rate of change of temperature control system previously analysed. This control strategy is widely used with great effect in electric motor based systems [(Roskilly, 1990)].

This concludes that with a slow heating system air temperature cannot be controlled directly as this does not satisfy the stability criteria. Thus to be able to control air temperature it is required to feedback air temperature plus an extra measured variable i.e. rate of change air temperature.

In this case the asymptotes are a function of the operating points such as internal & external CO₂ levels. It is also interesting to note that the asymptotes are not at an angle and thus variation in the operating points will not affect the controllability as the asymptotes will always be horizontal and negatively aligned. For controllability of air temperature it depends on the thermal mass of the floor. Thus, due to the thermal mass of the floor this will affect the responsivity of the heating system and thus the fast and accurate control of the air temperature. Here it is quite obvious that air temperature dynamics are very fast compared to the floor temperature dynamics. Thus this combination is not compatible to produce accurate and fast results.

With simple controls the solution for controlling air temperature with a slow heating system is to use dual loop control. The inner loop for controlling rate of change of air temperature and outer loop for controlling just air temperature. This is a simple solution to stability problem where basic PID controllers are being used. This would give satisfactory results however accurate control requires a high performance controller where bandwidth of each controller can be adjusted according to the response of the individual systems. In the case this is highly desirable where under-floor heating is very slow compared to mechanical ventilation.

As shown above, to make the stability matrix full rank requires the feedback of extra measurements such as rate of feedback. Upon analysing it is also found that in applications where comfort temperature is controlled with slow heating system these instability problems do not occur and also leads to a simpler control structure. This is shown as follows:

5.1.4 Stability of comfort temperature control

If in the feedback comfort temperature is fed back then the output equation of temperature is as follows: (based on the CIBSE comfort temperature))

$$T_{cm} = \frac{1}{3}T_a + \frac{1}{3}T_{mrad} \quad (5.69)$$

Where mean radiant temperature is given as follows:

$$T_{mrad} = \frac{T_{w1} + T_{w2} + T_{w3} + T_{w4} + T_s + T_r + T_m}{7} \quad (5.70)$$

Note: The CO₂ and lux level feedback equations remain the same as in the previous cases.

$$M = \begin{bmatrix} 0 & 0 & 0 & 0 & 0 & 0 & 0 & 0 & m_{19} & 0 & 0 \\ 0 & 0 & 0 & 0 & 0 & 0 & 0 & 0 & 0 & m_{210} & 0 \\ m_{31} & m_{32} & m_{33} & m_{34} & m_{35} & m_{36} & 0 & m_{38} & 0 & 0 & m_{311} \end{bmatrix}, D = \begin{bmatrix} 0 & 0 & 0 \\ 0 & 0 & 0 \\ 0 & 0 & 0 \end{bmatrix}$$

$$E = \begin{bmatrix} 0 & 0 & 0 & 0 & 0 & 0 & 0 & 0 & 0 & 0 & 0 & 0 \\ 0 & 0 & 0 & 0 & 0 & 0 & 0 & 0 & 0 & 0 & 0 & f_{213} \\ 0 & 0 & 0 & 0 & 0 & 0 & 0 & 0 & 0 & 0 & 0 & 0 \end{bmatrix}$$

The stability matrix for comfort temperature feedback is given as follows:

$$(MB + sD) = \begin{bmatrix} q_{mv} & u_L & \dot{Q}_p \\ m_{19}b_{91} & 0 & 0 \\ 0 & m_{210}b_{102} & 0 \\ m_{31}b_{11} & 0 & m_{36}b_{63} \end{bmatrix} \begin{bmatrix} CO_2 \\ Lux \\ Temp \end{bmatrix} \quad (5.71)$$

By feeding back comfort temperature the coupling of lighting with temperature is completely removed. Now the only coupling is between the CO₂ and temperature when operating the mechanical ventilation. Obviously this is an easier solution by

controlling comfort temperature rather than air temperature. Here the result is interesting that for controlling comfort temperature the stability is not dependent on the thermal mass or temperature of the walls and furniture (internal thermal mass) but only the mass of the heating system i.e. thermal mass of the floor. Thus a comfort temperature sensor where the contribution of air temperature is proportionally larger than the radiant temperature than the $m_{31}b_{11}$ term will be large and $m_{36}b_{63}$ term will be small and thus the matrix would be close to rank defective. Where as if radiant temperature dominant sensor is used this will cause the matrix to be more stable and diagonal and the $c_{31}b_{11}$ terms will be small. Hence resulting in a completely diagonal (singular) matrix where all the three control channels are completely decoupled. Thus there will be no need for a high performance controller design and simple PID controls will work very well. Only concern is that mechanical ventilation will have to be operated slower than its designed speed to prevent cross coupling with the heating and this is possible with slug filters that are commonly used in industry.

The transmission zeros for the control of comfort temperature with under-floor heating are given by the following determinant:

$$A = \det \begin{pmatrix} a_{11}-s & a_{12} & a_{13} & a_{14} & a_{15} & a_{16} & 0 & a_{18} & 0 & a_{110} & a_{111} & b_{11} & 0 & 0 \\ a_{21} & a_{22}-s & 0 & 0 & 0 & 0 & 0 & 0 & 0 & 0 & 0 & 0 & 0 & 0 \\ a_{31} & 0 & a_{33}-s & 0 & 0 & 0 & 0 & 0 & 0 & 0 & 0 & 0 & 0 & 0 \\ a_{41} & 0 & 0 & a_{44}-s & 0 & 0 & 0 & 0 & 0 & 0 & 0 & 0 & 0 & 0 \\ a_{51} & 0 & 0 & 0 & a_{55}-s & 0 & 0 & 0 & 0 & 0 & 0 & 0 & 0 & 0 \\ a_{61} & 0 & 0 & 0 & 0 & a_{66}-s & a_{67} & 0 & 0 & 0 & a_{611} & 0 & 0 & b_{63} \\ 0 & 0 & 0 & 0 & 0 & a_{76} & a_{77}-s & 0 & 0 & 0 & 0 & 0 & 0 & 0 \\ a_{81} & 0 & 0 & 0 & 0 & 0 & 0 & a_{88}-s & 0 & 0 & 0 & 0 & 0 & 0 \\ 0 & 0 & 0 & 0 & 0 & 0 & 0 & 0 & a_{99}-s & 0 & 0 & b_{91} & 0 & 0 \\ 0 & 0 & 0 & 0 & 0 & 0 & 0 & 0 & 0 & -s & 0 & 0 & b_{102} & 0 \\ a_{111} & 0 & 0 & 0 & 0 & a_{116} & 0 & 0 & 0 & 0 & a_{1111}-s & 0 & 0 & 0 \\ 0 & 0 & 0 & 0 & 0 & 0 & 0 & 0 & m_{19} & 0 & 0 & 0 & 0 & 0 \\ 0 & 0 & 0 & 0 & 0 & 0 & 0 & 0 & 0 & m_{210} & 0 & 0 & 0 & 0 \\ m_{31} & m_{32} & m_{33} & m_{34} & m_{35} & m_{36} & 0 & m_{38} & 0 & 0 & m_{311} & 0 & 0 & 0 \end{pmatrix} = 0$$

Symbolically this matrix can be reduced further to:

$$A = \det \begin{vmatrix} a_{11} - s & a_{12} & a_{13} & a_{14} & a_{15} & a_{16} & a_{18} & a_{111} \\ a_{21} & a_{22} - s & 0 & 0 & 0 & 0 & 0 & 0 \\ a_{31} & 0 & a_{33} - s & 0 & 0 & 0 & 0 & 0 \\ a_{41} & 0 & 0 & a_{44} - s & 0 & 0 & 0 & 0 \\ a_{51} & 0 & 0 & 0 & a_{55} - s & 0 & 0 & 0 \\ a_{81} & 0 & 0 & 0 & 0 & 0 & a_{88} - s & 0 \\ a_{111} & 0 & 0 & 0 & 0 & a_{116} & 0 & a_{1111} - s \\ m_{31} & m_{32} & m_{33} & m_{34} & m_{35} & m_{36} & m_{38} & m_{311} \end{vmatrix} = 0$$

This is still a very complex determinant to solve symbolically and instead needs numerical analysis. Although from the analysis earlier with controlling air temperature it is clear that transmission zeros are always stable for buildings. In this case they are very complex because the mean radiant temperature is a function of all the thermal masses. For comfort temperature the transmission zeros are shown in the simplified controllability case study where the symbolic analysis is a lot easier.

5.1.5 Conclusions

Thus for slow radiant heating systems a completely radiant temperature sensor will allow for accurate control without the cross coupling of the systems where there is no measurement of the air temperature (i.e. convective component) at all. However under-floor heating has both components radiative and convective. Thus this would produce heat input to the air point. These findings have been shown by experiments in the past (Bloomfield & Fisk, 1981) and are now confirmed through the science.

In theory the slow heating systems are better suited to controlling comfort temperature rather than purely air temperature. Even though air temperature can be controlled it is more difficult to implement due to measurement of rates of change which in practice will not be very accurate as in the zone the air change rates will always vary causing an error in the calculation of rate of change of air temperature accurately. Thus it is recommended that with slow heating systems in heating mode comfort temperature should be controlled for stability.

This is correct in theory however in practice it is not recommended to use a slow actuation heating system for controlling comfort temperature. Since comfort temperature is a function of the thermal mass, its dynamics are slowly varying and require fast acting heating system to influence its dynamics. Normally the brick walls have a time constant of days and with a very slow heating system control comfort temperature is not practical. Especially with under-floor heating, in cases where there is significant radiant component influencing the thermal mass temperature then this will be a very slow control system overall even though it is a stable system.

In this case study of slow actuation heating systems, the stability of: 1) controlling air temperature only, 2) air temperature plus its rate of change and 3) comfort temperature, were analysed. The fundamental conclusions can be drawn from this analysis are as follows:

1. Controlling air temperature with a slow acting heating system requires a more complex controller design. Based on the stability analysis a basic controller such as a PI will achieve satisfactory performance if a dual control loop is used where controlling air temperature plus its rate of change is used in the feedback.
2. Controlling comfort temperature with slow heating system requires a less complex controller design and based on the stability analysis using a basic PI controller will give good performance since through controlling comfort temperature the three systems are less coupled (i.e. MB matrix is near diagonal).
3. The choice of temperature sensors depends upon what you are trying to control. If it's air temperature then a purely air temperature sensor will cause the system to have oscillatory response [(Bradshaw & Counsell, 1998)]. So either a radiant component from the heater is required or rate of change of air temperature is required.

4. There is no impact of internal and external thermal mass on the stability of comfort temperature or air temperature with a slow actuation heating system. Only the thermal mass of the heating system is important and in the case of under-floor heating, it is the thermal properties of the screed ONLY.
5. There is one stable transmission zero when controlling air temperature with under-floor heating. This is because the MB matrix is rank defective due to which inverting the dynamics of the system is not possible. Since sliding mode not possible then it's eigen-values i.e. TZ are not observable. When controlling air temperature plus its rate of change then all transmission zeros are stable. Transmission zeros are not calculated for comfort temperature as they are too complex to be derived symbolically. However for a simpler model the transmission zeros are calculated and discussed for controlling comfort in practice in case studies 4-5.
6. Symbolic trackability and reachability are very complex for this case study due to the large model, hence it is recommended as part of further work for slow actuators.

5.2 Controllability of Heating Systems with Fast Actuation

A 4th order model is specifically developed to test the controllability of a nonlinear multivariable system with focus on fast heating systems. The model was derived from the results and modelling in the earlier case study. The dynamic model describes the energy and mass balance of air in the building zone having heating and ventilation.

The reason for proposing the 4th order reduced model is because the symbolic controllability analysis of the 11th order model proposed in the previous case study, showed that the transmission zeros corresponding to the thermal masses (i.e. walls, roof etc.) are all negative and will always remain negative. Thus there is no need for analysing the individual walls etc for their controllability and they can be treated as one single external thermal mass. The CB matrix analysis also showed that the lighting has a very small coupling with the temperature control due to its zeroth order dynamics and thus can be controlled accurately with a simple Proportional + Integral controller (PI). Thus the real coupling as shown to be is between the heating and ventilation controls. In this case study the controllability analysis of a fast heating system for controlling temperature and mechanical ventilation for control of humidity is presented. It is also shown that fast heating system with mechanical ventilation will be a better combination and thus here a fast heating system is assumed for controlling air temperature.

The 4th order model lumps the walls, floor and roof into a single external thermal mass with two resistance layers i.e. internal and external. This leads to a reduced model having four equations as follows:

1. Air temperature
2. External thermal mass: walls + floor + roof
3. Internal thermal mass: furniture + internal walls
4. Humidity level

5.2.1 Mathematical Modelling

The assumptions applied earlier regarding modelling of the air temperature are all applicable here. The temperature of the zone is modelled as a single node representing an average temperature of the zone.

$$\rho_a V_a c_{pa} \frac{dT_a}{dt} = \left[\begin{array}{l} (\dot{Q}_{sa} + \dot{Q}_L + \dot{Q}_{oc} + \dot{Q}_{ap})_{casual\ gains} \\ + (\dot{Q}_{wi} + \dot{Q}_{win} + \dot{Q}_m)_{structure} \\ + (\dot{Q}_{nt} + \dot{Q}_{nv} + \dot{Q}_{ni} + \dot{Q}_{mv})_{ventilation} \\ + (\dot{Q}_p)_{heating\ /cooling} \end{array} \right] \quad (5.72)$$

$$\text{Solar radiation : } \dot{Q}_{sa} = \alpha_a \sigma_s A_{win} I_{dr} \quad (5.73)$$

$$\text{Lighting : } \dot{Q}_L = k_e P_L \quad (5.74)$$

$$\text{Occupancy : } \dot{Q}_{oc} = n_p G_{pp} \quad (5.75)$$

$$\text{Appliances : } \dot{Q}_{ap} = \dot{Q}_{pc} + \dot{Q}_{laptops} + \dot{Q}_{peripherals} \quad (5.76)$$

$$\text{External thermal mass : } \dot{Q}_{wi} = 2U_{wi} A_w (T_w - T_a) \quad (5.77)$$

$$\text{Window : } \dot{Q}_{win} = U_{win} A_{win} (T_o - T_a) \quad (5.78)$$

$$\text{Internal thermal mass : } \dot{Q}_m = U_m A_m (T_m - T_a) \quad (5.79)$$

$$\text{Air change rate due to thermal forces : } \dot{Q}_{nt} = V_a n_t \rho_a c_{pa} (T_o - T_a) \quad (5.80)$$

$$\text{Air change rate due to external wind : } \dot{Q}_{nv} = V_a n_v \rho_a c_{pa} (T_o - T_a) \quad (5.81)$$

$$\text{Air tightness (infiltration) : } \dot{Q}_{ni} = V_a n_i \rho_a c_{pa} (T_o - T_a) \quad (5.82)$$

$$\text{Mechanical ventilation : } \dot{Q}_{mv} = q_{mv} \rho_a c_{pa} (T_o - T_a) \quad (5.83)$$

In this case study the fast actuation heating system considered is assumed to be transferring energy directly to the air node, i.e. a convector heater.

$$\text{Convection to zone air: } \dot{Q}_p \quad (5.84)$$

The rate of change of wall temperature is given by:

$$\rho_w V_w c_{pw} \frac{dT_w}{dt} = [\dot{Q}_{sw} + \dot{Q}_{wo} - \dot{Q}_{wi}] \quad (5.85)$$

Where heat exchange with:

$$\text{Outside: } \dot{Q}_{wo} = 2U_{wo} A_w (T_{sa} - T_w) \quad (5.86)$$

$$\text{Inside: } \dot{Q}_{wi} = 2U_{wi} A_w (T_w - T_a) \quad (5.87)$$

In the original model and the last case study, an overall heat transfer coefficient was assumed. In this case-study it is also investigated the effect of the two layers of insulation, inner and outer. Thus an inner and outer U values are considered in modelling the external thermal mass.

$$\text{Direct solar radiation through the window: } \dot{Q}_{sw} = \alpha_w \sigma_s A_w I_{dr} \quad (5.88)$$

The rate of change of thermal mass temperature is given by the following differential equation:

$$\rho_m V_m c_{pm} \frac{dT_m}{dt} = \dot{Q}_{sm} - \dot{Q}_m \quad (5.89)$$

Where the heat exchange with:

$$\text{Air: } \dot{Q}_m = 2U_m A_m (T_m - T_a) \quad (5.90)$$

$$\text{Solar gain through the window: } \dot{Q}_{sm} = \alpha_m \sigma_s A_w I_{dr} \quad (5.91)$$

The direct solar gain to the walls and internal mass was excluded in the last case study however here it is included. In this case study this has been added to see its effect however as mentioned this has little effect however for completeness this has been included to see what effect it has when the symbolic analysis is carried out.

The differential equation for water balances on the interior volume of the building are as follows:

$$\rho_a V_a \frac{dw_a(t)}{dt} = W_d - W_{nt} - W_{nv} - W_{ni} - W_{mv} \quad (5.92)$$

Where,

W_d is internal humidity gain (kg/s).

W_{nt} is humidity loss by thermal buoyancy: $W_{nt} = \rho_a n_{nv} V_a (w_a - w_o)$ (5.93)

W_{nv} is humidity loss by wind pressure: $W_{nv} = \rho_a n_{nv} V_a (w_a - w_o)$ (5.94)

W_{ni} is humidity loss by natural air change rate: $W_{ni} = \rho_a n_i V_a (w_a - w_o)$ (5.95)

W_{mv} is humidity loss by mechanical ventilation: $W_{mv} = \rho_a q_m (w_a - w_o)$ (5.96)

Sensors for the controller

A feedback control system can only control (i.e. track) what it feeds back as measured system outputs. Thus, to analyse the controllability of these measurements, they must be defined and are as follows:

Measured air Temperature level is given by: $T_{cm} = T_a$

Measured Humidity level is given by: $W_{cm} = W_a$,

The results of this linearisation enable the total system to be represented in the state-space form:

$$\dot{x}(t) = Ax(t) + Bu(t) + Fd(t)$$

$$y(t) = C(x)$$

This linear model (appendix) describes the dynamic behaviour of the building and its systems for a small amplitude perturbation δ about a steady state equilibrium condition. Where $y(t)$ is the measured output vector, $x(t)$ is a vector of state variables, $u(t)$ is a vector of system inputs (i.e. controller outputs) and $d(t)$ is a vector of disturbances. A, B, C and F are time invariant matrices consisting of constants. The vectors associated with these matrices are given as follows:

$$\begin{aligned}
 \dot{x} &= [\dot{T}_a, \dot{T}_w, \dot{T}_m, \dot{W}_a]^T \\
 x &= [T_a, T_w, T_m, W_a]^T \\
 u &= [\dot{Q}_p, q_{mv}]^T \\
 d &= [I_{dr}, P_L, \dot{Q}_{oc}, \dot{Q}_{ap}, T_o, v_o, T_{sa}, W_d, W_o]^T
 \end{aligned} \tag{5.97}$$

5.2.2 Stability of air temperature and humidity control

It was shown in first case-study that with a slow acting heating system i.e. under floor heating, when air temperature T_a is controlled for achieving the required comfort temperature i.e. $T_{cm} = T_a$, the matrix (CB+sD) is not of full rank (i.e. not invertible). This indicated that ISR of air temperature with slow heating systems is not feasible and thus extra measurements from the sensors are needed for ISR to be feasible. It was also shown that with the added rate of change of measured output feedback sensors i.e. feeding back rate of change of temperature with temperature resulted in a full rank CB+sD matrix which allowed for simple controls to be feasible. The findings proved that for perfect controllability of highly cross coupled heating and ventilation systems using simple controllers requires the heating system to be fast. Otherwise complex nonlinear MIMO controllers will be needed for stabilising the system. For the system discussed in this case study the CB stability matrix is given as follows:

$$CB = \begin{pmatrix} b_{11} & b_{12} \\ 0 & b_{42} \end{pmatrix} \tag{5.98}$$

The constants shown in the matrixes above are functions of building parameters and operating conditions as follows:

$$CB = \begin{pmatrix} Q_p & q_{mv} \\ \frac{\beta}{\rho_a V_a c_{pa}} & \frac{(\bar{T}_o - \bar{T}_a)}{V_a} \\ 0 & \frac{-(\bar{w}_a - \bar{w}_o)}{V_a} \end{pmatrix} \begin{matrix} T_a \\ w_a \end{matrix} \quad (5.99)$$

The CB matrix shows that there is cross coupling between temperature and humidity control through mechanical ventilation (b_{12}). The mechanical ventilation will affect both humidity and temperature. Whereas perimeter wall heating will only affect temperature. The reason is that heat losses due to evaporation of the water in the zone and the rate of moisture transfer from this evaporation emanate from the water contained in the contents of the zone. These factors have little influence on the thermal and moisture processes of the building indoor climate and can be considered as disturbances (Daskalov & Arvenitis, 2006). These factors are functions of the inside temperature and humidity. Hence direct heat input to the air node does not directly affect the water vapour content. The cross coupling of temperature is determined by the difference between operating indoor and outdoor temperatures (constant: b_{12}). In summer this cross coupling will be smaller as temperature difference will be less. Thus in summer this will be a nearly decoupled system where each control channel can be easily controlled using simple PID controls. Where as in winter the cross coupling will be stronger as temperature difference will be larger and thus in winter the mechanical ventilation will be a significant disturbance to the heating system.

It is clear that there is cross coupling between temperature and humidity controls via the mechanical ventilation. However, as can be seen, the coupling between the temperature and CO₂ controls is only one way, i.e. change in temperature control has no effect on humidity control directly. This is similar to the case study of slow systems. However the difference in the case study is that due to the fast heating

system the coupling is not due to rate of change of ventilation rate as was shown for slow systems.

The RIDE theory states that the asymptotes for a multivariable design are given by Eigen-values: $|sI + g(CB)\sigma| = 0$ where, g is the global gain from zero to infinity and σ is a scalar gain. Therefore the asymptotes are the solutions for s of the following determinant:

$$|sI + g(CB)\sigma| = \begin{vmatrix} s_1 + gb_{11}\sigma_1 & gb_{12} \\ 0 & s_2 + gb_{42}\sigma_2 \end{vmatrix} = 0 \quad (5.100)$$

$$(s_1 + gb_{11}\sigma_1)(s_2 + gb_{42}\sigma_2) = 0 \quad (5.101)$$

$$s_1 = -gb_{11}\sigma_1, \quad s_2 = -gb_{42}\sigma_2 \quad (5.102)$$

Hence, the asymptotes are defined by the following building parameters:

$$s_1 = -g_{0 \rightarrow \infty} \frac{\beta}{\rho_a V_a c_{pa}} (\sigma_1), \quad (5.103)$$

The asymptote for air temperature is negatively aligned and will result in stable fast transient temperature response without oscillation to reach steady state i.e. temperature control is stable and controllable.

$$s_2 = -g_{0 \rightarrow \infty} \frac{-(\bar{w}_a - \bar{w}_o)}{V_a} (\sigma_2) \quad (5.104)$$

The asymptote for humidity is positively aligned and will result in unstable transient response increasing in the right half plane i.e. humidity control is unstable and uncontrollable. As can be seen from the terms this is caused by the negative control b_{42} . To realign this asymptote to the negative real axis the gain σ_2 will have to be made negative.

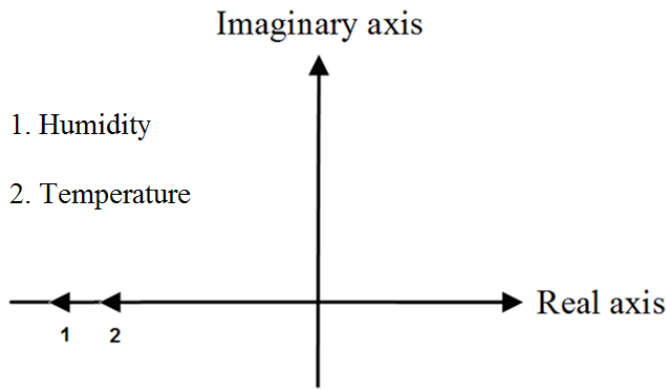


Figure 53 Asymptote directions on a root locus for a closed-loop system.

The asymptotes are a function of the operating points such as temperature difference between internal & external humidity levels. It is also interesting to note that the asymptotes are not at an angle and thus variation in the operating points will not affect the controllability as the asymptotes will always be horizontal and negatively aligned. Two fundamental conclusions can be drawn from this analysis as follows:

1. Easier to deploy high gain and high performance controls
2. Classical single input single output (SISO) controllers such as Proportional plus Integral control (PI) could be sufficient.

Transmission zeros

The matrix is given as follows:

$$TZ = \begin{vmatrix} a_{11} - s_1 & a_{12} & a_{13} & 0 & b_{11} & b_{12} \\ a_{21} & a_{22} - s_2 & 0 & 0 & 0 & 0 \\ a_{31} & 0 & a_{33} - s_3 & 0 & 0 & 0 \\ 0 & 0 & 0 & a_{44} - s_4 & 0 & b_{42} \\ c_{11} & 0 & 0 & 0 & 0 & 0 \\ 0 & 0 & 0 & c_{24} & 0 & 0 \end{vmatrix} = 0 \quad (5.105)$$

The determinant matrix can be reduced to:

$$TZ = \begin{vmatrix} a_{22} - s_2 & 0 \\ 0 & a_{33} - s_3 \end{vmatrix} = 0 \quad (5.106)$$

The equation is solved to find the values of s which are the transmission zeros. In this case study, there are two transmission zeros, which correspond to the external and internal thermal mass and are given by:

$$(a_{22} - s_2)(a_{33} - s_3) = 0 \quad (5.107)$$

The transmission zeros are:

$$s_2 = a_{22} = \left(\frac{-2U_{wo}A_w - 2U_{wi}A_w}{\rho_w V_w c_{pw}} \right) \quad (5.108)$$

$$s_3 = a_{33} = \left(\frac{-2U_m A_m}{\rho_m V_m c_{pm}} \right) \quad (5.109)$$

The transmission zeros are both in the left half plane and thus stable. Again they are a function of constants and thus will always remain stable. In this case they are not a function of operating conditions such as outside temperature, but are a function of thermal properties; area, mass and thermal capacitance and U values of the internal and external thermal mass.

The thermal transmittance of the walls, (the U-value) is generally required to be as low as economically possible; for purposes of energy costs saving, emissions reduction and to comply with the building regulations. If this is to be the case then the results of the transmission zero analysis (which proved that the location of the zero is a function of the heat transmitted through the fabric and the heat stored in the fabric) suggest that walls must have low thermal mass for to ensure speedy reaction

to control inputs. This implies that in an Adaptive Climatic Building, reducing thermal mass is important to responsive control.

This is in contrast to the ‘passive’ approach to the design of buildings, where thermal mass is used extensively for load levelling and heat storage. The results indicate that we can expect such ‘heavyweight’ buildings to be sluggish and respond slowly to control inputs. For passive buildings, this tends not to be a problem, as control of these buildings is likely to be minimal anyway. For actively controlled, adaptable buildings as are considered in the case studies, the implications of these findings are of great importance. Robust, responsive control is desired in Adaptive Climatic Buildings and it is clear that the choice of materials, and therefore the amount of thermal capacitance in these systems and the impact of this thermal mass must be given proper consideration in the design process. This analysis will allow the responsiveness of the proposed building to be quantified at an early stage and could allow for the cost effective evaluation of the impact of different material choices.

In the last case study the Reachability was not analysed as the model was too large for the symbolic analysis. In the light of the finding of the slow systems case study model was reduced and this model is just small enough for Reachability analysis to be carried out symbolically.

5.2.3 Trackability of air temperature and humidity control

It is shown that a good estimate of the $U_{trim}(t)$ enables the control system to accurately track the reference input and this is discussed in chapter 3. For a feedback control system steady state tracking of a constant reference input $v(0)$ can be expressed as,

$$\lim_{t \rightarrow \infty} e(t) = v(t) - y(t) \Rightarrow 0 \quad (5.110)$$

If this condition is satisfied then the tracking condition will be satisfied even in the presence of a disturbance vector $d(t)$. It is clear that the above condition depends on

what is being measured? Therefore it is important that what is measured in approaches the desired output $y(t)$ in steady state. In this case air temperature is measured and also controlled. Hence in this case study trackability is not a problem along as the system is stable. However in this last case study when air temperature was being controlled but the sensor used was measuring air temperature plus its rate of change. In this case measurement vector would be as follows:

$$w(t) = y(t) + k_D \dot{y}(t)$$

Here the trackability is satisfied as over time when the output becomes steady state, rate of change of output will come zero and $w(t)$ will equal $y(t)$ and therefore $w(t)$ will equal $v(t)$, meaning the measured variable equals the set-point.

5.2.4 Reachability of air temperature control

For a complete representation of a system given by the following state space equations:

$$\dot{x}(t) = Ax(t) + Bu(t) + Fd(t) \quad (5.111)$$

$$y(t) = Cx(t) \quad (5.112)$$

The RIDE theory can be applied to derive the equivalent control $U_{trim}(s)$ for the above system which is used for Reachability analysis and is given by:

$$U_{trim}(s) = \left[-(CB + sD)^{-1} CAX(s) - (CB + sD)^{-1} (CF + sE)d(s) \right] \quad (5.113)$$

As explained in previous chapters 3 & 4, the input $U_{trim}(t)$ uses inverse dynamics to determine the actuator inputs that are required to ensure zero rate of change of the outputs. It does this by taking into account the disturbances and system dynamics that would otherwise prevent the system from operating like an ideal integrating system.

The safe operation of the control system under disturbances and actuator nonlinearities is governed by the safe criteria for U_{trim} . The presence of limitations on the power of the system's actuators results in limitations on maintaining stable tracking and Reachability. In order to better understand this it is useful to derive a criterion which describes the limits of Reachability. When the actuator output, $u_a(s)$, has reached its upper (L_U) or lower (L_L) limits, the control signal to the actuator, $u(s)$, must either remain constant or decrease in order to avoid overdriving the actuator and to maintain safe control. As shown in earlier chapters, this criterion states that providing the closed-loop response is fast i.e. $K(s)$ is relatively large compared with rates of change of $U_{trim}(s)$ and that rate of change of $r(s)$ is made small then the limitation on tracking is that U_{trim} must remain between the upper and lower actuator limits. Using equation 4.10:

$$L_L \leq u_{trim}(s) \leq L_U \quad (5.114)$$

This criterion demonstrates that, when actuator limits are reached, safety can be ensured simply by setting the error signal to zero, providing that steady state is reachable (i.e. that the U_{trim} is within limits). This condition for Reachability can be readily inspected using dynamic simulation. Now the original expression for U_{trim} can be symbolically expanded to see which properties of the building and its control system affect the value of U_{trim} from staying between the actuator limits. This expression for U_{trim} can be reduced for the system presented in this case study where D and E matrices are zero and is given by:

$$u_{trim}(s) = \left[-(CB)^{-1} CAX(s) - (CB)^{-1} (CF)d(s) \right] \quad (5.115)$$

The matrices can be expanded and multiplied to give:

$$\begin{aligned}
U_{trim}(s) = & \\
& \left[\begin{array}{c} -\frac{1}{b_{11}b_{42}} \begin{pmatrix} b_{42} & -b_{12} \\ 0 & b_{11} \end{pmatrix} \begin{pmatrix} c_{11} & 0 & 0 & 0 \\ 0 & 0 & 0 & c_{24} \end{pmatrix} \begin{pmatrix} a_{11} & a_{12} & a_{13} & 0 \\ a_{21} & a_{22} & 0 & 0 \\ a_{31} & 0 & a_{33} & 0 \\ 0 & 0 & 0 & a_{44} \end{pmatrix} \begin{pmatrix} T_a(s) \\ T_w(s) \\ T_m(s) \\ w_a(s) \end{pmatrix} \\ \\ -\frac{1}{b_{11}b_{42}} \begin{pmatrix} b_{42} & -b_{12} \\ 0 & b_{11} \end{pmatrix} \begin{pmatrix} c_{11} & 0 & 0 & 0 \\ 0 & 0 & 0 & c_{24} \end{pmatrix} \begin{pmatrix} f_{11} & f_{12} & f_{13} & f_{14} & f_{15} & f_{16} & 0 & 0 & 0 \\ f_{21} & 0 & 0 & 0 & 0 & 0 & f_{27} & 0 & 0 \\ f_{31} & 0 & 0 & 0 & 0 & 0 & 0 & 0 & 0 \\ 0 & 0 & 0 & 0 & 0 & f_{46} & 0 & f_{48} & f_{49} \end{pmatrix} \begin{pmatrix} I_{dr}(s) \\ P_L(s) \\ \dot{Q}_{oc}(s) \\ \dot{Q}_{ap}(s) \\ T_o(s) \\ v_o(s) \\ T_{sa}(s) \\ W_d(s) \\ w_o(s) \end{pmatrix} \end{array} \right]
\end{aligned}
\tag{5.116}$$

Simplifying further gives:

$$\begin{aligned}
U_{trim}(s) = & \\
& \left[\begin{array}{c} -\frac{1}{b_{11}b_{42}} \begin{pmatrix} b_{42}a_{11} & b_{42}a_{12} & b_{42}a_{13} & -b_{12}a_{44} \\ 0 & 0 & 0 & b_{11}a_{44} \end{pmatrix} \begin{pmatrix} T_a(s) \\ T_w(s) \\ T_m(s) \\ w_a(s) \end{pmatrix} \\ \\ -\frac{1}{b_{11}b_{42}} \begin{pmatrix} b_{42}f_{11} & b_{42}f_{12} & b_{42}f_{13} & b_{42}f_{14} & b_{42}f_{15} & b_{42}f_{16} - b_{12}f_{46} & 0 & -b_{12}f_{48} & -b_{12}f_{49} \\ 0 & 0 & 0 & 0 & 0 & b_{11}f_{46} & 0 & b_{11}f_{48} & b_{11}f_{49} \end{pmatrix} \begin{pmatrix} I_{dr}(s) \\ P_L(s) \\ \dot{Q}_{oc}(s) \\ \dot{Q}_{ap}(s) \\ T_o(s) \\ v_o(s) \\ T_{sa}(s) \\ W_d(s) \\ w_o(s) \end{pmatrix} \end{array} \right]
\end{aligned}
\tag{5.117}$$

The vectors can be multiplied and the two U_{trim} equations of temperature and humidity control are given as follows:

$$u_{trim1}(s) = \frac{1}{b_{11}} \left(\begin{array}{l} -a_{11}T_a(s) - a_{12}T_w(s) - a_{13}T_m(s) + \frac{b_{12}a_{44}}{b_{42}}w_a(s) - f_{11}I_{dr}(s) - f_{12}P_L(s) - f_{13}\dot{Q}_{oc}(s) \\ -f_{14}\dot{Q}_{ap}(s) - f_{15}T_o(s) - f_{16}v_o(s) + \frac{b_{12}f_{46}}{b_{42}}v_o(s) + \frac{b_{12}f_{48}}{b_{42}}W_d(s) + \frac{b_{12}f_{49}}{b_{42}}w_o(s) \end{array} \right) \quad (5.118)$$

$$u_{trim2}(s) = \frac{1}{b_{42}} (-a_{44}w_a(s) - f_{46}v_o(s) - f_{48}W_d(s) - f_{49}w_o(s)) \quad (5.119)$$

Further rearranging gives:

$$u_{trim1}(s) = \frac{1}{b_{11}} \left(\begin{array}{l} \left(-a_{11}T_a(s) - a_{12}T_w(s) - a_{13}T_m(s) - f_{11}I_{dr}(s) - f_{12}P_L(s) - f_{13}\dot{Q}_{oc}(s) \right) \\ \left(-f_{14}\dot{Q}_{ap}(s) - f_{15}T_o(s) - f_{16}v_o(s) \right) \\ + \frac{b_{12}}{b_{42}} (+a_{44}w_a(s) + f_{46}v_o(s) + f_{48}W_d(s) + f_{49}w_o(s)) \end{array} \right) \quad (5.120)$$

$$u_{trim2}(s) = \frac{1}{b_{42}} (-a_{44}w_a(s) - f_{46}v_o(s) - f_{48}W_d(s) - f_{49}w_o(s)) \quad (5.121)$$

As shown above the Utrim of temperature control is also a function of Utrim of the humidity control. The different constants can be substituted for assessing Utrim.

The reachability equation for air temperature control with fast actuation system is given as follows:

NOTE: The U_{trim} equation does not depend on the system having cooling to be applicable. The U_{trim} calculates the actuator input required in response to the offset in temperature due to disturbances etc. Thus it is EQUALLY applicable for estimating heating or cooling requirements depending upon the climate.

$$\begin{aligned}
u_{trim1}(s) = & \left(\begin{array}{l} -\frac{1}{\rho_a V_a c_{pa}} \left(-2U_{wi} A_w - U_{win} A_{win} - U_m A_m - V_a \bar{n}_i \rho_a c_{pa} - V_a k_v \rho_a c_{pa} \bar{v}_o - V_a \bar{n}_i \rho_a c_{pa} \right) T_a(s) \\ -\left(\frac{2U_{wi} A_w}{\rho_a V_a c_{pa}} \right) T_w(s) - \left(\frac{U_m A_m}{\rho_a V_a c_{pa}} \right) T_m(s) - \left(\frac{\alpha_a \sigma_s A_w}{\rho_a V_a c_{pa}} \right) I_{dr}(s) - \left(\frac{k_e}{\rho_a V_a c_{pa}} \right) P_L(s) \\ -\left(\frac{1}{\rho_a V_a c_{pa}} \right) \dot{Q}_{oc}(s) - \left(\frac{1}{\rho_a V_a c_{pa}} \right) \dot{Q}_{ap}(s) \\ -\frac{1}{\rho_a V_a c_{pa}} \left(U_{win} A_{win} + V_a \bar{n}_i \rho_a c_{pa} + V_a k_v \rho_a c_{pa} \bar{v}_o + V_a \bar{n}_i \rho_a c_{pa} + \rho_a c_{pa} \bar{q}_m \right) T_o(s) \\ -\left((\bar{T}_o - \bar{T}_a) k_v \right) v_o(s) \end{array} \right) \\
& + \left(\frac{\bar{T}_o - \bar{T}_a}{-(\bar{w}_a - \bar{w}_o)} \right) \left(\begin{array}{l} +\left(-\bar{n}_i - k_v \bar{v}_o - \bar{n}_i - \frac{\bar{q}_m}{V_a} \right) w_a(s) + (-k_v (\bar{w}_a - \bar{w}_o)) v_o(s) + \left(\frac{1}{\rho_a V_a} \right) W_d(s) \\ +\left(\bar{n}_i + k_v \bar{v}_o + \bar{n}_i + \frac{\bar{q}_m}{V_a} \right) w_o(s) \end{array} \right)
\end{aligned} \tag{5.122}$$

For easier analysis of reachability the equation is rearranged as follows:

$$\begin{aligned}
u_{trim1}(s) = & \left(\begin{array}{l} \frac{1}{\rho_a V_a c_{pa}} \left(U_{win} A_{win} + V_a \bar{n}_i \rho_a c_{pa} + V_a k_v \rho_a c_{pa} \bar{v}_o + V_a \bar{n}_i \rho_a c_{pa} + \rho_a c_{pa} \bar{q}_m \right) (T_a(s) - T_o(s)) \\ +\left(\frac{2U_{wi} A_w}{\rho_a V_a c_{pa}} \right) (T_a(s) - T_w(s)) + \left(\frac{U_m A_m}{\rho_a V_a c_{pa}} \right) (T_a(s) - T_m(s)) - \left(\frac{\alpha_a \sigma_s A_w}{\rho_a V_a c_{pa}} \right) I_{dr}(s) \\ -\left(\frac{1}{\rho_a V_a c_{pa}} \right) \left(k_e P_L(s) + \dot{Q}_{oc}(s) + \dot{Q}_{ap}(s) \right) - \left((\bar{T}_o - \bar{T}_a) k_v \right) v_o(s) \\ +\left(\frac{\bar{T}_o - \bar{T}_a}{(\bar{w}_a - \bar{w}_o)} \right) \left(\begin{array}{l} \left(\bar{n}_i + k_v \bar{v}_o + \bar{n}_i + \frac{\bar{q}_m}{V_a} \right) (w_a(s) - w_o(s)) - (-k_v (\bar{w}_a - \bar{w}_o)) v_o(s) \\ -\left(\frac{1}{\rho_a V_a} \right) W_d(s) \end{array} \right) \end{array} \right)
\end{aligned} \tag{5.123}$$

In the first case study, due to the slow actuation heating system, the stability of air temperature control was dependent on the thermal properties of the heating and the building system. This case study has presented the controllability (i.e. STAR) of air temperature control with a fast acting heating system. As shown earlier, with the fast acting heating system the stability does not depend on thermal mass of the heater but still depends on the mass of walls and furniture. **However, the air temperature control reachability equation (5.129) has shown that for air temperature control the reachability does NOT depend on the thermal mass of walls or furniture but instead depends on their UA value ONLY (equation 5.129).**

The reason is the fast and slow decomposition of the overall system as explained by (Young, Kokotovic, & Utkin, 1977). In a building there are fast and slow dynamics or modes i.e. air temperature as being fast and wall (thermal mass) temperature being slowly varying. When the air temperature is being controlled using closed loop feedback control then the controller closes the loop in a short time i.e. the air temperature has reached within the control band of the set point in a short time. The time constant of air is very fast compared to the time constant of the wall and hence the air temperature dynamics have reached steady state before the walls could respond.

Thus when controlling air temperature only, the building system separates into fast and slow parts and the dynamics of slow parts have negligible effect on the fast parts and assumed steady state (Kokotovic, Khalil, & O'Reilly, 1999). Typically the time constant of walls with thermal mass is in hours where as for air it is in minutes. Thus compared to the dynamics of air the walls are considered steady state. When the walls have reached steady state then it means that they have no capacity to store heat hence input equals output. Therefore in steady state the transmission of heat is only dependent on the resistance i.e. U value of the wall and in this case $U_{wi}A_{wi}$. Hence the reachability of air temperature control (equation 5.129) depends on $U_{wi}A_{wi}$ value which determines the ability of the thermal mass to accept or reject heat only and there is NO effect of thermal mass on air temperature control because there is no capacity

or ability to store heat i.e. steady state. Further work is required to calculate the operative temperatures in the U_{trim} equation for walls etc.

For temperature control the U_{trim1} equation shows that the value of the U_{trim} depends on the difference between the sum of temperature differences and sum of casual gains. Hence in seasons where the temperature differences (i.e. $T_a - T_w$) and $U_{wi}A_{wi}$ (i.e. highly insulated) are small then casual gains will be the factor determining whether cooling is required or not. Thus in this case the equation would simplify to:

$$u_{trim1}(s) = \frac{1}{\beta} \left(-\alpha_a \sigma_s A_w I_{dr}(s) - \left(k_e P_L(s) + \dot{Q}_{oc}(s) + \dot{Q}_{ap}(s) \right) \right) \quad (5.124)$$

Hence the important terms in this are the casual gains i.e. solar, lighting, occupancy and appliances. Any significant casual gains will make the value of U_{trim} very large negative. Here it is important to note that negative limit of the plant represents the cooling limit and positive limit is the heating limit. Thus this equation will determine for a given climate the size of the cooling plant required.

In such a climate if there are very high casual gains consequently then the U_{trim} is more negative than the cooling limit is, then the system will be considered unreachable and the building will over heat. Equation 5.130 is for a climate where the temperature differences and the value of $U_{wi}A_{wi}$ is small (i.e. highly insulated).

Consider the case when internal temperature is equal to external temperature i.e. $T_a = T_o$ but $U_{wi}A_{wi}$ and $U_m A_m$ are large i.e. lower resistance and thermal mass can accept and reject heat easily. Where the value of $U_{wi}A_{wi}$ is large (low resistance) then the energy is transmitted quicker through the thermal mass due to higher heat transfer rate. If the $U_m A_m$ value is large then it means that the furniture has low resistances to heat transmission i.e. it can accept and reject heat energy easily. For the case the equation 5.129 can be simplified as follows:

$$u_{trim1}(s) = \frac{\rho_a V_a c_{pa}}{\beta} \left(\begin{aligned} &+ \left(\frac{2U_{wi}A_w}{\rho_a V_a c_{pa}} \right) (T_a(s) - T_w(s)) + \left(\frac{U_m A_m}{\rho_a V_a c_{pa}} \right) (T_a(s) - T_m(s)) - \left(\frac{\alpha_a \sigma_s A_w}{\rho_a V_a c_{pa}} \right) I_{dr}(s) \\ &- \left(\frac{1}{\rho_a V_a c_{pa}} \right) (k_e P_L(s) + \dot{Q}_{oc}(s) + \dot{Q}_{ap}(s)) \end{aligned} \right) \quad (5.125)$$

In this case of $T_a = T_o$, the higher U values will quickly saturate the thermal mass of walls and will not have any capacity to store heat. In this case if casual gains (e.g. solar, lighting, occupancy and appliances) are significant then over heating will occur even with high thermal mass and climate adaptive property of thermal is no longer useful. In this case active cooling techniques would have to be considered because passive stack or mechanical ventilation will not be useful. The above equation (5.131) can be used to assess the type of furniture and wall insulation needed for preventing overheating in this case whether cooling is installed or not. If active cooling is installed then amount of furniture and wall insulation can be used to reduce the need for active cooling.

In climates where temperature differences are significant such as in deep winter and in the height of summer season then the whole U_{trim1} equation (5.129) will have to be inspected. Hence this equation is useful for estimating the heating required in winter or cooling required in summer. If there is no cooling installed then equation 5.129 can be used to assess how much cooling would be required or an indication of the potential over heating impact. If it is a hot summer then $(T_a - T_o)$ will be a negative term. Internal temperature exchanges can be assumed small. The humidity terms in the U_{trim1} equation are dependent on the internal and external humidity levels and the vapour production rate. Thus in summer it all depends on the use of the zone. If it is a high occupancy zone such as a classroom then ventilation will be ON to control humidity (i.e. $(w_a(s) - w_o(s))$ positive). This is the reason why these terms are positive in the U_{trim1} equation because they will cause the temperature to drop making U_{trim1} more positive due to mechanical ventilation thus reducing the chance of overheating. On the other hand if

humidity control is not active i.e. ventilation is off then casual gains will have significant impact on the value of the U_{trim1} in summer for temperature control.

Hence the designer has to assess the case for overheating by inspecting the value of U_{trim} . If there is cooling installed and the value of U_{trim} is within the cooling limits then the temperature control is reachable and overheating can be avoided. If there is no cooling installed and passive strategy is specified then the designer has to do sensitivity analysis on the building parameters in the U_{trim} equation bring the value of U_{trim} to zero i.e. no cooling required. Here the designer has a lot of choice of parameters e.g. whether to increase the U value of the wall for larger heat transfer or increase the air change rate by installed passive stacks or vents etc. (For more detail about reachability see section 4.2.3 on reachability in chapter 4).

In deep winter $[T_a(s)-T_o(s)]$ term will be very large positive term. If at the same time the casual gains are small then the U_{trim1} will be positive. If the U_{trim1} value remains within the heating capacity of the plant then temperature will be reachable. This will also be helped with any casual gains generated in winter. However if the plant is under sized for heating then there is a change for temperature control being unstable and set point unreachable. On the other hand in situations where the control system is required to track temperature and there is only a heating system installed and the building requires cooling, then there is also a chance of control system becoming unstable. This could happen in winter season where there is a large demand for heating in the zone and the heating is required to come on but is not managed properly causing overheating.

Another important factor is air change rates in the building. If air change rate is very high (i.e. low insulated building) and coupled with a large temperature internal external temperature difference then this will cause the U_{trim1} to be more positive. In winter ($T_a(s)-T_o(s) > 0$) U_{trim1} will be positive and if above the upper plant limits then will indicate a cooling requirement. In summer ($T_a(s)-T_o(s) < 0$) this will be positive and if below the lower plant limits then will indicate heating requirement.

Overall for temperature control the reachability of set point depends on the temperature difference in the building and the casual and humidity gains. The designer has to inspect these variables in U_{trim1} to be able to determine the reachability of temperature control in this MIMO system.

5.2.5 Reachability of humidity control

The reachability equation for humidity control with fast actuation system is given as follows:

$$u_{trim2}(s) = \left(\frac{V_a}{-(\bar{w}_a - \bar{w}_o)} \right) \left(\begin{array}{l} \left(\bar{n}_t + k_v \bar{v}_o + \bar{n}_i + \frac{\bar{q}_m}{V_a} \right) (w_a(s) - w_o(s)) \\ + (k_v (\bar{w}_a - \bar{w}_o)) v_o(s) - \left(\frac{1}{\rho_a V_a} \right) W_d(s) \end{array} \right) \quad (5.126)$$

The above equation shows that the reachability of humidity depends on the humidity differences, the humidity gains, air change rates and external wind speed. If the term $(w_a - w_o)$ is small and there is a high water vapour generation rate then U_{trim} will become positive resulting in infiltration of air from the zone. The U_{trim2} will be simplified to:

$$u_{trim2}(s) = \left(\frac{V_a}{-(\bar{w}_a - \bar{w}_o)} \right) \left(- \left(\frac{1}{\rho_a V_a} \right) W_d(s) \right) \quad (5.127)$$

This indicates that U_{trim2} will be positive meaning moisture infiltration is required by the mechanical ventilation. This is because mathematically infiltration is assumed positive and extraction as negative. Thus a higher water vapour generation will cause a greater positive value of the U_{trim2} resulting in more extraction of air required from the zone.

In cases where the humidity levels inside and outside are significant and cannot be ignored. Here the whole of the U_{trim2} will have to be considered for determining the reachability of humidity.

$$u_{trim2}(s) = \left(\frac{V_a}{-(\bar{w}_a - \bar{w}_o)} \right) \left(\begin{array}{l} \left(\bar{n}_i + k_v \bar{v}_o + \bar{n}_i + \frac{\bar{q}_m}{V_a} \right) (w_a(s) - w_o(s)) \\ + (k_v (\bar{w}_a - \bar{w}_o)) v_o(s) - \left(\frac{1}{\rho_a V_a} \right) W_d(s) \end{array} \right) \quad (5.128)$$

However, very high generating rate, wind speeds and air change rate could cause U_{trim} to become negative. In winter, external humidity levels are lower than in internal and thus in this case infiltration cannot be used to increase the humidity level inside and will require extraction indicated by the negative U_{trim2} value. Here it is important that the plant is able to extract and infiltration depending on the situation as moisture generation is a disturbance and not a control variable.

5.2.6 Conclusions

Over all in winter season the controllability of this MIMO system is a lot more complex than in the summer season. Hence in winter the temperature and humidity control are more coupled and having both heating and cooling and bi-directional mechanical ventilation will allow good control of the internal environment.

Evaluation of the matrix CB, and the relationship between the input and output has shown the extent of the cross coupling between the parameters in the system. With the analysis in this paper the matrix was proved rank full due to temperature feedback with a fast heating system. The (CB) matrix is not aligned diagonally which will make fast and accurate control very difficult with independent SISO controllers for temperature, and humidity especially in winter. This undesirable coupling changes seasonally and throughout the day as the root-locus asymptote directions are a function of the operating conditions. By assessing the state-space model (CB) matrix, the suitability of the system for high performance control has been proven to

be seasonal (i.e. function of temperature difference) and not a function of the thermal mass of the construction or its U value. This analysis has shown the cross coupling which exists as a barrier to fast, non-interacting control. Any control system which is designed for this notional building must address the problem of this interaction.

Transmission zeros in the case study presented are both negative and thus stable. The transmission zero locations will allow a high performance high gain control to be successfully utilised when simultaneously controlling humidity and room temperature with a MIMO controller. As shown, the locations of the transmission zeros are a function of the building parameters. The impact on control performance of disturbances such as changes in outside temperature and also changes in thermal characteristics such as U values can be minimised through the use of the symbolic analysis of equivalent control input (U_{trim}). When sizing the system actuators, such as, mechanical ventilation rate and heater power, the conditions for U_{trim} derived in this case study must be satisfied for safe system operation and guaranteeing reachability.

The trackability in buildings is not very complex as long as the variables being measured approach the derived set-point. In the case of extra measurements such as rate feedback (e.g. first case study), the measured variable has to equal the set-point in steady state and this is explained in this case study in the trackability section. Hence in practice what is measured is tracked for easier implementation and this is the case with air and comfort temperature control. Therefore further case studies do not analyse trackability.

The reachability depends on U_{trim} to be within the power limits of the plant. If assuming ideally a bi-directional heating/cooling plant then negative U_{trim} will cause the plant power to become negative causing cooling. However if there is no cooling (i.e. lower limit of the plant is zero) then the negative value will show the breach of power limits meaning that overheating is occurring and there is no way to cool thus temperature is drifting away from the set point and not reachable. To avoid overheating the building parameters in the U_{trim} equation have to be modified. The

reachability of air temperature in summer depends heavily on having a method of cooling the building whether by passive or active means. The reachability of humidity control depends on having a mechanical ventilation plant which can extract and infiltrate depending on the season. In summer humidity levels will be higher outside than inside and in winter higher inside than outside. Hence having a mechanical plant which can extract and infiltrate will make reachability easy. Maximum humidity generation expected in the zone can be used to size the extraction ventilation plant. Overheating of buildings and humidity discomfort can be a difficult MIMO problem in buildings and these new criteria allows the designer inspect how vulnerable the building design and its systems as a whole are to overheating and humidity comfort. **Fundamentally the analysis has shown that reachability of air temperature control depends on the UA value ONLY and NOT on THERMAL MASS of the external walls and internal structure (furniture etc). The proof of this finding is further shown in the next case study with symbolic and numerical simulation results.**

In conclusion the controllability in this case study is very complex due to highly cross coupled system. However as shown that based on realistic assumptions the symbolic analysis can be simplified. Here it is clearly shown that in such a cross coupled system a fast heating/cooling system is essential to good controllability of the overall system. This case study is important in areas such as hospitals, animal building, pet houses where humidity and temperature are very important. However in the buildings industry generally humidity is not required to be controlled and is assumed to be free floating. In practice majority of the control systems are single input single output SISO systems where majority of the times a fast heating system is being controlled with a simple PID controller. In addition to this ventilation is present however is not actively controlled but normally is user operated such through windows or extractor fans. Thus the final case study presents a typical zone in practice where a radiator system is used to control the temperature and ventilation is treated as a disturbance to the system. In practice humidity is not required to be controlled thus simplifying the 4th order model and new 3rd order model is presented for simplified analysis of the controllability in industrial practice.

5.3 Simplified Controllability of Air Temperature for Systems with Fast Actuation (Convective Heater)

A simplified 3rd order model is specifically developed to test the controllability of a complex climate adaptive building with focus on fast heating systems in practice. The model was derived from the results of the previous two case studies. The dynamic model describes the energy and mass balance of air in the building zone having heating and ventilation. The assumptions inherent in constructing this model are numerous. However, the purpose of the model is not to emulate future reality but instead to be used for symbolic controllability analysis and simulation at the conceptual design state for building designers.

The reason for proposing the 3th order reduced model is because the symbolic controllability analysis of the 11th and 4th order models proposed in the earlier two case studies, showed that the control of CO₂ and humidity was not very complex as long as the mechanical ventilation was operated at a rate close to the responsiveness of the heating system. Then the mechanical ventilation can be treated as a disturbance by the heating resulting in a less complex control problem. Also in most common applications i.e. domestic, the control of CO₂ and humidity is not very important as much as temperature and are ignored and mechanical ventilation is purely used for cooling using on/off controls. Thus in this model CO₂ and humidity are not modelled.

From the work presented in the two previous case studies further simplifications to the model are proposed. It was proposed that primarily this model should be reduced further to include only the most fundamental causes and effects of a building system. These changes will allow for designers in industry to use this symbolic method quickly and effectively for producing meaningful results at the conceptual phase. Hence, the different air change rates induced by, buoyancy, external wind, infiltration and mechanical ventilation were combined into a single term for fundamentally analysing the effect of air change rate on the controllability.

5.3.1 Mathematical Modelling

The 3rd order model lumps the walls, floor and roof into a single external thermal mass with two resistance layers i.e. internal and external. This leads to a reduced model having three equations as follows:

1. Air temperature
2. External thermal mass: walls + floor + roof
3. Internal thermal mass: furniture + internal walls

The temperature of the zone is modelled as a single node representing an average temperature of the zone. The air temperature equation is given by:

$$\rho_a V_a c_{pa} \frac{dT_a}{dt} = \left[\begin{array}{l} (\dot{Q}_{sa} + \dot{Q}_L + \dot{Q}_{oc} + \dot{Q}_{ap})_{casual\ gains} \\ + (\dot{Q}_{wi} + \dot{Q}_{win} + \dot{Q}_m)_{structure} \\ + (\dot{Q}_n)_{ventilation} \\ + (\dot{Q}_p)_{heating/cooling} \end{array} \right] \quad (5.129)$$

$$\text{Solar radiation: } \dot{Q}_{sa} = \alpha_a \sigma_s A_{win} I_{dr} \quad (5.130)$$

$$\text{Lighting: } \dot{Q}_L = k_e P_L \quad (5.131)$$

$$\text{Occupancy: } \dot{Q}_{oc} = n_p G_{pp} \quad (5.132)$$

$$\text{Appliances: } \dot{Q}_{ap} = \dot{Q}_{pc} + \dot{Q}_{laptops} + \dot{Q}_{peripherals} \quad (5.133)$$

$$\text{External thermal mass: } \dot{Q}_{wi} = 2U_{wi} A_w (T_w - T_a) \quad (5.134)$$

$$\text{Window: } \dot{Q}_{win} = U_{win} A_{win} (T_o - T_a) \quad (5.135)$$

$$\text{Internal thermal mass: } \dot{Q}_m = U_m A_m (T_m - T_a) \quad (5.136)$$

$$\text{Air change rate due to thermal forces: } \dot{Q}_n = V_a n \rho_a c_{pa} (T_o - T_a) \quad (5.137)$$

The rate of change of temperature equation represents the major causes and effects that determine internal temperature of the zone. It takes into account the various

sources of heating and cooling from plants systems. For fast actuation systems it was assumed that majority of the energy is directly input or taken out from the air with some energy transfer to the internal and external thermal mass. One such type of model of a simple fast acting radiator was developed in the previous case study. This model was used for representing a fast acting heater and cooler. It was assumed that compared with the building zone, the radiator or cooler has a much smaller thermal inertia. The energy transfer from a radiator or cooler panel depends primarily on the temperature difference between the plant and the surrounding air. So the dynamics of the radiator can therefore be ignored and simplified as shown in previously case study. This can provide very rapid heating/cooling of a room.

The rate of change of wall temperature is given by:

$$\rho_w V_w c_{pw} \frac{dT_w}{dt} = [\dot{Q}_{sw} + \dot{Q}_{wo} - \dot{Q}_{wi}] \quad (5.138)$$

Where heat exchange with:

$$\text{Outside: } \dot{Q}_{wo} = 2U_{wo} A_w (T_{sa} - T_w) \quad (5.139)$$

$$\text{Inside: } \dot{Q}_{wi} = 2U_{wi} A_w (T_w - T_a) \quad (5.140)$$

$$\text{Direct solar radiation through the window: } \dot{Q}_{sw} = \alpha_w \sigma_s A_{win} I_{dr} \quad (5.141)$$

N.B: For heat transfer between external surroundings and the wall, the external temperature is taken to be the sol-air temperature. This allows for simpler treatment of the effect of the solar radiation and sky heat exchange with the wall.

The rate of change of thermal mass temperature is given by the following differential equation:

$$\rho_m V_m c_{pm} \frac{dT_m}{dt} = \dot{Q}_{sm} - \dot{Q}_m \quad (5.142)$$

Where the heat exchange with:

$$\text{Air: } \dot{Q}_m = U_m A_m (T_m - T_a) \quad (5.143)$$

$$\text{Solar gain through the window: } \dot{Q}_{sm} = \alpha_m \sigma_s A_{win} I_{dr} \quad (5.144)$$

The model equations represent the major causes and effects that determine internal temperature of the zone. They take into account the various sources of heating and cooling from plant systems.

Sensors for the Controller

A feedback control system can only control (i.e. track) what it feeds back as measured system outputs. Thus, to analyse the controllability of these measurements, they must be defined and are as follows:

In this case study two control strategies are fundamentally analysed.

1. Control and feedback of air Temperature level as given by: T_a
2. Control and feedback comfort temperature level as given by: $T_{cm} = k_a T_a + k_w T_w + k_m T_m$

In order to apply the aerospace controllability science, the nonlinear dynamic equations presented above must be linearised about a steady state operating point. The results of this linearisation enable the total system to be represented in the state-space form:

$$\dot{x}(t) = Ax(t) + Bu(t) + Fd(t) \quad (5.145)$$

$$y(t) = C(x) \quad (5.146)$$

Where $y(t)$ is the measured output vector, $x(t)$ is a vector of state variables, $u(t)$ is a vector of system inputs (i.e. controller outputs) and $d(t)$ is a vector of disturbances. A , B , C , E and F are time invariant matrices consisting of constants. The vectors associated with these matrices are given as follows:

$$\begin{aligned}
\dot{x} &= [\dot{T}_a, \dot{T}_w, \dot{T}_m]^T \\
x &= [T_a, T_w, T_m]^T \\
u &= [\dot{Q}_p]^T \\
d &= [I_{dir}, P_L, \dot{Q}_{oc}, \dot{Q}_{ap}, T_o, T_{sa}, n]^T
\end{aligned} \tag{5.147}$$

NOTE: For understanding the controllability analysis of systems in practice the SAP data was used for modelling and simulation. However the results are applicable generally.

5.3.2 Stability

The stability of air temperature is given by: $CB = \left(\frac{1}{\rho_a V_a c_{pa}} \right)$ (5.148)

The RIDE theory states that the asymptotes for a multivariable design are given by Eigen-values: $|sI + g(CB)\sigma| = 0$ where, g is the global gain from zero to infinity and σ is a scalar gain. In this case study a single-input single-output case of air temperature control is being presented therefore there is only one air temperature asymptote and the solution for s is given as follows:

$$s = -g_{0 \rightarrow \infty} \frac{1}{\rho_a V_a c_{pa}} (\sigma) \tag{5.149}$$

The asymptote for air temperature is negatively aligned and will result in stable fast transient temperature response without oscillation to reach steady state i.e. temperature control is stable and controllable. The main result is that the asymptote will always be negatively aligned hence this will produce a first order transient response with PI controller. What this result also shows is that the stability of this system is not dependent on the thermal mass of the external or internal envelope. This means that while increasing thermal mass slows the response of the building the control system will still be stable and thus able to control air temperature. The model

was constructed in ESL language for simulation of the step response using proportional + Integral Controller. Below shows a typical response of air temperature to a step change in set-point using a fast acting heater.

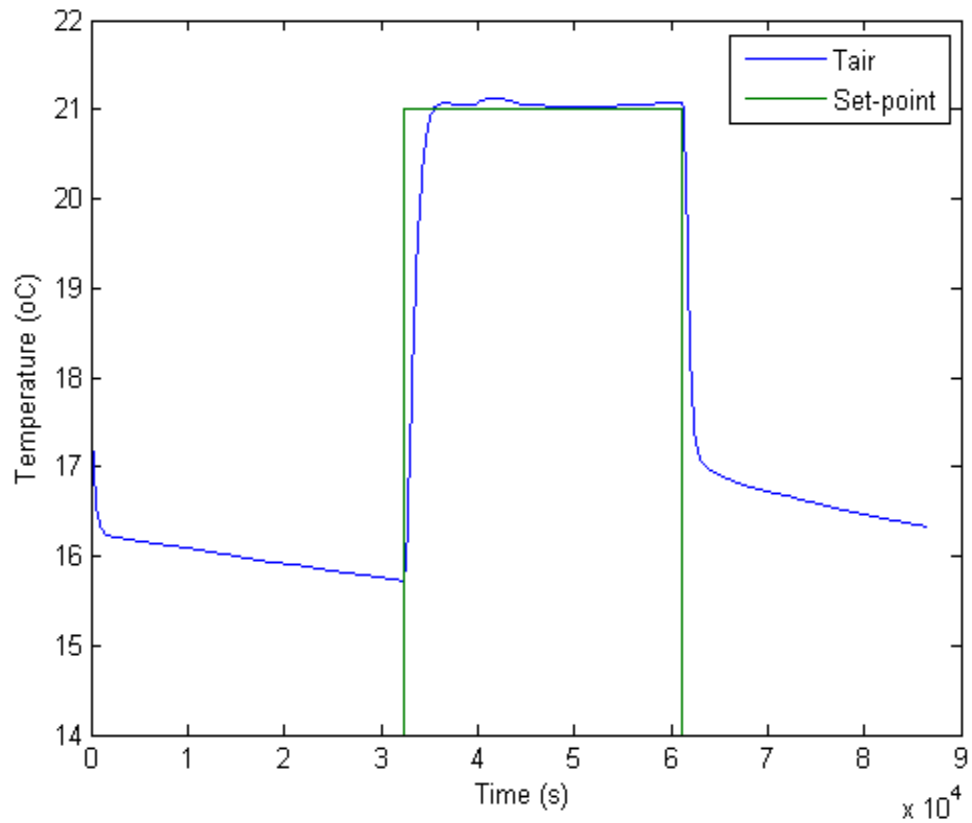


Figure 54: shows a typical response to a step change in the required temperature.

Now the external thermal capacity value is increased and decreased to see its effect on stability of the system.

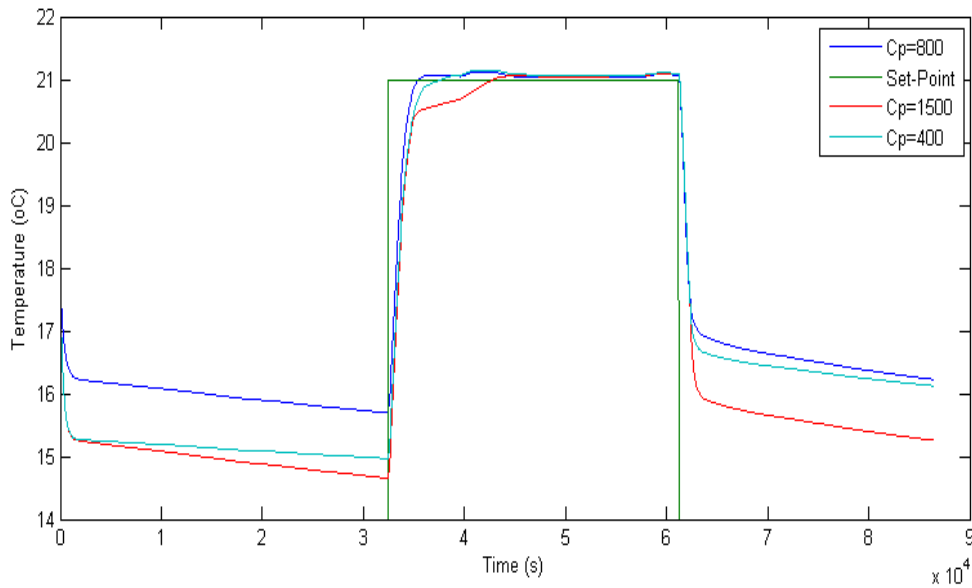


Figure 55: shows the response with varying external thermal mass values

The above figure shows the original response and response with high and low thermal mass values. As can be seen that the air temperature response is slower with the high thermal mass however the air temperature reaches steady state i.e. stable. Having a higher thermal mass for stabilising the internal air temperature will also require a faster and higher rated heater to compensate for the heat absorbed by the thermal mass to be able to achieve the require set point. With low thermal mass the building is more responsive and the set point is achieved quickly while being stable. This is a simple analysis and results to show the fundamental understanding that we generally have regarding thermal mass.

The control of the simple model is very easy when the asymptote is negative. As presented in the previous case studies generally the asymptotes are stable (negative). However for completeness, if the asymptote was to be made positive i.e. RHP, then the control system will be unstable i.e. uncontrollable as shown below. This can be done by making the gain (sigma) negative thus pointing the asymptote towards the unstable RHP. In the following figure this is shown as the air temperature is completely out of control. This is to illustrate the effect of unstable asymptotes.

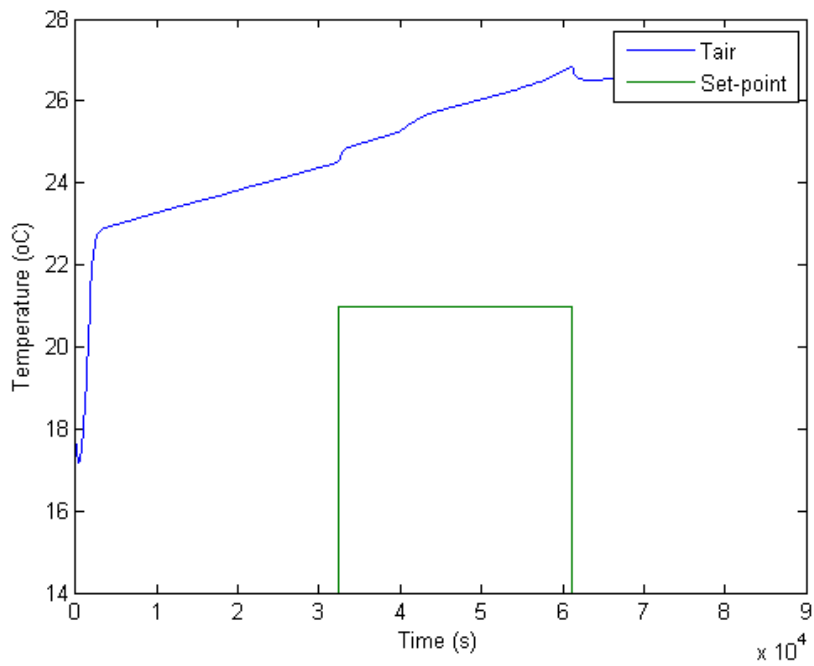


Figure 56: Unstable response with asymptote pointing towards RHP on the root-locus.

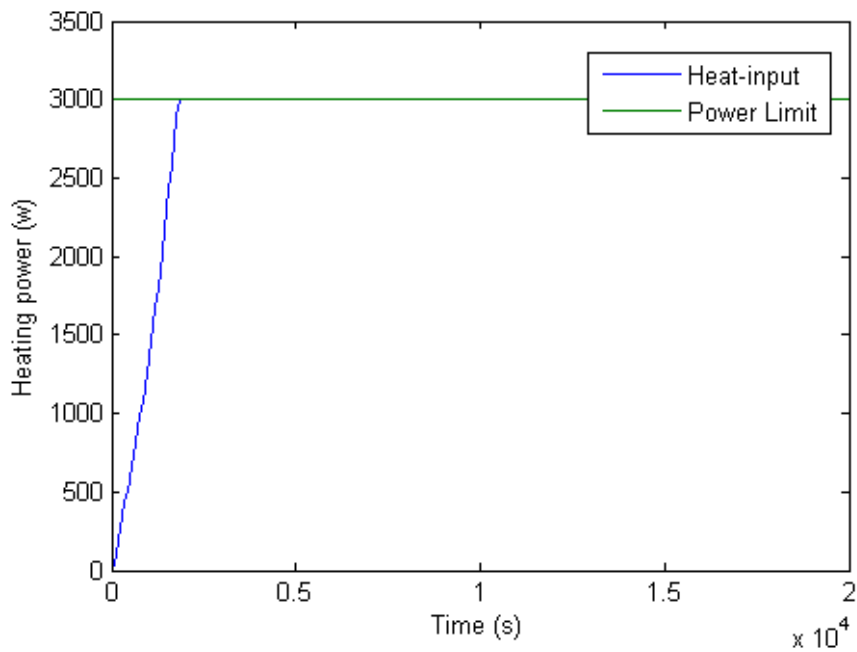


Figure 57: Unstable response of heating system with asymptote pointing towards RHP on the root-locus.

Due to unstable position of asymptotes the heating system is unstable and running at maximum even though the building is overheating.

The second stability property, transmission zeros, of this case are given by the following determinant:

$$(a_{22} - s_1)(a_{33} - s_1) = 0 \quad (5.150)$$

Thus the two transmission zeros are a_{22} and a_{33} . In terms of building parameters they are as follows:

$$s_1 = \left(\frac{-2U_{wo}A_w - 2U_{wi}A_w}{\rho_w V_w c_{pw}} \right), \quad s_2 = \left(\frac{-U_m A_m}{\rho_m V_m c_{pm}} \right) \quad (5.151)$$

Note: These transmission zeros correspond to the external and internal thermal masses. Of course in the external thermal mass there exists wall, roof, and floor. Therefore s_1 can be equally applied to walls, roof or floor for testing their stability individually by putting in the properties of these elements in the s_1 equation.

The transmission zeros are both in the left half plane and thus stable. Interestingly they are a function of constants and thus will always remain stable. In this case they are not a function of operating conditions such as outside temperature, but are a function of thermal properties; area, mass and thermal capacitance and U values of the internal and external thermal mass.

As proven by the previous two case studies the transmission zeros are not a problem in buildings as they are always stable. However they are still useful as building designers can inspect them for estimating the response of a building. A transmission zero far from origin (low insulation i.e. higher U value and low thermal mass i.e. low Cp value), will result in a responsive but also a very leaky building requiring fast and large heating system. On the other hand a transmission zero close to the origin will result in less responsive and but less leaky building.

5.3.3 Reachability

The reachability criterion equation U_{trim} is given as follows:

$$u_{trim}(s) = \left[-(CB)^{-1} CAX(s) - (CB)^{-1} (CF)d(s) \right] \quad (5.152)$$

Substituting the state space matrices gives the following equation:

$$u_{trim}(s) = \left[\begin{array}{c} -\frac{1}{b_{11}}(1 \ 0 \ 0) \begin{pmatrix} a_{11} & a_{12} & a_{13} \\ a_{21} & a_{22} & 0 \\ a_{31} & 0 & a_{33} \end{pmatrix} \begin{pmatrix} T_a(s) \\ T_w(s) \\ T_m(s) \end{pmatrix} \\ -\frac{1}{b_{11}}(1 \ 0 \ 0) \begin{pmatrix} f_{11} & f_{12} & f_{13} & f_{14} & f_{15} & 0 & f_{17} \\ f_{21} & 0 & 0 & 0 & 0 & f_{26} & 0 \\ f_{31} & 0 & 0 & 0 & 0 & 0 & 0 \end{pmatrix} \begin{pmatrix} I_{dr}(s) \\ P_L(s) \\ \dot{Q}_{oc}(s) \\ \dot{Q}_{ap}(s) \\ T_o(s) \\ T_{sa}(s) \\ n(s) \end{pmatrix} \end{array} \right] \quad (5.153)$$

Multiplying out the matrices:

$$u_{trim}(s) = \left[\begin{array}{c} -\frac{1}{b_{11}}(a_{11} \ a_{12} \ a_{13}) \begin{pmatrix} T_a(s) \\ T_w(s) \\ T_m(s) \end{pmatrix} \\ -\frac{1}{b_{11}}(f_{11} \ f_{12} \ f_{13} \ f_{14} \ f_{15} \ 0 \ f_{17}) \begin{pmatrix} I_{dr}(s) \\ P_L(s) \\ \dot{Q}_{oc}(s) \\ \dot{Q}_{ap}(s) \\ T_o(s) \\ T_{sa}(s) \\ n(s) \end{pmatrix} \end{array} \right] \quad (5.154)$$

And:

$$u_{trim}(s) = -b_{11}^{-1} \left[\begin{array}{l} a_{11}T_a(s) + a_{12}T_w(s) + a_{13}T_m(s) + f_{11}I_{dr}(s) + f_{12}P_L(s) + f_{13}\dot{Q}_{oc}(s) + f_{14}\dot{Q}_{ap}(s) \\ + f_{15}T_o(s) + f_{17}n(s) \end{array} \right] \quad (5.155)$$

Substituting the different building parameters corresponding to the constant from appendix gives the following U_{trim} equation:

$$u_{trim}(s) = \left[\begin{array}{l} (2U_{wi}A_w + U_{win}A_{win} + U_mA_m + V_a\rho_a c_{pa}\bar{n})T_a(s) \\ -2U_{wi}A_wT_w(s) - U_mA_mT_m(s) \\ -\alpha_a\sigma_s A_{win}I_{dr}(s) - k_eP_L(s) - \dot{Q}_{oc}(s) - \dot{Q}_{ap}(s) \\ - (U_{win}A_{win} + V_a\rho_a c_{pa}\bar{n})T_o(s) - (\bar{T}_o - \bar{T}_a)\rho_a V_a c_{pa}n(s) \end{array} \right] \quad (5.156)$$

And further simplification gives:

$$u_{trim}(s) = \left[\begin{array}{l} -V_a\rho_a c_{pa}\bar{n}(T_o(s) - T_a(s)) \\ -U_{win}A_{win}(T_o(s) - T_a(s)) \\ -2U_{wi}A_w(T_w(s) - T_a(s)) - U_mA_m(T_m(s) - T_a(s)) \\ -\alpha_a\sigma_s A_{win}I_{dr}(s) - k_eP_L(s) - \dot{Q}_{oc}(s) - \dot{Q}_{ap}(s) \\ -(\bar{T}_o - \bar{T}_a)\rho_a V_a c_{pa}n(s) \end{array} \right] \quad (5.157)$$

As can be seen from the above equation, the U_{trim} is a function of many building parameters and disturbances in the system. The criterion for safe tracking state that as long U_{trim} remains within the limits of the actuator i.e. minimum and maximum heater setting, then the air temperature will be easily reached.

In situations where the control system is required to track temperature and there is only a heating system installed and the building requires cooling, then there is a chance of control system becoming unstable. This could happen in winter season where there is a large demand for heating in the zone and the heating is required to come on. By mid-day the IT gains also start to increase the air temperature and in addition to this the sun comes out causing the air temperature to rise above the set point. This is shown in the figures below:

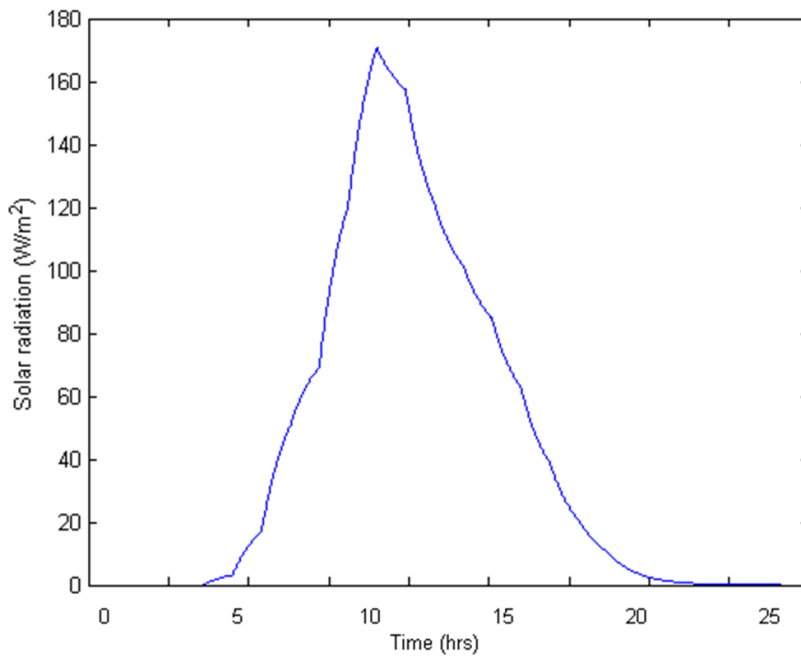
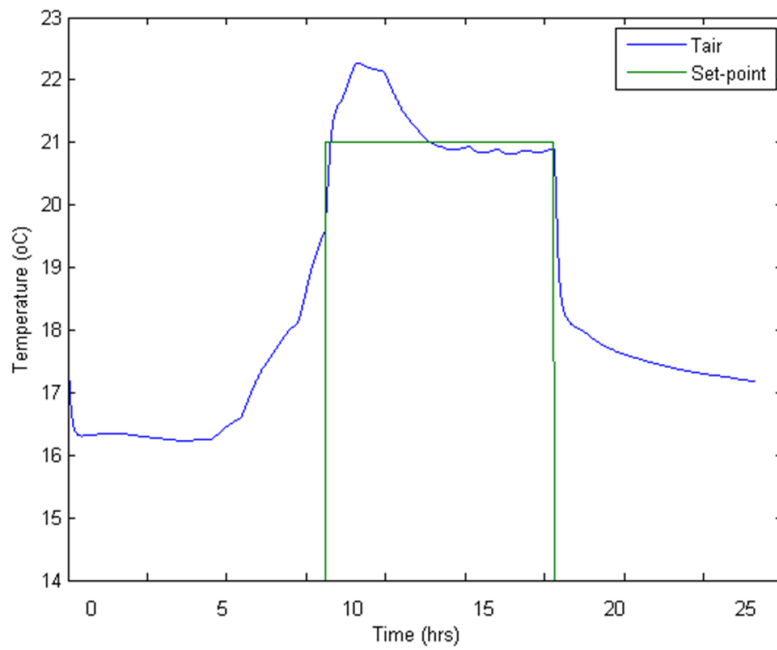


Figure 58: Air temperature response to solar gain (top), solar gain profile (bottom)

The above figure shows that as the solar gain increases during the day the air temperature goes above the set point. The casual gain causes the U_{trim} to become negative and the proportional plus integral control on heating system is unable to track temperature, this is shown below:

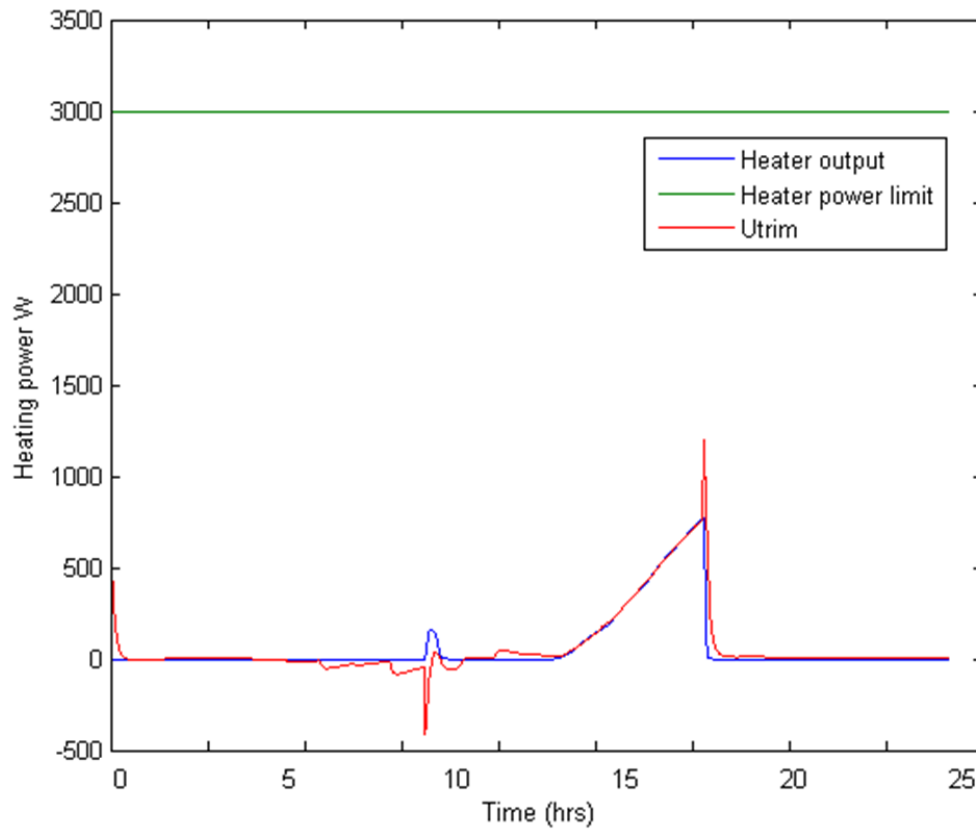


Figure 59: plot showing heater output and U_{trim}

As shown in the above figure when the U_{trim} is less than zero (i.e. since $L_L = 0$), the controller is not tracking the set-point and air temperature is above the set-point showing overheating. This is indicating a cooling requirement in heating mode. Clearly in this state the system is out of control because the criterion states that steady state is not reachable if the U_{trim} is out of limits. This is a very common problem of over-heating in buildings and this new criteria allows the designer to inspect how vulnerable the building design and its systems as a whole are to over-heating.

When the solar gains start to decrease the air temperature start to decrease and this is shown in the previous figures and U_{trim} becomes positive showing the air temperature is becoming more reachable until the air temperature hits the set-point and the heating system turns on to bring the temperature to steady state about the set point.

This is very useful for designers as they can test the design for the need for ventilation and its sizing to compensate for overheating. In buildings where the overheating is likely to happen, this problem can be minimised by increasing the air change rate, at times of overheating. This can be tested by varying the air change rate in the U_{trim} equation.

Also the following points are noted:

- 1) U_{trim} is more sensitive to casual gains with high internal insulation because this will reduce the effect of thermal capacitance on the air temperature control.
- 2) U_{trim} is less sensitive to casual gains with low internal insulation because this will allow for thermal mass capacitance to absorb heat from the air.

Hence by having low internal resistance gives more access to thermal storage and hence thermal mass has more effect on the air temperature response. This would cause the U_{trim} to be more insensitive to casual gains and thus easier reachability of air temperature. A highly insulated zone where there is no influence of thermal mass will find difficult to remove heat passively in cases of overheating as there will be no material to absorb heat. Thus in highly insulated buildings high conductivity furniture will be very useful. Hence up to an extent having some internal and external thermal mass is useful for controllability of air temperature. Otherwise for U_{trim} to be insensitive to casual gains with highly insulated zone is only possible if there is also fast acting provision for cooling in the building as well. Also, by varying the value of internal resistance U_{wi} , it is effectively varying the level of access to the thermal mass heat storage capacity in the wall.

Furthermore the reachability U_{trim} equation (5.163) is NOT a function of the thermal mass of the internal and external structure i.e. Cp value. This is confirmed and explained in the previous case study and the case study also analysis concludes that the thermal masses of the internal and external structures have NO effect on reachability of air temperature control. The reachability ONLY depends on the UA value of the thermal masses. Here this symbolic result is confirmed by the simulation results as follows:

Consider the same case as above. A 3kW heater is used for heating a 5 m³ zone. The results show that for a fixed amount of thermal mass in the external wall and varying the U value:

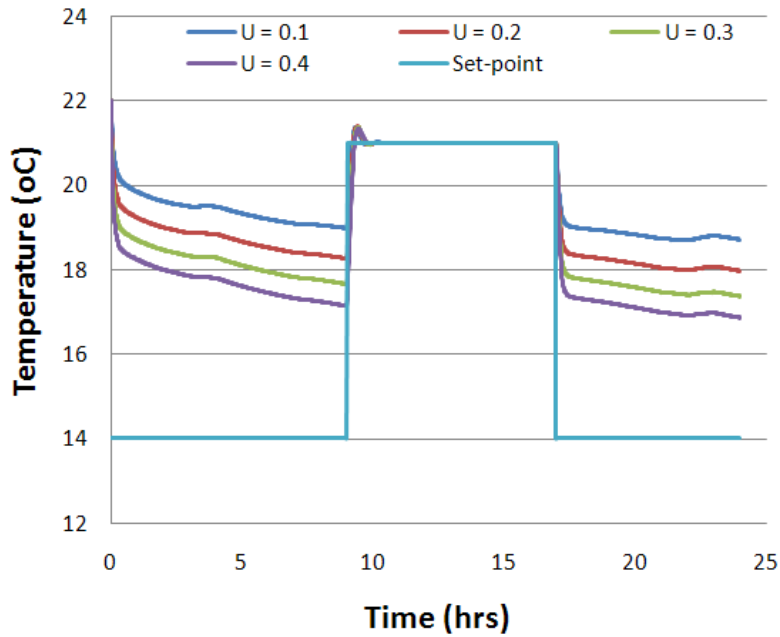


Figure 60: Temperature response with different U values of the wall

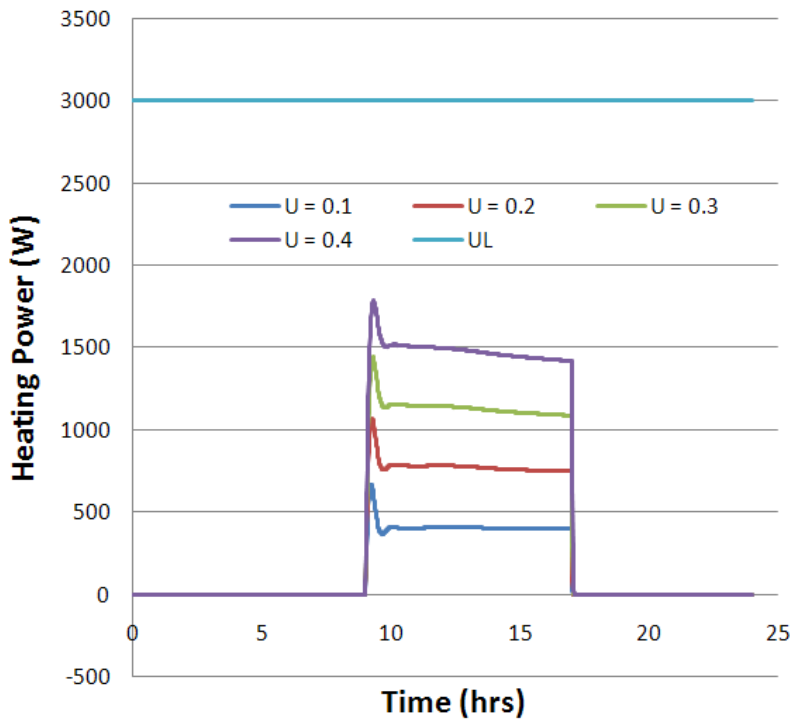


Figure 61: Heating power consumed for different U values of the wall

The two plots above show that changes in U value affects the ability of the thermal mass to accept or reject heat. If the building has low U value i.e. it is well insulated then the ability for thermal mass of wall to accept or reject heat is minimised. In this case thermal mass has negligible effect on the air temperature reachability. However with higher U values the thermal mass socks more heat from the air and thus energy consumption has increased.

It can be argued that the reachability of air temperature control depends on the thermal mass because the U_{trim} equation (5.162) is the function of wall temperature T_w and internal thermal mass T_m that are functions of the thermal mass. This is true **but** as the rate of change of wall temperature tends to zero (i.e. steady state) the effect of capacitance is less and less on the air temperature reachability. This is because the structure reaches steady state when there is no capacity left in the structure to store heat. Hence amount of heat entering is equal to amount of heat leaving. This can also be shown from the RC circuit analogy as follows:

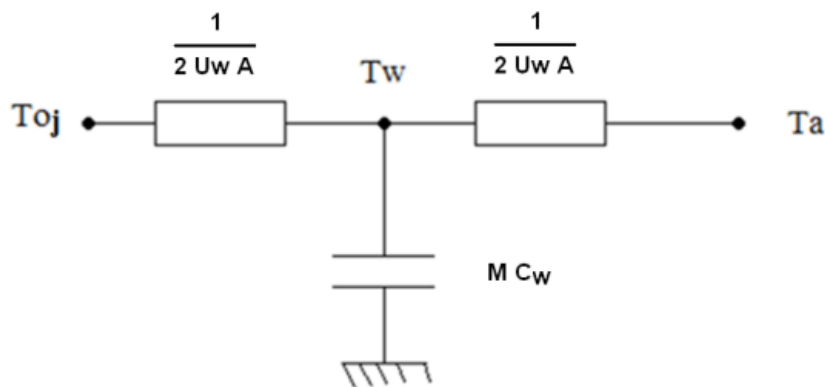


Figure 62 Resistance capacitance circuit of the wall

The figure shows that the T_w is anchored with the capacitance of the wall. When the wall cannot hold anymore heat i.e. it's capacity is full, then the wall temperature stops changing i.e. there is equal rate of heat passing through the resistors the capacitance has no effect and can be removed.



Figure 63 Steady state resistance circuit of the wall

Note: In this thesis the value resistances have been assumed equal (i.e. $0.5U$) for the internal and external surfaces. This is just one case and generally the U value will be higher on the internal surfaces (due to insulation, plaster etc.) than on the external surfaces of the wall.

$$R_1 + R_2 = \frac{1}{U} \rightarrow R_1 = R_2 = \frac{1}{2U} \Rightarrow \frac{1}{2U} + \frac{1}{2U} = \frac{1}{U} \text{ or } \frac{1}{3U} + \frac{2}{3U} = \frac{1}{U}$$

The external surface U value is easy to calculate as it is of one material layer where the internal U value is a function of different material layer. Hence subtracting the external layer U value from the overall U value used in industry will result in the required internal U value.

Hence it is important to use the right amount of thermal mass for the wall temperature to remain near constant so that thermal mass does not affect the reachability of air temperature control. Otherwise using the wrong amount of thermal mass might result in a dynamic wall that will affect reachability of air temperature.

To show how only up to a certain amount of thermal mass affects the reachability of air temperature with casual gain the model was simulated for increasing values of thermal mass from 100 to 1500 J/kgK for internal U value of 0.22:

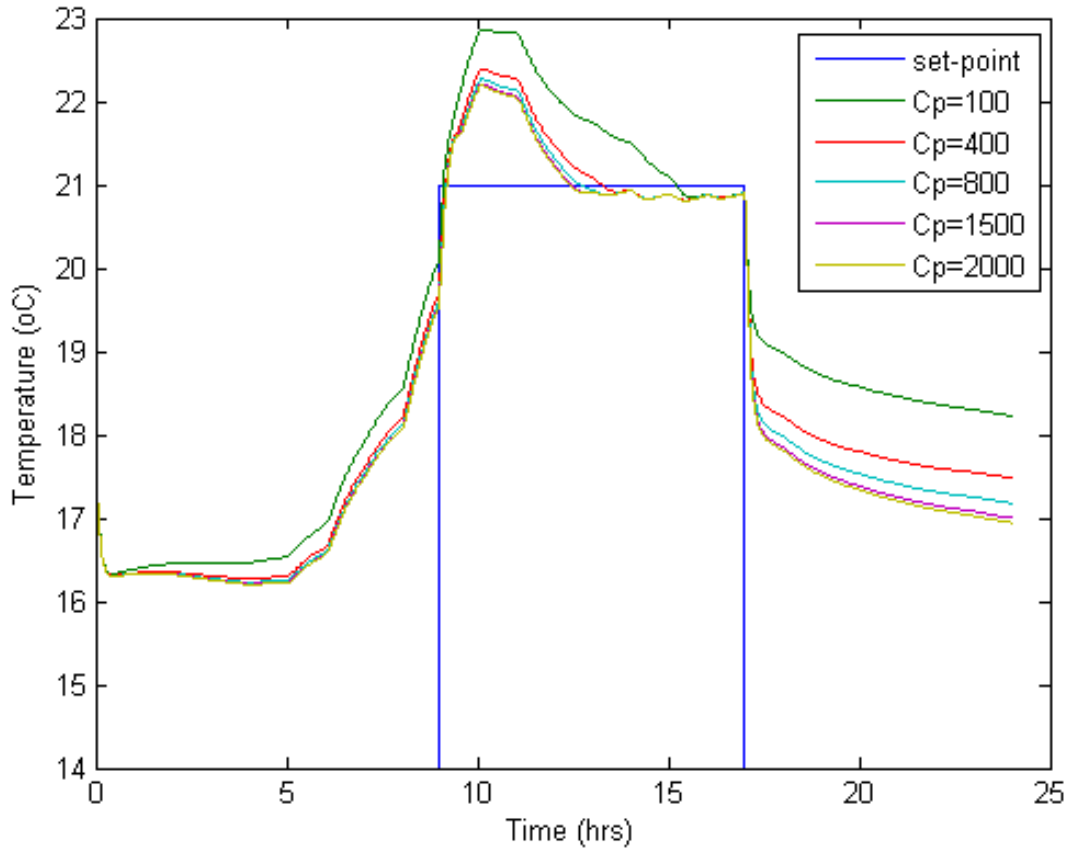


Figure 64: Temperature response with varying C_p values with constant U value of 0.22

As the results show in the above figure, depending on the resistance value i.e. U_{wi} value, only up to a certain amount of thermal mass will be useful in damping and compensating for casual gain affecting the air temperature reachability. After that, any amount of thermal mass will have negligible effect on the air temperature reachability. As shown that $C_p = 800 \text{ J/kgK}$ is for a brick wall and increasing further leads to a concrete wall at $C_p=2000 \text{ J/kgK}$. Increasing the C_p value from 800 to 2000 has no effect on the response of air temperature. Hence with U value of 0.22 as a good insulated building, increasing the thermal mass above 400 J/kgK has no effect on the damping of temperature and thus no effect on air temperature reachability and therefore not useful in absorbing the effect of casual gain.

The proof of this result can be shown symbolically as follows:

$$U_{trim} = f(T_w) \quad (5.158)$$

$$m_w c_{pw} \frac{dT_w}{dt} = 2UA(T_o - T_w) - 2UA(T_w - T_a) \quad (5.159)$$

In Laplace transform this can be written as follows:

$$m_w c_{pw} s T_w + 4UA T_w = 2UA(T_o + T_a) \quad (5.160)$$

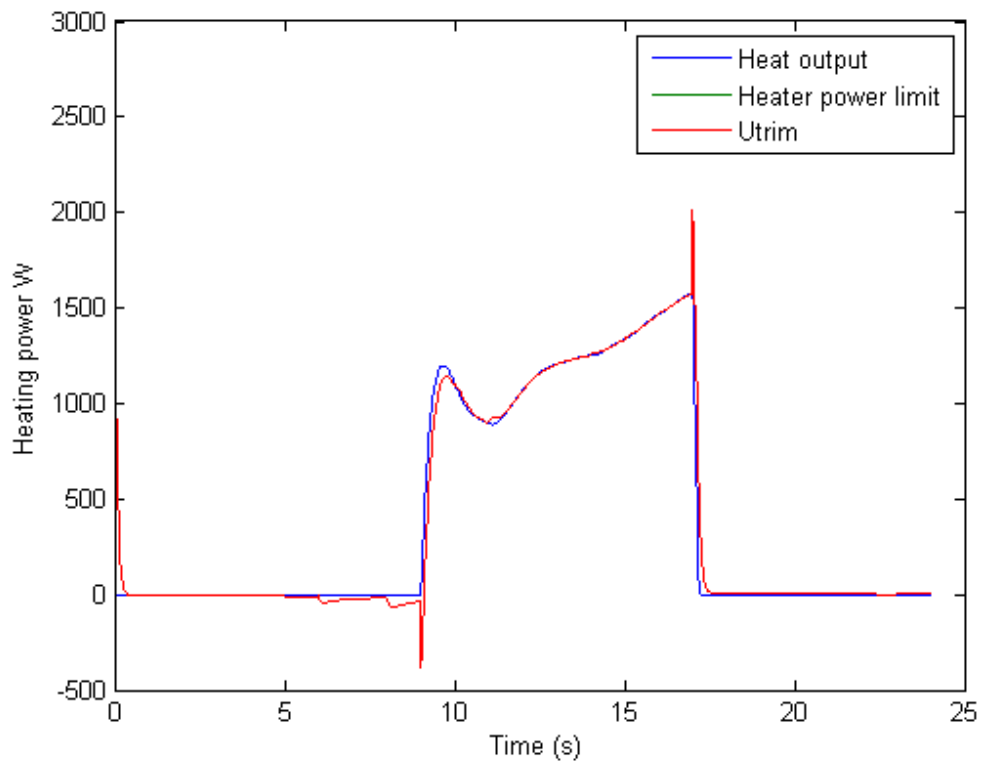
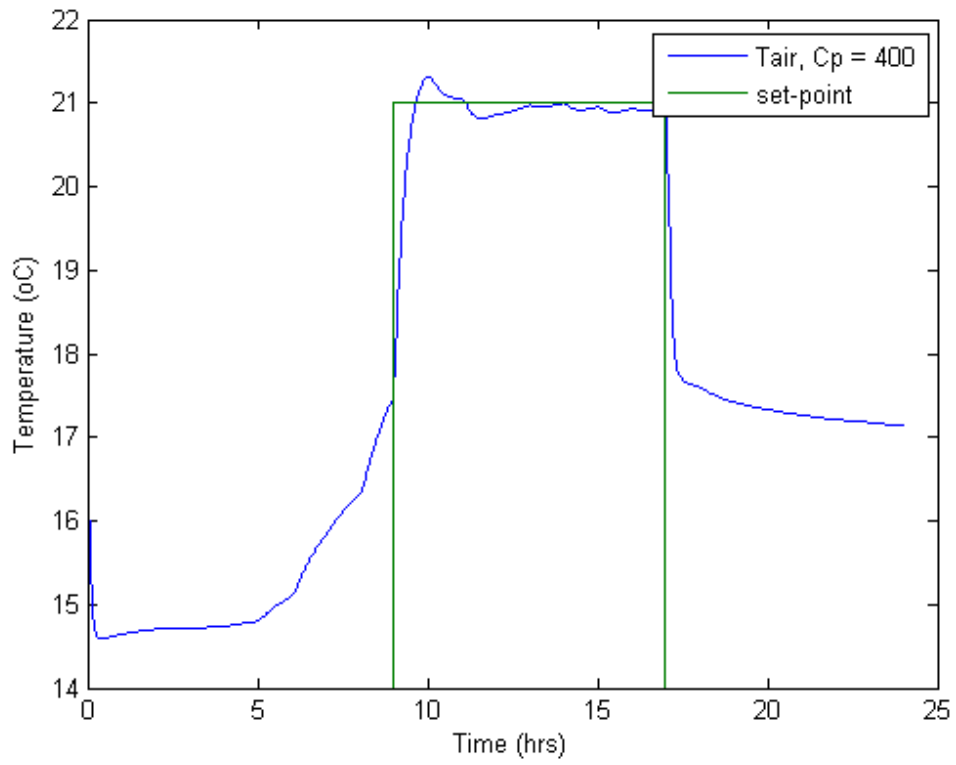
$$T_w = \frac{2UA(T_o + T_a)}{(m_w c_{pw} s + 4UA)} \rightarrow s T_w = \frac{2UA(T_o + T_a)}{(m_w c_{pw} s + 4UA)} s \quad (5.161)$$

$$\text{Case 1: } m_w \rightarrow 0 \Rightarrow T_w = \frac{(T_o + T_a)}{2} = \text{Steady State Value} \quad (5.162)$$

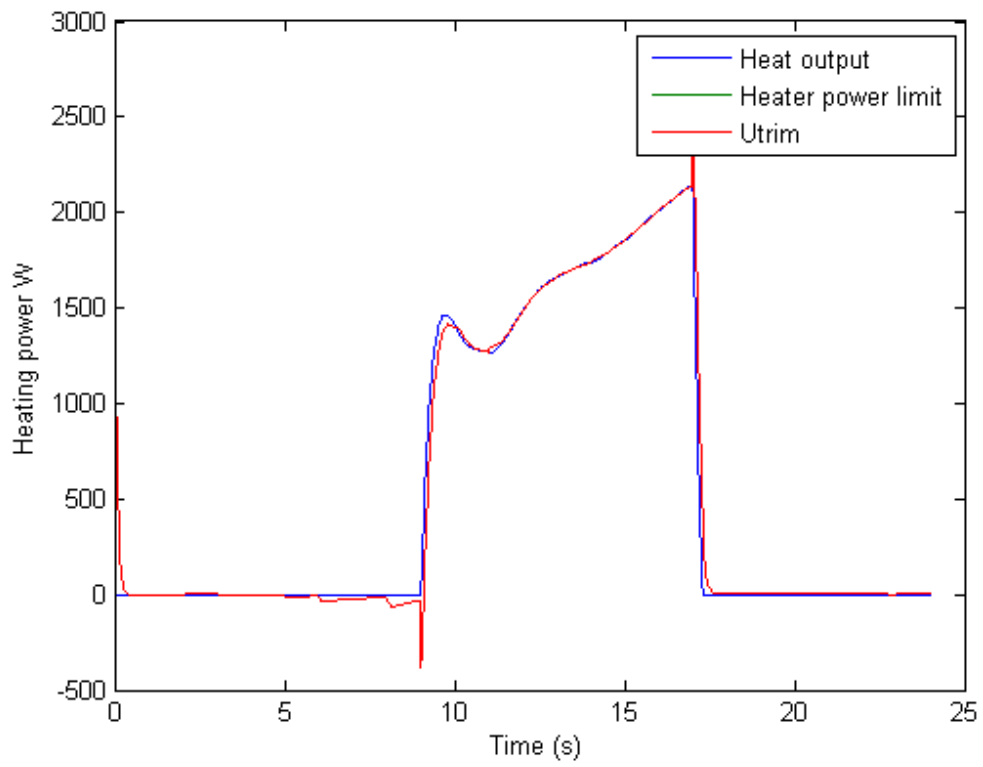
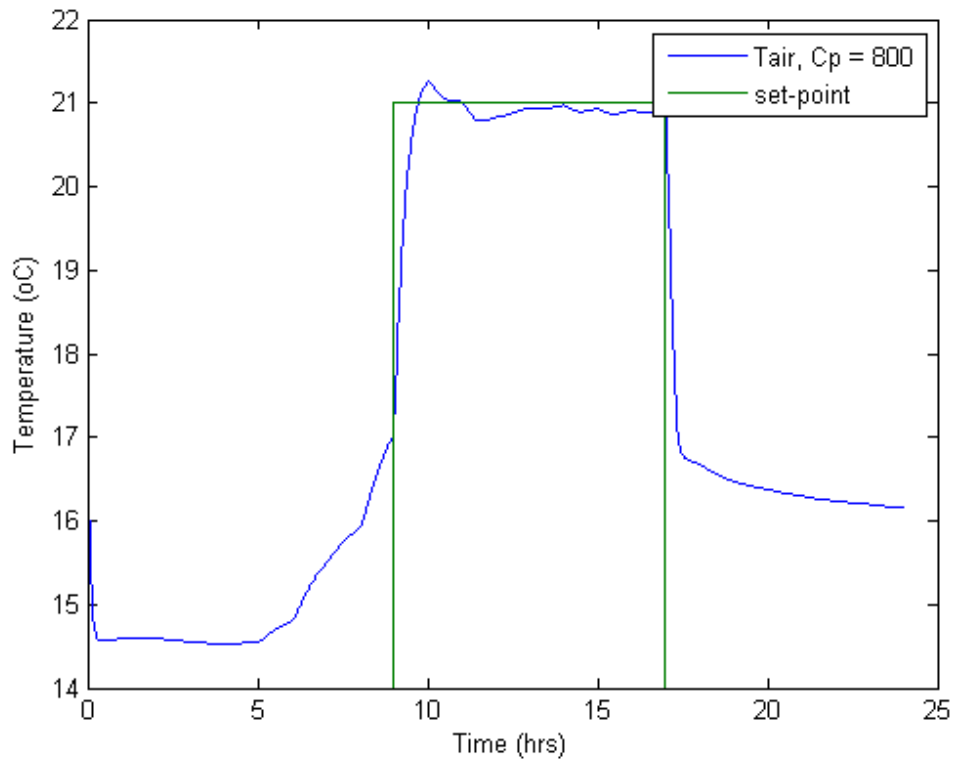
$$\text{Case 2: } m_w \rightarrow \infty \Rightarrow s T_w = 0 = \text{Steady State Value} \quad (5.163)$$

The results also show that by increasing thermal mass for damping the transient response of the air temperature also means that more energy is used for controlling air temperature due to thermal mass absorbing the initial heat input. The figure below shows temperature response with negligible internal wall build up resistance (i.e. more access to thermal mass) and with increasing values of thermal mass.

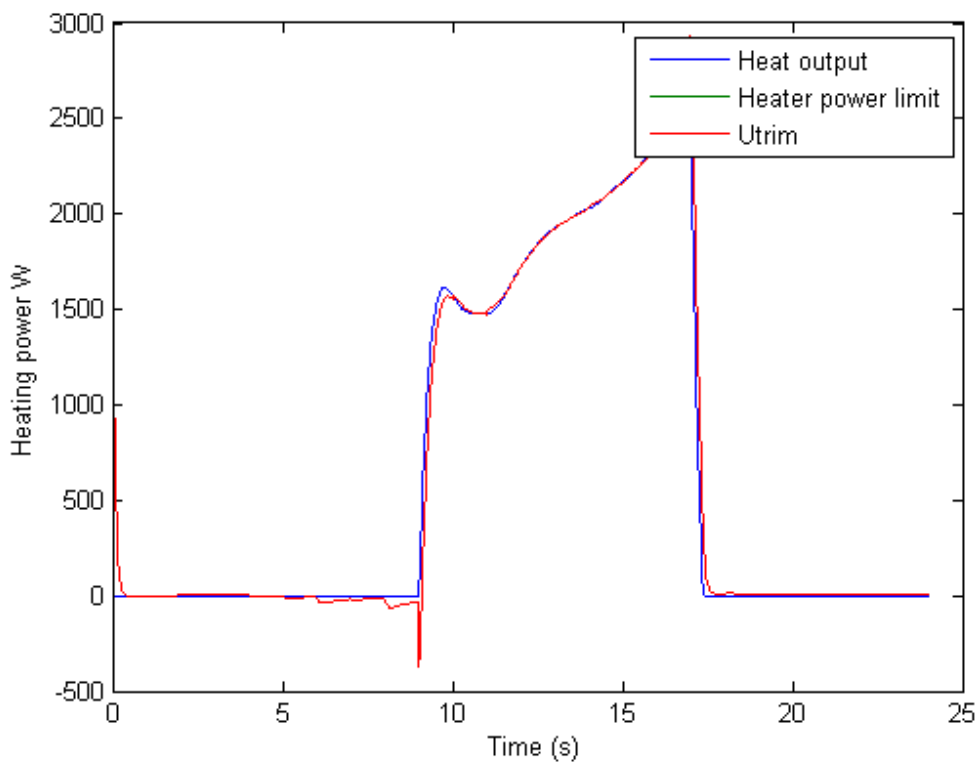
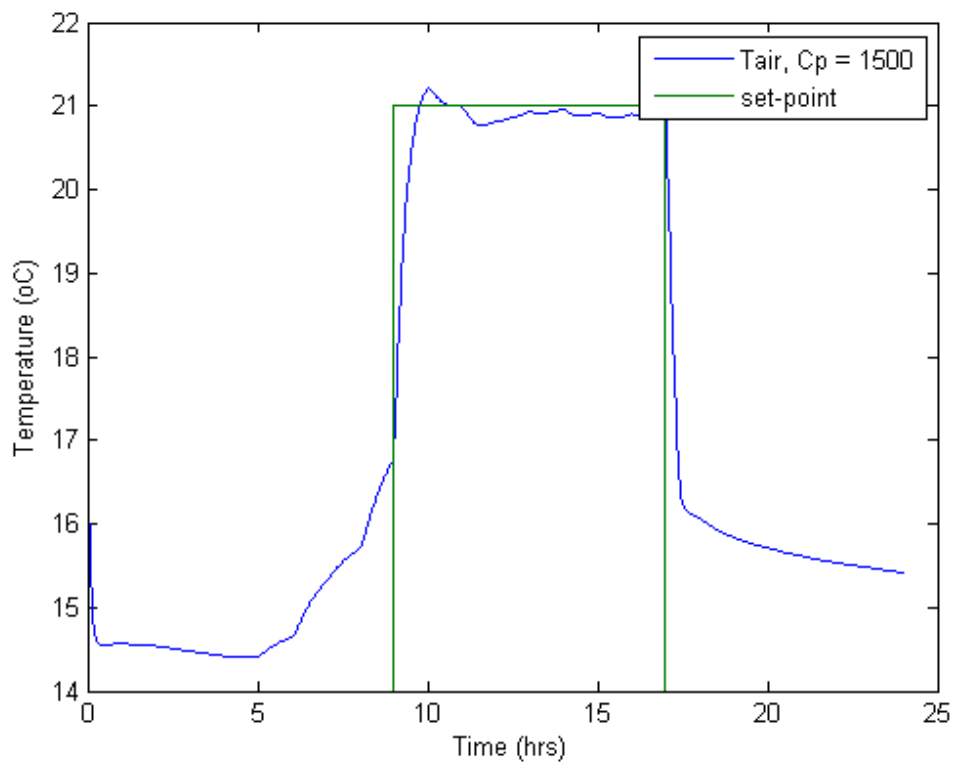
Hence increasing thermal mass does have affect on air temperature response however at the cost of increased energy consumption. Where the U_{trim} equation states that instead if you insulate the building and have fast response cooling is more cost effective. The results are as follows:



a) $C_p = 400$



b) $C_p = 800$



c) $C_p = 1500$

Figure 65: Effect of thermal mass on tracking air temperature a) 400 b) 800 c) 1500 (J/kgK).

With increasing thermal mass as shown in the above figures the peak of air temperature is cut down which is caused by the high solar gain in comparison to values previous figure where the peak was very large. And as the thermal mass is increased further the effect of solar gain is completely removed and the air temperature set point is being tracked accurately. However, increasing the thermal mass further leads to poor energy performance.

5.3.4 Conclusions

Stability of air temperature with fast actuation heating system is very simple. The asymptotes are a function of the air thermal properties only. The reason is that the fast heating system is taken as a convector heater which only has a direct impact on the air temperature.

The transmission zeros are both in the left half plane and thus stable. Interestingly they are a function of properties that are constants and thus will always remain stable. In this case they are not a function of operating conditions such as outside temperature, but are a function of thermal properties; area, mass and thermal capacitance and U values of the internal and external thermal mass.

The U_{trim} equation which determines the reachability of air temperature control is sensitive to casual gains with highly insulated building (i.e. low U values) and using thermal mass helps in damping the air temperature for easier control depending on the U value. However as discussed earlier, air temperature stability doesn't depend on thermal mass and having an efficient heating and cooling system is more important. This is not to say that thermal mass is useless and shouldn't be used in buildings because further analysis shows that thermal mass is very important to controllability as will be illustrated in the next case study.

Hence from the analysis so far it can be concluded that for air temperature reachability:

1. If insulation on the internal side of the wall is very high then any amount of thermal mass will have no effect.
2. If insulation on the internal side of the wall is low then it all depends on the amount of thermal mass in the wall:
 - a. If thermal mass is very little then it will NOT have any effect on air temperature response because it will reach steady state very quickly.
 - b. If thermal mass is very high then it will NOT have any effect on air temperature because the thermal mass will be near steady state most of the time.

Hence the fundamental conclusion about air temperature control reachability is that:

Using low internal insulation, the thermal mass of the wall has no effect on air temperature reachability providing there is enough thermal mass available for the wall temperature to be near steady state. If the amount of thermal mass in the wall is moderate then it will affect the air temperature reachability because its temperature will be dynamic and cannot be assumed steady state.

This leads to the next section on controllability with comfort temperature control.

NOTE: There is a difference between air temperature control and comfort temperature control as explained at the start of chapter 1.

5.4 Simplified Controllability of Comfort temperature for Systems with Fast Actuation (Convective heater)

In chapter 1 as discussed, the thermal comfort is a function of three temperatures, 1) internal air, 2) external thermal mass & 3) internal thermal mass (i.e. air temperature plus mean radiant temperature). In the previous section air temperature alone was controlled in a zone and its controllability was assessed. In this section controllability of comfort temperature is analysed.

In this section the control system feedback temperature is the measured comfort temperature level given by the following equation: $T_{cm} = k_a T_a + k_w T_w + k_m T_m$.

So the C matrix in the state space model is given as follows:

$$C = (c_{11} \quad c_{12} \quad c_{13}) \quad (5.164)$$

5.4.1 Stability

The stability of comfort temperature control is given by:

$$CB = \left(\frac{k_a}{\rho_a V_a c_{pa}} \right) \quad (5.165)$$

$$s = -g_{0 \rightarrow \infty} \frac{k_a}{\rho_a V_a c_{pa}} (\sigma) \quad (5.166)$$

The asymptote of comfort temperature control is still negatively aligned as its position on the negative real axis is determined by the fraction of air temperature contribution to the comfort temperature, k_a . The bigger the percentage of air temperature affecting comfort temperature the further the pole position will be on the negative real axis resulting in a more accurate transient first order response.

Here it is interesting to note that by controlling comfort temperature the asymptotes are unaffected and are not a function of the thermal mass. This goes back to the discussion in the first case study that because there is no lag in transferring heat to the air the thermal mass of the structure has no effect on the asymptote.

The second stability property, transmission zeros, of this case are given by the following determinant:

$$TZ = \det \begin{vmatrix} a_{11} - s & a_{12} & a_{13} & b_{11} \\ a_{21} & a_{22} - s & 0 & 0 \\ a_{31} & 0 & a_{33} - s & 0 \\ c_{11} & c_{12} & c_{13} & 0 \end{vmatrix} = 0 \quad (5.167)$$

The definition of environmental (Comfort) temperature is given by CIBSE Guide A as follows:

$$T_{cm} = \frac{1}{3}T_a + \frac{2}{3}T_r, \quad T_r = \frac{T_w + T_m}{2} \Rightarrow T_{cm} = \frac{1}{3}T_a + \frac{1}{3}T_w + \frac{1}{3}T_m \quad (5.168)$$

$$k_a = k_w = k_m = 1/3 \Rightarrow c_{11} = c_{12} = c_{13} = 1/3 \quad (5.169)$$

And given that $a_{31} = -a_{33}$

Solving the determinant gives the following equation:

$$s^2 + (a_{21} - a_{22} - 2a_{33})s + a_{33}(2a_{22} - a_{21}) = 0 \quad (5.170)$$

$$a_{21} = \left(\frac{2U_{wi}A_w}{\rho_w V_w c_{pw}} \right), \quad a_{22} = -2 \left(\frac{U_{wo}A_w + U_{wi}A_w}{\rho_w V_w c_{pw}} \right), \quad a_{33} = - \left(\frac{U_m A_m}{\rho_m V_m c_{pm}} \right) \quad (5.171)$$

Substituting the constants above gives the follow determinant equation:

$$s^2 + \left(\frac{2U_{wi}A_w}{\rho_w V_w c_{pw}} + 2 \left(\frac{U_{wo}A_w + U_{wi}A_w}{\rho_w V_w c_{pw}} \right) + 2 \left(\frac{U_m A_m}{\rho_m V_m c_{pm}} \right) \right) s + \left(\frac{U_m A_m}{\rho_m V_m c_{pm}} \right) \left(4 \left(\frac{U_{wo}A_w + U_{wi}A_w}{\rho_w V_w c_{pw}} \right) + \left(\frac{2U_{wi}A_w}{\rho_w V_w c_{pw}} \right) \right) = 0 \quad (5.172)$$

$$s^2 + \left(\left(\frac{2U_m A_m}{\rho_m V_m c_{pm}} \right) + \left(\frac{2U_{wo}A_w + 4U_{wi}A_w}{\rho_w V_w c_{pw}} \right) \right) s + \left(\frac{U_m A_m}{\rho_m V_m c_{pm}} \right) \left(\frac{4U_{wo}A_w + 6U_{wi}A_w}{\rho_w V_w c_{pw}} \right) = 0 \quad (5.173)$$

The above equation can be expressed as a quadratic equation of the form:

$as^2 + bs + c = 0$, where:

$$a = 1, \quad b = \left(\frac{2U_m A_m}{\rho_m V_m c_{pm}} \right) + \left(\frac{2U_{wo}A_w + 4U_{wi}A_w}{\rho_w V_w c_{pw}} \right), \quad c = \left(\frac{U_m A_m}{\rho_m V_m c_{pm}} \right) \left(\frac{4U_{wo}A_w + 6U_{wi}A_w}{\rho_w V_w c_{pw}} \right)$$

The value of s is given by: $s = \frac{-b \pm \sqrt{b^2 - 4ac}}{2a} \Rightarrow s = \frac{-b \pm \sqrt{b^2 - 4c}}{2}$

Thus the transmission zeros are:

$$s_1 = \frac{-b - \sqrt{b^2 - 4c}}{2}, \text{ for this transmission zero to be stable i.e. negative, } b^2 \geq 4c$$

$$s_2 = \frac{-b + \sqrt{b^2 - 4c}}{2}, \text{ for this transmission zero to be stable, } \sqrt{b^2 - 4c} \leq b$$

However in the case that $\sqrt{b^2 - 4c} = b$ then $s_2=0$, i.e. there will be a transmission at the origin, which will exhibit oscillatory response of the thermal mass temperature.

For the standard case with the values given in appendix 10, it is estimated that in the quadratic equation, b^2 will be about 1.5 times higher than $4c$. In reality the parameters of the building don't vary that much from the values given in appendix 11 which are the standard SAP values for modern dwellings, **it can be safely said that the transmission zeros will always be stable for comfort temperature control.**

5.4.2 Reachability

The reachability criterion equation U_{trim} is given as follows:

$$u_{trim}(s) = \left[-(CB)^{-1} CAX(s) - (CB)^{-1} (CF)d(s) \right] \quad (5.174)$$

$$u_{trim}(s) = \left[\begin{array}{c} -\frac{1}{b_{11}}(k_a \quad k_w \quad k_m) \begin{pmatrix} a_{11} & a_{12} & a_{13} \\ a_{21} & a_{22} & 0 \\ a_{31} & 0 & a_{33} \end{pmatrix} \begin{pmatrix} T_a(s) \\ T_w(s) \\ T_m(s) \end{pmatrix} \\ -\frac{1}{b_{11}}(k_a \quad k_w \quad k_m) \begin{pmatrix} f_{11} & f_{12} & f_{13} & f_{14} & f_{15} & 0 & f_{17} \\ f_{21} & 0 & 0 & 0 & 0 & f_{26} & 0 \\ f_{31} & 0 & 0 & 0 & 0 & 0 & 0 \end{pmatrix} \begin{pmatrix} I_{dr}(s) \\ P_L(s) \\ \dot{Q}_{oc}(s) \\ \dot{Q}_{ap}(s) \\ T_o(s) \\ T_{sa}(s) \\ n(s) \end{pmatrix} \end{array} \right] \quad (5.175)$$

As given earlier, $k_a=k_w=k_m$, thus for simplification these constants will be taken as k_c .

$$u_{trim}(s) = \left[\begin{array}{c} -\frac{1}{b_{11}}(k_c \quad k_c \quad k_c) \begin{pmatrix} a_{11} & a_{12} & a_{13} \\ a_{21} & a_{22} & 0 \\ a_{31} & 0 & a_{33} \end{pmatrix} \begin{pmatrix} T_a(s) \\ T_w(s) \\ T_m(s) \end{pmatrix} \\ -\frac{1}{b_{11}}(k_c \quad k_c \quad k_c) \begin{pmatrix} f_{11} & f_{12} & f_{13} & f_{14} & f_{15} & 0 & f_{17} \\ f_{21} & 0 & 0 & 0 & 0 & f_{26} & 0 \\ f_{31} & 0 & 0 & 0 & 0 & 0 & 0 \end{pmatrix} \begin{pmatrix} I_{dr}(s) \\ P_L(s) \\ \dot{Q}_{oc}(s) \\ \dot{Q}_{ap}(s) \\ T_o(s) \\ T_{sa}(s) \\ n(s) \end{pmatrix} \end{array} \right] \quad (5.176)$$

Multiplying out the brackets further simplification gives:

$$\mathbf{u}_{trim}(s) = \begin{bmatrix} -\frac{1}{b_{11}} \begin{pmatrix} k_c(a_{11} + a_{21} + a_{31}) & k_c(a_{12} + a_{22}) & k_c(a_{13} + a_{33}) \end{pmatrix} \begin{pmatrix} T_a(s) \\ T_w(s) \\ T_m(s) \end{pmatrix} \\ -\frac{1}{b_{11}} \begin{pmatrix} k_c(f_{11} + f_{21} + f_{31}) & k_c f_{12} & k_c f_{13} & k_c f_{14} & k_c f_{15} & k_c f_{26} & k_c f_{17} \end{pmatrix} \begin{pmatrix} I_{dr}(s) \\ P_L(s) \\ \dot{Q}_{oc}(s) \\ \dot{Q}_{ap}(s) \\ T_o(s) \\ T_{sa}(s) \\ n(s) \end{pmatrix} \end{bmatrix} \quad (5.177)$$

$$\mathbf{u}_{trim}(s) = -\frac{1}{b_{11}} k_c \begin{bmatrix} (a_{11} + a_{21} + a_{31})T_a(s) + (a_{12} + a_{22})T_w(s) + (a_{13} + a_{33})T_m(s) \\ (f_{11} + f_{21} + f_{31})I_{dr}(s) + f_{12}P_L(s) + f_{13}\dot{Q}_{oc}(s) + f_{14}\dot{Q}_{ap}(s) \\ f_{15}T_o(s) + f_{26}T_{sa}(s) + f_{17}n(s) \end{bmatrix} \quad (5.178)$$

Substituting the building parameters corresponding to the constants gives the following \mathbf{U}_{trim} for comfort temperature control:

$$\mathbf{u}_{trim}(s) = \begin{bmatrix} \left(\frac{1}{\rho_a V_a c_{pa}} (-2U_{wi}A_w - U_{win}A_{win} - U_m A_m - V_a \rho_a c_{pa} \bar{n}) + \left(\frac{2U_{wi}A_w}{\rho_w V_w c_{pw}} \right) + \left(\frac{U_m A_m}{\rho_m V_m c_{pm}} \right) \right) T_a(s) \\ + \left(\left(\frac{2U_{wi}A_w}{\rho_a V_a c_{pa}} \right) + \left(\frac{-2U_{wo}A_w - 2U_{wi}A_w}{\rho_w V_w c_{pw}} \right) \right) T_w(s) + \left(\left(\frac{U_m A_m}{\rho_a V_a c_{pa}} \right) + \left(\frac{-U_m A_m}{\rho_m V_m c_{pm}} \right) \right) T_m(s) \\ -\frac{1}{b_{11}} k_c + \left(\left(\frac{\alpha_a \sigma_s A_{win}}{\rho_a V_a c_{pa}} \right) + \left(\frac{\alpha_w \sigma_s A_{win}}{\rho_w V_w c_{pw}} \right) + \left(\frac{\alpha_m \sigma_s A_{win}}{\rho_m V_m c_{pm}} \right) \right) I_{dr}(s) + \left(\frac{k_e}{\rho_a V_a c_{pa}} \right) P_L(s) \\ + \left(\frac{1}{\rho_a V_a c_{pa}} \right) \dot{Q}_{oc}(s) + \left(\frac{1}{\rho_a V_a c_{pa}} \right) \dot{Q}_{ap}(s) + \frac{1}{\rho_a V_a c_{pa}} (U_{win}A_{win} + V_a \rho_a c_{pa} \bar{n}) T_o(s) \\ + \left(\frac{2U_{wo}A_w}{\rho_w V_w c_{pw}} \right) T_{sa}(s) + (\bar{T}_o - \bar{T}_a) n(s) \end{bmatrix} \quad (5.179)$$

The above equation shows that because of controlling comfort temperature rather than air temperature the reachability equation is now a function of the internal and external thermal mass. The simulation results confirm this that by varying the internal and external thermal mass the reachability of comfort temperature is affected. Consider the same case as above. A 3kW heater is used for heating a 5 m³ zone, with an external temperature profile as shown in the figure below. The response of air temperature is very fast and accurate. With the same setting the response of comfort temperature is as follows:

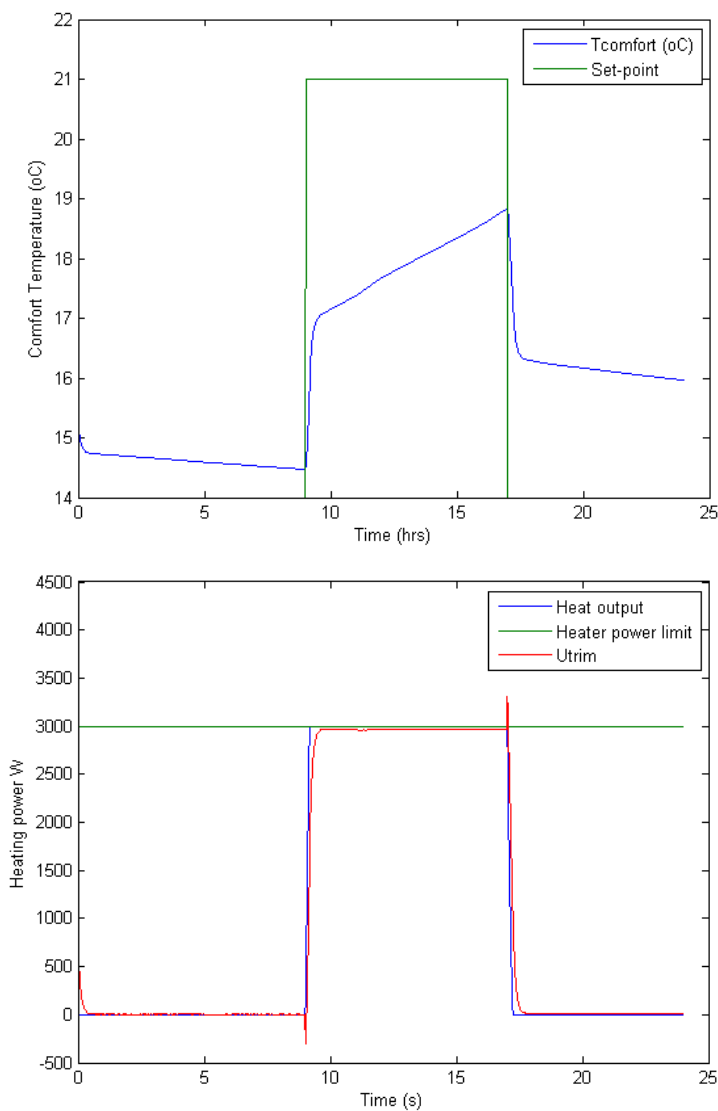


Figure 66: Comfort Temperature response to step change in set-point (top) & power output from the heater and U_{trim} plot (bottom) with 3 kW heater

As can be seen from the above figures the comfort temperature was not able to reach set-point. The reason for this is that due to the damping of the thermal mass the comfort temperature is very slowly varying. As can be seen from the bottom plot, that the energy required for reaching set point is also a lot more compare to when controlling the air temperature. This is because the internal and external thermal masses also need to be heated up as their temperatures are a function of the comfort temperature. A lot of heat energy is required to change their temperature. These results confirm the symbolic analysis in the first case study where it was shown that for effective controlling it is better to use a radiant system for comfort temperature rather than completely convective heater. The reason is shown in the previous plot that with convector heater it takes a lot of time absorb the heat from the air into thermal masses to raise their temperature for influencing the comfort temperature. Thus it is recommended to use a radiant heater with comfort temperature as this have a faster control on the comfort temperature.

The previous figure also shows that the U_{trim} is exactly following the heater output. This is because the rate of change of comfort temperature is very small thus U_{trim} is almost equal to u_a . This means that the comfort temperature reachability is guaranteed provided there is a high rated heating system need for heating thermal mass i.e. radiant heater. This is shown in the next figure, as the power limits of the heater are increased the temperature is able to reach set-point.

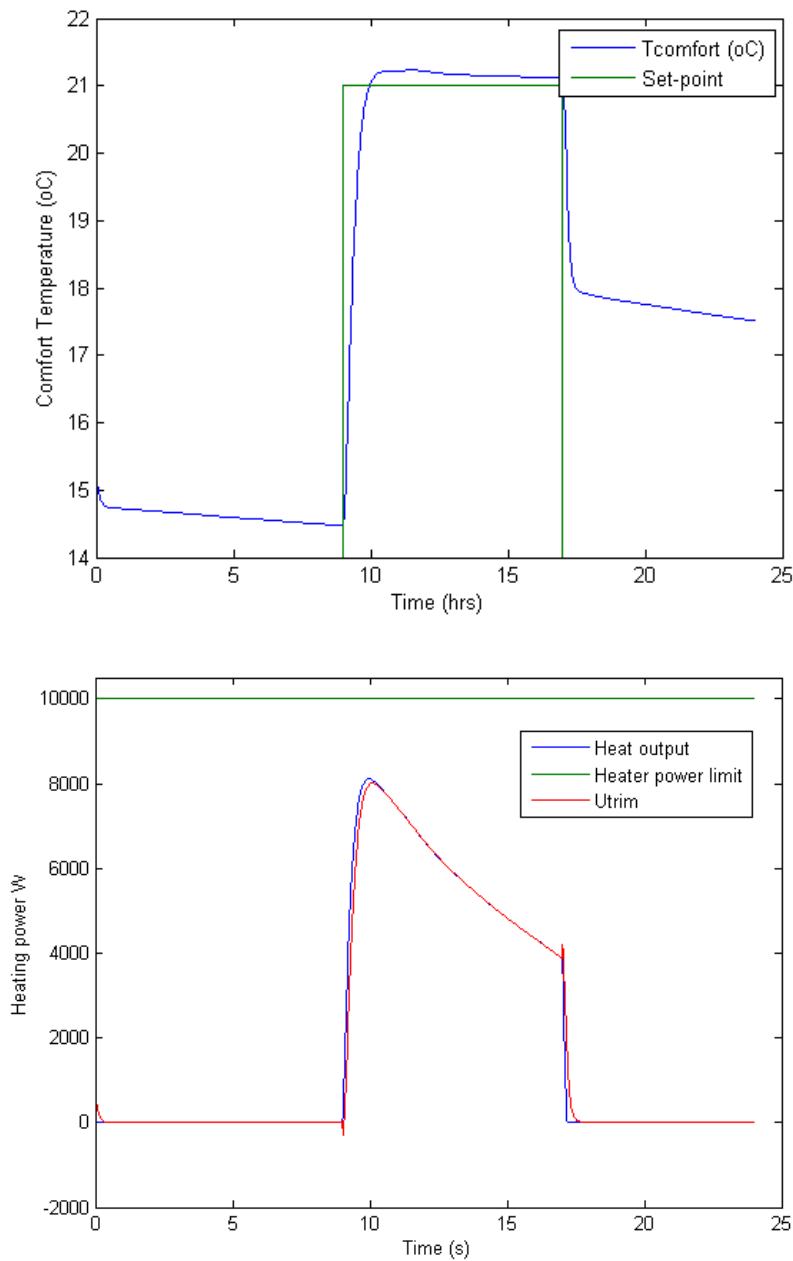


Figure 67: Comfort Temperature response with a 10 kW heating system

As can be seen from the above figure with a higher rated heating system the control system is able to reach the comfort temperature set-point. These results obviously suggest that comfort temperature require more energy for reachability than air temperature with a purely convective heater. **But does the amount thermal mass matter when controlling comfort temperature with convector heater?**

It is shown below that by varying the amount of thermal mass in the wall structure the reachability of **comfort temperature** is **NOT** affected significantly when using a convector heater.

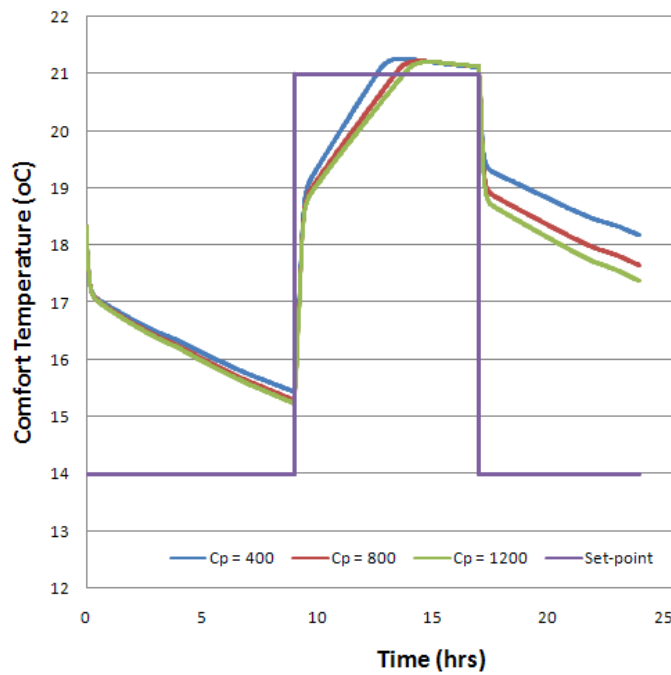


Figure 68: Comfort temperature response with varying thermal mass

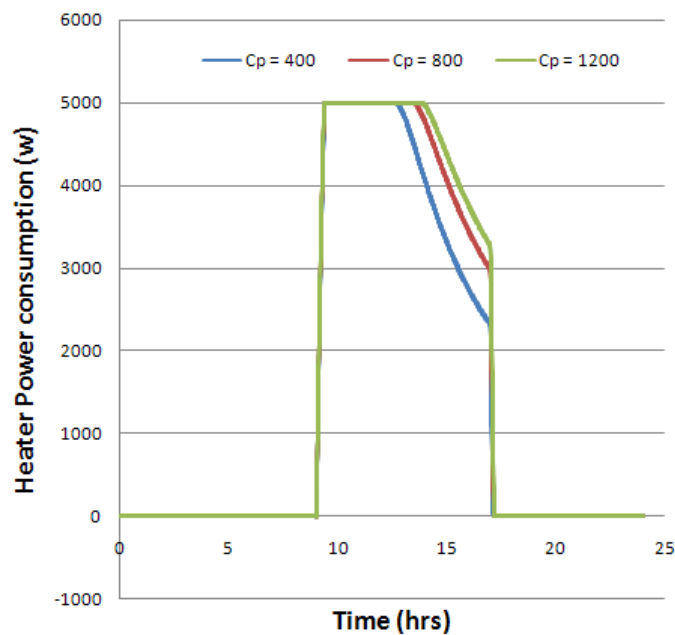


Figure 69 Heating power consumed for different Cp values of the wall

The results clearly show that because the convector heater is only affecting air temperature in the comfort equation then varying thermal mass has little impact on reachability. The thermal mass temperature is pretty much steady state and adding more thermal mass does not affect the value of comfort temperature as long as convector heater is used. This is because the thermal mass is not heated directly by the convector heater.

5.4.3 Conclusions

The stability of comfort temperature is not any different from air temperature control because of using convector heater which only affects the air temperature. The asymptotes are stable and are function of the thermal mass of air, same as in the previous case study. The transmission zeros are complex because of the comfort temperature feedback control however as discussed they are stable.

In the reachability of air temperature (equation 5.162) the U value was important but in this case study the reachability of comfort temperature (equation 5.179) is a lot more complex and **is a function of the thermal mass** of external and internal structure i.e. wall and furniture. The reason for this is that comfort temperature is a function of wall, furniture and air temperatures.

How it is important that the designer selects the correct actuator system depending on the variable being controlled. As shown in this case study controlling comfort temperature with a convector heater is not recommended as it only influences the air temperature term in the comfort equation. Hence changing the thermal mass properties of the wall has no effect on reachability as convector heater has no direct link to the wall and furniture temperatures through radiant component. The convector heater has fast actuation but having no radiant component results in a slow system as it has to heat the air and then the heat in the air through convection goes into the wall thermal mass.

This is one of the reasons why the conventional radiator is successful as it is able to provide both convective and radiative components of heat transfer and thus has a direct effect on the air and thermal mass temperature. Hence the radiator is able to provide better reachability of comfort temperature as long as it is exposed to the walls and internal thermal mass and air.

Thus using a radiator system is the better solution to controllability of comfort temperature than convector heater. With a radiator system the mathematical model changes and thus the controllability also changes. This is shown as follows:

5.5 Simplified Controllability of Comfort temperature control with a conventional Radiator

For this case study the state space matrices and the symbolic coefficients are given in appendix. For the air temperature control the state space was given as follows:

$$A = \begin{pmatrix} a_{11} & a_{12} & a_{13} \\ a_{21} & a_{22} & 0 \\ a_{31} & 0 & a_{33} \end{pmatrix} B = \begin{pmatrix} b_{11} \\ 0 \\ 0 \end{pmatrix} F = \begin{pmatrix} f_{11} & f_{12} & f_{13} & f_{14} & f_{15} & 0 & f_{17} \\ f_{21} & 0 & 0 & 0 & 0 & f_{26} & 0 \\ f_{31} & 0 & 0 & 0 & 0 & 0 & 0 \end{pmatrix} \quad (5.180)$$

However if assumed a conventional radiator then the component of heat from radiator Q_p will have three components, i.e. air, internal mass and external mass each taking a share from the Q_p . Thus the B matrix will change and the rest of the system will remain the same and hence the new state space form is given as follows:

$$A = \begin{pmatrix} a_{11} & a_{12} & a_{13} \\ a_{21} & a_{22} & 0 \\ a_{31} & 0 & a_{33} \end{pmatrix} B = \begin{pmatrix} b_{11} \\ b_{21} \\ b_{31} \end{pmatrix} F = \begin{pmatrix} f_{11} & f_{12} & f_{13} & f_{14} & f_{15} & 0 & f_{17} \\ f_{21} & 0 & 0 & 0 & 0 & f_{26} & 0 \\ f_{31} & 0 & 0 & 0 & 0 & 0 & 0 \end{pmatrix} \quad (5.181)$$

$$C = (c_{11} \quad c_{12} \quad c_{13})$$

5.5.1 Stability

In the previous case study for air temperature feedback it is given as follows:

$$CB = \left(\frac{k_a}{\rho_a V_a c_{pa}} \right) \quad (5.182)$$

With the following asymptote:

$$s = -g_{0 \rightarrow \infty} \frac{k_a}{\rho_a V_a c_{pa}} (\sigma) \quad (5.183)$$

However with comfort temperature control with radiator the CB matrix is given as follows:

$$CB = (c_{11}b_{11} + c_{12}b_{21} + c_{13}b_{31}) = \left(\frac{c_{11}k_a}{\rho_a V_a c_{pa}} + \frac{c_{12}k_b}{\rho_w V_w c_{pw}} + \frac{c_{13}k_c}{\rho_m V_m c_{pm}} \right) \quad (5.184)$$

With the following asymptote:

$$s = -g_{0 \rightarrow \infty} \left(\frac{c_{11}k_a}{\rho_a V_a c_{pa}} + \frac{c_{12}k_b}{\rho_w V_w c_{pw}} + \frac{c_{13}k_c}{\rho_m V_m c_{pm}} \right) (\sigma) \quad (5.185)$$

In this case the asymptote is stable and the asymptotic stability is dependent on the thermal mass of air, wall and furniture because of using a radiator having both convective and radiant components. Although the asymptote for this system will never go unstable as it is a function of building parameters that are constant in reality. It is also clear that this asymptote is aligned along the negative real axis of the root locus and thus will result in a response close to the ISR.

The transmission zeros are given by the following determinant matrix:

$$TZ = \det \begin{vmatrix} a_{11} - s & a_{12} & a_{13} & b_{11} \\ a_{21} & a_{22} - s & 0 & b_{21} \\ a_{31} & 0 & a_{33} - s & b_{31} \\ c_{11} & c_{12} & c_{13} & 0 \end{vmatrix} = 0 \quad (5.186)$$

Symbolically the determinant equation is given as follows:

$$\begin{aligned} & -(a_{11} - s)(a_{22} - s)c_{13}b_{31} - (a_{11} - s)(a_{33} - s)(b_{21}c_{12} + b_{11}c_{11}) \\ & + (a_{33} - s)(a_{12}b_{21}c_{11} + b_{11}a_{21}c_{11}) + (a_{22} - s)(a_{13}b_{31}c_{11} + b_{11}a_{31}c_{13}) \\ & + (a_{21}b_{31} + b_{21}a_{31})(a_{12}c_{13} + a_{12}c_{12}) = 0 \end{aligned} \quad (5.187)$$

This is very difficult to solve for its roots symbolically hence numerically the results are given as follows:

$$TZ = \det \begin{vmatrix} -0.00296 - s & 0.000428 & 0.0023 & 0.0000019 \\ 0.0000023 & -0.0000046 - s & 0 & 0.00000001 \\ 0.000032 & 0 & -0.000032 - s & 0.000000036 \\ 0.33 & 0.33 & 0.33 & 0 \end{vmatrix} = 0 \quad (5.188)$$

By solving this determinant in Matlab the transmission zeros are given as follows:

$$s_1 = -0.0000064 \quad s_2 = -0.0001778 \quad (5.189)$$

There are two transmission zeros corresponding to the internal and external masses. They are both negative real and hence stable, hence they aligned with the negative real axis of the root locus. Overall control of comfort temperature with a radiator is stable.

5.5.2 Reachability

The reachability criterion equation U_{trim} is given as follows:

$$u_{trim}(s) = \left[\begin{aligned} & \left(\frac{1}{\rho_a V_a c_{pa}} (-2U_{wi} A_w - U_{win} A_{win} - U_m A_m - V_a \rho_a c_{pa} \bar{n}) + \left(\frac{2U_{wi} A_w}{\rho_w V_w c_{pw}} \right) + \left(\frac{U_m A_m}{\rho_m V_m c_{pm}} \right) \right) T_a(s) \\ & + \left(\left(\frac{2U_{wi} A_w}{\rho_a V_a c_{pa}} \right) + \left(\frac{-2U_{wo} A_w - 2U_{wi} A_w}{\rho_w V_w c_{pw}} \right) \right) T_w(s) + \left(\left(\frac{U_m A_m}{\rho_a V_a c_{pa}} \right) + \left(\frac{-U_m A_m}{\rho_m V_m c_{pm}} \right) \right) T_m(s) \\ & - (cb)^{-1} k_{cm} + \left(\left(\frac{\alpha_a \sigma_s A_{win}}{\rho_a V_a c_{pa}} \right) + \left(\frac{\alpha_w \sigma_s A_{win}}{\rho_w V_w c_{pw}} \right) + \left(\frac{\alpha_m \sigma_s A_{win}}{\rho_m V_m c_{pm}} \right) \right) I_{dr}(s) + \left(\frac{k_e}{\rho_a V_a c_{pa}} \right) P_L(s) \\ & + \left(\frac{1}{\rho_a V_a c_{pa}} \right) \dot{Q}_{oc}(s) + \left(\frac{1}{\rho_a V_a c_{pa}} \right) \dot{Q}_{ap}(s) + \frac{1}{\rho_a V_a c_{pa}} (U_{win} A_{win} + V_a \rho_a c_{pa} \bar{n}) T_o(s) \\ & + \left(\frac{2U_{wo} A_w}{\rho_w V_w c_{pw}} \right) T_{sa}(s) + (\bar{T}_o - \bar{T}_a) n(s) \end{aligned} \right] \quad (5.190)$$

$$\text{Where: } (cb)^{-1} = \frac{\rho_a V_a c_{pa} \rho_w V_w c_{pw} \rho_m V_m c_{pm}}{c_{11} k_a \rho_w V_w c_{pw} \rho_m V_m c_{pm} + c_{12} k_b \rho_a V_a c_{pa} \rho_m V_m c_{pm} + c_{13} k_c \rho_a V_a c_{pa} \rho_w V_w c_{pw}}$$

The U_{trim} equation (5.190) (above) clearly shows that the reachability of comfort temperature with a radiator **IS A FUNCTION OF THERMAL MASS** OF WALLS, FURNITURE AND AIR.

This result is the same as the previous case study however here the difference is in the $(CB)^{-1}$ matrix which is now a function of thermal mass of walls and furniture. Whereas in the previous case study the $(CB)^{-1}$ matrix was only a function of heat capacity of air. This is because in the previous case study a convector heater was being used and now a radiator is used with both convective as well as radiant components. Because of using a radiator and controlling comfort temperature the thermal mass of walls and furniture cannot be ignored. The dynamics of comfort temperature are close to the dynamics of thermal mass of walls and furniture; hence they are now IMPORTANT to reachability and cannot be set to steady state. **Thus, now the reachability of comfort temperature with radiator depends on the ability of the structure to store heat.** The simulation results confirm this as follows:

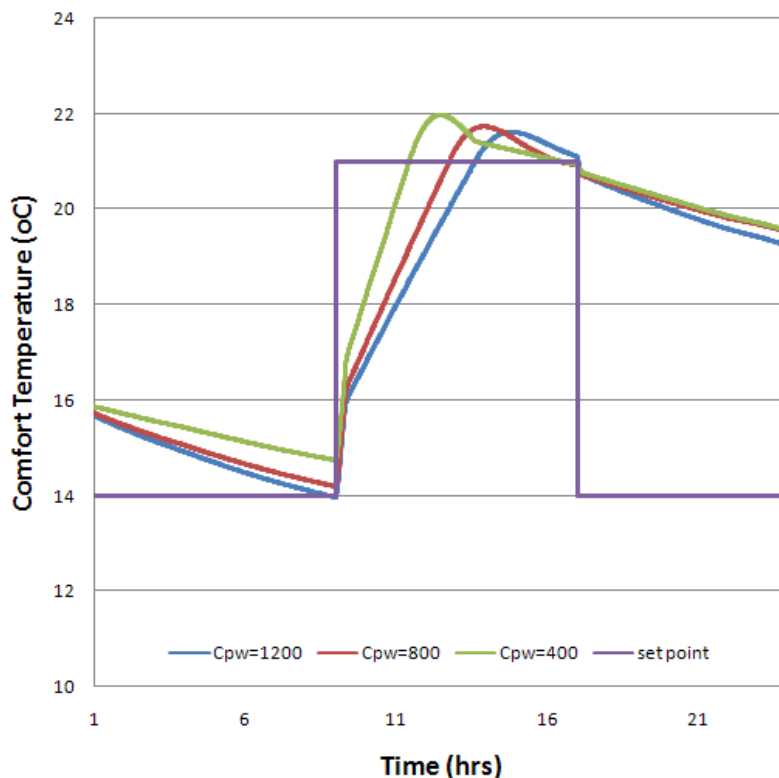


Figure 70: Comfort Temperature response to change in set point with varying the thermal mass of the wall

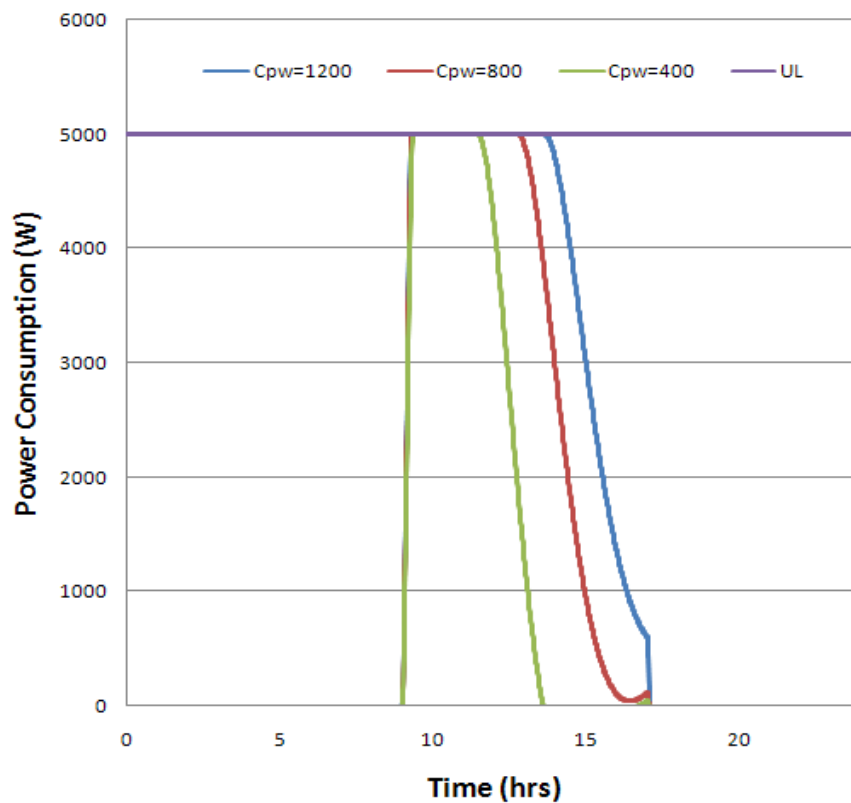


Figure 71: Radiator power consumption for comfort temperature control with varying the thermal mass of the wall

The results show that increasing the thermal mass has significant effect on the comfort temperature reachability and power consumption. As the thermal mass of the wall is increased the reachability becomes more and more difficult and the power consumption also increases.

5.5.3 Conclusions

The stability of the comfort temperature depends on the thermal mass of the air, walls and furniture. The asymptotes and transmission zeros are very complex and are a function of the thermal mass properties of the walls, furniture and air. However they are permanently stable and thus do not need further analysis.

The reachability is also complex when using a radiator to control comfort temperature. The comfort temperature dynamics are strongly coupled with the dynamics of the thermal masses. This is the reason why the thermal masses cannot be assumed steady state and hence reachability is a function of thermal mass and not just the U value as was the case with controlling air temperature. The analysis shows that the ability of the structure to store heat becomes very important when the comfort temperature is controlled because its time constant is close to the time constant of the walls and furniture.

The designer can use the U_{trim} equation (5.190) to calculate reachability of comfort temperature with a radiator. The sensitivity of thermal mass with other building parameters in the equation can be investigated to satisfy the reachability criteria.

Hence in general it can also be shown that U_{trim} can also be used to design operational reachability band of buildings for assessment of overheating and need for cooling based on the comfort criteria and building parameters e.g. high or low thermal mass.

6 : Conclusions, industrial impact and further work



“The closer one gets to the top, the more one finds there is no "top"” Nancy Barcus

6.1 Conclusions

In the first case study a slow heating system (under floor heating) was used for controlling air temperature and the stability of such a system was assessed. It was found that such a system is not stable and requires extra measurements. It was found that measuring air plus its rate of change, makes the system stable for achieving the Ideal System Response. This measurement was particularly used because it also satisfied the tracking of the system. Trackability requires that what is measured and feedback to create the error signal approaches the desired output $y(t)$ in steady state. It was also found that this measurement made the system more complex in terms of controller design as a very slow system was being used to control a fast variable with fast disturbances. A better solution was shown to be controlling comfort temperature which is slowly varying and is not quickly affected by the disturbances to air temperature through mechanical ventilation. Comfort temperature being also a function of the temperature of thermal mass is slowly varying and thus easier for a slow heating system to respond to necessary changes in time. The lighting and CO₂ control channels were less coupled when controlling comfort temperature, due to the slowly varying nature of the cross coupling.

In the second case study a fast heating system (convector heater) was used for controlling air temperature and mechanical ventilation for humidity. Here the assessment Stability, Trackability and Reachability (STAR) were assessed symbolically. This stability of this system is not as complex as the slow actuation case as the control channels were less coupled and operating at similar bandwidths (i.e. speed of response). The trackability was also simpler as no extra sensor measurements were required. The reachability was very complex and symbolic analysis was performed to derive the expression of U_{trim} in terms of building parameters. The reachability criteria for humidity control is very simple, however for temperature it was more complex. For air temperature control it was found that the reachability is dominated by the UA value of the wall and NOT it's thermal mass as the temperature of the walls is much slower to change than the air temperature. In many cases as shown in this thesis there will be sufficient thermal mass in the wall

to keep the wall temperature near steady state compared to the transient response of the air temperature. Thus, in most cases except extremely light weight structures the thermal mass will not be so important for determining the reachability of the air temperature and thus its controllability. It was also found that when the building is highly insulated (i.e. UA value is small) and the temperature difference between inside and outside is small then the reachability is depends on the magnitude of the casual gains.

In the case where the UA value is large (i.e. less internal insulation and more ability for the thermal mass to accept heat) and also inside temperature is close to the outside temperature for a long period of time, then in this case active cooling will be needed. This is because over time the thermal mass will be saturated with heat and there will be no temperature gradient for the heat to leave the room and hence active cooling would be required, especially if there are large casual and solar gains. In most cases the thermal mass will have a response time much greater than a day and thus it will not always passively cool during lower outside temperature periods e.g. at night. A proportion of stored heat will carry over to the next day and the mass acts as a storage heater to the point at which the required building air temperature can not be reached without active cooling. Thus, in spring and autumn thermal mass will help reduce cooling power required, however during sustained periods of high outside temperature the building will be out of control.

In the third case study humidity control was removed to simplify the controllability analysis of a buildings with a fast heating system for air temperature control ONLY. Stability and reachability of the system were assessed. The symbolic STaR results of the second case study were confirmed using dynamic simulation.

Fundamental conclusion was that:

When using low internal wall insulation, the thermal mass of the wall has no effect on air temperature reachability providing there is enough thermal mass available for the wall temperature to be near steady state. If the amount of thermal mass in the wall is moderate to low then it will affect the air

temperature reachability because its temperature will be dynamic and cannot be assumed steady state.

The fourth case study assessed the stability and reachability of comfort temperature with using convector heater. With a convector heater the response of the system is slow. Because comfort temperature is a function of air and mean radiant temperature. The convector heater has no effect on the mean radiant temperature and thus the system requires more energy to be injected in the air to see a change in the radiant temperature because it takes time for the heat in the air to convect into the mass. Over all this is a stable system. **The reachability of comfort temperature with convector heater is a function of the thermal mass of the wall and furniture. When heating and controlling the comfort temperature with a convector heater the effect of thermal mass on the reachability is negligible as shown in the results. However, further work is required to assess the impact of thermal mass on the reachability of comfort temperature in buildings which are naturally ventilated such as Climate Adaptive Cooling (i.e. no active cooling) during warmer months of the year. The symbolic tools presented in this thesis can be applied to such cases.**

The fifth case study is controlling comfort temperature with a conventional radiator which is more typical than using a convector. The radiator delivers heat as part convective and part radiant. This system is again stable, however this time the stability is a function of the stored thermal energy in the mass of the wall, the furniture and the zone's air. This also resulted in a complex reachability analysis which was so complex it prevented a symbolic solution being found, this is area for further work. **Fundamentally, when controlling comfort temperature with a radiator, THE THERMAL MASS IS VERY IMPORTANT TO REACHABILITY.** This was also confirmed with the simulation results which showed the dramatic impact of the thermal mass on the speed of response in the system. In the case of a building in warmer months with no cooling, then it is clear that the thermal mass will have an impact on the thermal comfort in the building and

the symbolic analysis tools presented in this case study can also be used in this case. This is also an area for further work.

Overall the results show that comfort temperature generally requires more energy than the air temperature control. The effect of thermal mass on controllability depends on the response of the heating system and the choice of controlling air or comfort temperatures. If air temperature is controlled then it is important to estimate the suitable amount of thermal mass in the wall that would prevent the wall temperature dynamics to affect air temperature control. If comfort temperature is controlled then thermal mass is very important because the dynamics of the thermal mass affect the dynamics of the comfort temperature. For fast and accurate control a convector heater is ideal for controlling air temperature and radiator for controlling comfort temperature.

It is shown in the case studies that the controllability science is equally applicable to buildings with heating and cooling, heating only and cooling only. The science determines the controllability of the system from the design of the building, its systems and sensors. The second and third case studies show and discuss how the reachability is assessed of buildings without conventional cooling. Also the effect of thermal mass internally has been discussed in detail in these case studies. In particular these two case studies have also shown that reachability is also a function of the solar and other casual gains. The science presented can be used by the designer to assess the impact of solar gains on reachability to be able to decide whether solar shading is required. The second and third case studies discuss this to an extent. In this thesis one of the aims was to investigate the impact of thermal mass in buildings, although this thesis has only shown case studies with heating, the theory is applicable to the cooling case also, with or without an active cooling system. Further work is required to assess the importance of solar shading with respect to the conclusions on thermal mass in this thesis. Fourth and fifth case studies also address the impact of mean radiant temperature when controlling comfort temperature in a building using convector and radiator heating systems.

Based on the results in this thesis the following conclusions are drawn about controllability of buildings:

6.2 Industrial Impact for Heating System Control

A question that has exercised industry thinking for a considerable time is how to improve the commissioning of systems and give the building occupier a system that not only operates correctly, but is energy efficient and easy to manage. Ideally the commissioning process should start at the design stage and remain a major focus throughout the construction phase of the building. In terms of controllability this is not the case and the majority of the time commissioning of the control systems is done after the building has been built, and there are no penalties for this in the building processes. Controllability problems can lead to high energy costs and ideally it should be taken into account during all the phases of the project — including design, system engineering, off-site testing and simulation, site testing, post-occupancy, and handover phases. From the aerospace industry it is known that this is carried out heavily at the conceptual design stage where maximum effort is done to get the design right, of course this is essential for pilot and passenger safety. The case studies presented in the thesis investigated the controllability of the three standard choices every designer faces when designing a building and its control system:

- 4) Design a building with high or low thermal mass?**
- 5) Use fast or a slow heating system?**
- 6) Control comfort temperature or air temperature?**

To understand the implications of these choices on the controllability of the building is presented in the thesis. Consideration of the fundamental physical dynamic processes in a notional building single zone has allowed mathematical models of an Adaptive Climatic Building to be constructed. These models were re-arranged in a form suitable for analysis using modern state space methods and then the control theory of ISR was utilised to assess the controllability of various systems. The results

from these case studies provide a unique insight into the performance of buildings and Advanced Control Systems.

Stability was identified as a prerequisite for controllability, and calculation of the value of the stability matrices and transmission zeros before a control system is considered, is essential to ensure stability in the system. The locations of the transmission zeros determine the internal stability of the system. There is not a problem from a stability point of view in buildings as they remain stable always providing actuator and sensor dynamics are fast compare to with the closed loop response i.e. bandwidth. In buildings they are function of density, volume, thermal capacity, surface area and U values of the structure i.e. walls, roof, floor and furniture. However these are fundamental parameters and by changing their values affect the position of the transmission zeros on the stability chart which can change the response of the building.

Majority of buildings utilise three fundamental building materials, timber (wood), brick and concrete. As the case studies showed that for plant systems with radiant heating component will radiate to internal furniture in the building as well as the internal side of the external wall. And also as shown in the last case study that fundamentally there are only two transmission zeros in a building, 1) internal thermal mass (furniture) 2) external thermal mass (walls). Hence homes with more furniture are going to be less responsive and will cost more to run. As with flat panel radiators 67% of heat is radiant and thus majority of the time the heating systems in the houses are heating up the furniture as they are located either behind a sofa or a bed or a table. Hence houses with little furniture or low thermal capacity furniture are less costly to run and are more responsive. Thus designers can use transmission zeros to determine the amount of thermal mass needed in the walls and type of furniture to shape the response of the building to match the specification at the conceptual design stage. Thus the closer the value of transmission zero is to the zero the slower the response of that furniture and higher the thermal capacity thus that furniture should cost more. This would also encourage buying of furniture made of renewable materials and with low thermal mass and higher transmission zero values. This also

leads to proposal for furniture of the future where phase change materials can be used in furniture to provide comfort heat on the spot. This type of furniture can change its response by change its thermal capacity based on the temperature in building.

Evaluation of the matrix $(CB)^{-1}$, and the relationship between the input and output has shown the extent of the cross coupling between the parameters in the system. The asymptotic analysis has shown the cross coupling which exists as a barrier to fast, non-interacting control. Any control system which is designed for this notional building must address the problem of this interaction. The stability matrix $CB+sD$ has shown that the asymptotes (i.e. infinite poles) can easily be obtained for the building if the parameters (material properties and dimensions etc) are known through simple controllability symbolic analysis. The stability matrices for the case studies presented earlier showed that the asymptotes are the function of the properties of the plant and the variable being controlled. For example with under floor heating the asymptote directions were a function of the thermal mass of the screed and air. It was found that operating fast systems such as mechanical ventilation with slow systems such as under-floor heating is a source of cross coupling between different control channels. Hence it is recommended that in practice for using MIMO building control system the plant systems are operated with closed-loop bandwidths well separated from each other as this will result in a decoupled system that will be controllable with simple controllers such as PID.

Fundamentally using a slow system such as under-floor heating for controlling air temperature is not recommended as shown in the first case study. This is not a controllable system however it can be made controllable by sensing air temperature plus its rate of change. In the case that mechanical ventilation is being used as shown in the first case study which has direct influence on the air temperature it is better to control comfort temperature which is less affected by the disturbances in the air temperature. Thus for slow heating systems it is recommended to control comfort temperature rather than air temperature. Slow heating systems are more stable with controlling comfort temperature than air temperature. On the other hand fast heating

systems such as warm air system are recommended for controlling air temperature. This is because they have a direct influence on air temperature. For fast acting radiant systems it is recommended to control comfort temperature as electric radiant systems have less influence on the air temperature. For wall panel radiators as shown in the last section of the third case study controlling air temperature yields low energy consumption and controlling comfort temperature yields high energy consumption. Thus for such plant systems (i.e. panel radiators) which have both convective and radiant components it is recommended to control comfort temperature but with dominant air temperature sensor. This will ensure that radiant component is taken into account but at the same time controlling air temperature will result in less energy consumption.

The calculation and derivation of the property of Inverse dynamics ' U_{trim} ' is essential to understanding the reachability of the system. With simple calculations by entering parameters in the U_{trim} equation can quickly allow designers to determine plant sizes. Another fundamental question that arises is when to control comfort or air temperature. As shown in the last case study this is shown by inspecting the U_{trim} equation symbolically, it has shown a deep insight into the various parameters affecting the response of air temperature and comfort temperature. Fundamentally it was found that thermal mass has no effect on the control of air temperature where as it has an effect on the control of comfort temperature. When the U_{trim} equation is derived for air temperature control only the thermal mass of air was the only important factor and thus using a warm air convector system is the best option for fast accurate response. On the other hand for controlling **comfort temperature (i.e. air plus mean radiant)** it is recommended to use a fast radiant system for ideal response. Actually a conventional radiator system is a good balance of the two requirements.

In reality people want to control their comfort temperature, not air temperature, so building and systems have to be designed such to satisfy that criteria in the most efficient way. Looking at the current situation, the current wet flat panel radiator system commonly used today is best, radiant and air borne system at the same time!

It full fills two separate functions. The radiant effect warms the internal mass, and warms the air that rises up through buoyancy. This is recommended to be the most efficient way of satisfying the comfort criteria.

Literature is full of implications on controlling thermal comfort. It is said that thermal comfort is very important to many work-related factors. It can affect the distraction levels of the workers, and in turn affect their performance and productivity of their work. Also, thermal discomfort has been known to lead to Sick Building Syndrome symptoms. The US EPA BASE study found that higher indoor temperatures, even within the recommended thermal comfort range, increased worker symptoms. The occurrence of symptoms increased much more with raised indoor temperatures in the winter than in the summer due to the larger difference created between indoor and outdoor temperatures. On top of all this fundamentally it must be acknowledged that to satisfy the comfort criteria of a zone with many people is very difficult. Hence it is recommended not to control comfort temperature as it is expensive and difficult to control. Instead it is recommended that the ideal, most sustainable and energy efficient solution is to control air temperature to a standard set point which is a measure of good comfort based on PPD & PMV (24°C suggested by BCO 2009) and on top of that people who are not satisfied can manage their own comfort temperature through their clothing. This recommendation is in agreement with BCO (2009). Now, how to control air temperature and what systems to use and what should be the control strategy whether to use high or low thermal mass? The following question answers these questions:

What is the point of heating a room that you don't use most of the day?

The solution recommended is to design highly insulated homes/buildings with minimum thermal mass using fast warm air electric heater systems i.e. Control Volume and Variable Temperature CVVT system to control air temperature. These systems are commonly used in hotels at the moment such as Travel Lodge or Premier Inn and are highly effective. The control strategy is very simple; each room has its own heater with a feedback control system using an air temperature sensor situation

on the other side of the room. For commercial building and open plan offices variable volume variable temperature VVVT systems are recommended that can be installed in the roof. These systems are fast and controllable as they can directly heat the air before blowing the air into the zone and can be powered by heat pumps, wind energy and solar, thus making them sustainable.

As the building and construction industry adapts to meet the new challenges it faces, there has been an increase in early multi-disciplinary work on projects. No longer can the designer simply design the building and pass it on to the engineer to fit the environmental services around the design. Holistic, integrated design at all stages of a building's life cycle is now recognised as a fundamental requirement to ensure that buildings are fit for purpose, and meet the requirements of occupant health and comfort, reduced energy footprints and lower emissions.

Lastly, the Control Theory was developed to design feedback controllers that remove uncertainty to poor prediction where as modelling was developed to improve prediction. For the purposes of feedback control highly accurate models are desired. However, such accuracy often requires that complicated high order models be used, which in turn lead to more difficult control design problems from both an engineering and a computational perspective. In high technology disciplines such as aerospace, emphasis is on the development of methods for reducing the size and complexity of the model while retaining the essential features of the system description. Their aim is to find a simplified system model which describes the physical system accurately enough so that controllers designed based on this simplified model perform well when implemented on the real system [(Doyle, 1997)].

In this context, the science presented in this thesis for analysing controllability of building systems is particularly suitable. By allowing controllability and performance to be evaluated at an early stage, the methods outlined in this thesis, combined with other tools available to the building design team, can assist in facilitating this integrated design. Where previously the control of buildings was left until the end of

the design (and often construction) process, where there was little flexibility to adapt the design to improve the control, the effect of changing certain parameters can now be assessed while there remains room for manoeuvre. Furthermore, these effects, now can be quantified, can be used to justify decision making, and assist in the selection of the optimal design. However the work in this thesis is a contribution to this goal and requires further work.

6.3 Further work

In this thesis the science and method of controllability assessment of buildings is presented with a focus on heating system. However in some building types e.g. CAB, the requirement is to minimise energy costs by passively maintaining the internal thermal environment. To apply this science to the climate adaptive building case requires further work as detailed below:

In Climate Adaptive Buildings (CAB), distinct thermal comfort regions may be identified for summer and winter conditions. The internal gains, natural ventilation and thermal mass of walls and furniture may be expected to be useful to limit overheating in CAB type buildings during summer and cooler period of the year. Consequently for temperature control of these buildings, it is useful to use operational limits of the air temperature. A reasonable tolerance for CAB type buildings defined by BCO (2009) is a minimum of 20°C and a maximum of 28°C for air temperature. For such type of buildings, the actual temperature has to be floating within the minimum and maximum allowable temperature limits. In BCO (2009) it is also stated: “For mixed mode and naturally ventilated offices, the internal temperatures should not exceed 28°C for more than 5% of the occupied hours and 28°C for no more than 1%”.

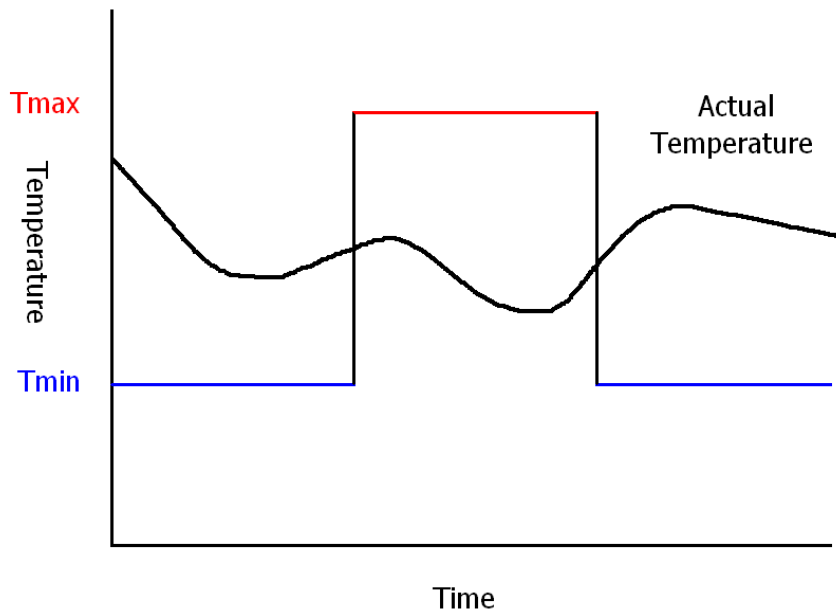


Figure 72: Limits on operational range of temperature

To assess the reachability in this case requires the U_{trim} for upper and lower limits of the operational band to be calculated separately. Two U_{trim} equations for temperature will be formed: 1) Upper limit U_{trim} at 28°C temperature and 2) lower limit at 20°C temperature. And the actual U_{trim} has to remain within these limits.

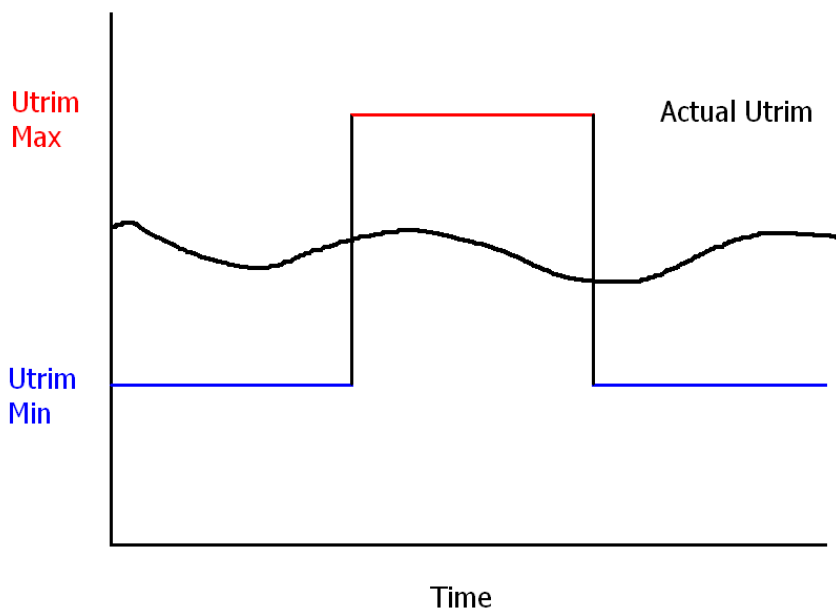


Figure 73: Limits of U_{trim} for reachability

As long as the actual U_{trim} remains within the limits no heating or cooling will be required. However if U_{trim} is less than $U_{\text{trim min}}$ then heating will not be required and if U_{trim} is more than $U_{\text{trim max}}$ then cooling will be required.

For a building with HEATING ONLY, then as long as the upper limit $U_{\text{trim max}}$ is less than the maximum power of the heater then reachability is guaranteed. To completely remove the need to for active cooling the lower limit $U_{\text{trim min}}$ should NOT be negative otherwise either the building parameters (e.g. thermal mass, Passive Stack ventilation etc) would have to be modified or active cooling would be required. Then the temperature will regulate within the operational limits and reachability will be satisfied. The U_{trim} limits correspond to the maximum flexibility of the building when in operation. By modifying the building properties in the U_{trim} these reachability bands can be extended or contracted to allow for passive and active building types to be designed.

Note: As mentioned before the U_{trim} is the inverted dynamics of the building system, depending on the variable you are trying to control e.g. temperature. The calculation of U_{trim} does not depend on the building to have an automatic control system. The U_{trim} can still be calculated for a free running building for air or comfort temperature monitoring to see whether the building is able to main temperature without the need for cooling or heating.

The benefits mentioned above of the controllability science cannot be attained without the mathematical models of the building and systems. As discussed in detail in chapter two these models are based on many assumptions that are based on experiments and observations. It is clear that applying the techniques outlined in this thesis to the design process when constructing Adaptive Climatic Buildings has the potential to improve the design process and lead to better performance, however, the model as derived above is likely to require refinement and validation before it is suitable for application in practice. There are certain areas which can be identified as priorities for further work, so that the methods can be utilized as a meaningful and productive part of the design process.

Temperature gradients in the buildings fabric are assumed one dimensional in most programs as well as in this thesis. It is proposed that this is needed to be confirmed through a thorough look at U_{trim} in the CFD domain to see whether temperature gradients in other directions has any effect on the U_{trim} dynamics and controllability. The fully mixed assumption is not valid as air temperature in different parts of the zone is changing due to disturbances. The effect of and dynamics of stratification need to be considered and a simplified method needs to be established. Obviously a relationship needs to be established which in a simple way describes the stratification and its relation to air change rate. This is being investigated by the current research in the BRE centre on complex fluidic based systems involving CFD modelling and system identification technique using neural networks.

The indoor air change rates and stratification is affected by occupancy and appliances. Thus further work is required for proper dynamic models of occupancy behaviour and appliances models that affect the internal conditions significantly and also their validation. These models are being developed in another project in the BRE Centre looking at assessment methodologies for ICT equipment in buildings.

As mentioned in the validation section the models of humidity and CO_2 have been verified in other research papers however for controllability the equations presented need to be validated with empirical data and intermodal comparisons. The lighting equations also need verification possibly using ESP-r where detail models of daylight and solar positions are present. Sol air temperature is commonly used for taking account of the solar gains on the external envelope of the building. From the results it is obvious that long wave radiation exchange with sky at night is either negligible or is not transmitted into the zone and this needs to be researched further to clarify this effect.

There is much less work done on thermal properties of internal thermal mass (i.e. furniture) and their transient behaviour. It is recommended that further work needs research into double layer thermal mass where internal layer is uniform temperature and external layer that has faster dynamics interacting with indoor air. This

assumption needs to be confirmed that the outer layer of the furniture etc acts a buffer for extra heat in the zone and the internal layer of the furniture has little affect on the air temperature. As results show that the internal thermal mass affects the comfort temperature and therefore affects the energy consumption of the zone.

Sensor placement and position of the internal mass also affects the controllability of the building. This is going to be researched as part of the CFD project mentioned above. This is an important topic as air change rate and stratification will also affect the sensor measurement. The passive stack ventilation effect has shown in the thesis and this needs to be also validated with real test data.

In terms of modelling and validation a project is underway in a partnership between Newcastle and Strathclyde universities on energy modelling and sensor networks. Where a test case modern climate adaptive building is being used to for sensing detailed data of the building environment for validation of the model in this thesis.

Future considerations in terms of more case studies on controllability science include:

- 1) Effect of occupant behaviour on the Air change rate and controllability.
- 2) Influence of the sensor position on controllability (symbolic analysis).
- 3) Influence of different arrangements of thermal mass and insulation on dynamic thermal characteristics of walls and system controllability.
- 4) Controllability in the Digital domain.

As was discussed in the introductory chapters, the level of detail of a model should depend on its proposed use. As was identified in the rationale for this thesis, the early stages of design are often when the most meaningful results can be obtained. The controllability analysis method, as outlined in this thesis, is ideally suited to this early design stage, both because it requires mainly early stage design information (orientation, glazing sizes, construction materials), rather than detailed design information (zoning, occupation rates, plant specification) and also because it

provides results which are most suited to this stage, such as whether the proposed design is stable, controllable and responsive.

For introducing the controllability analysis methods outlined in this thesis into the design process then due consideration must be given to validation. Validation is an essential part of building confidence in a model/method. The tools which are most widely used in the industry tend also to be well established. Practitioners must be convinced of the benefits that this method offers, or even the inadequacy of traditional methods, before they will consider applying it. Few methods (even theoretically superior ones) will be applied by practitioners unless they are shown to be economic.

The full validation is not carried out in this project mainly due to restriction on the time duration of the project. The validation of the model has started as part of a wider project looking at design and operation of buildings in future. Empirical validation and inter-model comparisons are being carried out. This is being done through the collaboration of Newcastle University where a sensor rich building is being used for recording of real data which will be utilised for empirical validation and verification of the assumptions taken in this thesis. This collaboration is for investigation of building management linking energy demand, distributed conversion and storage using dynamic modelling and a pervasive sensor infrastructure [<http://www.ncl.ac.uk/energy/research/project/3198>]. At the same time this sensor rich building is being modelled in high detail using ESP-r modelling and simulation package. The combination of high quality empirical data and the detailed model will be used for complete validation of the simple model for controllability analysis presented in this thesis.

Currently a tool is being developed at the BRE Centre as part energy utilisation and advanced controllability research to be utilised in practice in industry. At the moment research is being done to validate this tool for use in the design context.

Bring this science into practice is being done through three important projects for industry:

For Academic community: If the controllability analysis suggests that advanced controlled systems are needed for a building and simple PID will not work then. This project has focussed on the use of non-linear controller design method Variable Transient Response to supersede traditional controller designs such as PID in building systems. This project is developing further the RIDE controller algorithms.

For designers and buildings industry: To incorporate the controllability science into the buildings industry there is a dynamic simplified tool for quick answers is being developed. This project aims to develop methodologies and tools to assist in the process of introducing new technologies into the standard assessment procedure (SAP). With the renewed sense of urgency to reduce carbon emissions in new and refurbished homes, it is vital that new technologies can be readily included in SAP without delay and be given a fair rating. Existing and new dynamic simulation of homes and their systems are being utilised to create a new framework to speed up SAP method approval for new technologies.

For building services: U_{trim} is the magical input that calculates the input required to reach steady state i.e. perfect. How can this U_{trim} be derived from a real building to help in easier commissioning of PID requires measurement of U_{trim} of the real life building. This project aims to bridge the gap between high-performance control systems and model predictive controls through the development of a novel method which incorporates the benefits of both control strategies. This method can then be used for the development of high-performance building controllers.

Finally increased regulation, higher energy prices and greater demand for excellent indoor comfort are just some of the challenges facing the building design and construction industry. It is essential that the buildings of the future are designed to overcome these difficult challenges. Buildings designed with an Adaptive Climatic Philosophy are one way in which these challenges might be met. Robust, responsive

and accurate control of these buildings has been identified as a pre-requisite for good performance and without this even otherwise well designed buildings will perform below their optimum. While both simple tools and (to a lesser extent) more advanced simulation programs continue to be the mainstay of design in the building industry, the controllability analysis method can become another tool that is available to the designer and which contributes in a unique fashion to the improved design of buildings and their enhanced performance.

7 : References

- A.L.Dexter, Geng, G., & Haves, P. (1990). Application of Self-Tuning PID Control to HVAC Systems. *IEE Colloquium (Digest) (93)*, 3.
- Adamy, J., & Flemming, A. (2004). Soft variable-structure controls: a survey. *Automatica* (40), 1821-1844.
- Aglan, H. A. (2003). Predictive model for CO₂ generation and decay in building envelopes. *Journal of Applied Physics* , 93 (2), 1287-1290.
- Ahmed, A., Schwartz, H., & Aitken, V. (2004). Sliding mode control for singularly perturbed system. *5th Asian Control Conference*, 3, pp. 1946-1950.
- Ahmed, O., Mitchell, J., & Klein, S. (1996). Application of general regression neural network (GRNN) in HVAC process identification and control. *ASHRAE Transactions* , 102 (1) , 1147.
- AlSwailem, S. I. (2004). Application of Robust Control in Unmanned Vehicle Flight control system Design. *P.hD Thesis* . Cranfield University.
- Andersen, K. (2003). Theory for natural ventilation by thermal buoyancy in one zone with uniform temperature. *Building and Environment* , 38 (11), 1281-1289.
- Arguello, B., & Reyes, M. V. (1999). Nonlinear Control of Heating, Ventilating and Air Conditioning System with Thermal Load Estimation. *IEEE transactions on control systems technology* , 7 (1).
- ASHRAE. (2009). *ASHRAE Handbook: Fundamentals*. ASHRAE Inc.
- ASHRAE, H. (2008). *HVAC Systems and Equipment*.
- ASHRAE-Standard-55-2004. (n.d.). Thermal Environmental Conditions for Human Occupancy.
- Balaras, C. (1996). The role of thermal mass on the cooling load of buildings. An overview of computational methods. *Energy and Buildings* , 24, 1-10.

- Barrio, E., & Lefebvre, G. (2000). Using model size reduction techniques for thermal control applications in buildings. *Energy and Buildings* , 33, 1-14.
- Bartholomew, D., & Robinson, D. (1998). Building Energy and Environmental Modelling. *Application Manual AM11* . CIBSE.
- BCO, B. C. (2009). Best practice in the specification for offices. *BCO Guide to Specification* .
- Beghi, A., & Cesshinato, L. (2008). A dynamic model for the thermal-hygrometric simulation of buildings, . *Proceedings of the 17th world congress, The international Federation of Automatic Control*. Seoul.
- Berger, X., & Buriot, D. (1984). About the equivalent radiative temperature for clear skies. *Solar Energy* , 32 (6), 725-733.
- Berkeley, N. L. (2003). *SPARK 2.0 Reference Manual, Simulation problem analysis and research kernel*. U.S Department of Energy.
- Berkerley, L. L. (1993). *DOE-2 Supplement Version 2.1 E*. Berkerley, CA.
- Bland, B. (1992). Conduction in dynamic thermal models: analytical tests for validation. *Building Services Engineering Research and Technology* , 13 (4), 197-208.
- Bloomfield, B., Lornas, K., & Martin, C. (1992). Assessing programs which predict the thermal performance of buildings. *BRE Information Paper IP 7/92* .
- Bloomfield, D., & Fisk, D. (1981). Room thermal response and control stability. *Building services Engineering Research & Technology* , 2 (2), 88-99.
- Boiko, I. (2009). *Discontinuous Control Systems Frequency- Domain Analysis and Design*. Birkhauser Doston - ISBN 9780817647520.
- Bownass, D. (2001). *Building services Design Methodology A Practical Guide*. SPON Press.

- Bradshaw, A., & Counsell, J. (1992). Design of autopilots for high performance missiles. *IMechE Journal of Systems & Control* , 75-84.
- Bradshaw, A., & Counsell, J. M. (1998). A knowledge based mechatronics approach to controller design. *UKACC International Conference on CONTROL '98* (pp. 1723-1727). Publication No. 455 IEE.
- BRE. (2006). Part L explained - The BRE guide. *Guide* .
- BRE-NCM. (n.d.). iSBEM User manual 04 Jun10. *EPBD-NCM* .
- BRE-SAP. (2005). Standard Assessment Procedure for Energy Rating of Dwellings. *Compliance Method , revision 3*. Building Research Establishment.
- Brown, Z. B. (2009). Occupant comfort and engagement in green buildings: Examining the effects of knowledge, feedback and workplace culture. *PhD* . The University of British Columbia.
- Brugmann, J. (2009). Welcome to the Urban Revolution: How Cities are Changing the World. *ICLEI* . London, UK: Bloomsbury Press.
- Calafiore, G., & Carabelli, S. (1997). Structural interpretation of transmission zeros for matrix second order systems. *Automatica* , 33 (4), 745-748.
- Cengel, Y. A. (1998). *Heat transfer - A Practical Approach*. New York: McGrawHill.
- Cengel, Y. A., & Turner, R. H. (2001). *Fundamentals of Thermal-Fluid Sciences*. McGrawHill.
- CIBSE. (1998). Building Energy and Environmental Modelling. *Applications Manual 11* . London: CIBSE.
- CIBSE. (2006). *Environmental Design, Guide A*. London: CIBSE.
- Clarke, J. A. (2001). *Energy Simulation in Building Design*. Oxford: Butterworth - Heinemann.

- Clarke, J. A., & Johnstone, C. M. (2008). The role of built environment energy efficiency in a sustainable UK energy economy. *Energy Policy* (36), 4605-4609.
- Clarke, J. (2006). Trends in building energy modelling and simulation. *Proceedings of the world renewable energy congress IX*. Pergamon Press ISBN 00844671.
- Corrado, V., & Mechri, H. E. (2007). Building energy performance assessment through simplified models: application of the ISO 13790 Quasi-steady state method. *Building Simulation*.
- Corriou, J.-P. (2004). *Process Control: Theory and applications*. Springer - ISBN 1852337761.
- Counsell, J. M. (1992). Optimum and safe control algorithm (OSCA) for modern missile autopilot design. *P.hD* . Lancaster University.
- Counsell, J., & Porter, I. (1999). Schemebuilder: computer aided knowledge based design of mechatronic systems. *Journal of Industrial Automation* , 19 (2), 129-138.
- Counsell, J., Brindley, J., & Macdonald, M. (2009). Non-linear autopilot design using the philosophy of variable transient response. *AIAA Guidance, Navigation and Control Conference*, (pp. 10-13). Chicago.
- Crawley, D. B., & Hand, J. W. (2008). Contrasting the capabilities of building energy performance simulation programs. *Building and Environment* , 43 (4), 661-673.
- Darby, S., & White, R. (2005). *Thermal Comfort*. Environmental Change Institute, University of Oxford.
- Daskalov, P. I., & Arvenitis, K. G. (2006). Nonlinear adaptive temperature and humidity control in animal buildings. *Biosystems Engineering* , 93 (1), 1-24.
- Davidson, E., & Goldenberg, A. (1975). The robust control of a general servo mechanism problem: the servo compensation. *Automatica* , 11, 461-471.

- Davies, M. (1990). Room heat needs in relation to comfort temperature: Simplified calculation methods. *Building Services Engineering Research Technology* , 4 (11), 123-139.
- Deque, F., Ollivier, F., & Poblador, A. (2000). Grey boxes used to represent buildings with a minimum number of geometric and thermal parameters. *Energy and Buildings* , 30 (1), 29-35.
- DeRosa, A., & Ferraro, V. (2008). Simplified correlations of global, direct and diffuse luminous efficacy on horizontal and vertical surfaces. *Energy and Buildings* , 40, 1991-2001.
- Distefano, J. J. (1995). *Schaum's Outlines: Feedback and Control Systems 2nd Edition*. McGrawHill.
- Dounis, A., & Caraiscos, C. (2009). Advanced control systems engineering for energy and comfort management in a building environment - A review. *Renewable and Sustainable Energy Reviews* , 13 (6-7), 1246-1261.
- Doyle, J. C. (1997). *Nonlinear Robust Control Theory and Applications*. California Institute of Technology.
- EN15251, E. S. (n.d.). EN 15251:2007 Indoor environmental input parameters for design and assessment of energy performance of buildings addressing indoor air quality, thermal environment, lighting and acoustics.
- Enai, M., & Kawaguchi, Y. (1999). Control of the humidity and temperature in an atrium by cooling the surface of a pond in the atrium. *IBPSA Conference Proceedings*. Kyoto.
- Energy, U. S. (2010). Retrieved from <http://apps1.eere.energy.gov/buildings/energyplus/>
- Erbe, H. H. (2006). The Relevance of energy saving control. *IFAC WS ESC 06, energy saving control in plants and buildings*. Banskó.

- ESRU. (2010). *ESP-r*. Retrieved from Energy Systems Research Unit:
<http://www.esru.strath.ac.uk/Programs/ESP-r.htm>
- EST, E. S. (2004). *CE84 Energy efficiency best practice in housing Scotland: Assessing U values of existing housing*. BRE/ EST.
- Falb, P. L., & Wolovich, W. A. (1967). Decoupling in the design and synthesis of Multivariable control systems. *IEEE transactions on automatic control* , AC-12 (6), 651-659.
- Fanger, P. O. (1973). Assessment of man's thermal comfort in practice. *British Journal of Industrial Medicine* (30), 313-324.
- Fissore, A. (1997). Effect of internal long wave radiation and convection on fenestration simulation. *CLIMA 2000*. Brussels.
- Fontoynt, M. (2002). Perceived performance of Daylighting Systems: Lighting Efficacy and Agreeableness. *Solar Energy* , 73 (2), 83-94.
- Franklin, G., & Powell, J. (2005). *Feedback Control of Dynamic Systems*. Prentice Hall - ISBN 0131499300.
- French, M. J. (1985). *Conceptual Design for Engineers* (2nd ed.). London: Design Council.
- Friedman, T. L. (2009). Hot, Flat and crowded: Why we need a green revolution - and how it can renew America. *Picador* . New York, USA.
- FSTC. (n.d.). *Muslim Heritage*. Retrieved from <http://www.muslimheritage.com/>.
- Garcia, J. *A review of general and local thermal comfort models for controlling indoor ambiances*. University of A Coruna & Department of Energy - Spain.
- Gebremedhin, K. G., & Wu, B. X. (2003). Characterization of flow field in a ventilation space and simulation of heat exchange between cows and their environment. *Journal of Thermal Biology* , 28, 301-319.

- Gouda, M., & Danaher, S. (2002). Building thermal model reduction using nonlinear constrained optimization. *Building and Environment* , 37 (12), 1255-1265.
- Gouda, M., Danaher, S., & Underwood, C. (2000). Low-order model for the simulation of a building and its heating system. *Building Services Engineering Research and Technology* (21), 199-208.
- Gouda, M., Underwood, C. P., & Danaher, S. (2003). Modelling the robustness properties of HVAC plant under feedback control. *Building Services engineering research technology* , 24, 271.
- Gough, M. (1982). Modelling heat flow in buildings: an eigenfunction approach. *Ph.D. Thesis* . University of Cambridge.
- Grimm, C., & Mahlknecht, S. (2011). *Embedded Systems for Smart Appliances and Energy Management*. Springer 1st Edition, ISBN 1441987940.
- Guthrie, J. P. (2003). *Architect's Portable Handbook: First step rules of thumb for building design* (3rd ed.). McGraw-Hill Professional - ISBN: 0071409815.
- Hanan, J. J. (1997). *Horticulture, Greenhouses: Advanced Technology for Protected*. CRC Press.
- Hanie, O., & Aryan, A. (2010). Understanding the Importance of Sustainable Buildings in Occupants Environmental Health and Comfort. *Journal of Sustainable Development* , 3 (2), 194-200.
- Health & safety Executive, H. (1995). How to deal with Sick building Syndrome. *Series: Health and Safety Guidance* . HSE Books.
- Holman, J. P. (2009). *Heat Transfer* (10th Edition ISBN: 0071267697 ed.). McGraw-Hill Higher Education.
- Holmes, M. J. (1980). Dynamic computer models are flawed but useful. *AIRAH Journal* , 42 (4), 51-54.
- Hudson, G., & Underwood, C. (1999). A simple building modelling procedure for matlab/simulink. *Proceedings of Building Simulation '99*, 2, pp. 777-83.

- Irving, A. D. (1988). Validation of dynamic thermal models. *Energy and Buildings* , 10, 213-220.
- Jian, W., & Wenjian, C. (2000). Development of an Adaptive Neuro-Fuzzy Method for Supply Air Pressure Control in HVAC System. *International Conference on Systems, Man and Cybernetics*, 5, pp. 3806-3809.
- Judkoff, R., & Neymark, J. (1994). A testing and diagnostic procedure for building simulation programs. *Building environmental performance* .
- Kampf, J. H., & Robinson, D. (2007). A simplified thermal model to support analysis of urban resource flows. *Energy and Buildings* , 39, 445-453.
- Kavolelis, B., & Bleizgys, R. (2008). Natural Ventilation of animal sheds due to thermal buoyancy and wind. *Journal of Environmental engineering and landscape management* , 16 (4), 188-194.
- Keyser, R. M., & Dumortier, F. A. (1984). Modelling, simulation and adaptive control of a domestic floor heating system. *International Symposium on the Performance of HVAC Systems and Controls in Buildings*. Garston (UK).
- Kokotovic, P., Khalil, K., & O'Reilly, J. (1999). *Singular Perturbation Methods in Control Analysis and Design*. SIAM - ISBN 10987654321.
- Laknera, R., & Hangos, K. M. (2005). On minimal models of process systems. *Chemical Engineering Science* , 60 (4), 1127-1142.
- Lechner, N. (2001). *Heating, Cooling, lighting; Design Methods for Architects*. John Wiley and sons, ISBN: 0471241431.
- Lee, B., & Kim, Y. (1999). A study on the improvement of controllability of chemical processes based on structural analysis. *Computers and Chemical Engineering Supplement* , S35-S38.
- Lefebvre, G., Bransier, J., & Neveu, A. (1987). Simulation of the thermal behaviour of a room by reduced order numerical methods. *Revue Generale de Thermique* , 26 (302), 106-114.

- Levermore, G. (2000). *Building energy management systems: applications to low-energy HVAC and Natural Ventilation Control* (2nd ed.). Taylor & Francis.
- Li, Y., & Delsante, A. (2001). Natural Ventilation induced by combined wind and thermal forces. *Bulding and Environment* , 36 (1), 59-71.
- Li, Y., & Delsante, A. (2000). Prediction of natural ventilation in buildings with large openings. *Buildings and Environment* , 35 (3), 191-206.
- Liao, Z., & Dexter, A. (2004). A simplified physical model for estimating the average air temperature in multi-zone heating systems. *Building and Environment* , 39, 1013-1022.
- Liesen, R., & Pedersen, C. (1997). An evaluation of inside surface heat balance models for cooling load calculations. *ASHRAE Transactions* , 4 (3), 485-502.
- Littlefair, P. J. (1988). Measurements of the luminous efficacy of daylight. *Lighting Research and Technology* , 20, 177.
- Lomas, K., Eppel, H., Martin, C., & Bloomfield, D. (1997). Empirical validation of building energy simulation programs. *Energy and Buildings* , 26 (3), 253-276.
- Lorenz, F., & Masy, G. (1982). *Methode d'evaluation de l'economic d'energie apportee par l'intermittence de chauffage dans les batiments. Traitement par differences finies d'un model a deux constantes de temps*. University de Liege, Belgium.
- Lui, J., & Cai, W.-J. (2009). Design and Application of Handheld Auto-tuning PID instrument used in HVAC. *Industrial Electronics and Applications, ICIEA 2009, 4th IEEE conference*, (pp. 1695-1698).
- Luo, Z., & Zhao, J. (2007). Estimating natural ventilation potential considering both thermal comfort and IAQ issues. *Building and Environment* , 42 (6), 2289-2298.
- Macqueen, J. (1997, August). P.hD. *The modelling and simulation of energy management control systems* . University of Strathclyde.

- Magni, J.-F., & Bennani, S. (1997). Lecture Notes in Control and Information Sciences. *Robust Flight Control: A Design Challenge* , 224. Springer-Verlag.
- Mardaljevic, J., & Heschong, L. (2009). Daylight metrics and energy savings. *Lighting Research and Technology* , 41, 261-283.
- Mayr, O. (1975). *The Origins of Feedback Control*. The MIT Press - ISBN 0-262-63056-7.
- McMullan, R. (2007). *Environmental Science in Building*. Palgrave Macmillan.
- Meerov, M. V. (1947). Automatic control systems stable with indefinitely large values of gain. *Automatika i Telemekhanika* , 8 (4).
- Merz, H., Hansemann, T., & Hubner, C. (2009). *Building Automation communication systems with EIB/KNX, LON, and BACnet*. Springer.
- Milbank, N., & Lynn, J. (1974). Thermal response and the admittance procedure. *Building services Engineering* , 42, 38-50.
- Minister, O. o. (2005). Building Regulations . *Explanatory Booklet* . Welsh Assembly Government.
- Mitalas, G. (1965). An assessment of common assumptions in estimating cooling loads and space temperatures. *ASHRAE Transactions* , 71 (Part II), 72-80.
- Morbitzer, C. A. (2003). Towards the Integration of Simulation into the Building Design Process. *PhD* . Glasgow: University of Strathclyde.
- Muir, E., & Bradshaw, A. (1996). Control law design for thrust vectoring fighter aircraft using robust inverse dynamics estimation (RIDE). *Proceedings of IMechE* , 210, 333-343.
- Naidu, D. (1988). *Singular Perturbation methodology in control systems*. Peter Peregrinus Ltd - ISBN 086341107x.
- Nakanishi et al, E. (1973). Simultaneous control of temperature and humidity in a confined space Part 1. *Building Science* , 8, 39-49.

- Never, N. (1995). *Air Pollution Control Engineering*. Singapore: McGraw-Hill.
- Newsham, G., & C. Donnelly. (2006). The effect of ramps in temperature and electric light level on office occupants: a literature review and a laboratory experiment. *ACEEE Summer study on energy efficiency in buildings* (pp. 252-264). California: Pacific Grove.
- Orosa, J. A. (2011). A new modelling methodology to control HVAC systems. *Expert systems with applications*, 38, 4505-4513.
- Phelan, R. M. (1977). *Automatic Control Systems*. Cornell University Press - ISBN 0801410338.
- Pirez, R., & Ineichen, P. (1990). Modelling daylight availability and irradiance components from direct and global irradiance. *Solar Energy*, 40 (5), 271-289.
- Qui, L., & Davison, E. (1993). Performance Limitations of Non-Minimum phase systems in the Servomechanism problem. *Automatica*, 29 (2), 337-349.
- Ralegaonkar, R. V., & Gupta, R. (2010). Review of intelligent building construction: A passive solar architecture approach. *Renewable and Sustainable Energy Reviews*.
- Richard C. Dorf, R. H. (2008). *Modern Control Systems* (eleventh ed.). Pearson Prentice Hall.
- Robins, D. (2007, June). Delivering An Effective Control System. *Modern Building Services journal*.
- Robinson, D. (1996). Energy model usage in building design: A qualitative assessment. *Building Services Engineering Research and Technology*, 17 (2), 89-95.
- Roskilly, A. P. (1990). Nonlinear modelling of robust controllers for robotic manipulators. *IMechE*.
- S. Virk, G., & Loveday, D. L. (1994). Model-Based Control for HVAC applications. *IEEE Conference on Control Applications*, 3, p. 1861.

- Salsbury, T. I. (2005). A survey of control technologies in the building automation industry. *International Federation of Automatic Control World Congress*. Prague.
- Salsbury, T. I. (2006). Control performance assessment for building automation systems. *Energy Saving Control in Plants and Buildings*. Bansko.
- SEL. (2000). *TRNSYS, A Transient system simulation program, User Guide Version 15*. . Solar Energy Lab, University of Wisconsin-Madison.
- Shakir, B. (. (1979). *The Book of Ingenious Devices (Kitab al-hiyal)*. (D. R. Hill, Trans.) D. Reidel - ISBN 9027708339.
- Singh, J., & Yu, C. W. (2010). Building Pathology, Investigation of Sick Buildings Toxic Moulds. *Indoor and Built Environment* , 19 (1), 40-47.
- Singh, S. (2009). *Process Control Concepts, Dynamics and Applications*. New Delhi: PHI Learning Private Limited: ISBN 9788120336780 Page:331.
- Skogestad, S. (1996). A procedure for siso controllability analysis with application to design of pH neutralization processes. *Computers & Chemical Engineering* , 20 (4), 373-386.
- Slotine, J., & Li, W. (1991). *Applied nonlinear control*. Prentice Hall - ISBN 0130408905.
- Smith, P. (2007). *Sustainability at the Cutting Edge: Emerging Technologies for low energy buildings* (2nd ed.). Architectural Press.
- Sodja, A., & Zupancic, B. (2009). Modelling thermal processes in buildings using an object orientated approach and modelica. *Simulation modelling practice and theory* , 17, 1143-1159.
- Sodja, A., & Zupancic, B. (2008). Some aspects of thermal and radiation flows modelling in buildings using Modelica. *Tenth International conference on Computer Modeling and Simulation*, (pp. 637-642).

- Sourbron, M., & Helsen, L. (2011). Evaluation of adaptive thermal comfort models in moderate climates and their impact on energy use in office buildings. *Energy and Buildings* (43), 423-432.
- Straete, H. J. (1995). Physical Meaning of Zeros and Transmission Zeros from Bond Graph Models. *Thesis* . MIT.
- Swinbank, W. C. (1963). Long-wave radiation from clear skies. *Quarterly Journal of the Royal Meteorological Society* , 89 (381), 339-348.
- Tan, W. W., & Dexter, A. L. (2000). Self-Learning Fuzzy Controller for Embedded Applications. *Automatica* , 36 (8), 1189.
- Tashtoush, B., & Molhim, M. (2005). Dynamic model of an HVAC system for control analysis. *Energy* , 30, 1729-1745.
- Tindale, A. (1993). Third-order lumped-parameter simulation method. *Building services engineering research technology* , 14, 127-37.
- Toepfer, K. (2007). Architecture - Urban Planning - Environment in T. Herzog. *Solar Charter* . Munich, Germany: Prestel Publisher.
- Truong, P. H. (2010, September). Improving the Fanger Model's Thermal Comfort Predictions for Naturally Ventilated Spaces. *Phd* . MIT.
- Tung, T. L. (2008, December). solar radiation and daylight illuminance modelling and implications for building integrated photovoltaic system designs. *Ph.D Thesis* . City University of Hong Kong.
- Tunstall, G. (2006). *Managing the building Design process* (2nd edition ed.). Butterworth-Heinemann, ISBN - 0750667913.
- UK Government, D. o. (2006). *code for sustainable homes: a step change in sustainable home building practice*. Crown.
- Underwood, C. P. (2000). Robust Control of HVAC plant I: modelling, II: Controller design. *Building services engineering research technology* , 21.

- Utkin, V. I. (1971). Equations of the slipping regime in discontinuous systems II. *Automation and Remote Control* .
- Utkin, V. I. (1977). Variable structure systems with sliding modes. *IEEE Transactions on Automatic control* , 22 (2), 212-222.
- Wang, S. (2010). *Intelligent Buildings and Building Automation*. Spon Press: ISBN 0203890817.
- Wellstead, P. E. (1979). *Introduction to Physical System Modelling*. New York: Academic Press.
- Wetter, M. (2009). Modelica-based modelling and simulation to support research and development in building energy and control systems. *Building Performance Simulation* , 2 (2), 143-161.
- Wigginton, M., & Harris, J. (2002). *Intelligent Skins*. Oxford: Architectural Press.
- Xia, C., & Zhu, Y. (2008). Building simulation as assistance in the conceptual design. *Building simulation* (1), 46-52.
- Xiaoshu, L., Derek, C., & Martti, V. (2009). Past, present and future mathematical models for buildings: focus on intelligent buildings (Part 1 & 2). *Intelligent Buildings International* , 1 (1), 23-38, 131-141.
- Xu, X., & Wang, S. (2008). A simplified dynamic model for existing buildings using CTF and thermal network models. *International Journal of Thermal Sciences* , 47, 1249-1262.
- Yam, J., & Li, Y. (2003). Natural coupling between thermal mass and natural ventilation in buildings. *International Journal of heat and mass transfer* , 40, 1251-1264.
- Yam, J., & Li, Y. (2002). Nonlinear coupling between thermal mass and natural ventilation in buildings. *International Journal of Heat and Mass Transfer* , 46, 1251-1264.

- Yam, J., & Li, Y. (2003). Nonlinear coupling between thermal mass and natural ventilation in buildings. *International Journal of heat and mass transfer* , 40, 1251-1264.
- Yang, L., & Zhang, G. (2005). Investigation potential of natural driving forces for ventilation in four major cities in China. *Building and Environment* , 40 (1), 734-736.
- Young, K.-K. D., Kokotovic, P. V., & Utkin, V. I. (1977). A singular perturbation analysis of high gain feedback systems. *IEEE Transactions of Automatic Control* , Ac-22 (6), 931-938.
- Young, P. C., & Lees, M. J. (1993). The active mixing volume: a new concept in modelling environmental systems. *Statistics for the environment* .
- young, P., & Price, L. (2000). Recent developments in the modelling of imperfectly mixed air spaces. *Computer and Electronics in Agriculture* , 26, 239-254.
- Yuan, S., & O'Neill, Z. (2008). Testing and validating an equation-based dynamic building program with ASHRAE Standard method of test. *Third National Conference of IBPSA-USA*, (pp. 45-52). California.
- Zhang, H., & Yoshino, H. (2010). Analysis of indoor humidity environment in Chinese residential buildings. *Building and Environment* , 45 (10), 2132-2140.
- Zhang, J., & Jacobson, L. (1989). Modelling natural ventilation induced by combined thermal buoyancy and wind. *Transaction of the ASAE* , 32b, 2165-2174.
- Zhou, J., & Zhang, G. (2008). Coupling of thermal mass and natural ventilation in buildings. *Energy and Buildings* , 40, 979-986.
- Zhou, J., & Zhang, G. (2008). Coupling of thermal mass and natural ventilation in buildings. *Energy and Buildings* , 40, 979-986.
- Zinober, A. (1990). *Deterministic control of uncertain systems*. Peter Peregrinus Ltd - ISBN 0863411703.

8 : Appendix 1 - Thermodynamics

Heat transfer, Q : Heat transfer to a system (heat gain) increases the energy of the molecules and thus the internal energy of the system, and heat transfer from a system (heat loss) decreases it since the energy transferred with a fixed mass or closed system are heat transfer and work [(Cengel & Turner, 2001)].

1st Law of thermodynamics

$$E_{in} - E_{out} = \Delta E_{sys}$$

Energy can be transferred to or from a system in three forms: heat, work, and mass flow. Energy interactions are recognised at the system boundary as they cross it and they represent the energy gained or lost by a system during a process. Noting that energy can be transferred in the forms of heat, work, and mass, and that the net transfer of a quantity is equal to the difference between the amounts transferred in and out, the energy balance can be written more explicitly as:

$$E_{in} - E_{out} = (Q_{in} - Q_{out})_{net} + (W_{in} - W_{out})_{net} + (E_{mass,in} - E_{mass,out})_{net} = \Delta E_{system}$$

Where the subscripts “in” and “out” denote quantities that enter and leave the system, respectively. All six quantities on the right side of the equation represent “amounts”, and thus they are positive quantities. Heat gain is assumed positive where as heat loss is assumed to be negative.

Work can be cancelled because the energy interaction is caused by a temperature difference between the system and its surroundings. The heat entering the building by mass flow due to mechanical air ventilation is also included but assumed to be a heat transfer rather than mass flow or mechanical work. Thus the equation simplifies to:

$$E_{in} - E_{out} = (Q_{in} - Q_{out})_{net} = \Delta E_{system}$$

The change in the total energy of a system during a process is the sum of the changes in its internal kinetic and potential energies and can be expressed as;

$$\Delta E = \Delta U + \Delta KE + \Delta PE$$

For stationary systems such as buildings, the changes in kinetic and potential energies are zero (that is $\Delta KE = \Delta PE = 0$), and the total energy change relation above reduces to $\Delta E = \Delta U$ for such systems.

$$(Q_{in} - Q_{out}) = \Delta E = \Delta U = C_p \Delta T$$

$$\Delta U = mu \quad C_p = mc_p = \rho V c_p$$

$$Q_{in} - Q_{out} = \Delta E = \Delta U = \rho V c_p \Delta T$$

For incompressible substances (liquids and solids), both the constant-pressure and constant-volume specific heats are identical and denoted by C:

$$C_p + C_v = C$$

Thus;

$$\rho V c_p \Delta T = Q_{in} - Q_{out}$$

In the rate of change form,

$$\rho V c_p \Delta \dot{T} = \dot{Q}_{in} - \dot{Q}_{out}$$

The energy balance can be expressed in the differential equation form as;

$$\rho V c_p \frac{dT}{dt} = \dot{Q}_{in} - \dot{Q}_{out}$$

This equation will be used to sum all the heat transfers in and out of the building envelop:

$$\rho V c_p \frac{dT}{dt} = \sum \dot{Q}_{in} - \sum \dot{Q}_{out}$$

Heat energy always tends to migrate in the direction of decreasing temperature.

9 : Appendix 2 – external thermal mass equation derivation

Consider a basic structure with heat entering and leaving the structure:

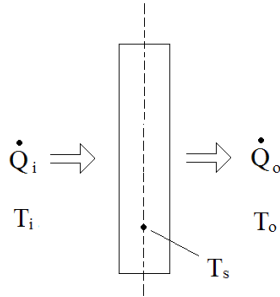


Figure 74: Basic thermal mass with heat transfer across it

In steady state conditions:

$$T_s = \frac{T_i + T_o}{2}$$

$$\dot{Q}_i = \dot{Q}_o \rightarrow UA(T_i - T_s) = UA(T_s - T_o)$$

Substituting T_s into the heat equations gives:

$$\dot{Q}_i = \dot{Q}_o \rightarrow UA\left(\frac{T_i - T_o}{2}\right) = UA\left(\frac{T_i - T_o}{2}\right)$$

This shows that when steady state is reached the heat transfer is halved. Therefore, the original equations for \dot{Q}_i & \dot{Q}_o , need to be multiplied by a factor of 2 to prevent the heat transfer to be halved at steady state. The window equation doesn't need to be multiplied by a factor of 2 because the windows are already in steady state.

10 : Appendix 3 – Test house data

The house used for this work was a mid terraced house.



Figure 75: Test House

The house was of timber framed construction, with weather boarding to the front and back facades above the ground floor windows and other areas being brick clad. The windows were made of PVCu framed double glazing. The roof is of simple dual-pitch design with pitch angle of 42° .

Details of the construction and design heat losses for the houses are as follows:

Ground floors: 50mm screed on 100mm concrete on DPM over 50mm foamed polystyrene on blinded hardcore. U-value $0.33 \text{ W/m}^2 \text{ }^{\circ}\text{C}$, area (each house) 44 m^2 , heat loss $14.7 \text{ W/}^{\circ}\text{C}$.

Walls: Plasterboard on polyethylene vapour barrier on 92mm studs at 400mm spacing, space between studs filled with 92mm glass

fibre quilt. 9mm sheathing ply, breather felt, then either 40mm cavity and facing brickwork, or weatherboarding on 25mm battens. U-value $0.36 \text{ W/m}^2 \text{ }^\circ \text{C}$, areas: end of terrace house [54.1] excluding gable triangle 80 m^2 giving heat loss $28.8 \text{ W/}^\circ \text{C}$, centre house [54.2] 39 m^2 giving heat loss $14 \text{ W/}^\circ \text{C}$.

Windows: PVCu double glazed, U-value $3.0 \text{ W/m}^2 \text{ }^\circ \text{C}$, area 9.6 m^2 , heat loss $28.8 \text{ W/}^\circ \text{C}$.

Doors: Timber, U-value $2.6 \text{ W/m}^2 \text{ }^\circ \text{C}$, area 0.9 m^2 , heat loss $2.5 \text{ W/}^\circ \text{C}$.

Glazed, U-value $4.3 \text{ W/m}^2 \text{ }^\circ \text{C}$, area 3.3 m^2 , heat loss $14 \text{ W/}^\circ \text{C}$.

Roof: 100mm fibreglass between joists of first floor ceiling; U-value $0.29 \text{ W/m}^2 \text{ }^\circ \text{C}$, area 44 m^2 , heat loss $12.8 \text{ W/}^\circ \text{C}$.

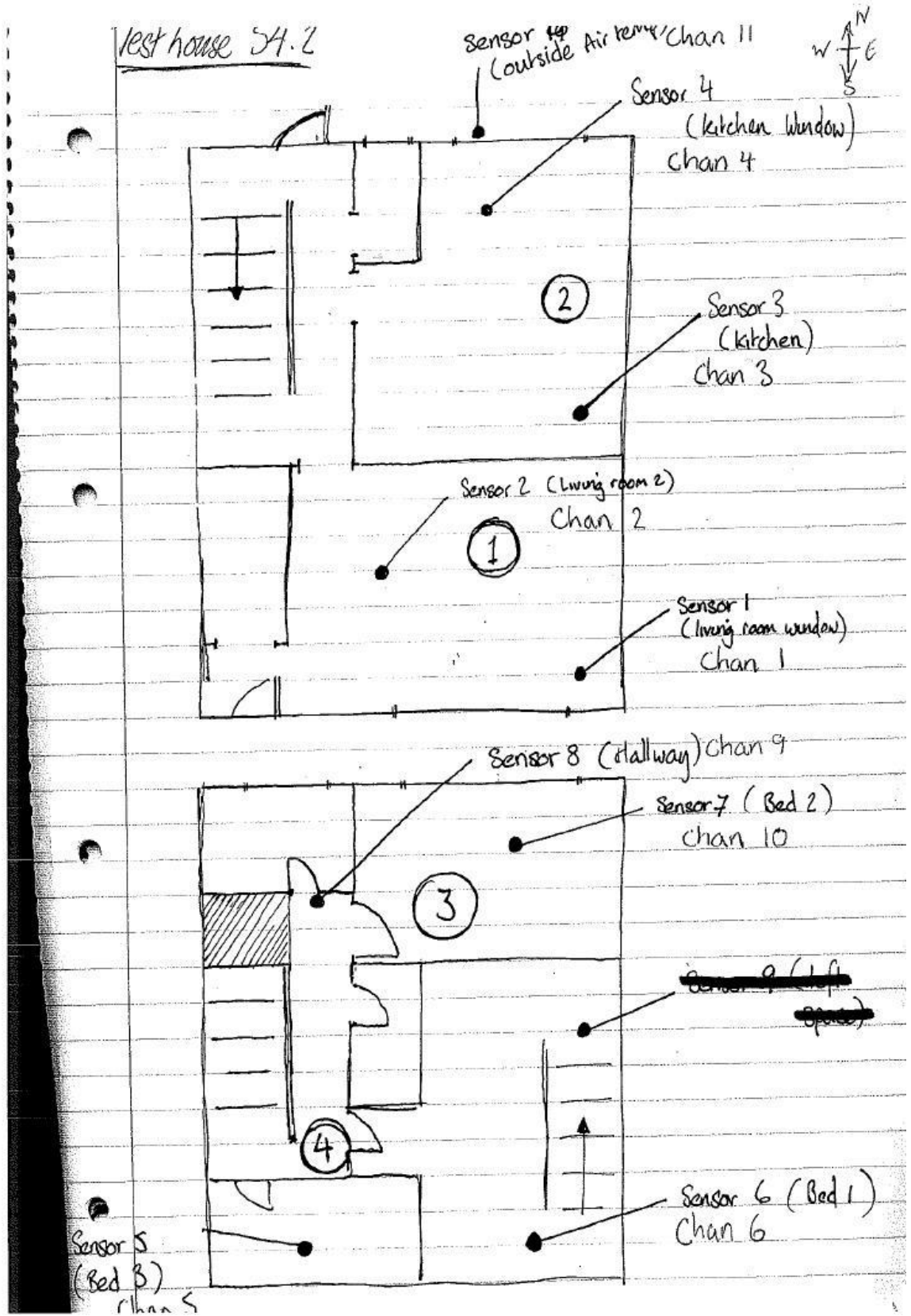
Total design fabric heat losses:

Centre terrace house [54.2]: $86.8 \text{ W/}^\circ \text{C}$ (1823 Watts @ $20 \text{ }^\circ \text{C}$ indoor, $-1 \text{ }^\circ \text{C}$ outdoor)

It is assumed that there is no heat loss across partition walls between houses (one wall for the end house [54.1] and two walls for the centre house [54.2]). The third test house in the terrace [54.3] was being used for experiments during the monitoring periods but was essentially unheated (a 1kW heater was used in one room for about 1 hour per day when experiments were running and that room was separated from the centre house by the hall and stairs of 54.3). If the indoor temperature in 54.3 is assumed to be $10 \text{ }^\circ \text{C}$ with a partition wall u-value assumed to be 0.36 this would mean about $14 \text{ W/}^\circ \text{C}$ more heat loss from the centre house [54.2] than indicated above.

Each house has internal dimensions of 5.36 m width (front and back walls), 8.1 m depth (front t back) and 4.96m height (ground floor to upstairs ceiling), giving a gross volume of 215 m³. However, during the sealing measures, described later in this report, it was convenient to seal off some built in cupboards leaving an effective internal volume of 190 m³, which is the volume used in calculations for the project.

For the purposes of this project the houses were heated by oil filled electric panel heaters with integral thermostats placed in the kitchen, living room and three bedrooms. The bathrooms were heated by electric convector heaters with separate thermostats. All the heating appliances were controlled by time switches, the □on□ period being from 07:00 to 23:00 every day. The use of electric heating simplified the energy monitoring (compared with the alternative of gas central heating) by ensuring that all the energy use recorded contributed to the heating of the houses, and by making it easier to ensure temperatures in the two houses were balanced.



Modelling data:

As said the house is of timber frame construction:

Walls:

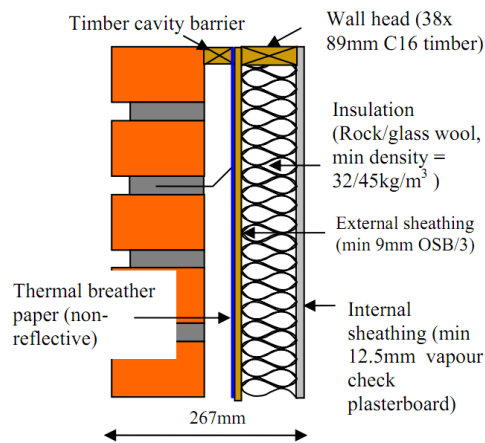


Figure 2 Standard timber frame wall detail

Reference: Development of the Optimum Sustainable Timber Frame Wall Detail

Robert Hairstan, Robin Dodyk, Abdy Kermani

Walls:

Note: the weather boarding is for the first floor not the ground floor. From the picture it is clear that on the ground floor the wall detail is as given above in the diagram. These walls can be assumed to be on the three sides of the zone and the fourth wall is the internal wall connected to the kitchen. There is no insulation on the external side of the brick wall and all the insulation is on the internal side of the brick wall.

Exact materials are as follows: Plasterboard on polyethylene vapour barrier on 92mm studs at 400mm spacing, space between studs filled with 92mm glass fibre quilt. 9mm sheathing ply, breather felt, then either 40mm cavity and facing brickwork, or weatherboarding on 25mm battens. U value $0.36 \text{ W/m}^2 \text{ } ^\circ \text{C}$.

Based upon the materials used in the wall and their arrangement, it can be assumed that the insulation is steady state and is considered a resistance and the differential equation will model the brick wall as it's a thermal mass.

For a brick (outer leaf) the thermal properties are as follows:

Density (kg/m³) = 1700, Thermal conductivity (W/mK) = 0.84, Specific heat capacity (J/kgK) = 800, thickness = 10.5 cm = 0.105 m. This applies to all the walls, 1-4 from the diagram.

Volumes: = $t * L * h$ = thickness x length x height

$$\text{wall 2} = 0.0105 * 3.15 * 2.5 = 0.104 \text{ m}^3$$

$$\text{wall 3} = (0.0105) * (A_{\text{wall}} (4.32*2.5) - A_{\text{win}} (1.54*0.83)) = 0.1 \text{ m}^3$$

$$\text{wall 4} = \text{wall 2} = 0.104 \text{ m}^3$$

$$\text{wall 1} = 0.0105*4.32*2.5 = 0.1134$$

For internal wall (no. 1) it is assumed to be a brick wall as well but without insulation i.e. a higher U value of 3.0. [The calculation of energy use in dwellings, Uglow, 1977]

Areas:

$$\text{Wall 2} = 7.875 \text{ m}^2$$

$$\text{Wall 3} = 10.8 - 1.28 = 9.52 \text{ m}^2$$

$$\text{Wall 4} = 7.875 \text{ m}^2$$

$$\text{Wall 1} = 10.8 \text{ m}^2$$

Suspended roof/floor:

Density (kg/m³) = 650, Thermal conductivity (W/mK) = 0.12, Specific heat capacity (J/kgK) = 1200.0, U = 0.65 for suspender floor (timber), thickness (m) = 0.18

The thickness was calculated using the formula $U=1/(L/K)$

$$\text{Area} = 4.32 * 3.15 = 13.608 \text{ m}^2, \text{ volume} = \text{area} * 0.18 = 2.45 \text{ m}^3$$

Ground floor:

The concrete will be modelled with the differential equation.

Cast concrete: density (kg/m³) = 2000, Thermal conductivity (W/mK) = 1.13, specific heat capacity (J/kgK) = 1000, thickness = 0.1 m, U values of 0.33.

The insulation is on outer side of the floor. There is no need to model the screed. It can be assumed to be an insulation material with a U value of 8 J/kgK.

Exact details are:

50mm screed on 100mm concrete on DPM over 50mm foamed polystyrene on blinded hardcore. U-value 0.33 W/m²°C, area (each house) 44 m², heat loss 14.7 W/°C.

Area: 4.32*3.15 = 13.608 m², volume = 1.36 m³

Internal Thermal mass:

The internal thermal mass such as furniture is assumed to be lumped mass in the zone floating in the air.

Volume (m³) = 3 m³ for a 3 piece suite, Density (kg/m³) = 500, Specific heat capacity (J/kg K) = 1600, Area: 13.0 m²

Plant (oil radiator properties):

[reference: low-order model for the simulation of a building and its heating system: Gouda, Danaher and Underwood]

A_a = emitter external area **

A_{cross} = emitter cross-sectional area

A_w = emitter internal area

C_m = thermal capacity of the emitter material

C_{pw} = specific heat capacity of water J/kgk

h_e = air side heat emitter heat transfer coefficient W/m²K = U value

k_w = thermal conductivity of water (W/mK)

m_w = emitter water flow rate (kg/s)

n = heat emission index

Q_w = heat transfer from water

Q_p = plant heat output (W)

T_g = earth temperature

T_m = emitter material temperature



For the thermal model of the emitter:

Volume (of oil or internal volume): $\text{Area} \times \text{thickness} = (3.142 \times 0.083 \times 2) \times 0.365 = 0.19$
m³

Density: 0.9 kg/m³

Specific heat capacity: 2500 J/kgK

For convection need to take the surface area of the radiator: looking at the diagram there are about 5 fins:

Each fin is about 0.5 m in height, 0.1 m wide, thus

Total surface area = $0.5 \times 0.1 \times 5 = 0.25$ m²

The same area will be used for radiation as well.

11 : Appendix 4 – chapter two symbolic models and data

The proposed model is specifically developed to test the controllability of a nonlinear multivariable system. The dynamic model describes the energy and mass balance of air in the building zone having heating, ventilation and lighting.

Some suppositions were considered in mathematical modelling procedures and listed as follows:

1. Temperature gradients along the layers of the structure i.e. walls, floor, roof and window panes are small in comparison to those perpendicular to the surface and can be neglected. All elements of the envelope are thus simplified to one-dimensional heat transfer.
2. The simplified model assumes that the indoor zone air is fully mixed at constant pressure. This leads to far less complex dynamic equations, but are still detailed enough to analyse controllability. Note that the air volume V_a used in the balances is the temperature active mixing volume (AMV) respectively [(Young & Lees, 1993) (young & Price, 2000)]. Shortcuts in the air path and stagnant zones exist in ventilated spaces and the AMV (that is, the air volume computed from real measurements of the reactions assuming perfect mixing) is typically significantly less than the calculated total volume. The AMV of a ventilated space may easily be as small as 60–70% of the geometric volume. This, of course, means indoor air temperature is unlikely to be uniform throughout the air space. However, in a model with only one state for the temperature, the effective heat capacity must be taken larger than the one corresponding to the AMV, to encompass some of the heat capacity contributed by the construction materials. The use of the concept of AMV

allows considering perfect mixing, when modelling the building (Daskalov & Arvenitis, 2006).

3. Air change rate is the result buoyancy effect and tightness of the building that are due to air velocity pressure difference or temperature difference. With passively driven ventilation, it is known that indoor airflow is thermally stratified in some circumstances. However the fully mixed assumption is used here because it leads to relatively simple equations, which nonetheless display interesting cause and effect behaviour.
4. Thermal corner effects are neglected so that internal and external structural areas can be assumed to be the same. U-Values (overall thermal transmittance coefficient) are used to model the heat transfer through the building fabric.
5. While a multilayer representation of the structure will add to the accuracy for calculating energy consumption, it does not improve the calculation of the dynamics of the zone. Thus it was found through simulation that a second order representation of the walls, floor and roof produced accurate dynamic responses in comparison to an equivalent multi-layer construction. This allowed for simplification of the model for controllability analysis while retaining the essential dynamics characteristics. Due to low thermal mass of windows they are considered to be in steady state.
6. It is assumed that the thermal mass is not in equilibrium with the indoor air. Here all the internal masses are represented by one mass however in reality the mass will be spread on the zone floor. The temperature distribution in the thermal mass materials is also assumed to be uniform. This means that the thermal diffusion process is much faster than the convective heat transfer at the thermal mass surface [(Zhou & Zhang, 2008) (Yam & Li, Natural coupling between thermal mass and natural ventilation in buildings, 2003)].

7. Solar radiation on cooling load were compared and discussed in (Liesen & Pedersen, 1997), and it's shown that projecting all the solar on the floor matches actual behaviours in many cases. In most cases the floor will be obscured with the internal thermal mass such as furniture and thus it is sensible to include solar gains in the thermal mass equation. Also due to direct solar radiation penetrating the window will cause the window temperature to rise. Thus a small part of the solar radiation will be included in the air due heat transfer between the window and air. Because the window is assumed to be in steady state thus this gain is treated as a direct heat gain to the air temperature node.
8. Most solar heat gain to a building space is by direct radiation through windows. The heat gain in a building by radiation from the sun depends upon site-specific factors and dynamic factors. The former consist of the surface area and angle of tilt of the glass, the composition of the glass, the geographic location of the site, the orientation of the building on the site and any local shading factors. These factors are more important for energy consumption calculation where the orientation of the building with respect to its setting will have a signification impact on the calculation results. However for controllability analysis a reasonable estimate of the amount of solar gain entering the zone is sufficient and thus a simplified model is used.
9. For the purposes of modelling, the level of light can be treated as three components, the artificial light, the direct light from the sun and the background, or reflected light from the surrounding environment. The objective of this work is not to model accurate position of the sun in the sky for formulating luminance levels. A reasonable daylight factor will allow for simulating the causes and effects in the zone by the external solar data.
10. The fabric solar heat gains through walls and roofs may be considered negligible for most UK applications. Little solar heat reaches the interior of the building because the high thermal capacity of 'heavy' constructions tends to delay transmission of the heat until its direction of flow is reversed with

the arrival of evening. Low thermal capacity construction, on the other hand, tends to be well insulated, ensuring that solar heat transmission is minimised.

NOTE: sol air temperature is being used thus there is no need to make this assumption

11. The model is assumed to have casual heat gains. Casual heat gains take account of the heat given off by various activities and equipment, the major sources being people, lighting, and electrical appliances.

Long-wave radiation exchange between internal surfaces of the zone is ignored.

Full order model:

$$\rho_a V_a c_{pa} \frac{dT_a}{dt} = \left[\begin{array}{l} \alpha_a \sigma_s A_{win} I_{dr} + 2U_{w1} A_{w1} (T_{w1} - T_a) + 2U_{w2} A_{w2} (T_{w2} - T_a) \\ + 2U_{w3} A_{w3} (T_{w3} - T_a) + 2U_{w4} A_{w4} (T_{w4} - T_a) + 2U_f A_f (T_f - T_a) \\ + 2U_r A_r (T_r - T_a) + U_{win} A_{win} (T_{o3} - T_a) + h_m A_m (T_m - T_a) + h_c A_p (T_p - T_a) \end{array} \right]$$

$$\rho_{w1} V_{w1} c_{pw1} \frac{dT_{w1}}{dt} = [2U_{w1} A_{w1} (T_{o1} - T_{w1}) - 2U_{w1} A_{w1} (T_{w1} - T_a)]$$

$$\rho_{w2} V_{w2} c_{pw2} \frac{dT_{w2}}{dt} = [2U_{w2} A_{w2} (T_{o2} - T_{w2}) - 2U_{w2} A_{w2} (T_{w2} - T_a)]$$

$$\rho_{w3} V_{w3} c_{pw3} \frac{dT_{w3}}{dt} = [2U_{w3} A_{w3} (T_{o3} - T_{w3}) - 2U_{w3} A_{w3} (T_{w3} - T_a)]$$

$$\rho_{w4} V_{w4} c_{pw4} \frac{dT_{w4}}{dt} = [2U_{w4} A_{w4} (T_{o4} - T_{w4}) - 2U_{w4} A_{w4} (T_{w4} - T_a)]$$

$$\rho_f V_f c_{pf} \frac{dT_f}{dt} = [2U_f A_f (T_{o5} - T_f) - 2U_f A_f (T_f - T_a)]$$

$$\rho_r V_r c_{pr} \frac{dT_r}{dt} = [2U_r A_r (T_{o6} - T_r) - 2U_r A_r (T_r - T_a)]$$

$$\rho_m V_m c_{pm} \frac{dT_m}{dt} = [\alpha_m \sigma_s A_{win} I_{dr} + h_r A_p (T_p - T_m) - h_m A_m (T_m - T_a)]$$

$$\rho_p V_p c_{pp} \frac{dT_p}{dt} = [\dot{Q}_p - h_r A_p (T_p - T_m) - h_c A_p (T_p - T_a)]$$

$$\tau_p \frac{d\dot{Q}_p}{dt} = [\dot{Q}_c - \dot{Q}_p]$$

$$\delta x = [\delta T_a \quad \delta T_{w1} \quad \delta T_{w2} \quad \delta T_{w3} \quad \delta T_{w4} \quad \delta T_f \quad \delta T_r \quad \delta T_m \quad \delta T_p \quad \delta \dot{Q}_p]^T$$

$$\delta b = [\delta \dot{Q}_p]^T$$

$$\delta d = [\delta I_{dr} \quad \delta T_{o1} \quad \delta T_{o2} \quad \delta T_{o3} \quad \delta T_{o4} \quad \delta T_{o5} \quad \delta T_{o6} \quad \delta \dot{Q}_c]^T$$

$$A = \begin{bmatrix} a_{11} & a_{12} & a_{13} & a_{14} & a_{15} & a_{16} & a_{17} & a_{18} & a_{19} & 0 \\ a_{21} & a_{22} & 0 & 0 & 0 & 0 & 0 & 0 & 0 & 0 \\ a_{31} & 0 & a_{33} & 0 & 0 & 0 & 0 & 0 & 0 & 0 \\ a_{41} & 0 & 0 & a_{44} & 0 & 0 & 0 & 0 & 0 & 0 \\ a_{51} & 0 & 0 & 0 & a_{55} & 0 & 0 & 0 & 0 & 0 \\ a_{61} & 0 & 0 & 0 & 0 & a_{66} & 0 & 0 & 0 & 0 \\ a_{71} & 0 & 0 & 0 & 0 & 0 & a_{77} & 0 & 0 & 0 \\ a_{81} & 0 & 0 & 0 & 0 & 0 & 0 & a_{88} & a_{89} & 0 \\ a_{91} & 0 & 0 & 0 & 0 & 0 & 0 & a_{98} & a_{99} & 0 \\ 0 & 0 & 0 & 0 & 0 & 0 & 0 & 0 & 0 & 0 \end{bmatrix}, B = \begin{bmatrix} 0 \\ 0 \\ 0 \\ 0 \\ 0 \\ 0 \\ 0 \\ 0 \\ 0 \\ b_{91} \\ b_{101} \end{bmatrix},$$

$$F = \begin{bmatrix} f_{11} & 0 & 0 & f_{14} & 0 & 0 & 0 & 0 \\ 0 & f_{22} & 0 & 0 & 0 & 0 & 0 & 0 \\ 0 & 0 & f_{33} & 0 & 0 & 0 & 0 & 0 \\ 0 & 0 & 0 & f_{44} & 0 & 0 & 0 & 0 \\ 0 & 0 & 0 & 0 & f_{55} & 0 & 0 & 0 \\ 0 & 0 & 0 & 0 & 0 & f_{66} & 0 & 0 \\ 0 & 0 & 0 & 0 & 0 & 0 & f_{77} & 0 \\ f_{81} & 0 & 0 & 0 & 0 & 0 & 0 & 0 \\ 0 & 0 & 0 & 0 & 0 & 0 & 0 & 0 \\ 0 & 0 & 0 & 0 & 0 & 0 & 0 & f_{108} \end{bmatrix}$$

$$C = [1 \quad 0 \quad 0], D = [0], E = [0 \quad 0 \quad 0]$$

$$a_{11} = \frac{(-2U_{w1}A_{w1} - 2U_{w2}A_{w2} - 2U_{w3}A_{w3} - 2U_{w4}A_{w4} - 2U_fA_f - 2U_rA_r - U_{win}A_{win} - h_mA_m - h_cA_p)}{\rho_a V_a c_{pa}}$$

$$a_{12} = \frac{2U_{w1}A_{w1}}{\rho_a V_a c_{pa}}, a_{13} = \frac{2U_{w2}A_{w2}}{\rho_a V_a c_{pa}}, a_{14} = \frac{2U_{w3}A_{w3}}{\rho_a V_a c_{pa}}, a_{15} = \frac{2U_{w4}A_{w4}}{\rho_a V_a c_{pa}}, a_{16} = \frac{2U_fA_f}{\rho_a V_a c_{pa}}, a_{17} = \frac{2U_rA_r}{\rho_a V_a c_{pa}}$$

$$a_{18} = \frac{h_mA_m}{\rho_a V_a c_{pa}}, a_{19} = \frac{h_cA_p}{\rho_a V_a c_{pa}}, f_{11} = \frac{\alpha_a \sigma_s A_{win}}{\rho_a V_a c_{pa}}, f_{14} = \frac{U_{win}A_{win}}{\rho_a V_a c_{pa}}$$

$$a_{21} = \frac{2U_{w1}A_{w1}}{\rho_{w1}V_{w1}c_{pw1}}, a_{22} = \frac{-4U_{w1}A_{w1}}{\rho_{w1}V_{w1}c_{pw1}}, f_{22} = \frac{2U_{w1}A_{w1}}{\rho_{w1}V_{w1}c_{pw1}}$$

$$a_{31} = \frac{2U_{w2}A_{w2}}{\rho_{w2}V_{w2}c_{pw2}}, a_{33} = \frac{-4U_{w2}A_{w2}}{\rho_{w2}V_{w2}c_{pw2}}, f_{33} = \frac{2U_{w2}A_{w2}}{\rho_{w2}V_{w2}c_{pw2}}$$

$$a_{41} = \frac{2U_{w3}A_{w3}}{\rho_{w3}V_{w3}c_{pw3}}, a_{44} = \frac{-4U_{w3}A_{w3}}{\rho_{w3}V_{w3}c_{pw3}}, f_{44} = \frac{2U_{w3}A_{w3}}{\rho_{w3}V_{w3}c_{pw3}}$$

$$a_{51} = \frac{2U_{w4}A_{w4}}{\rho_{w4}V_{w4}c_{pw4}}, a_{55} = \frac{-4U_{w4}A_{w4}}{\rho_{w4}V_{w4}c_{pw4}}, f_{55} = \frac{2U_{w4}A_{w4}}{\rho_{w4}V_{w4}c_{pw4}}$$

$$a_{61} = \frac{2U_fA_f}{\rho_fV_fc_{pf}}, a_{66} = \frac{-4U_fA_f}{\rho_fV_fc_{pf}}, f_{66} = \frac{2U_fA_f}{\rho_fV_fc_{pf}}$$

$$a_{71} = \frac{2U_rA_r}{\rho_rV_rc_{pr}}, a_{77} = \frac{-4U_rA_r}{\rho_rV_rc_{pr}}, f_{77} = \frac{2U_rA_r}{\rho_rV_rc_{pr}}$$

$$a_{81} = \frac{h_mA_m}{\rho_mV_mc_{pm}}, a_{88} = \frac{(-h_rA_p - h_mA_m)}{\rho_mV_mc_{pm}}, a_{89} = \frac{h_rA_p}{\rho_mV_mc_{pm}}, f_{81} = \frac{\alpha_m \sigma_s A_{win}}{\rho_mV_mc_{pm}}$$

$$a_{91} = \frac{h_cA_p}{\rho_pV_pc_{pp}}, a_{98} = \frac{h_rA_p}{\rho_pV_pc_{pp}}, a_{99} = \frac{(-h_rA_p - h_cA_p)}{\rho_pV_pc_{pp}}, b_{91} = \frac{1}{\rho_pV_pc_{pp}}$$

$$b_{101} = \frac{-1}{\tau_p}, f_{108} = \frac{1}{\tau_p}$$

Model for industry:

$$\rho_a V_a c_{pa} \frac{dT_a}{dt} = \left[\begin{array}{l} \alpha_a \sigma_s A_{win} I_{dr} + U_{w1} A_{w1} (T_{o1} - T_a) + U_{w2} A_{w2} (T_{o2} - T_a) \\ + 2U_{w3} A_{w3} (T_{w3} - T_a) + U_{w4} A_{w4} (T_{o4} - T_a) + U_f A_f (T_{o5} - T_a) \\ + U_r A_r (T_{o6} - T_a) + U_{win} A_{win} (T_{o3} - T_a) + h_m A_m (T_m - T_a) \\ + h_c A_p (T_p - T_a) \end{array} \right]$$

$$\rho_{w3} V_{w3} c_{pw3} \frac{dT_{w3}}{dt} = [2U_{w3} A_{w3} (T_{o3} - T_{w3}) - 2U_{w3} A_{w3} (T_{w3} - T_a)]$$

$$\rho_m V_m c_{pm} \frac{dT_m}{dt} = [\alpha_m \sigma_s A_{win} I_{dr} + h_r A_p (T_p - T_m) - h_m A_m (T_m - T_a)]$$

$$\delta x = [\delta T_a \quad \delta T_{w3} \quad \delta T_m]^T$$

$$\delta b = [\delta \dot{Q}_p]^T$$

$$\delta d = [\delta I_{dr} \quad \delta T_{o1} \quad \delta T_{o2} \quad \delta T_{o3} \quad \delta T_{o4} \quad \delta T_{o5} \quad \delta T_{o6}]^T$$

$$A = \begin{bmatrix} a_{11} & a_{12} & a_{13} \\ a_{21} & a_{22} & 0 \\ a_{31} & 0 & a_{33} \end{bmatrix}, B = \begin{bmatrix} b_{11} \\ 0 \\ b_{31} \end{bmatrix}, F = \begin{bmatrix} f_{11} & f_{12} & f_{13} & f_{14} & f_{15} & f_{16} & f_{17} \\ 0 & 0 & 0 & f_{24} & 0 & 0 & 0 \\ f_{31} & 0 & 0 & 0 & 0 & 0 & 0 \end{bmatrix}$$

$$C = [1 \quad 0 \quad 0], D = [0], E = [0 \quad 0 \quad 0 \quad 0 \quad 0 \quad 0 \quad 0]$$

$$\frac{dT_a}{dt} = \left[\begin{array}{l} a_{11}T_a + a_{12}T_{w3} + a_{13}T_m + b_{11}\dot{Q}_p + f_{11}I_{dr} + f_{12}T_{o1} + f_{13}T_{o2} + f_{14}T_{o3} \\ + f_{15}T_{o4} + f_{16}T_{o5} + f_{17}T_{o6} \end{array} \right]$$

$$a_{11} = \frac{(-U_{w1}A_{w1} - U_{w2}A_{w2} - 2U_{w3}A_{w3} - U_{w4}A_{w4} - U_fA_f - U_rA_r - U_{win}A_{win} - h_mA_m + h_c^2A_p / (h_r + h_c) - h_cA_p)}{\rho_a V_a c_{pa}}$$

$$a_{12} = \frac{2U_{w3}A_{w3}}{\rho_a V_a c_{pa}}, a_{13} = \frac{1}{\rho_a V_a c_{pa}} \left(\frac{h_c h_r A_p}{(h_r + h_c)} + h_m A_m \right), b_{11} = \frac{h_c}{\rho_a V_a c_{pa} (h_r + h_c)}$$

$$f_{11} = \frac{\alpha_s \sigma_s A_{win}}{\rho_a V_a c_{pa}}, f_{12} = \frac{U_{w1}A_{w1}}{\rho_a V_a c_{pa}}, f_{13} = \frac{U_{w2}A_{w2}}{\rho_a V_a c_{pa}}, f_{14} = \frac{U_{win}A_{win}}{\rho_a V_a c_{pa}}, f_{15} = \frac{U_{w4}A_{w4}}{\rho_a V_a c_{pa}}$$

$$f_{16} = \frac{U_f A_f}{\rho_a V_a c_{pa}}, f_{17} = \frac{U_r A_r}{\rho_a V_a c_{pa}}$$

$$\frac{dT_{w3}}{dt} = [a_{21}T_a + a_{22}T_{w3} + f_{24}T_{o3}]$$

$$a_{21} = \frac{2U_{w3}A_{w3}}{\rho_{w3} V_{w3} c_{pw3}}, a_{22} = \frac{-4U_{w3}A_{w3}}{\rho_{w3} V_{w3} c_{pw3}}, f_{24} = \frac{2U_{w3}A_{w3}}{\rho_{w3} V_{w3} c_{pw3}}$$

$$\rho_m V_m c_{pm} \frac{dT_m}{dt} = [a_{31}T_a + a_{33}T_m + b_{31}\dot{Q}_p + f_{31}I_{dr}]$$

$$a_{31} = \frac{1}{\rho_m V_m c_{pm}} \left(\frac{h_r h_c A_p}{(h_r + h_c)} + h_m A_m \right),$$

$$a_{33} = \frac{1}{\rho_m V_m c_{pm}} \left(\frac{h_r^2 A_p}{(h_r + h_c)} - h_r A_p - h_m A_m \right)$$

$$b_{31} = \frac{h_r}{\rho_m V_m c_{pm} (h_r + h_c)}, f_{31} = \frac{\alpha_m \sigma_s A_{win}}{\rho_m V_m c_{pm}}$$

Parameter values:

Dimensions:

Elements	Length (m)	Width (m)	Height (m)	Thickness (m)
Zone	4.32	3.15	4.96	
Wall 1	4.32	2.5		0.1
Wall 2	3.15	2.5		0.1
Wall 3	4.32	2.5		0.1
Wall 4	3.15	2.5		0.1
Floor	4.32	3.15		0.1
Roof	4.32	3.15		0.1
Mass	2.0	1.5		1.0
Window	1.42	0.83		
Plant	0.854	0.586		0.011

Thermal properties:

Elements	Density (kg/m ³)	Heat capacity (J/kgK)	U values (W/m ² K)
Zone air	1.22	1012.0	
Wall 1	1700.0	800.0	0.36
Wall 2	1700.0	800.0	0.36
Wall 3	1700.0	800.0	0.36
Wall 4	1700.0	800.0	0.36
Floor	2000.0	1000.0	0.33
Roof	12.0	840.0	0.29
Mass	400.0	900.0	1.57
Window			
Plant	2094.0	1964.0	$h_r: 5.0$ $h_c: 6.5$

Other constants:

τ_p	300.0 (s)		
α_a	0.2		
α_m	0.8		
σ_s	0.5		
ϵ	0.5		
σ_b	0.0000000567		

Higher order model numerical state space model for matlab implementation:

```
A=[-0.000688 0.0000984 0.0000717 0.0000876 0.0000717 0.000114 0.0000998
0.0000596 0.0000412 0;
0.00000529 -0.0000106 0 0 0 0 0 0 0;
0.00000529 0 -0.0000106 0 0 0 0 0 0;
0.00000529 0 0 -0.0000106 0 0 0 0 0;
0.00000529 0 0 0 -0.0000106 0 0 0 0;
0.00000330 0 0 0 0 -0.0000066 0 0 0;
0.000575 0 0 0 0 0 -0.00115 0 0;
0.00000377 0 0 0 0 0 0 -0.00000577 0.000002 0;
0.000144 0 0 0 0 0 0 0.000111 -0.000254 0;
0 0 0 0 0 0 0 0 0]
```

```
B=[0;0;0;0;0;0;0;0;0.0000442;-0.00333]
```

```
C=[1 0 0 0 0 0 0 0 0]
```

```
D=[0]
```

Third order numerical state space model for matlab

W=[-0.000437 0.0000876 0.0000775; 0.00000529 -0.0000106 0;
0.00000490 0 -0.00000547]

X=[0.00000715; 0; 0.000000348]

Y=[1 0 0]

Z=[0]

4th order numerical state space model for matlab:

I=[-0.000461 0.0000876 0.0000596 0.0000412; 0.00000529 -0.0000106 0 0;
0.00000377 0 -0.00000577 0.000002; 0.000144 0 0.000110 -0.000254]

J=[0; 0; 0; 0.0000442]

K=[1 0 0 0]

L=[0]

12 : Appendix 5 – U_{trim} equation derivation for proof

$$\dot{x}(t) = Ax(t) + Bu(t) + Fd(t)$$

$$w(t) = Mx(t) + Du(t) + Ed(t)$$

Differentiate $w(t)$

$$\dot{w}(t) = M\dot{x}(t) + D\dot{u}(t) + E\dot{d}(t)$$

Substitute $\dot{x}(t)$ into $\dot{w}(t)$ gives:

$$\dot{w}(t) = MAx(t) + MBu(t) + MFd(t) + D\dot{u}(t) + E\dot{d}(t)$$

Rearranging and converting to laplace gives:

$$sW(s) = MAx(s) + (MB + sD)u(s) + (MF + sE)d(s)$$

If $u(s) = u_c(s) + U_{trim}(s)$:

$$sW(s) = MAx(s) + (MB + sD)(u_c(s) + U_{trim}(s)) + (MF + sE)d(s)$$

If U_{trim} is given as below and substituted into the above equation:

$$U_{trim}(s) = \left[-(MB + sD)^{-1} MAx(s) - (MB + sD)^{-1} (MF + sE)d(s) \right]$$

This systems reduces to as follows:

$$sW(s) = (MB + sD)u_c(s)$$

13 : Appendix 6 – Case-study 1

$$\rho_a V_a c_{pa} \frac{dT_a}{dt} = \left[\begin{array}{l} \alpha_a \sigma_s A_{win} I_{dr} + k_e P_L + g_{oc} n_{oc} + 2U_{w1} A_{w1} (T_{w1} - T_a) + 2U_{w2} A_{w2} (T_{w2} - T_a) \\ + 2U_{w3} A_{w3} (T_{w3} - T_a) + 2U_{w4} A_{w4} (T_{w4} - T_a) + 2U_r A_r (T_r - T_a) \\ + U_{win} A_{win} (T_o - T_a) + h_m A_m (T_m - T_a) + V_a n_t \rho_a c_{pa} (T_o - T_a) \\ + V_a n_v \rho_a c_{pa} (T_o - T_a) + V_a n_{in} \rho_a c_{pa} (T_o - T_a) + q_{mv} \rho_a c_{pa} (T_o - T_a) \\ + h_c A_s (T_s - T_a) \end{array} \right]$$

$$\frac{d\delta T_a}{dt} = \left[\begin{array}{l} \frac{1}{\rho_a V_a c_{pa}} \left(-2U_{w1} A_{w1} - 2U_{w2} A_{w2} - 2U_{w3} A_{w3} - 2U_{w4} A_{w4} - 2U_r A_r - U_{win} A_{win} \right) \delta T_a \\ + \frac{2U_{w1} A_{w1}}{\rho_a V_a c_{pa}} \delta T_{w1} + \frac{2U_{w2} A_{w2}}{\rho_a V_a c_{pa}} \delta T_{w2} + \frac{2U_{w3} A_{w3}}{\rho_a V_a c_{pa}} \delta T_{w3} + \frac{2U_{w4} A_{w4}}{\rho_a V_a c_{pa}} \delta T_{w4} \\ + \frac{h_c A_s}{\rho_a V_a c_{pa}} \delta T_s + \frac{2U_r A_r}{\rho_a V_a c_{pa}} \delta T_r + \frac{k_e}{\rho_a V_a c_{pa}} \delta P_L + \frac{h_m A_m}{\rho_a V_a c_{pa}} \delta T_m \\ + \frac{\rho_a c_{pa} (\bar{T}_o - \bar{T}_a)}{\rho_a V_a c_{pa}} \delta q_{mv} + \frac{\alpha_a \sigma_s A_{win}}{\rho_a V_a c_{pa}} \delta I_{dr} + \frac{g_{oc}}{\rho_a V_a c_{pa}} \delta n_{oc} \\ + \frac{1}{\rho_a V_a c_{pa}} \left(\begin{array}{l} U_{win} A_{win} + V_a \bar{n}_t \rho_a c_{pa} + V_a \rho_a c_{pa} \bar{n}_v \\ + V_a \bar{n}_{in} \rho_a c_{pa} + \rho_a c_{pa} \bar{q}_{mv} \end{array} \right) \delta T_o + (\bar{T}_o - \bar{T}_a) \delta n_v \end{array} \right]$$

$$\frac{d\delta T_a}{dt} = \left[\begin{array}{l} a_{11} \delta T_a + a_{12} \delta T_{w1} + a_{13} \delta T_{w2} + a_{14} \delta T_{w3} + a_{15} \delta T_{w4} \\ + a_{16} \delta T_s + a_{18} \delta T_r + a_{110} \delta P_L + a_{111} \delta T_m + b_{11} \delta q_{mv} \\ + f_{11} \delta I_{dr} + f_{12} \delta n_{oc} + f_{13} \delta T_o + f_{110} \delta n_v \end{array} \right]$$

$$a_{11} = \frac{1}{\rho_a V_a c_{pa}} \left(-2U_{w1} A_{w1} - 2U_{w2} A_{w2} - 2U_{w3} A_{w3} - 2U_{w4} A_{w4} - 2U_r A_r - U_{win} A_{win} \right) \\ - \frac{h_m A_m}{\rho_a V_a c_{pa}} - \frac{V_a \bar{n}_t \rho_a c_{pa}}{\rho_a V_a c_{pa}} - \frac{V_a \rho_a c_{pa} \bar{n}_v}{\rho_a V_a c_{pa}} - \frac{V_a \bar{n}_{in} \rho_a c_{pa}}{\rho_a V_a c_{pa}} - \frac{\rho_a c_{pa} \bar{q}_{mv}}{\rho_a V_a c_{pa}} - \frac{h_c A_s}{\rho_a V_a c_{pa}}$$

$$a_{12} = \frac{2U_{w1} A_{w1}}{\rho_a V_a c_{pa}}, a_{13} = \frac{2U_{w2} A_{w2}}{\rho_a V_a c_{pa}}, a_{14} = \frac{2U_{w3} A_{w3}}{\rho_a V_a c_{pa}}, a_{15} = \frac{2U_{w4} A_{w4}}{\rho_a V_a c_{pa}}, a_{16} = \frac{h_c A_s}{\rho_a V_a c_{pa}}$$

$$a_{18} = \frac{2U_r A_r}{\rho_a V_a c_{pa}}, a_{110} = \frac{k_e}{\rho_a V_a c_{pa}}, a_{111} = \frac{h_m A_m}{\rho_a V_a c_{pa}}, b_{11} = \frac{(\bar{T}_o - \bar{T}_a)}{V_a}, f_{11} = \frac{\alpha_a \sigma_s A_{win}}{\rho_a V_a c_{pa}},$$

$$f_{12} = \frac{g_{oc}}{\rho_a V_a c_{pa}}, f_{13} = \frac{1}{\rho_a V_a c_{pa}} \left(\begin{array}{l} U_{win} A_{win} + V_a \bar{n}_t \rho_a c_{pa} + V_a \rho_a c_{pa} \bar{n}_v \\ + V_a \bar{n}_{in} \rho_a c_{pa} + \rho_a c_{pa} \bar{q}_{mv} \end{array} \right), f_{110} = (\bar{T}_o - \bar{T}_a)$$

$$\rho_{w1}V_{w1}c_{pw1}\frac{dT_{w1}}{dt} = [2U_{w1}A_{w1}(T_{o1} - T_{w1}) - 2U_{w1}A_{w1}(T_{w1} - T_a)]$$

$$\frac{d\delta T_{w1}}{dt} = \left[\frac{2U_{w1}A_{w1}}{\rho_{w1}V_{w1}c_{pw1}}\delta T_a + \frac{-4U_{w1}A_{w1}}{\rho_{w1}V_{w1}c_{pw1}}\delta T_{w1} + \frac{2U_{w1}A_{w1}}{\rho_{w1}V_{w1}c_{pw1}}\delta T_{o1} \right]$$

$$\frac{d\delta T_{w1}}{dt} = [a_{21}\delta T_a + a_{22}\delta T_{w1} + f_{22}\delta T_{o1}]$$

$$a_{21} = \frac{2U_{w1}A_{w1}}{\rho_{w1}V_{w1}c_{pw1}}, a_{22} = \frac{-4U_{w1}A_{w1}}{\rho_{w1}V_{w1}c_{pw1}}, f_{22} = \frac{2U_{w1}A_{w1}}{\rho_{w1}V_{w1}c_{pw1}}$$

$$\rho_{w2}V_{w2}c_{pw2}\frac{dT_{w2}}{dt} = [2U_{w2}A_{w2}(T_{o2} - T_{w2}) - 2U_{w2}A_{w2}(T_{w2} - T_a)]$$

$$\frac{d\delta T_{w2}}{dt} = \left[\frac{2U_{w2}A_{w2}}{\rho_{w2}V_{w2}c_{pw2}}\delta T_a + \frac{-4U_{w2}A_{w2}}{\rho_{w2}V_{w2}c_{pw2}}\delta T_{w2} + \frac{2U_{w2}A_{w2}}{\rho_{w2}V_{w2}c_{pw2}}\delta T_{o2} \right]$$

$$\frac{d\delta T_{w2}}{dt} = [a_{31}\delta T_a + a_{33}\delta T_{w2} + f_{33}\delta T_{o2}]$$

$$a_{31} = \frac{2U_{w2}A_{w2}}{\rho_{w2}V_{w2}c_{pw2}}, a_{33} = \frac{-4U_{w2}A_{w2}}{\rho_{w2}V_{w2}c_{pw2}}, f_{33} = \frac{2U_{w2}A_{w2}}{\rho_{w2}V_{w2}c_{pw2}}$$

$$\rho_{w3}V_{w3}c_{pw3}\frac{dT_{w3}}{dt} = [2U_{w3}A_{w3}(T_{o3} - T_{w3}) - 2U_{w3}A_{w3}(T_{w3} - T_a)]$$

$$\frac{d\delta T_{w3}}{dt} = \left[\frac{2U_{w3}A_{w3}}{\rho_{w3}V_{w3}c_{pw3}}\delta T_a + \frac{-4U_{w3}A_{w3}}{\rho_{w3}V_{w3}c_{pw3}}\delta T_{w3} + \frac{2U_{w3}A_{w3}}{\rho_{w3}V_{w3}c_{pw3}}\delta T_{o3} \right]$$

$$\frac{d\delta T_{w3}}{dt} = [a_{41}\delta T_a + a_{44}\delta T_{w3} + f_{44}\delta T_{o3}]$$

$$a_{41} = \frac{2U_{w3}A_{w3}}{\rho_{w3}V_{w3}c_{pw3}}, a_{44} = \frac{-4U_{w3}A_{w3}}{\rho_{w3}V_{w3}c_{pw3}}, f_{44} = \frac{2U_{w3}A_{w3}}{\rho_{w3}V_{w3}c_{pw3}}$$

$$\rho_{w4}V_{w4}c_{pw4}\frac{dT_{w4}}{dt} = [2U_{w4}A_{w4}(T_{o4} - T_{w4}) - 2U_{w4}A_{w4}(T_{w4} - T_a)]$$

$$\frac{d\delta T_{w4}}{dt} = \left[\frac{2U_{w4}A_{w4}}{\rho_{w4}V_{w4}c_{pw4}}\delta T_a + \frac{-4U_{w4}A_{w4}}{\rho_{w4}V_{w4}c_{pw4}}\delta T_{w4} + \frac{2U_{w4}A_{w4}}{\rho_{w4}V_{w4}c_{pw4}}\delta T_{o4} \right]$$

$$\frac{d\delta T_{w4}}{dt} = [a_{51}\delta T_a + a_{55}\delta T_{w4} + f_{44}\delta T_{o4}]$$

$$a_{51} = \frac{2U_{w4}A_{w4}}{\rho_{w4}V_{w4}c_{pw4}}, a_{55} = \frac{-4U_{w4}A_{w4}}{\rho_{w4}V_{w4}c_{pw4}}, f_{55} = \frac{2U_{w4}A_{w4}}{\rho_{w4}V_{w4}c_{pw4}}$$

$$\rho_s V_s c_{ps} \frac{dT_s}{dt} = [U_{in}A_{in}(T_c - T_s) + \dot{Q}_p - h_c A_s(T_s - T_a) - h_r A_s(T_s - T_m)]$$

$$\frac{d\delta T_s}{dt} = \left[+ \frac{h_c A_s}{\rho_s V_s c_{ps}} \delta T_a + \frac{(-U_{in}A_{in} - h_c A_s - h_r A_s)}{\rho_s V_s c_{ps}} \delta T_s + \frac{U_{in}A_{in}}{\rho_s V_s c_{ps}} \delta T_c + \frac{h_r A_s}{\rho_s V_s c_{ps}} \delta T_m + \frac{1}{\rho_s V_s c_{ps}} \delta \dot{Q}_p \right]$$

$$\frac{d\delta T_s}{dt} = [a_{61}\delta T_a + a_{66}\delta T_s + a_{67}\delta T_c + a_{611}\delta T_m + b_{63}\delta \dot{Q}_p]$$

$$a_{61} = \frac{h_c A_s}{\rho_s V_s c_{ps}}, a_{66} = \frac{(-U_{in}A_{in} - h_c A_s - h_r A_s)}{\rho_s V_s c_{ps}}, a_{67} = \frac{U_{in}A_{in}}{\rho_s V_s c_{ps}}, a_{611} = \frac{h_r A_s}{\rho_s V_s c_{ps}}, b_{63} = \frac{1}{\rho_s V_s c_{ps}}$$

$$\rho_c V_c c_{pc} \frac{dT_c}{dt} = [U_c A_c (T_{o5} - T_c) - U_{in} A_{in} (T_c - T_s)]$$

$$\frac{d\delta T_c}{dt} = \left[+ \frac{U_{in}A_{in}}{\rho_c V_c c_{pc}} \delta T_s + \frac{(-U_c A_c - U_{in}A_{in})}{\rho_c V_c c_{pc}} \delta T_c + \frac{U_c A_c}{\rho_c V_c c_{pc}} \delta T_{o5} \right]$$

$$\frac{d\delta T_c}{dt} = [a_{76}\delta T_s + a_{77}\delta T_c + f_{78}\delta T_{o5}]$$

$$a_{76} = \frac{U_{in}A_{in}}{\rho_c V_c c_{pc}}, a_{77} = \frac{(-U_c A_c - U_{in}A_{in})}{\rho_c V_c c_{pc}}, f_{78} = \frac{U_c A_c}{\rho_c V_c c_{pc}}$$

$$\rho_r V_r c_{pr} \frac{dT_r}{dt} = [2U_r A_r (T_{o6} - T_r) - 2U_r A_r (T_r - T_a)]$$

$$\frac{dT_r}{dt} = \left[\frac{2U_r A_r}{\rho_r V_r c_{pr}} T_a + \frac{-4U_r A_r}{\rho_r V_r c_{pr}} T_r + \frac{2U_r A_r}{\rho_r V_r c_{pr}} T_{o6} \right]$$

$$\frac{dT_r}{dt} = [a_{81}T_a + a_{88}T_r + f_{88}T_{o6}]$$

$$a_{81} = \frac{2U_r A_r}{\rho_r V_r c_{pr}}, a_{88} = \frac{-4U_r A_r}{\rho_r V_r c_{pr}}, f_{88} = \frac{2U_r A_r}{\rho_r V_r c_{pr}}$$

$$\rho_{co2}V_a \frac{dC_a}{dt} = \left[\begin{array}{l} S - q_{mv}\rho_{co2}(C_a - C_o) - \rho_{co2}n_tV_a(C_a - C_o) \\ -\rho_{co2}n_vV_a(C_a - C_o) - \rho_{co2}n_iV_a(C_a - C_o) \end{array} \right]$$

$$\frac{d\delta C_a}{dt} = \left[\begin{array}{l} \frac{(-\rho_{co2}\bar{n}_tV_a - \rho_{co2}\bar{n}_vV_a - \bar{q}_{mv}\rho_{co2} - \rho_{co2}\bar{n}_iV_a)\delta C_a}{\rho_{co2}V_a} \\ + \frac{-(\bar{C}_a - \bar{C}_o)}{V_a}\delta q_{mv} + (-\bar{C}_a - \bar{C}_o)\delta n_v + \frac{1}{\rho_{co2}V_a}\delta S \\ + \frac{(n_tV_a + \bar{n}_vV_a + \bar{q}_{mv} + n_iV_a)}{V_a}\delta C_o \end{array} \right]$$

$$\frac{d\delta C_a}{dt} = [a_{99}\delta C_a + b_{91}\delta q_{mv} + f_{910}\delta n_v + f_{911}\delta S + f_{912}\delta C_o]$$

$$a_{99} = \frac{(-\rho_{co2}\bar{n}_tV_a - \rho_{co2}\bar{n}_vV_a - \bar{q}_{mv}\rho_{co2} - \rho_{co2}\bar{n}_iV_a)}{\rho_{co2}V_a}, b_{91} = \frac{-(\bar{C}_a - \bar{C}_o)}{V_a}$$

$$f_{910} = (-\bar{C}_a - \bar{C}_o), f_{911} = \frac{1}{\rho_{co2}V_a}, f_{912} = \frac{(n_tV_a + \bar{n}_vV_a + \bar{q}_{mv} + n_iV_a)}{V_a}$$

$$\frac{dP_L}{dt} = u_L$$

$$\frac{d\delta P_L}{dt} = \delta u_L$$

$$b_{102} = 1$$

$$\rho_m V_m c_{pm} \frac{d\delta T_m}{dt} = [\alpha_m \sigma_s A_{win} \delta I_{dr} + h_r A_s (\delta T_s - \delta T_m) - h_m A_m (\delta T_m - \delta T_a)]$$

$$\frac{d\delta T_m}{dt} = \left[+ \frac{h_m A_m}{\rho_m V_m c_{pm}} \delta T_a + \frac{h_r A_s}{\rho_m V_m c_{pm}} \delta T_s + \frac{-h_r A_s - h_m A_m}{\rho_m V_m c_{pm}} \delta T_m + \frac{\alpha_m \sigma_s A_{win}}{\rho_m V_m c_{pm}} \delta I_{dr} \right]$$

$$\frac{d\delta T_m}{dt} = [a_{111}\delta T_a + a_{116}\delta T_s + a_{1111}\delta T_m + f_{111}\delta I_{dr}]$$

$$a_{111} = \frac{h_m A_m}{\rho_m V_m c_{pm}}, a_{116} = \frac{h_r A_s}{\rho_m V_m c_{pm}}, a_{1111} = \frac{-h_r A_s - h_m A_m}{\rho_m V_m c_{pm}}, f_{111} = \frac{\alpha_m \sigma_s A_{win}}{\rho_m V_m c_{pm}}$$

Control strategy 1, Ta control:

$$C_{cm} = C_a$$

$$\delta C_{cm} = m_{19} \delta C_a, m_{19} = 1$$

$$L_{cm} = L_i + L_s = k_L P_L + \lambda \alpha_L I_{df}$$

$$\delta L_{cm} = m_{210} \delta P_L + f_{213} \delta I_{df}$$

$$m_{210} = k_L, f_{213} = \lambda \alpha_L$$

$$T_{cm} = T_a$$

$$\delta T_{cm} = m_{31} \delta T_a, m_{31} = 1$$

Control strategy 2: Ta plus its Rate of change control

$$C_{cm} = C_a$$

$$\delta C_{cm} = m_{19} \delta C_a, m_{19} = 1$$

$$L_{cm} = L_i + L_s = k_L P_L + \lambda \alpha_L I_{df}$$

$$\delta L_{cm} = m_{210} \delta P_L + f_{213} \delta I_{df}$$

$$m_{210} = k_L, f_{213} = \lambda \alpha_L$$

$$T_{cm} = T_a + \dot{T}_a = \delta T_a + \frac{d\delta T_a}{dt} = \left[\begin{array}{l} (a_{11} + 1) \delta T_a + a_{12} \delta T_{w1} + a_{13} \delta T_{w2} + a_{14} \delta T_{w3} + a_{15} \delta T_{w4} + a_{16} \delta T_s + a_{18} \delta T_r \\ + a_{110} \delta P_L + a_{111} \delta T_m + b_{11} \delta q_{mv} + f_{11} \delta I_{dr} + f_{12} \delta n_{oc} + f_{13} \delta T_o + f_{110} \delta n_v \end{array} \right]$$

Control strategy 3: Comfort temperature control

$$C_{cm} = C_a$$

$$\delta C_{cm} = m_{19} \delta C_a, m_{19} = 1$$

$$L_{cm} = L_i + L_s = k_L P_L + \lambda \alpha_L I_{df}$$

$$\delta L_{cm} = m_{210} \delta P_L + f_{213} \delta I_{df}$$

$$m_{210} = k_L, f_{213} = \lambda \alpha_L$$

$$T_{cm} = \frac{1}{3} T_a + \frac{1}{21} T_{w1} + \frac{1}{21} T_{w2} + \frac{1}{21} T_{w3} + \frac{1}{21} T_{w4} + \frac{1}{21} T_s + \frac{1}{21} T_r + \frac{1}{21} T_m$$

$$T_{cm} = m_{31} T_a + m_{32} T_{w1} + m_{33} T_{w2} + m_{34} T_{w3} + m_{35} T_{w4} + m_{36} T_s + m_{38} T_r + m_{311} T_m$$

$$m_{31} = \frac{1}{3}, m_{32} = \frac{1}{21}, m_{33} = \frac{1}{21}, m_{34} = \frac{1}{21}, m_{35} = \frac{1}{21}, m_{36} = \frac{1}{21}, m_{38} = \frac{1}{21}, m_{311} = \frac{1}{21}$$

14 : Appendix 7 – Case study 2

Temperature:

$$\dot{Q}_{nt} = V_a n_t \rho_a c_{pa} (T_o - T_a) \Rightarrow \delta \dot{Q}_{nt} = V_a \bar{n}_t \rho_a c_{pa} \delta T_o - V_a \bar{n}_t \rho_a c_{pa} \delta T_a$$

$$\dot{Q}_{nv} = V_a n_v \rho_a c_{pa} (T_o - T_a) \Rightarrow \delta \dot{Q}_{nv} = -V_a k_v \rho_a c_{pa} \bar{v}_o \delta T_a + V_a k_v \rho_a c_{pa} \bar{v}_o \delta T_o + V_a k_v \rho_a c_{pa} (\bar{T}_o - \bar{T}_a) \delta v_o$$

$$\dot{Q}_{ni} = V_a n_i \rho_a c_{pa} (T_o - T_a) \Rightarrow \delta \dot{Q}_{ni} = V_a \bar{n}_i \rho_a c_{pa} (\delta T_o - \delta T_a)$$

$$\dot{Q}_{mv} = q_{mv} \rho_a c_{pa} (T_o - T_a) \Rightarrow \delta \dot{Q}_{mv} = -\rho_a c_{pa} \bar{q}_m \delta T_a + (\bar{T}_o - \bar{T}_a) \rho_a c_{pa} \delta q_m + \rho_a c_{pa} \bar{q}_m \delta T_o$$

Humidity:

$$W_{nt} = \rho_a n_t V_a (w_a - w_o) \Rightarrow \delta W_{nt} = \rho_a \bar{n}_t V_a \delta w_a - \rho_a \bar{n}_t V_a \delta w_o$$

$$W_{nv} = \rho_a n_v V_a (w_a - w_o) \Rightarrow \delta W_{nv} = \rho_a V_a k_v \bar{v}_o \delta w_a + \rho_a V_a k_v (\bar{w}_a - \bar{w}_o) \delta v_o - \rho_a V_a k_v \bar{v}_o \delta w_o$$

$$W_{ni} = \rho_a n_i V_a (w_a - w_o) \Rightarrow \delta W_{ni} = \rho_a \bar{n}_i V_a \delta w_a - \rho_a \bar{n}_i V_a \delta w_o$$

$$W_{mv} = \rho_a q_m (w_a - w_o) \Rightarrow \delta W_{mv} = \rho_a \bar{q}_m \delta w_a + (\bar{w}_a - \bar{w}_o) \rho_a \delta q_m - \rho_a \bar{q}_m \delta w_o$$

Substituting the nonlinear parts into the equations gives:

$$\rho_a V_a c_{pa} \frac{d\delta T_a}{dt} = \left[\begin{array}{l} \left(\alpha_a \sigma_s A_w I_{dr} + k_e \delta P_L + \delta \dot{Q}_{oc} + \delta \dot{Q}_{ap} \right)_{\text{casual gains}} \\ + \left(2U_{wi} A_w (\delta T_w - \delta T_a) + U_{win} A_{win} (\delta T_o - \delta T_a) + U_m A_m (\delta T_m - \delta T_a) \right)_{\text{structure}} \\ + \left(\begin{array}{l} V_a \bar{n}_i \rho_a c_{pa} \delta T_o - V_a \bar{n}_i \rho_a c_{pa} \delta T_a \\ - V_a k_v \rho_a c_{pa} \bar{v}_o \delta T_a + V_a k_v \rho_a c_{pa} \bar{v}_o \delta T_o + V_a k_v \rho_a c_{pa} (\bar{T}_o - \bar{T}_a) \delta v_o \\ + V_a \bar{n}_i \rho_a c_{pa} (\delta T_o - \delta T_a) \\ - \rho_a c_{pa} \bar{q}_m \delta T_a + (\bar{T}_o - \bar{T}_a) \rho_a c_{pa} \delta q_m + \rho_a c_{pa} \bar{q}_m \delta T_o \end{array} \right)_{\text{ventilation}} \\ + \left(\beta \delta Q_{pwh} \right)_{\text{heating / cooling}} \end{array} \right]$$

$$\rho_w V_w c_{pw} \frac{d\delta T_w}{dt} = \left[\alpha_w \sigma_s A_w \delta I_{dr} + 2U_{wo} A_w (\delta T_{sa} - \delta T_w) - 2U_{wi} A_w (\delta T_w - \delta T_a) \right]$$

$$\rho_m V_m c_{pm} \frac{d\delta T_m}{dt} = \alpha_m \sigma_s A_w \delta I_{dr} - 2U_m A_m (\delta T_m - \delta T_a)$$

$$\rho_a V_a \frac{dw_a}{dt} = \left[\begin{array}{l} W_d - \rho_a \bar{n}_i V_a \delta w_a + \rho_a \bar{n}_i V_a \delta w_o \\ - \rho_a V_a k_v \bar{v}_o \delta w_a - \rho_a V_a k_v (\bar{w}_a - \bar{w}_o) \delta v_o + \rho_a V_a k_v \bar{v}_o \delta w_o \\ - \rho_a \bar{n}_i V_a \delta w_a + \rho_a \bar{n}_i V_a \delta w_o - \rho_a \bar{q}_m \delta w_a - (\bar{w}_a - \bar{w}_o) \rho_a \delta q_m + \rho_a \bar{q}_m \delta w_o \end{array} \right]$$

Rearranging the equations gives:

$$\frac{d\delta T_a}{dt} = \left[\begin{array}{l} \frac{1}{\rho_a V_a c_{pa}} \left(-2U_{wi} A_w - U_{win} A_{win} - U_m A_m - V_a \bar{n}_i \rho_a c_{pa} - V_a k_v \rho_a c_{pa} \bar{v}_o - V_a \bar{n}_i \rho_a c_{pa} \right) \delta T_a \\ + \left(\frac{2U_{wi} A_w}{\rho_a V_a c_{pa}} \right) \delta T_w + \left(\frac{U_m A_m}{\rho_a V_a c_{pa}} \right) \delta T_m + \left(\frac{\beta}{\rho_a V_a c_{pa}} \right) \delta Q_{pwh} + \left(\frac{(\bar{T}_o - \bar{T}_a)}{V_a} \right) \delta q_m \\ + \left(\frac{\alpha_a \sigma_s A_w}{\rho_a V_a c_{pa}} \right) \delta I_{dr} + \left(\frac{k_e}{\rho_a V_a c_{pa}} \right) \delta P_L + \left(\frac{1}{\rho_a V_a c_{pa}} \right) \delta \dot{Q}_{oc} + \left(\frac{1}{\rho_a V_a c_{pa}} \right) \delta \dot{Q}_{ap} \\ + \frac{1}{\rho_a V_a c_{pa}} \left(U_{win} A_{win} + V_a \bar{n}_i \rho_a c_{pa} + V_a k_v \rho_a c_{pa} \bar{v}_o + V_a \bar{n}_i \rho_a c_{pa} + \rho_a c_{pa} \bar{q}_m \right) \delta T_o + \left((\bar{T}_o - \bar{T}_a) k_v \right) \delta v_o \end{array} \right]$$

$$\frac{dT_w}{dt} = \left(\frac{2U_{wi}A_w}{\rho_w V_w c_{pw}} \right) T_a + \left(\frac{-2U_{wo}A_w - 2U_{wi}A_w}{\rho_w V_w c_{pw}} \right) T_w + \left(\frac{\alpha_w \sigma_s A_w}{\rho_w V_w c_{pw}} \right) I_{dr} + \left(\frac{2U_{wo}A_w}{\rho_w V_w c_{pw}} \right) T_{sa}$$

$$\frac{dT_m}{dt} = \left(\frac{2U_m A_m}{\rho_m V_m c_{pm}} \right) T_a + \left(\frac{-2U_m A_m}{\rho_m V_m c_{pm}} \right) T_m + \left(\frac{\alpha_m \sigma_s A_w}{\rho_m V_m c_{pm}} \right) I_{dr}$$

$$\frac{dw_a}{dt} = \left[\begin{array}{l} \left(-\bar{n}_i - k_v \bar{v}_o - \bar{n}_i - \frac{\bar{q}_m}{V_a} \right) \delta w_a + \left(\frac{-(\bar{w}_a - \bar{w}_o)}{V_a} \right) \delta q_m + (-k_v (\bar{w}_a - \bar{w}_o)) \delta v_o \\ + \left(\bar{n}_i + k_v \bar{v}_o + \bar{n}_i + \frac{\bar{q}_m}{V_a} \right) \delta w_o + \left(\frac{1}{\rho_a V_a} \right) W_d \end{array} \right]$$

Identifying the coefficients:

$$\frac{d\delta T_a}{dt} = \left[\begin{array}{l} a_{11} \delta T_a + a_{12} \delta T_w + a_{13} \delta T_m + b_{11} \delta Q_{pwh} + b_{12} \delta q_m + f_{11} \delta I_{dr} + f_{12} \delta P_L + f_{13} \delta \dot{Q}_{oc} + f_{14} \delta \dot{Q}_{ap} \\ + f_{15} \delta T_o + f_{16} \delta v_o \end{array} \right]$$

$$\frac{dT_w}{dt} = [a_{21} T_a + a_{22} T_w + f_{21} I_{dr} + f_{27} T_{sa}]$$

$$\frac{dT_m}{dt} = a_{31} T_a + a_{33} T_m + f_{31} I_{dr}$$

$$\frac{dw_a}{dt} = [a_{44} \delta w_a + b_{42} \delta q_m + f_{46} \delta v_o + f_{48} W_d + f_{49} \delta w_o]$$

Where the coefficients are given by:

$$a_{11} = \frac{1}{\rho_a V_a c_{pa}} \left(\begin{array}{l} -2U_{wi}A_w - U_{win}A_{win} - U_m A_m - V_a \bar{n}_t \rho_a c_{pa} - V_a k_v \rho_a c_{pa} \bar{v}_o - V_a \bar{n}_i \rho_a c_{pa} \\ -\rho_a c_{pa} \bar{q}_m \end{array} \right)$$

$$a_{12} = \left(\frac{2U_{wi}A_w}{\rho_a V_a c_{pa}} \right), a_{13} = \left(\frac{U_m A_m}{\rho_a V_a c_{pa}} \right), b_{11} = \left(\frac{\beta}{\rho_a V_a c_{pa}} \right), b_{12} = \left(\frac{(\bar{T}_o - \bar{T}_a)}{V_a} \right)$$

$$f_{11} = \left(\frac{\alpha_a \sigma_s A_w}{\rho_a V_a c_{pa}} \right), f_{12} = \left(\frac{k_e}{\rho_a V_a c_{pa}} \right), f_{13} = \left(\frac{1}{\rho_a V_a c_{pa}} \right), f_{14} = \left(\frac{1}{\rho_a V_a c_{pa}} \right)$$

$$f_{15} = \frac{1}{\rho_a V_a c_{pa}} \left(U_{win}A_{win} + V_a \bar{n}_t \rho_a c_{pa} + V_a k_v \rho_a c_{pa} \bar{v}_o + V_a \bar{n}_i \rho_a c_{pa} + \rho_a c_{pa} \bar{q}_m \right)$$

$$f_{16} = \left((\bar{T}_o - \bar{T}_a) k_v \right)$$

$$a_{21} = \left(\frac{2U_{wi}A_w}{\rho_w V_w c_{pw}} \right), a_{22} = \left(\frac{-2U_{wo}A_w - 2U_{wi}A_w}{\rho_w V_w c_{pw}} \right), f_{21} = \left(\frac{\alpha_w \sigma_s A_w}{\rho_w V_w c_{pw}} \right), f_{27} = \left(\frac{2U_{wo}A_w}{\rho_w V_w c_{pw}} \right)$$

$$a_{31} = \left(\frac{2U_m A_m}{\rho_m V_m c_{pm}} \right), a_{33} = \left(\frac{-2U_m A_m}{\rho_m V_m c_{pm}} \right), f_{31} = \left(\frac{\alpha_m \sigma_s A_w}{\rho_m V_m c_{pm}} \right)$$

$$a_{44} = \left(-\bar{n}_t - k_v \bar{v}_o - \bar{n}_i - \frac{\bar{q}_m}{V_a} \right), b_{42} = \left(\frac{-(\bar{w}_a - \bar{w}_o)}{V_a} \right), f_{46} = \left(-k_v (\bar{w}_a - \bar{w}_o) \right) f_{48} = \left(\frac{1}{\rho_a V_a} \right)$$

$$f_{49} = \left(\bar{n}_t + k_v \bar{v}_o + \bar{n}_i + \frac{\bar{q}_m}{V_a} \right), c_{11} = 1, c_{24} = 1$$

The state space model is given as follows:

$$A = \begin{pmatrix} a_{11} & a_{12} & a_{13} & 0 \\ a_{21} & a_{22} & 0 & 0 \\ a_{31} & 0 & a_{33} & 0 \\ 0 & 0 & 0 & a_{44} \end{pmatrix}, B = \begin{pmatrix} b_{11} & b_{12} \\ 0 & 0 \\ 0 & 0 \\ 0 & b_{42} \end{pmatrix}, C = \begin{pmatrix} c_{11} & 0 & 0 & 0 \\ 0 & 0 & 0 & c_{24} \end{pmatrix}$$

$$D = 0, E = 0, F = \begin{pmatrix} f_{11} & f_{12} & f_{13} & f_{14} & f_{15} & f_{16} & 0 & 0 & 0 \\ f_{21} & 0 & 0 & 0 & 0 & 0 & f_{27} & 0 & 0 \\ f_{31} & 0 & 0 & 0 & 0 & 0 & 0 & 0 & 0 \\ 0 & 0 & 0 & 0 & 0 & f_{46} & 0 & f_{48} & f_{49} \end{pmatrix}$$

15 : Appendix 8 – Case study 3

Linearisations:

$$\dot{Q}_n = V_a n \rho_a c_{pa} (T_o - T_a) \Rightarrow \delta \dot{Q}_n = -V_a \rho_a c_{pa} \bar{n} \delta T_a + V_a \rho_a c_{pa} \bar{n} \delta T_o + V_a \rho_a c_{pa} (\bar{T}_o - \bar{T}_a) \delta n$$

State-space model representation

Substituting the nonlinear parts into the equations gives:

$$\rho_a V_a c_{pa} \frac{d\delta T_a}{dt} = \left[\begin{array}{l} \left(\alpha_a \sigma_s A_{win} I_{dr} + k_e \delta P_L + \delta \dot{Q}_{oc} + \delta \dot{Q}_{ap} \right)_{casual \ gains} \\ + \left(2U_{wi} A_w (\delta T_w - \delta T_a) + U_{win} A_{win} (\delta T_o - \delta T_a) + U_m A_m (\delta T_m - \delta T_a) \right)_{structure} \\ + \left(-V_a \rho_a c_{pa} \bar{n} \delta T_a + V_a \rho_a c_{pa} \bar{n} \delta T_o + V_a \rho_a c_{pa} (\bar{T}_o - \bar{T}_a) \delta n \right)_{ventilation} \\ + \left(\delta Q_p \right)_{heating \ / \ cooling} \end{array} \right]$$

$$\rho_w V_w c_{pw} \frac{d\delta T_w}{dt} = \left[\alpha_w \sigma_s A_{win} \delta I_{dr} + 2U_{wo} A_w (\delta T_{sa} - \delta T_w) - 2U_{wi} A_w (\delta T_w - \delta T_a) \right]$$

$$\rho_m V_m c_{pm} \frac{d\delta T_m}{dt} = \left[\alpha_m \sigma_s A_{win} \delta I_{dr} - U_m A_m (\delta T_m - \delta T_a) \right]$$

Rearranging the equations gives:

$$\frac{d\delta T_a}{dt} = \left[\begin{array}{l} \frac{1}{\rho_a V_a c_{pa}} \left(-2U_{wi} A_w - U_{win} A_{win} - U_m A_m - V_a \rho_a c_{pa} \bar{n} \right) \delta T_a \\ + \left(\frac{2U_{wi} A_w}{\rho_a V_a c_{pa}} \right) \delta T_w + \left(\frac{U_m A_m}{\rho_a V_a c_{pa}} \right) \delta T_m + \left(\frac{1}{\rho_a V_a c_{pa}} \right) \delta Q_p + \left(\frac{\alpha_a \sigma_s A_{win}}{\rho_a V_a c_{pa}} \right) \delta I_{dr} \\ + \left(\frac{k_e}{\rho_a V_a c_{pa}} \right) \delta P_L + \left(\frac{1}{\rho_a V_a c_{pa}} \right) \delta \dot{Q}_{oc} + \left(\frac{1}{\rho_a V_a c_{pa}} \right) \delta \dot{Q}_{ap} \\ + \frac{1}{\rho_a V_a c_{pa}} \left(U_{win} A_{win} + V_a \rho_a c_{pa} \bar{n} \right) \delta T_o + (\bar{T}_o - \bar{T}_a) \delta n \end{array} \right]$$

$$\frac{dT_w}{dt} = \left[\left(\frac{2U_{wi} A_w}{\rho_w V_w c_{pw}} \right) T_a + \left(\frac{-2U_{wo} A_w - 2U_{wi} A_w}{\rho_w V_w c_{pw}} \right) T_w + \left(\frac{\alpha_w \sigma_s A_{win}}{\rho_w V_w c_{pw}} \right) I_{dr} + \left(\frac{2U_{wo} A_w}{\rho_w V_w c_{pw}} \right) T_{sa} \right]$$

$$\frac{dT_m}{dt} = \left(\frac{U_m A_m}{\rho_m V_m c_{pm}} \right) T_a + \left(\frac{-U_m A_m}{\rho_m V_m c_{pm}} \right) T_m + \left(\frac{\alpha_m \sigma_s A_{win}}{\rho_m V_m c_{pm}} \right) I_{dr}$$

$$A = \begin{pmatrix} a_{11} & a_{12} & a_{13} \\ a_{21} & a_{22} & 0 \\ a_{31} & 0 & a_{33} \end{pmatrix} B = \begin{pmatrix} b_{11} \\ 0 \\ 0 \end{pmatrix} F = \begin{pmatrix} f_{11} & f_{12} & f_{13} & f_{14} & f_{15} & 0 & f_{17} \\ f_{21} & 0 & 0 & 0 & 0 & f_{26} & 0 \\ f_{31} & 0 & 0 & 0 & 0 & 0 & 0 \end{pmatrix}$$

$$TZ = \det \begin{vmatrix} a_{11} - s & a_{12} & a_{13} & b_{11} \\ a_{21} & a_{22} - s & 0 & b_{21} \\ a_{31} & 0 & a_{33} - s & b_{31} \\ c_{11} & c_{12} & c_{13} & 0 \end{vmatrix} = 0$$

Air temperature feedback

$$C = (1 \ 0 \ 0), D = 0, E = 0$$

Comfort temperature feedback

$$C = (c_{11} \ c_{12} \ c_{13}), D = 0, E = 0$$

With a radiator the Q_p is divided into three components, affecting air, internal thermal mass and external thermal mass, hence the B matrix will change for radiator as follows:

$$A = \begin{pmatrix} a_{11} & a_{12} & a_{13} \\ a_{21} & a_{22} & 0 \\ a_{31} & 0 & a_{33} \end{pmatrix} B = \begin{pmatrix} b_{11} \\ b_{21} \\ b_{31} \end{pmatrix} F = \begin{pmatrix} f_{11} & f_{12} & f_{13} & f_{14} & f_{15} & 0 & f_{17} \\ f_{21} & 0 & 0 & 0 & 0 & f_{26} & 0 \\ f_{31} & 0 & 0 & 0 & 0 & 0 & 0 \end{pmatrix}$$

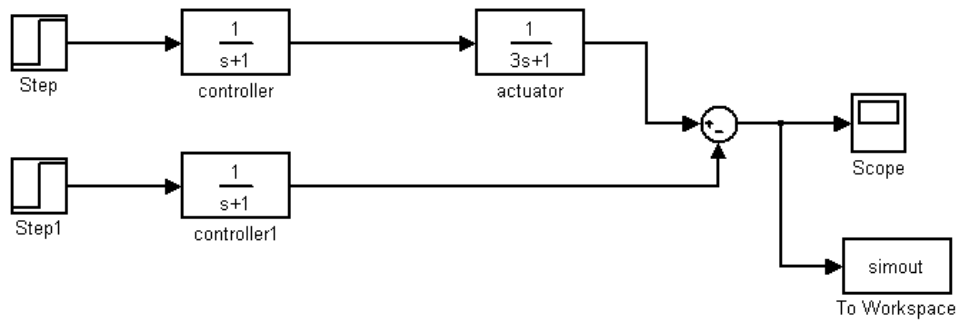
Where:

$$b_{11} = k_a Q_p, b_{21} = k_b Q_p, b_{31} = k_c Q_p$$

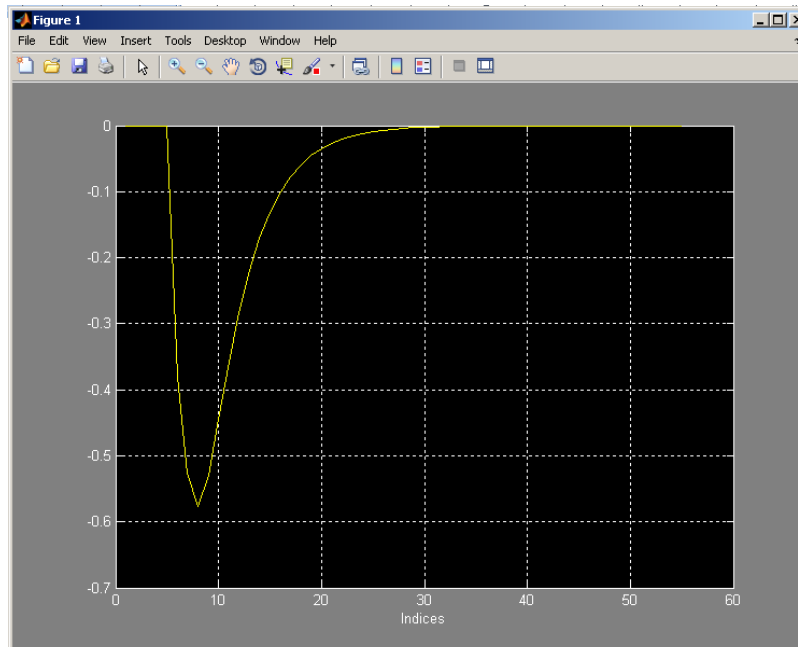
16 : Appendix 9 – Proof of controller bandwidth to be 3 times slower

To prove that actuator dynamics can be assumed to be fast it can shown as follows:

A block diagram was created in simulink:



In the first row of blocks the controller is assumed having a third of the time constant of the actuator. And in the second row of the actuator is assumed fast i.e. transfer function = 1. A step input is applied to both systems and the errors between the two signals are compared.



The figure above clearly shows that the error between the two systems is about 0.5 and in time the error is zero as the system reaches steady state. Hence the error between assuming a fast actuator i.e. Transfer function =1 or taking actuator bandwidth as 3 times the controller is very small and thus proves the assumption.

17 : Appendix 10 – standard SAP values

3) Well Insulated House Information (based upon: 20110206 - IDEAS - Well Insulated House B Matrix = 1 0 0.xlsx)

Definition of Figures and Variables

Mv	0.037035971	kg/s	Mass of the Dwelling Air
Ca	1012	J/(kg.K)	Specific Heat Capacity of Air
Us	0.3	(W/m ² K)	Heat Transfer Co-Efficient of the Structure
As	85.6	(m ²)	Surface Area of Structure
Ur	0.13	(W/m ² K)	Heat Transfer Co-Efficient of the Roof
Ar	44.4	(m ²)	Area of Roof
Uw	1.5	(W/m ² K)	Heat Transfer Co-Efficient of the Windows
Aw	16.9	(m ²)	Area of the Windows
Ma	249.795	kg	Mass of the air
Pa	1.22	kg/m ³	Density of Air
Va	204.75	m ³	Volume of Air
Ms	13696	kg	Mass of Structure
Cs	800	J/(kg.K)	Specific Heat Capacity of Structure
Uf	0.2	(W/m ² K)	Heat Transfer Co-Efficient
Af	44.4	(m ²)	Area of the Floor
Pb	800	kg/m ³	Brick density
Mft	6900	kg	Mass of the Furniture
Pft	400	kg/m ³	Density of Furniture
Vft	17.25	m ³	Volume of Furniture
Cft	900	J/(kg.K)	Specific Heat Capacity of Furniture
Uft	2.574	(W/m ² K)	Heat Transfer Co-Efficient of the Furniture
Aft	34.5	m ²	Area of Internal Mass in a Dwelling
Tfur	0.5	m	Thickness of Furniture

18 : Appendix 11 – ESL code for dynamic simulation

SIMPLIFIED 3RD ORDER MODEL

SIMULATION (EXPERIEMNT) FILE

```
STUDY
INCLUDE "DERIV";
INCLUDE "LIMIT";
INCLUDE "PA_DATA";
INCLUDE "SM_BUILDING";
INCLUDE "SM_ACTUATOR";
INCLUDE "SM_CONTROLLER";

MODEL ZONE();
REAL: ua,uc,y,tday;

INITIAL

DYNAMIC

y,tday:=SM_BUILDING(ua);
ua:=SM_ACTUATOR(uc);
uc:=SM_CONTROLLER(y,tday);

END ZONE;

-- Experiment

ALGO :=2; -- FOURTH ORDER RUNGE KUTTA
TSTART:=0.0;--START TIME
TFIN :=86400;--FINISH TIME -- days 86400s = 1 day profile
CINT:=60;--COMMUNICATION INTERVAL; -- 30.0 s
NSTEP:=5;-- i.e. integration step is 30 seconds.

ZONE;

END_STUDY
```

SUBMODEL DATA FILE

PACKAGE pa_data;

REAL:UL/5000.0/;

REAL:LL/0.0/;

-- zone dimensions (m)

REAL: L/5.0/;

REAL: w/5.0/;

REAL: h/5.0/;

-- densities kg/m³

REAL: rhoa/1.22/;

REAL: rhow/800.0/;

REAL: rhom/400.0/;

-- data transmission zero calculation

-- these are the ratio of heat from radiator going into air, wall and furniture

REAL: ka/0.3/; -- 0.3

REAL: kb/0.3/; -- 0.3

REAL: kc/0.4/; -- 0.4

-- c constants are the comfort temperature constants

REAL: c11/0.33/;

REAL: c12/0.33/;

REAL: c13/0.33/;

REAL: kcm/0.33/;

-- Volumes m³

REAL: Va/125.0/;

REAL: Vw/45.0/;

REAL: Vm/69.0/;

-- specific heat capacities units = J/kg k

REAL: cpa/1012.0/;

REAL: cpw/800.0/; -- 400, 800, 1200

REAL: cpm/400.0/;

-- Areas m²

REAL: Aw/150.0/;

REAL: Awin/16.9/;

REAL: Am/138.0/;

```

-- constants

REAL: alpa/1.0/;
REAL: alpw/0.0/;
REAL: alpm/0.0/;
REAL: sigs/0.8/;
REAL: ke/1.0/;
REAL: ksa/0.026/;

-- U values W/m^2K

REAL: Uwi/0.22/; --0.1, 0.2, 0.3, 0.4
REAL: Uwo/0.22/;
REAL: Uwin/1.5/;
REAL: Um/2.57/;

-- others

REAL: n/0.0000694/; -- ACR
REAL: np/5.0/; -- no. of occupants
REAL: Gpp/60.0/; -- occupancy heat generation rate

END pa_data;

```

SUBMODEL ACTUATOR FILE

```

SUBMODEL sm_actuator(REAL:ua:=REAL:uc);
USE pa_data;

-- upper and lower limits

REAL:x,ux;
REAL:tau/50.0/;

-- if you increase tau the time of decay of the control input will be slower

INITIAL

ux := 0.0;

DYNAMIC

x := Limit(LL,UL,uc);
ux' := (1.0/tau)*(x-ux);

ua:= ux;
COMMUNICATION

--PLOT "heat",t,uc[ua],0.0,TFIN,-3000.0,7000.0;
END sm_actuator;

```

BUILDING MODEL FILE

```
SUBMODEL sm_building (REAL:y,tday:=REAL:ua);
```

```
USE pa_data;
```

```
-- variables for Heat transfers
```

```
REAL:Qsa,QL,Qoc,Qap,Qwi,Qwin,Qm,Qn,Qp,Qsw,Qwo,Qsm;
```

```
REAL:Tw,Tm,Ta;
```

```
REAL:ldr,PL,To,Tsa,setT;
```

```
REAL:Tadot;
```

```
REAL:hour,day,ueq,ueq2,ydot;
```

```
REAL:a11,a12,a13,b11,a21,a22,b21,a31,a33,b31,cbinv,setTdot,utrim1,utrim2,utrim  
3;
```

```
REAL: f11,f21,f31,f12,f13,f14,f15,f26,f17;
```

```
--external weather variables
```

```
FILE:file1;          -- File Handler
```

```
REAL:x(8000,2);      -- File Buffer
```

```
INTEGER:J,I;         -- Counter
```

```
INTEGER:Comm_Sync;   -- To sync an hourly weather data to communication  
interval
```

```
REAL: v1,v2,v3,v4;
```

```
INITIAL
```

```
-- initial temperatures
```

```
Ta:=295.0;
```

```
Tw:=284.0;
```

```
Tm:=295.0;
```

```
day:= 0.0;
```

```
-- code for reading from a data file
```

```
OPEN file1,"weather1.csv";
```

```
READ file1,x;
```

```
J:=1;
```

```
Comm_Sync:=0;
```

```
v1:=283.4;
```

```
v3:=0.0;
```

```
DYNAMIC
```

```
-- Disturbances
```

```
--PL:=135.0;
```

```
Qp:=ua;
```

```

-- air temperature

Tadot:=(1.0/(rhoa*Va*cpa))*(Qsa+QL+Qoc+Qap+Qwi+Qwin+Qm+Qn+(ka*Qp));
Ta' := Tadot;

-- Casual gains
-- lighting gain is based on 5.4 W/m2, QL:=ke*PL, lights on at 9am and off at 5 pm
QL:= if tday >(9.0*3600.0) and tday < (17.0*3600.0) then ke*5.4*25.0 else 0.0;

-- occupancy gains, people in at 9am and leave at 5pm, Qoc:=np*Gpp;
Qoc:= if tday >(9.0*3600.0) and tday < (17.0*3600.0) then np*Gpp else 0.0;

-- appliance gains
Qap:=0.0;

Qsa:=alpa*sigs*Aw*Idr;
Qwi:=2.0*Uwi*Aw*(Tw-Ta);
Qwin:=Uwin*Aw*(To-Ta);
Qm:=Um*Am*(Tm-Ta);
Qn:=Va*n*rhoa*cpa*(To-Ta);

-- external thermal mass

Tw':=(1.0/(rhow*Vw*cpw))*(Qsw+Qwo-Qwi+(kb*Qp));

Qwo:=2.0*Uwo*Aw*(Tsa-Tw);
Qsw:=alpw*sigs*Aw*Idr;

-- internal thermal mass

Tm':=(1.0/(rhom*Vm*cpm))*(Qsm-Qm+(kc*Qp));

Qsm:=alpm*sigs*Aw*Idr;

-- Sol-air temperature model

Tsa:=To+(ksa*Idr);

-- Weather Data input

-- day counter

tday:= t - (day*3600*24);

When (tday/(24*3600)) > 1.0 then
day := day + 1;
end_when;

-- Hour counter for reading the weather file
hour:= t - (J*3600);
When (hour/3600) > 1.0 then

```

```

J:=J+1;
end_when;

-- external temperature
v2:=x(J,1)+273;
v1'=(1.0/3600.0)*(v2-v1);
To:=v1;

-- direct solar radiation
v4:=x(J,2);
v3'=(1.0/3600.0)*(v4-v3);
ldr:=v3;

setT:= if tday >(9.0*3600.0) and tday < (17.0*3600.0) then 294.0 else 287.0;

-- UTRIM = -Cbinv ydot + Ua

-- For air temperature control

--ueq:=-(((rhoa*Va*cpa)/3)*ydot)+(ua);

-- For comfort temperature control

cbinv:=
(1/(((c11*ka)/(rhoa*Va*cpa))+((c12*kb)/(rhov*Vw*cpw))+((c13*kc)/(rhom*Vm*cpm)))
);

ueq:=(-cbinv*(ydot))+(Qp);
ueq2:=(-cbinv*(setTdot))+(Qp);

-- ORIGINAL UTrim

utrim1:=
cbinv*kcm*(((a11+a21+a31)*(setT))+((a12+a22)*Tw)+((a13+a33)*Tm)+((f11+f21+f3
1)*ldr)+(f12*QL)+(f13*Qoc)+(f14*Qap*0.0)+(f15*To)+(f26*Tsa)+(f17*n*0.0));
utrim2:=
cbinv*kcm*(((a11+a21+a31)*(Ta))+((a12+a22)*Tw)+((a13+a33)*Tm)+((f11+f21+f31)
*ldr)+(f12*QL)+(f13*Qoc)+(f14*Qap*0.0)+(f15*To)+(f26*Tsa)+(f17*n*0.0));

-- Sensor equation

-- air temperature
--y:=Ta;

-- Comfort temperature
y:=(Ta/3)+(Tw/3)+(Tm/3);

-- Rate of change calculation

ydot:=DERIV(0.0,y);
setTdot:=DERIV(0.0,setT);

```

-- State Space parameters calculation

```
a11:=(1/(rhoa*Va*cpa))*(-(2.0*Uwi*Aw)-(Uwin*Aw)-(Um*Am)-(Va*rhoa*cpa*n));
a12:=(2.0*Uwi*Aw)/(rhoa*Va*cpa);
a13:=(Um*Am)/(rhoa*Va*cpa);
b11:=ka/(rhoa*Va*cpa);
a21:=(2.0*Uwi*Aw)/(rhow*Vw*cpw);
a22:=(-(2.0*Uwo*Aw)-(2.0*Uwi*Aw))/(rhow*Vw*cpw);
b21:=kb/(rhow*Vw*cpw);
a31:=(Um*Am)/(rhom*Vm*cpm);
a33:=(-Um*Am)/(rhom*Vm*cpm);
b31:=kc/(rhom*Vm*cpm);
```

```
f11:=(alpa*sigs*Aw)/(rhoa*Va*cpa);
f21:=(alpw*sigs*Aw)/(rhow*Vw*cpw);
f31:=(alpm*sigs*Aw)/(rhom*Vm*cpm);
f12:=ke/(rhoa*Va*cpa);
f13:=1/(rhoa*Va*cpa);
f14:=1/(rhoa*Va*cpa);
f15:=((Uwin*Aw)+(Va*rhoa*cpa*n))/(rhoa*Va*cpa);
f26:=(2.0*Uwo*Aw)/(rhoa*Va*cpa);
f17:=(To-Ta);
```

COMMUNICATION

```
--PLOT "Temp",t,y-273.0[setT-273.0],0.0,TFIN,263.0-273.0,314.0-273.0;
--PLOT "heat",t,utrim1[utrim2],0.0,TFIN,-80000.0,30500.0;
--PLOT "heat",t,ueq[ueq2],0.0,TFIN,0.0,6000.0;
TABULATE "datanew.txt",t/3600.0,y-273.0,setT-273.0,UL,ueq,ueq2;
--TABULATE "data400.txt",t/3600.0,ua,UL;
--PRINT "variables1",a22,b21,a31,a33,b31;
--PRINT "variables2",a11,a12,a13,b11,a21;
--PRINT "cbinv",cbinv,;
```

END sm_building;

CONTROLLER MODEL FILE

SUBMODEL sm_controller (REAL:uc:=REAL:y,tday);

USE pa_data;

REAL:set,Tset,edot,elast;
REAL:e,z;

REAL: kp/0.3/; --0.3
REAL: ki/0.9/;
REAL: kd/0.0/;

REAL:V/294.0/;

INITIAL

z:=0.0;

DYNAMIC

set:= if tday >(9.0*3600.0) and tday < (17.0*3600.0) then V else 287.0;

e:= set-y;

z':= e;

uc := kp*e + (ki*z);

COMMUNICATION

if uc > UL then
z:=(1.0/ki)*(UL-(kp*e));
end_if;
if uc < LL then
z:=(1.0/ki)*(LL-(kp*e));
end_if;

END sm_controller;

FULL 6TH ORDER MODEL

SIMULATION (EXPERIEMNT) FILE

STUDY

```
INCLUDE "DERIV";
INCLUDE "LIMIT";
INCLUDE "PA_DATA";
INCLUDE "SM_BUILDING";
INCLUDE "SM_ACTUATOR";
INCLUDE "SM_CONTROLLER";
```

```
MODEL ZONE();
REAL: ua,uc,y,tday;
```

INITIAL

DYNAMIC

```
y,tday:=SM_BUILDING(ua);
ua:=SM_ACTUATOR(uc);
uc:=SM_CONTROLLER(y,tday);
```

END ZONE;

-- Experiment

```
ALGO :=2; -- FOURTH ORDER RUNGE KUTTA
TSTART:=0.0;--START TIME
TFIN :=86400;--FINISH TIME -- days 86400s = 1 day profile -- 900
CINT:=900;--60COMMUNICATION INTERVAL; -- 30.0 s
NSTEP:=2;-- i.e. integration step is 30 seconds.
```

ZONE;

END_STUDY

SUBMODEL DATA FILE

PACKAGE pa_data;

-- globalspec engineering search engine

REAL: UL/1000.0/;

REAL: LL/0.0/;

-- zone and elements dimensions (m)

REAL: lz/4.32/; -- facade width

REAL: wz/3.15/;

REAL: hz/4.96/;

REAL: lw1/4.32/;

REAL: lw2/3.15/;

REAL: lw3/4.32/;

REAL: lw4/3.15/;

REAL: lf/4.32/;

REAL: lr/4.32/;

REAL: lm/2.0/;

REAL: lwin/1.42/;

REAL: ww1/2.5/;

REAL: ww2/2.5/;

REAL: ww3/2.5/;

REAL: ww4/2.5/;

REAL: wf/3.15/;

REAL: wr/3.15/;

REAL: wm/1.5/; --check

REAL: wwin/0.83/;

REAL: thw1/0.1/; -- 100 mm width internal wall *** check

REAL: thw2/0.1/; -- 100 mm width facing brick work

REAL: thw3/0.1/; -- 100 mm width facing brick work

REAL: thw4/0.1/; -- 100 mm width facing brick work

REAL: thf/0.1/; -- 100 mm cast concrete

REAL: thr/0.1/; -- 100 mm fibre glass

REAL: thm/1.0/; -- wrong ***

REAL: lp/0.854/;

REAL: wp/0.586/;

REAL: thp/0.011/;

-- densities kg/m³

REAL: rhoa/1.22/;

REAL: rhow1/1700.0/; -- uter leaf brick work

REAL: rhow2/1700.0/; --

REAL: rhow3/1700.0/; --

REAL: rhow4/1700.0/; --

REAL: rhof/2000.0/; -- cast concrete (bath university)

REAL: rhor/12.0/; -- fibre glass (bath university)

REAL: rhom/400.0/; -- wrong **** 500 for wood and 100 for furniture (i.e foam part of chairs etc)

REAL: rhop/2094.0/; -- 0.9 for oil, 7850 for low carbon steel weighted average 2094

```

-- specific heat capacities units = J/kg k
REAL: cpa/1012.0/;
REAL: cpw1/800.0/; -- outer leaf brick work
REAL: cpw2/800.0/; -- outer leaf brick work
REAL: cpw3/800.0/; -- outer leaf brick work
REAL: cpw4/800.0/; -- outer leaf brick work
REAL: cpf/1000.0/; -- cast concrete (bath university)
REAL: cpr/840.0/; -- fibre glass (bath university)
REAL: cpm/900.0/; -- wrong*** or 1600
REAL: cpp/1964.0/; -- 2500 of oil, 490 of steel wrong***** weightedf average 1964

-- U values W/m^2K
REAL: Uw1/0.36/;
REAL: Uw2/0.36/;
REAL: Uw3/0.36/;
REAL: Uw4/0.36/;
REAL: Uf/0.33/;
REAL: Ur/0.29/;

REAL: Uwi1/0.36/; -- *
REAL: Uwi2/0.36/; -- *
REAL: Uwi3/0.36/; -- *
REAL: Uwi4/0.36/; -- *
REAL: Uwin/3.0/; -- * check
REAL: hm/1.57/; -- check
REAL: hp/6.5/; -- hp:=1.78*(abs(Tp-Ta)**0.32)
REAL: Ufi/0.33/; -- *
REAL: Ufo/0.33/; -- *
REAL: Uri/0.29/; -- *
REAL: Uro/0.29/; -- *
REAL: Uwo1/0.36/; -- *
REAL: Uwo2/0.36/; -- *
REAL: Uwo3/0.36/; -- *
REAL: Uwo4/0.36/; -- *
REAL: krd/2.5/; --krd:=em*bolt*Ap*((Tp**2)+(Tm**2))*(Tp+Tm);
REAL: kc/0.8/; --- convection constant for reduced model
REAL: kr/0.2/; --- radiation constant for reduced model
--REAL: Up/158.0/; check

-- others
REAL: taup/300.0/;
REAL: alpa/0.2/;
REAL: alpm/0.8/;
REAL: sigs/0.5/;
REAL: ke/1.0/;
REAL: ksa/0.026/;
REAL: em/0.5/;
REAL: bolt/0.000000567/;
REAL: ni/0.0000694/; --
REAL: np/5.0/; --
REAL: Gpp/60.0/; --
REAL: cd/1.0/; --

```

```

REAL: gv/9.81; --
REAL: dh/1.0; --
REAL: cv/1.0; --
REAL: PL/1.0; --
REAL: To5/283.0; -- ground temperature

```

```

END pa_data;

```

SUBMODEL ACTUATOR FILE

```

SUBMODEL sm_actuator(REAL:ua:=REAL:uc);
USE pa_data;

```

```

-- upper and lower limits

```

```

REAL:x,ux;
REAL:tau/300.0;

```

```

-- if you increase tau the time of decay of the control input will be slower

```

INITIAL

```

ux := 0.0;

```

DYNAMIC

```

x := Limit(LL,UL,uc);
ux' := (1.0/tau)*(x-ux);

```

```

ua:= ux;

```

```

END sm_actuator;

```

BUILDING MODEL FILE

```

--*****
--*****
--***** SUBMODEL: BUILDING PHYSICS *****
--*****
--*****

```

```

-- for this case study the zone is a mid terraced house. its walls 1 and 4
-- have no heat loss (i.e. no heat loss between houses) thus Qwo1=Qwo4=0.
-- Also the external wall is connected to the outside temperature thus
-- To3=Tsa; where Tsa is the sol-air temperature. To4 is the temperature
-- in the kitchen ** wrong. This model is for thermal analysis only. there is no
-- passive stack or mechanical ventilation thus Qnt=Qnv=Qmv=0, also

```

-- Qoc=Qap=QL=0

SUBMODEL sm_building (REAL:y,tday:=REAL:ua);
USE pa_data;

----- Declaration of Variables -----

----- variables in equations -----

REAL:Ta,Qsa,QL,Qoc,Qap,Qwi1,Qwi2,Qwi3,Qwi4,Qfi,Qri,Qwin,Qm,Qnt,Qnv,Qni;
REAL:Qmv,Qcp,ldr,Tw1,Tw2,Tw3,Tw4,Tf,Tr,Tm,Tp,Tsa,Tadot,Qsw1,Qsw2,Qsw3;
REAL:Qsw4,Qwo1,Qwo2,Qwo3,Qwo4,To1,To2,To3,To4,To6,Qfo,Qsf,Qsm,Qro;
REAL:Qrpm,Qrpw1,Qrpw2,Qrpw3,Qrpw4,kv,nv,vo,Qp,Qpac,z3,z6,nt,Tac,Um1;
REAL:Va,Vw1,Vw2,Vw3,Vw4,Vf,Vr,Vm,Aw1,Aw2,Aw3,Aw4,Awin,Am,Af,Ar,Tac2;
REAL:Tac1,Qpac2,Qpac1,Tk1,Tk2,Tk,Up,Ap,Vp;

REAL:setT,Qtot,Q_in,Q_out,Q_stor;
REAL:time,day,ueq,ueq2,ydot,per;
REAL:a11,a12,a13,a14,a15,a16,a17,a18,a19,f11;
REAL:f14,a21,a22,f22,a31,a33,f33,a41,a44,f44;
REAL:a51,a55,f55,a61,a66,f66,a71,a77,f77,a81;
REAL:a88,a89,f81,a91,a98,a99,b91,b101,f108;
REAL: b11,f12,f13,f15,f16,f17,f24,b31,f31; -- 3om

----- External weather data -----

-- The weather file is declared by the file handler
-- then the file buffer reads from the rows and columns
-- the counter counts the rows and columns and then a
-- integer is assigned to synchronise the weather data
-- with the communication interval.

FILE:file1;
REAL:x(1056,11);
INTEGER:J,I;
INTEGER:Comm_Sync;
REAL:
v1,v2,v3,v4,v5,v6,v7,v8,v9,v10,v11,v12,v13,v14,v15,v16,v17,v18,v19,v20,v21,v22;

----- INITIALISE VARIABLES -----

INITIAL

----- Building parameters -----

Ta:=297.6;
Tw1:=297.15;
Tw2:=297.6;
Tw3:=297.15;
Tw4:=297.6;
Tf:=294.3;
Tr:=297.55;
Tm:=296.6;
Tp:=330.6;

day:= 0.0;

----- weather file -----

OPEN file1,"weather.csv";

READ file1,x;

J:=1;

Comm_Sync:=0;

v1:=3.6+273.0;

v3:=22.0;

v5:=23.7+273.0;

v7:=4.3;

v9:=24.5+273.0;

v11:=173.0;

v13:=24.6+273.0;

v15:=24.6+273.0;

v17:=243.0;

v19:=25.1+273.0;

v21:=23.5+273.0;

----- DYNAMIC REGION -----

DYNAMIC

-- Dimensions

-- Areas

Aw1:=lw1*ww1;

Aw2:=lw2*ww2;

Aw3:=(lw3*ww3)-(Awin);

Aw4:=lw4*ww4;

Awin:=lwin*wwin;

Am:=lm*wm;

Af:=lf*wf;

Ar:=lr*wr;

Ap:=lp*wp;

-- volumes

Va:=(Lz*wz*hz)-Vm;

Vw1:=Aw1*thw1;

Vw2:=Aw2*thw2;

Vw3:=Aw3*thw3;

Vw4:=Aw4*thw4;

Vf:=Af*thf;

Vr:=Ar*thr;

Vm:=0.05141*(Lz*wz*hz); -- 0.05141kg/m3 Am*thm;

Vp:=Ap*thp;

-- note area and volume of the plant radiator (Vp, Ap) are given in data file

-- due to volume calculation being different from the external surface area

-- this is why these variables have been defined individually.

----- Air temperature equation -----

-- Differential equation

```

Tadot:=(1.0/(rhoa*Va*cpa))*(Qsa+Qwi1+Qwi2+Qwi3+Qwi4+Qfi+Qri+Qwin+Qm+Qcp
+(Qpac*0.0));
Ta':= Tadot;
Qsa:=alpa*sigs*Aw1*Idr;
Qwi1:=2.0*Uwi1*Aw1*(Tw1-Ta);
Qwi2:=2.0*Uwi2*Aw2*(Tw2-Ta);
Qwi3:=2.0*Uwi3*Aw3*(Tw3-Ta);
Qwi4:=2.0*Uwi4*Aw4*(Tw4-Ta);
Qfi:=2.0*Ufi*Af*(Tf-Ta);
Qri:=2.0*Uri*Ar*(Tr-Ta);
Qwin:=Uwin*Aw1*(To3-Ta);
Qm:=hm*Am*(Tm-Ta);
Qcp:=hp*Ap*(Tp-Ta);
--hp:=1.78*(abs(Tp-Ta)**0.32); -- equation 11 ashrae systems 2008 s06
----- Wall temperature equations -----
-- Differential equation
Tw1':=(1.0/(rho1*Vw1*cpw1))*(Qwo1-Qwi1);
Tw2':=(1.0/(rho2*Vw2*cpw2))*(Qwo2-Qwi2);
Tw3':=(1.0/(rho3*Vw3*cpw3))*(Qwo3-Qwi3);
Tw4':=(1.0/(rho4*Vw4*cpw4))*(Qwo4-Qwi4);
-- External heat transfer
Qwo1:=2.0*Uwo1*Aw1*(Tk-Tw1); -- To1 - original Kitchn Temp, Avergae = Tk
Qwo2:=0.0;--2.0*Uwo2*Aw2*(283.0-Tw2); -- To2 = 10 degree = 283
Qwo3:=2.0*Uwo3*Aw3*(Tsa-Tw3);
Qwo4:=0.0;--2.0*Uwo4*Aw4*(283.0-Tw4); -- To4 = 10 Degree

----- Floor temperature equations -----
-- Differential equation
Tf':=(1.0/(rho5*Vf*cpf))*(Qfo-Qfi);
-- External heat transfer
Qfo:=2.0*Ufo*Af*(To5-Tf);

----- Roof temperature equations -----
-- Differential equation
Tr':=(1.0/(rho6*Vr*cpr))*(Qro-Qri);
-- External heat transfer
Qro:=2.0*Uro*Ar*(To6-Tr);

----- Mass temperature equations -----
-- Differential equation
Tm':=(1.0/(rho7*Vm*cpm))*(Qsm-Qm+Qrpm+(Qpac*0.0));
-- Mass solar heat gain
Qsm:=alpm*sigs*Aw1*Idr;
-- Heat gain from plant
Qrpm:=em*bolt*Ap*((Tp**4)-(Tm**4));
--krd:=em*bolt*Ap*((Tp**2)+(Tm**2))*(Tp+Tm);
----- Plant thermal equations -----
-- Differential equation
Tp':=(1.0/(rho8*Vp*cpp))*((Qpac)-Qrpm-Qcp);
-- Power input to the plant
Qp:=ua;

----- Weather data input -----

```

```

-- Sol air temperature
Tsa:=To3+(ksa*(ldr));
-- day counter
tday:= t - (day*3600*24);
When (tday/(24*3600)) > 1.0 then
day := day + 1;
end_when;

-- counter for reading the weather file
per:=900.0; -- in seconds
time:= t - (J*per);
When (time/per) > 1.0 then
J:=J+1;
end_when;
-- external air temperature zone 3 (To3)
v2:=x(J,1)+273;
v1'=(1.0/per)*(v2-v1);
To3:=v1;
-- direct solar radiation
v4:=x(J,2);
v3'=(1.0/per)*(v4-v3);
ldr:=v3;
-- zone 1 (kitchen temperature) (To1)
v6:=x(J,3)+273;
v5'=(1.0/per)*(v6-v5);
To1:=v5;
-- external wind speed
v8:=x(J,4);
v7'=(1.0/per)*(v8-v7);
vo:=v7;
-- zone 6 above the roof (another room) (To6)
v10:=x(J,5)+273;
v9'=(1.0/per)*(v10-v9);
To6:=v9;
-- Qp heat output
v12:=x(J,6);
v11'=(1.0/per)*(v12-v11);
Qpac1:=v11;
-- actual measured zone air temp TAC
v14:=x(J,7)+273;
v13'=(1.0/per)*(v14-v13);
Tac1:=v13;
-- actual measured zone air temp TAC2
v16:=x(J,8)+273;
v15'=(1.0/per)*(v16-v15);
Tac2:=v15;
-- Qp from heater two
v18:=x(J,9);
v17'=(1.0/per)*(v18-v17);
Qpac2:=v17;
-- actual measured kitchen temperature Tk1
v20:=x(J,10)+273;
v19'=(1.0/per)*(v20-v19);

```

```

Tk1:=v19;
-- actual measured kitchen temperature Tk2
v22:=x(J,11)+273;
v21'=(1.0/per)*(v22-v21);
Tk2:=v21;

Tk:=(Tk1+Tk2)/2;

-- Qpac is now the average measured heat from the two values
Qpac:=Qpac1+(Qpac2*0.2);
-- Tac is now the average measured temperatures from the two values
Tac:=((Tac1)+(Tac2))/2;

-- setT:= if tday >(9.0*3600.0) and tday < (17.0*3600.0) then 294.0 else 287.0;

setT:= if t < 309600 then 297.0 else 301.0;

y:=Ta;

-- ***** SCRAP *****
-- UTRIM
--ueq:=-((3*rhoa*Va*cpa*ydot)+(ua);
--ueq2:=-Qn-Qwin-Qwi-Qm-Qsa-QL-Qoc-Qap;
-- output
--y:=(Ta/3)+(Tw/3)+(Tm/3);
--ydot:=DERIV(0.0,y);
-- *****

-- conservation of energy
--
Q_in:=Qsa+Qwi1+Qwi2+Qwi3+Qwi4+Qfi+Qri+Qwin+Qm+Qcp+Qsw1+Qrpw1+Qwo
1+Qsw2+Qrpw2+
--
Qwo2+Qsw3+Qrpw3+Qwo3+Qsw4+Qrpw4+Qwo4+Qsf+Qfo+Qro+Qsm+Qrpm+Qp;

--Q_out:=-Qwi1-Qwi2-Qwi3-Qwi4-Qfi-Qri-Qm-Qrpm-Qrpw1-Qrpw2-Qrpw3-Qrpw4-
Qcp;

--
Q_stor:=(Qsa+Qwi1+Qwi2+Qwi3+Qwi4+Qfi+Qri+Qwin+Qm+Qcp)+(Qsw1+Qrpw1+
Qwo1-Qwi1)
--+(Qsw2+Qrpw2+Qwo2-Qwi2)+(Qsw3+Qrpw3+Qwo3-
Qwi3)+(Qsw4+Qrpw4+Qwo4-Qwi4)
--+(Qsf+Qfo-Qfi)+(Qro-Qri)+(Qsm+Qrpm-Qm)+(Qp-Qrpm-Qrpw1-Qrpw2-Qrpw3-
Qrpw4-Qcp);

--Qtot:=Q_in+Q_out-Q_stor;

-----
-- frequency response

a11:=(-(2*Uw1*Aw1)-(2*Uw2*Aw2)-(2*Uw3*Aw3)-(2*Uw4*Aw4)-(2*Uf*Af)-(2*Ur*Ar)-
(Uwin*Aw1)-(hm*Am)-(hp*Ap))/(rhoa*Va*cpa);

```

```

a12:=(2*Uw1*Aw1)/(rhoa*Va*cpa);
a13:=(2*Uw2*Aw2)/(rhoa*Va*cpa);
a14:=(2*Uw3*Aw3)/(rhoa*Va*cpa);
a15:=(2*Uw4*Aw4)/(rhoa*Va*cpa);
a16:=(2*Uf*Af)/(rhoa*Va*cpa);
a17:=(2*Ur*Ar)/(rhoa*Va*cpa);
a18:=(hm*Am)/(rhoa*Va*cpa);
a19:=(hp*Ap)/(rhoa*Va*cpa);
f11:=(alpa*sigs*Aw1n)/(rhoa*Va*cpa);
f14:=(Uwin*Aw1n)/(rhoa*Va*cpa);
a21:=(2*Uw1*Aw1)/(rhow1*Vw1*cpw1);
a22:=((-4)*Uw1*Aw1)/(rhow1*Vw1*cpw1);
f22:=(2*Uw1*Aw1)/(rhow1*Vw1*cpw1);
a31:=(2*Uw2*Aw2)/(rhow2*Vw2*cpw2);
a33:=((-4)*Uw2*Aw2)/(rhow2*Vw2*cpw2);
f33:=(2*Uw2*Aw2)/(rhow2*Vw2*cpw2);
a41:=(2*Uw3*Aw3)/(rhow3*Vw3*cpw3);
a44:=((-4)*Uw3*Aw3)/(rhow3*Vw3*cpw3);
f44:=(2*Uw3*Aw3)/(rhow3*Vw3*cpw3);
a51:=(2*Uw4*Aw4)/(rhow4*Vw4*cpw4);
a55:=((-4)*Uw4*Aw4)/(rhow4*Vw4*cpw4);
f55:=(2*Uw4*Aw4)/(rhow4*Vw4*cpw4);
a61:=(2*Uf*Af)/(rhof*Vf*cpf);
a66:=((-4)*Uf*Af)/(rhof*Vf*cpf);
f66:=(2*Uf*Af)/(rhof*Vf*cpf);
a71:=(2*Ur*Ar)/(rhor*Vr*cpr);
a77:=((-4)*Ur*Ar)/(rhor*Vr*cpr);
f77:=(2*Ur*Ar)/(rhor*Vr*cpr);
a81:=(hm*Am)/(rhom*Vm*cpm);
a88:=(-krd-(hm*Am))/(rhom*Vm*cpm);
a89:=krd/(rhom*Vm*cpm);
f81:=(alpm*sigs*Aw1n)/(rhom*Vm*cpm);
a91:=(hp*Ap)/(rhop*Vp*cpp);
a98:=krd/(rhop*Vp*cpp);
a99:=(-krd-(hp*Ap))/(rhop*Vp*cpp);
b91:=1/(rhop*Vp*cpp);
b101:=(-1)/(taup);
f108:=(1)/(taup);

```

COMMUNICATION

```
-- 3om state space vairables
```

```
--TABULATE
```

```
"SS3om.txt",t,a11,a12,a13,b11,f11,f12,f13,f14,f15,f16,f17,a21,a22,f24,a31,a33,b31,f31;
```

```
TABULATE
```

```
"SS6om.txt",t,a11,a12,a13,a14,a15,a16,a17,a18,a19,f11,f14,a21,a22,f22,a31,a33,f33,a41,a44,f44,a51,a55,f55,a61,a66,f66,a71,a77,f77,a81,a88,a89,f81,a91,a98,a99,b91,b101,f108;
```

```
PLOT "Temp",t,Ta-273.0[Tac-273.0],0.0,TFIN,296.0-273.0,303.0-273.0;
```

```
--PLOT "Temp",t,Tp-273[Ta-273],0.0,TFIN,263.0-273.0,370.0-273.0;
```

```
--PLOT "heat",t,Qpac[Qp],0.0,TFIN,-500.0,500.0;
```

```

--PLOT "heat",t,Qwi1[Qwi2,Qwi3,Qwi4,Qfi,Qri,Qwin,Qm],0.0,TFIN,-500.0,500.0;
--PLOT "heat",t,krd,0.0,TFIN,0.0,10.0;
--PLOT      "Temp",t,Tw1-273[Tw2-273,Tw3-273,Tw4-273,Tf-273,Tr-273,Tm-
273],0.0,TFIN,263.0-273.0,320.0-273.0;
--TABULATE "plot9.txt",t/86400.0,Tp-273.0,Ta-273.0;
--TABULATE "plot2.txt",t/86400.0,Tac-273,Ta-273,To3-273,Qpac,Qp;
--TABULATE "plot3.txt",t/86400.0,Qtot,Q_in,Q_out,Q_stor;
--TABULATE "plot6.txt",t/86400.0,Tw1-273,Tw2-273,Tw3-273,Tw4-273;
--TABULATE "plot7.txt",t/86400.0,Tf-273,Tr-273,Tm-273;
--PRINT "variables",Ta;
--PLOT "Temp",t,Ta-273.0[Tp-273.0],0.0,TFIN,263.0-273.0,350.0-273.0;
--PLOT "",t,Ta-273.0[Tp-273.0],0.0,TFIN,263.0-273.0,350.0-273.0;
--TABULATE "plot8Tp.txt",t/86400.0,Ta-273,Tp-273;
END sm_building;

```

CONTROLLER MODEL FILE

```
SUBMODEL sm_controller (REAL:uc:=REAL:y,tday);
```

```
USE pa_data;
```

```

REAL:set,Tset,edot,elast;
REAL:e,z;

REAL: kp/0.0009/--0.000019/; --0.3
REAL: ki/0.03/--0.01/; -- 0.9
REAL: kd/0.0/;

REAL:V/294.0/;

INITIAL

z:=0.0;

DYNAMIC

set:= if t < 309600 then 297.0 else 301.0;
--set:= if tday >(9.0*3600.0) and tday < (17.0*3600.0) then V else 287.0;

e:= set-y;

z':= e;

uc := kp*e + (ki*z);

COMMUNICATION

if uc > UL then
z:=(1.0/ki)*(UL-(kp*e));
end_if;
if uc < LL then
z:=(1.0/ki)*(LL-(kp*e));
end_if;

END sm_controller;

```

DETAILED RIDE MODEL

SIMULATION (EXPERIEMNT) FILE

STUDY

```

INCLUDE "LIMIT";
INCLUDE "LIMINT";
Include "RAMP";
INCLUDE "DERIV";
INCLUDE "PA_SMCPARR";
INCLUDE "SM_CONTROLLER";
INCLUDE "SM_ACTUATOR";
INCLUDE "SM_BUILDING";
INCLUDE "SM_RATES";

MODEL ZONE(:=REAL:utswitch);
REAL:y(1..3),uc1,uc2,uc3,ua(1..3),invcgx(1..3,1..3),tday,T1,utrim(1..3),utrimdot(1..3)
,ucdot(1..3),uadot(1..3),Dm(1..3,1..3);

INITIAL

DYNAMIC

uc1,uc2,uc3,utrim:=SM_CONTROLLER(ua,T1,invcgx,y,tday,utswitch,utrimdot,ucdot
,uadot,Dm);
ua:=SM_ACTUATOR(uc1,uc2,uc3);
invcgx,y,T1,tday,Dm:= SM_BUILDING(ua);
utrimdot,ucdot,uadot:=SM_RATES(uc1,uc2,uc3,ua,utrim);
END ZONE;

-- Experiment
REAL:utswitch/1.0/;

ALGO :=2; -- FOURTH ORDER RUNGE KUTTA
TSTART:=0.0;--START TIME
TFIN :=432000.0;--FINISH TIME;
CINT:=60.0;--COMMUNICATION INTERVAL;
NSTEP:=2;-- i.e. integration step is 30 seconds.
READ utswitch;

ZONE(:=utswitch);

END_STUDY

SUBMODEL DATA FILE

PACKAGE pa_smcpar;
PARAMETER REAL: co2_pp/0.0000125/; -- co2 per person kg/s: co2 paper
PARAMETER REAL: co2_rho/1.97/; -- co2 density kg/m^3
PARAMETER REAL: rho_air/1.205/; -- density of air kg/m^3

```

PARAMETER REAL: Cp_air/1005.0/; -- Cp of air J/kgC
PARAMETER REAL: h/2.961/; -- Zone height m
PARAMETER REAL: v1/1817.82/; -- volume of zone m³
PARAMETER REAL: floor_area/613.92/; -- floor area m
PARAMETER REAL: ke/1.0/; -- heat coefficient for lighting
PARAMETER REAL: Uw1/0.15/; -- U wall 1 W/m²C
PARAMETER REAL: Uw2/0.15/; -- U wall 2 W/m²C
PARAMETER REAL: Uw3/0.15/; -- U wall 3 W/m²C
PARAMETER REAL: Lw1/91.6/; -- wall 1 length m
PARAMETER REAL: Lw2/9.2/; -- wall 2 length m
PARAMETER REAL: Lw3/14.4/; -- wall 3 length m
PARAMETER REAL: rho_w1/517.28/; -- density wall 1 kg/m³
PARAMETER REAL: rho_w2/517.28/; -- density wall 2 kg/m³
PARAMETER REAL: rho_w3/517.28/; -- density wall 3 kg/m³
PARAMETER REAL: Cp_w1/1054.96/; -- Cp wall 1 J/kgk
PARAMETER REAL: Cp_w2/1054.96/; -- Cp wall 2 J/kgk
PARAMETER REAL: Cp_w3/1054.96/; -- Cp wall 3 J/kgk
PARAMETER REAL: t_w1/0.103/; -- wall 1 thickness m
PARAMETER REAL: t_w2/0.103/; -- wall 2 thickness m
PARAMETER REAL: t_w3/0.103/; -- wall 3 thickness m
PARAMETER REAL: Aw1/199.1976/; -- area of wall 1 m²
PARAMETER REAL: Aw2/27.2412/; -- area of wall 2 m²
PARAMETER REAL: Aw3/42.6384/; -- area of wall 3 m²
PARAMETER REAL: Uwin/0.17/; -- U windows W/m²k
PARAMETER REAL: Awin/72.03/; -- total Area of windows m²
PARAMETER REAL: Ufs/6.25/; -- U screed W/m²k
PARAMETER REAL: Ufc/4.55/; -- U concrete W/m²k
PARAMETER REAL: Urf/0.12/; -- u roof W/m²k
PARAMETER REAL: t_fs/0.065/; -- thickness of screed m
PARAMETER REAL: rho_fs/1200.0/; -- density of screed kg/m³
PARAMETER REAL: Cp_fs/840.0/; -- Cp of screed J/kgC
PARAMETER REAL: t_fc/0.3/; -- thickness of concrete m
PARAMETER REAL: rho_fc/2000.0/; -- density of concrete kg/m³
PARAMETER REAL: Cp_fc/1000.0/; -- Cp of concrete J/kgC
PARAMETER REAL: kL/0.52/; -- Lux per unit W lighting 500lux/108W
= 4.6 for 1 room BH p164 -- for whole zone 500lux/9*108w (9 rooms) =

0.52

PARAMETER REAL: ks/0.01/; -- w/m² per unit lux
PARAMETER REAL: alpha/0.05/; -- transmissivity of window
PARAMETER REAL: Anv/2.142/; -- 2.142 effective area of ventilation

openings

PARAMETER REAL: Uin/0.04/; -- insulation u value
PARAMETER REAL: bolt/0.0000000567/; -- boltzmans constant from radiation
PARAMETER REAL: Fr/0.87/; -- radiation exchange factor
PARAMETER REAL: g_acc/9.81/; -- gravitational acceleration
PARAMETER REAL: h_d/2.0/; -- height difference between inlet and

outlet vents

PARAMETER REAL: C_d/0.65/; -- discharge coefficient in NV equation
PARAMETER REAL: delta_cp/0.5/; -- winter coefficient of pressure is 0.5
PARAMETER REAL: now/14.0/; -- number of windows
PARAMETER REAL: Pf/800.0/; -- fan power per unit volume air flow

rate w/m³/s

```
PARAMETER REAL: kf/1.0;          -- proportion of fan power converted to
heat
END pa_smcparr;
```

SUBMODEL ACTUATOR FILE

```
SUBMODEL sm_actuator(REAL:ua(1..3):=REAL:uc1,uc2,uc3);
```

```
-- upper and lower limits
```

```
CONSTANT REAL:UL(1..3)[ 1.0,
                        100000.0,
                        50000.0 ];
```

```
CONSTANT REAL:LL(1..3)[ 0.0,
                        -100000.0,
                        0.0 ];
```

```
-- vector elements in the above limits are: ventilation (co2), light power
(Lights),Heating (temperature)
```

```
REAL:x,y,z,ua1,ua2,ua3;
CONSTANT REAL: tau1/180.0/,tau2/180.0/,tau3/180.0/;
```

```
-- if you increase tau the time of decay of the control input will be slower
```

INITIAL

```
ua1 := 0.0;
ua2 := 0.0;
ua3 := 0.0;
```

DYNAMIC

```
x := Limit(LL(1),UL(1),uc1);
y := Limit(LL(2),UL(2),uc2);
z := Limit(LL(3),UL(3),uc3);
```

```
ua1' := (1.0/tau1)*(x-ua1);
ua2' := (1.0/tau2)*(y-ua2);
ua3' := (1.0/tau3)*(z-ua3);
```

```
PROCEDURAL(ua := ua1,ua2,ua3);
  ua(1):= ua1;
  ua(2):= ua2;
  ua(3):= ua3;
END_PROCEDURAL;
```

```
END sm_actuator;
```

-- Note:
 -- That the PROCEDURAL region is required because you cannot set individual vector elements directly in the DYNAMIC region.

BUILDING MODEL FILE

SUBMODEL sm_building
 (Real:invcgx(1..3,1..3),y(1..3),T1,tday,Dm(1..3,1..3):=Real:ua(1..3));

USE pa_smcparr;

REAL:fen_in,fen_out;
 REAL:qmv,ucL,Qdoth,Qdotin,Qdotwin,Qdothmv;
 REAL:Qdotsol,QdotL,Qdotcon,Qdotrad,Qdotocc,Qdotapp,Qdotw1,Qdotmv,Qdotnv;
 REAL:Qdotfs,Qdotrf,Qdotni;
 REAL:Qdotw1i,Qdotw1o,Qdotw2i,Qdotw2o,Qdotw3i,Qdotw3o;
 REAL:Qdotfco;
 REAL:S,Cdotg,Cdotmv,Cdotnv,Cdotni;
 REAL:Lo,CLo,To,vo,lux_L,lux_S;
 REAL:Tfs,Tfc,PL,C1,Cc,Lc,Tc,Tw1,Tw2,Tw3;
 REAL:vnv,knv,DELTA_T;
 REAL:Vw1,Vw2,Vw3,Afs,Afc,Arf,Vfs,Vfc;
 REAL:ydot(1..3),b71,c28,b11,c31,b53,c35,c17,b82,T1dot,c38,d31,d31dot,d31last;
 REAL:u(1..3),ulast(1..3),ylast(1..3);
 REAL:day; -- 250 day counter and time of
 day in seconds.
 PARAMETER REAL: pupils/175.0/; -- normally 25*7 number
 of pupils in the class, 250 is extreme.
 -- PARAMETER REAL: vo/3.0/; -- external wind speed
 m/s Ref: standard
 PARAMETER REAL: Tomin/280.0/; -- kelvin : Minimum outside
 temp design day -1.0 degrees celcius
 PARAMETER REAL: Tomax/285.0/; -- kelvin : Maximum
 outside temp
 PARAMETER REAL: T2/283.0/; -- kelvin : 24.0 degrees
 celcius
 PARAMETER REAL: T6/283.0/; -- kelvin : 24.0 degrees
 celcius
 PARAMETER REAL: T4/283.0/; -- kelvin : 24.0 degrees
 celcius
 PARAMETER REAL: PLo/1075.0/; -- External lux level
 PARAMETER REAL: n/0.000069/; -- air exchange rate
 PARAMETER REAL: Co/0.000732/; -- kg/m^3 outside co2
 level 400 ppm

```
-- *****
-- ***** INITIAL REGION
-- *****
-- *****
```

INITIAL

```

T1:=288.0; -- initial air temp (K) 15.0 C
Tfs:=T1; -- initial screed temp
Tfc:=288.0; -- initial concrete temp
Tw1:=(T1+Tomin)/2.0; -- initial wall 1 temp
Tw2:=(T6+Tomin)/2.0; -- initial wall 2 temp
Tw3:=(T4+Tomin)/2.0; -- initial wall 3 temp

C1:=0.001098; -- initial co2 level 600 ppm
day:= 0.0; -- day counter
Vw1:=Aw1*t_w1; -- volume of wall 1
Vw2:=Aw2*t_w2; -- volume of wall 2
Vw3:=Aw3*t_w3; -- volume of wall 3
Afs:=floor_area; -- floor area of screed
Afc:=floor_area; -- floor area of concrete
Arf:=floor_area; -- roof area
Vfs:=Afs*t_fs; -- volume of screed slab
Vfc:=Afc*t_fc; -- volume of concrete slab
fen_in :=0.0;
fen_out:=0.0;

d31last:=0.0;

-- *****
-- ***** DYNAMIC REGION *****
-- *****

DYNAMIC

tday:= t - (day*3600*24);

When (tday/(24*3600)) > 1.0 then
day := day + 1;
end_when;

To := -((Tomax-Tomin)/2.0)*cos((2*3.142*tday)/(24*3600)) + ((Tomin + Tomax)/2.0);

qmv:=ua(1); -- mechanical ventilation rate
ucL:=ua(2); -- control input to lights
Qdoth:=ua(3); -- underfloor heat
fen_in':= Qdoth;

-- Heat transfer rates for air temperature equation

CLo := -PLo*cos((tday/(24.0*3600.0))*2.0*3.142);
Lo := if tday > (6.0*3600.0) and tday < (18.0*3600.0) then CLo
else 0.0;
Qdothmv:=Pf*kf*qmv; -- heat from the mechanical vent
plant
Qdotsol:=Lo*ks*AwIn; -- solar radiation
QdotL:=ke*PL; -- internal lights
Qdotcon:=Afs*2.13*((abs(Tfs-T1))**0.31)*(Tfs-T1); -- convection

```

```

Qdotrad:=Afs*bolt*Fr*((Tfs**4.0)-(T1**4.0));           -- radiation
Qdotocc:= if tday > (9.0*3600.0) and tday < (16.0* 3600.0) then 63.0*pupils
else 0.0;                                           -- occupants
Qdotapp:=0.0;                                       -- appliances
Qdotwin:=Uwin*Aw1*(T1-To);                           -- windows
Qdotfs:=Qdotcon+Qdotrad;                             -- screed
fen_out':=Qdotfs;
Qdotrf:=Urf*Arf*(T1-To);                             -- roof

DELTA_T:= (T1-To);
vo:=2*cos((tday/(24.0*3600.0))*4*3.142)+3;
knv:= If (T1-To) < 0.0 Then (To-T1)/(To) Else (T1-To)/(T1);
vnv:=C_d*(((g_acc*h_d*knv)+((vo**2)*delta_cp*0.5))**0.5);

Qdotnv:=vnv*Anv*rho_air*Cp_air*(T1-To);             -- natural ventilation
Qdotni:=V1*n*rho_air*Cp_air*(T1-To);                 -- air infiltration
Qdotmv:=qmv*rho_air*Cp_air*(T1-To);                 -- mechanical ventilation

-- Heat transfer rates for walls temperature equation

Qdotw1i:=Uw1*Aw1*(T1-Tw1);                           -- heat entering the wall
1
Qdotw1o:=Uw1*Aw1*(Tw1-To);                           -- heat leaving the wall 1
Qdotw2i:=Uw2*Aw2*(T1-Tw2);                           -- heat entering the wall
2
Qdotw2o:=Uw2*Aw2*(Tw2-T6);                           -- heat leaving the wall 2
Qdotw3i:=Uw3*Aw3*(T1-Tw3);                           -- heat entering the wall
3
Qdotw3o:=Uw3*Aw3*(Tw3-T4);                           -- heat leaving the wall 3

-- Floor insulation

Qdotin := Uin*Afs*(Tfc-Tfs);                           -- Steady heat flow through
insulation.

-- Heat transfer rates for floor temperature equation

Qdotfco:=Ufc*Afc*(T2-Tfc);                             -- heating leaving concrete

-- CO2 transfer rates for zone 1

S:= if tday > (9.0*3600.0) and tday < (16.0*3600) then co2_pp*pupils
else 0.0;
Cdotg := S;                                           -- internal co2 gains
Cdotmv:=qmv*(C1-Co);                                 -- mechanical vent
Cdotnv:=Anv*vnv*(C1-Co);                             -- natural vent
Cdotni:=v1*n*(C1-Co);                                 -- infiltration

-- mathematical differential equations for rates of change of building states

-- rate of change of indoor air
temperature for zone 1

```

```

T1dot:=(1.0/(rho_air*V1*Cp_air))*(Qdothmv+Qdotsol+QdotL+Qdotcon+Qdotrad+Qdotoccc+Qdotapp-Qdotw1i-Qdotw2i-Qdotw3i-Qdotwin-Qdotrf-Qdotni-Qdotmv-Qdotnv);
T1' := T1dot;
Tw1':=(1.0/(rho_w1*Vw1*Cp_w1))*(Qdotw1i-Qdotw1o);           -- rate of change
of temperature of wall 1
Tw2':=(1.0/(rho_w2*Vw2*Cp_w2))*(Qdotw2i-Qdotw2o);           -- rate of change
of temperature of wall 2
Tw3':=(1.0/(rho_w3*Vw3*Cp_w3))*(Qdotw3i-Qdotw3o);           -- rate of change
of temperature of wall 3
Tfs':=(1.0/(rho_fs*Vfs*Cp_fs))*(Qdotin+Qdoth-Qdotfs);        -- rate of change
of screed
Tfc':=(1.0/(rho_fc*Vfc*Cp_fc))*(Qdotfco - Qdotin);           -- rate of change of
concrete
C1':=(1.0/v1)*(Cdotg-Cdotmv-Cdotnv-Cdotni);                  -- rate of change
of co2 level in zone 1
PL := LIMINT(0.0,0.0,972.0,ucL);                               -- rate of change of
power in to lights

-- output equations

Cc:=C1;                                                         -- comfort co2 level
lux_L:=kL*PL;                                                  -- lux from lights entering
the zone
lux_S:=Lo*alpha;                                              -- lux from sun entering
the zone
Lc:=(lux_L)+(lux_S);                                          -- comfort lighting level in
the zone
Tc:=(0.33*T1)+(0.1504*Tw1)+(0.0206*Tw2)+(0.0322*Tw3)+(0.4635*Tfs);-- comfort
temp

Procedural(y:=C1,T1dot,Lc);
y(1) := C1;
y(2) := Lc;
y(3) := T1dot;
End_procedural;

-- CB inverse matrix calculation based on constant nominal values for CB terms
-- b71:=- (0.001098-Co)/V1;

b71:= if (C1-Co) > 0.01 then -(C1-Co)/v1
else -0.01;
c17:=1.0;
b82:=1.0;
c28:=kL;
b11:=((Pf*kf)-(rho_air*Cp_air*(T1-To)))/(rho_air*V1*Cp_air);

c31:=(-(Afs*2.13*((abs(Tfs-T1))**0.31))-(Afs*bolt*Fr*(T1**3.0))-(Uw1*Aw1)-
(Uw2*Aw2)-(Uw3*Aw3)-(Uwin*Awin)-(Ufs*Afs)-(Urf*Arf)-(vnv*Anv*rho_air*Cp_air)-
(V1*n*rho_air*Cp_air))/(rho_air*V1*Cp_air);
d31:=((Pf*kf)-(rho_air*Cp_air*(T1-To)))/(rho_air*V1*Cp_air);
b53:=(1.0/(rho_fs*Vfs*Cp_fs));
c35:=(((Afs*2.13*((abs(Tfs-
T1))**0.31)))+(Afs*bolt*Fr*(Tfs**3.0)))/(rho_air*V1*Cp_air);

```

```
c38:=(Ke/(rho_air*V1*Cp_air));
```

```
Procedural(invcgx:= b71,c17,b82,c28,b11,c31,b53,c35,c38,c31);  
invcgx(1,1):=1.0/(b71*c17);  
invcgx(1,2):=0.0;  
invcgx(1,3):=0.0;  
invcgx(2,1):=0.0;  
invcgx(2,2):=1.0/(b82*c28);  
invcgx(2,3):=0.0;  
invcgx(3,1):=-(b11*c31)/(b53*b71*c17*c35);  
invcgx(3,2):=-c38/(b53*c28*c35);  
invcgx(3,3):=1.0/(b53*c35);  
end_procedural;
```

```
Procedural(Dm:= d31);  
Dm(1,1):=0.0;  
Dm(1,2):=0.0;  
Dm(1,3):=0.0;  
Dm(2,1):=0.0;  
Dm(2,2):=0.0;  
Dm(2,3):=0.0;  
Dm(3,1):=d31;  
Dm(3,2):=0.0;  
Dm(3,3):=0.0;  
end_procedural;
```

```
END sm_building;
```

CONTROLLER MODEL FILE

```
SUBMODEL sm_controller  
(REAL:uc1,uc2,uc3,utrim(1..3):=REAL:ua(1..3),T1,invcgx(1..3,1..3),y(1..3),tday,utswi  
tch,utrimdot(1..3),ucdot(1..3),uadot(1..3),Dm(1..3,1..3));
```

```
USE pa_smcparr;
```

```
REAL:set1,set2,set3,e1,e2,e3,int_e1,int_e2,int_e3,ki11,ki22,ki33,ki31,ki32,int_e1las  
t,int_e2last,int_e3last,  
kp11,kp22,kp33,kp31,kp32,tidotset3,uc(1..3),ylast(1..3),ydot(1..3),utrim_qmv,uc_qmv  
,u_qmv;
```

```
REAL: KT/0.00035/;
```

```
REAL:rho(1..3,1..3)[ 8.0e-08,0.0,0.0,  
0.0,0.00000225,0.0,  
0.0,0.0,0.0000025];
```

```
-- rho 3,3 0.0000025
```

```
REAL:zigma(1..3,1..3)[ 0.0056,0.0,0.0,  
0.0,0.03,0.0,
```

```

0.0,0.0,0.01667];

-- vector elements in the above limits are:qmv (CO2),ucL (Lights),Qdoth (heater)

REAL:UL(1..3)[ 1.4,
               100000.0,
               50000.0 ];
REAL:LL(1..3)[ 0.0,
               -100000.0,
               0.0 ];

--vector v1 = Tcr required comfort temperature
--vector v2 = Lcr required lux level
--vector v3 = Ccr required co2 level

REAL:v(1..3)[ 0.002745,    -- 1500ppm
              500.0,      -- lux level for the whole zone
              294.0 ];   -- 21 oc

REAL: Tset;                -- actual set point for temperature
PARAMETER REAL: g/0.1/;    -- gain
PARAMETER REAL: Co/0.000732/; -- kg/m^3 outside co2 level 400 ppm

INITIAL

int_e1 := g*(1.0/rho(1,1))*sigma(1,1)*y(1);
int_e2 := g*(1.0/rho(2,2))*sigma(2,2)*y(2);
int_e3 := g*(1.0/rho(3,3))*sigma(3,3)*y(3);

ki11:=invcgx(1,1)*rho(1,1);
ki22:=invcgx(2,2)*rho(2,2);
ki31:=invcgx(3,1)*rho(1,1);
ki32:=invcgx(3,2)*rho(2,2);
ki33:=invcgx(3,3)*rho(3,3);

kp11:=g*invcgx(1,1)*sigma(1,1);
kp22:=g*invcgx(2,2)*sigma(2,2);
kp31:=g*invcgx(3,1)*sigma(1,1);
kp32:=g*invcgx(3,2)*sigma(2,2);
kp33:=g*invcgx(3,3)*sigma(3,3);

ylast(1):=y(1);
ylast(2):=y(2);
ylast(3):=y(3);

int_e1last :=0.0;
int_e2last :=0.0;
int_e3last :=0.0;

uc1:=0.0;
uc2:=0.0;
uc3:=0.0;

```

DYNAMIC

```
set1 := if tday >(8.0*3600.0) and tday < (17.0*3600.0) then V(1)
else 0.000732;
```

```
set2 := if tday >(6.0*3600.0) and tday < (17.0*3600.0) then V(2)
else 0.0;
```

```
set3 := if tday >(4.0*3600.0) and tday < (15.0*3600.0) then V(3)
else 282.0;
```

```
Tset:= set3 + 6.0;
```

COMMUNICATION

```
tdotset3 := KT*(set3-T1); -- temperature control outer-loop of RIDE loop
```

```
e1 := set1-y(1);
e2 := set2-y(2);
e3 := tdotset3-y(3);
```

```
int_e1:= int_e1 + CINT*e1;
int_e2:= int_e2 + CINT*e2;
int_e3:= int_e3 + CINT*e3;
```

```
ydot:=(1.0/CINT)*(y-y1ast);
```

```
utrim:=-(invcgx*ydot)-(invcgx*(Dm*utrimdot))+ua+(invcgx*(Dm*uadot));
```

```
--utrim_qmv:=invcgx(1,1)*ydot(1)+ua(1);
--uc_qmv:=ki11*int_e1 - kp11*y(1);
```

```
--u_qmv:=uc_qmv+utrim_qmv;
```

```
-- utrim:=((-invcgx)*ydot)+ua;
```

```
uc1 := ki11*int_e1 - kp11*y(1) + utswitch*utrim(1);
uc2 := ki22*int_e2 - kp22*y(2) + utswitch*utrim(2);
```

```
uc3 := ki31*int_e1 + ki32*int_e2 + ki33*int_e3 - kp31*y(1) - Kp32*y(2) - kp33*y(3) +
(utswitch*utrim(3))-(invcgx(3,3)*ucdot(1)*Dm(3,1));
```

```
--uc3 := ki33*int_e3 - kp33*y(3) + 0.0*(ki31*int_e1 + ki32*int_e2 - kp31*y(1) -
Kp32*y(2) + utswitch*utrim(3) );
```

```
if uc1 > UL(1) then
```

```
int_e1 := (1.0/ki11)*(UL(1)+kp11*y(1) - utswitch*utrim(1));
```

```

end_if;
if uc1 < LL(1) then
int_e1 := (1.0/ki11)*(LL(1)+kp11*y(1) - utswitch*utrim(1));
end_if;
if uc2 > UL(2) then
int_e2 := (1.0/ki22)*(UL(2)+kp22*y(2)- utswitch*utrim(2));
end_if;
if uc2 < LL(2) then
int_e2 := (1.0/ki22)*(LL(2)+kp22*y(2)- utswitch*utrim(2));
end_if;
if uc3 > UL(3) then
int_e3 := (1.0/ki33)*(UL(3)-ki31*int_e1 - ki32*int_e2 + kp31*y(1) + Kp32*y(2) +
kp33*y(3) - (utswitch*utrim(3))+(invcgx(3,3)*ucdot(1)*Dm(3,1)));
end_if;
if uc3 < LL(3) then
int_e3 := (1.0/ki33)*(LL(3)-ki31*int_e1 - ki32*int_e2 + kp31*y(1) + Kp32*y(2) +
kp33*y(3) - (utswitch*utrim(3))+(invcgx(3,3)*ucdot(1)*Dm(3,1)));
end_if;

uc(1) := uc1;
uc(2) := uc2;
uc(3) := uc3;

int_e1last :=int_e1;
int_e2last :=int_e2;
int_e3last :=int_e3;

ylast:=y;

END sm_controller;

```

19 : Table of figures

Figure 1: Schematic of the Fanger's comfort criteria	8
Figure 2 Current building design process (✓= included x = not included) [see (French, 1985) for conceptual and detailed design stages]	17
Figure 3 Graph of cost of error removal over time in design process.....	30
Figure 4 2D representation of a model zone building case study	36
Figure 5 Schematic of the building's energy flows, CO ₂ and lux balance showing the factors affecting the internal environment of the zone.....	37
Figure 6 Internal model multilayer comparison of simplified model and ESP-r model for temperature response	38
Figure 7 Internal model single layer comparison of simplified model and ESP-r model for temperature response	38
Figure 8 lumped capacitance model – building energy transfer function paths	41
Figure 9 Resistance capacitance thermal circuit for the wall.....	48
Figure 10 Resistance capacitance thermal circuit for the floor.....	50
Figure 11 An electrical node through which current are entering and exiting.....	72
Figure 12 Linear transfer function with sine wave input	76
Figure 13 Presentation of frequency response data: Bode Plot.....	77
Figure 14 Response of a system to high frequency excitation (input).....	78
Figure 15 Frequency response specification	79
Figure 16 Three dimensional representation of the test house living room.....	80
Figure 17 Comparison of the measured and estimated zone air temperature in the test house with measured heat power output	83
Figure 18 Measured heater power output in the test house.....	84
Figure 19 Comparison of the measured and estimated air temperature in the test house with model heater.....	85
Figure 20 Comparison of the measured and estimated heat power output	86
Figure 21 Thermal mass temperatures with heating (Closed loop)	87
Figure 22 Thermal mass temperatures without heating (open loop).....	88

Figure 23 Comparison of dynamics of radiator temperature and air temperature for closed loop system	89
Figure 24 Bode plots of the two models for the test case house	96
Figure 25 Comparison of the reduced and full order temperature response with measured temperature	97
Figure 26 Bode plots of the 4 th and 10 th order models for the test case house.....	100
Figure 27 Comparison of the reduced and full order temperature response with measured temperature	101
Figure 28 Comparison of the dynamic and steady state temperature predictions of the plant temperature.....	102
Figure 29 Decision impact vs. Building life [(Lechner, 2001)]	104
Figure 30: First order temperature response to step change in temperature	106
Figure 31 Block diagram of the ISR Philosophy	107
Figure 32 Temperature response as the proportional gain is increased	108
Figure 33 The simplest controller – a gain.....	109
Figure 34 As $k \rightarrow \infty$, the controller becomes a relay.....	110
Figure 35 Block diagram of the control system with controller matrix $K(t)$ and dynamic inverse input $U_{eq}(t)$ where: $u_r(t)$ = reference input to the controller, $u_c(t)$ = controller output, $u(t)$ = control signal to the actuator, $u_a(t)$ = actuator output, $y(t)$ = actual output of the system and $r(t)$ = desired output.....	114
Figure 36 Block diagram of a simple feedback control system with controller matrix K	115
Figure 37 simple block diagram of a generic control system	119
Figure 38 first order system block diagram	119
Figure 39 Second order system block diagram	121
Figure 40 Second order system with derivative feedback block diagram	121
Figure 41 Generic feedback control system.....	124
Figure 42 U_{eq} feedback makes a MIMO system behave like an ideal integrator (i.e. First Order).....	133
Figure 43 PDF control system block diagram	134
Figure 44 Simplified PDF and first order system	135

Figure 45: Block diagram of a simple feedback control system with controller matrix $K(s)$ Where: r = set-point, y = output, g = scalar gain and K = controller gain matrix	138
Figure 46 Block diagram of closed system with U_{trim}	139
Figure 47 RIDE control system block diagram	149
Figure 48 Proposed design process flow diagram for controllability assessment and controller design.....	154
Figure 49 Case study School Design Concept	170
Figure 50 Heating mode, showing inputs of the whole system, where MV = Mechanical ventilation, PL = lighting power and UFH = Under-floor heating.....	171
Figure 51 Asymptote directions on a root locus for the three control channels with control strategy 1.....	179
Figure 52 Asymptote directions on a root locus for the three control channels with control strategy 2.....	183
Figure 53 Asymptote directions on a root locus for a closed-loop system.	200
Figure 54: shows a typical response to a step change in the required temperature.	221
Figure 55: shows the response with varying external thermal mass values.....	222
Figure 56: Unstable response with asymptote pointing towards RHP on the root-locus.	223
Figure 57: Unstable response of heating system with asymptote pointing towards RHP on the root-locus.....	223
Figure 58: Air temperature response to solar gain (top), solar gain profile (bottom)	227
Figure 59: plot showing heater output and U_{trim}	228
Figure 60: Temperature response with different U values of the wall.....	230
Figure 61: Heating power consumed for different U values of the wall.....	230
Figure 62 Resistance capacitance circuit of the wall	231
Figure 63 Steady state resistance circuit of the wall	232
Figure 64: Temperature response with varying C_p values with constant U value of 0.22.....	233
Figure 65: Effect of thermal mass on tracking air temperature a) 400 b) 800 c) 1500 (J/kgK).	237

Figure 66: Comfort Temperature response to step change in set-point (top) & power output from the heater and U_{trim} plot (bottom) with 3 kW heater	245
Figure 67: Comfort Temperature response with a 10 kW heating system.....	247
Figure 68: Comfort temperature response with varying thermal mass	248
Figure 69 Heating power consumed for different C_p values of the wall.....	248
Figure 70: Comfort Temperature response to change in set point with varying the thermal mass of the wall	254
Figure 71: Radiator power consumption for comfort temperature control with varying the thermal mass of the wall	255
Figure 72: Limits on operational range of temperature	269
Figure 73: Limits of U_{trim} for reachability	269
Figure 76: Basic thermal mass with heat transfer across it.....	294
Figure 77: Test House	295